Characterization of swarm-colony development reveals the release of a distinct cell type facilitating dissemination of *Vibrio parahaemolyticus*

Dissertation

zur
Erlangung des Doktorgrades
der Naturwissenschaften
(Dr. rer. nat.)

dem Fachbereich Biologie
der Philipps-Universität Marburg
vorgelegt

von

Carolina Duarte de Freitas

aus Lisboa, Portugal

Marburg (Lahn), im Juli 2019

Die Untersuchungen zur vorliegenden Arbeit wurden von Oktober 2015 bis Juli 2019 am Max-Planck-Institut für Terrestrische Mikrobiologie unter der Leitung von Dr. Simon Ringgaard durchgeführ.

Vom Fachbereich Biologie der Philipps-Universität Marburg als Dissertation angenommen am:

Erstgutachter: Dr. Simon Ringgaard
Zweitgutachter: Prof. Dr. Martin Thanbichler

Weitere Mitglieder der Prüfungskommission:

Prof. Dr. Knut Drescher

Prof. Dr. Michael Bölker

Tag der mündlichen Prüfung am: 24.09.2019

Die während der Promotien erzielten Erebbnisse wurden zum Teil in folgenden Originalpublikationen veröffentlicht:

Muraleedharan, S., Freitas, C., Mann, P., Glatter, T. and Ringgaard, S. (2018).

A cell length-dependent transition in MinD-dynamics promotes a switch in division-site placement and preservation of proliferating elongated *Vibrio parahaemolyticus* swarmer cells. *Molecular Microbiology* 109(3): 365-384

Unpublished work:

Freitas, C., Glatter, T. and Ringgaard, S. The release of a distinct cell type from swarm colonies facilitates dissemination of *Vibrio parahaemolyticus* in the environment. *Under review,* The ISME Journal

To my family

Table of contents

Contents

List of figures

List of tables

Abbreviations

µ-	Micro
µL	Microliter
aa	Amino acid
Amp	Ampicillin
ATP	Adenosine triphosphate
A.U.	Arbitrary unit
C	Cells from the Center of swarm colonies
CCW	Counterclockwise
c-di-GMP	Cyclic diguanylate
CFU	Colony forming unit
Cm	Chloramphenicol
CW	Clockwise
DNA	Deoxyribonucleic acid
FC	Fold change
FDR	False discovery rate
GO	Gene ontology
h	Hour
L	Cells grown in Liquid LB
LB	Luria-Bertani medium
LC-MS	Liquid chromatography mass spectrometry
LFQ	Label-free quantification
LPS	Lipopolysaccharide
GlcNAc	monosaccharide N-acetylglucosamine
mCherry	Monomeric Cherry (fluorescent protein)
MCP	Methyl-accepting chemotaxis protein
min	Minutes
mL	Mililiter
nm	Nanometer
OD	Optical density
P	Cells from the Periphery of swarm colonies
pH	Negative decimal logarithmic of the hydrogen ion activity
PTS	Phosphotransferase system
R	Released cells
RNA	Ribonucleic acid

SEM	Standard error of the mean
sfGFP	Superfolder green fluorescent protein
SS	Statistically significant
S	Cells grown on an LB solid plate
TIIISS	Type III secretion system
TVISS	Type VI secretion system
vs.	versus
w/v	weight/volume

Abstract

Bacteria often experience changes in their external environment and have developed various strategies to respond accordingly. One mechanism to accommodate such changes involves the differentiation into specialized cell types suitable for the particular conditions. *Vibrio parahaemolyticus* exists as a swimmer cell, adapted for liquid conditions, and as a swarmer cell, specialized to grow on solid surfaces. Swarmer cells undergo a differentiation process that leads to elongation and production of multiple lateral flagella along the cell body, which are essential for swarming behavior. According to the position within a swarm colony, *V. parahaemolyticus* cells display different sizes. Particularly, long swarmer cells are only found in the periphery of the colony while the center consists of much shorter cells. Nonetheless, how the architecture develops over time or in response to environmental fluctuations is unknown. As *V. parahaemolyticus* is a marine bacterium and the leading agent of seafood borne gastroenteritis, the worldwide distribution of *V. parahaemolyticus* accentuates the need for understanding the factors contributing to its dissemination.

In this study, by characterizing the swarm-colony architecture and development we revealed that a new distinct cell type is released from the swarm colony into the environment. Through mass spectrometry and confocal microscopy analysis we show that released cells comprise of a cell type that is morphologically short and distinct from cells belonging to the center and periphery of the swarm colony. Surprisingly, the cell length distribution of released cells was very homogenous and almost no long cells were detected. Thus, suggesting that long swarmer cells are not released into the liquid environment but stay surface-attached during flooding. We also revealed that released cells are capable of spreading in the liquid environment and attach to new submerged surfaces. Moreover, our data shows that released cells are optimized for swimming behavior and can chemotax towards the chitin component, N-acetylglucosamine. By using fluorescence microscopy and stereomicroscopy, we determine the temporal development of swarm colonies and show how the swarm colony architecture fluctuates with changing environmental conditions. Importantly, we show that swarm colonies act as a continuous source of cells that are released from the swarm colony into the environment. Overall, these results indicate that release of a distinct cell type from swarm colonies facilitates the dissemination of *V. parahaemolyticus* in the environment, likely influencing the ecology of this marine bacterium.

Additionally, our research revealed the degree to which the *V. parahaemolyticus* proteome changes according to its distinct environmental circumstances. Particularly, we define which proteins are present specifically in the swarm flares, in the center of the swarm colony and in a planktonic condition. By performing single deletions we identified potential regulators of swarming differentiation. At last, we define which proteins are constitutively expressed in this bacterium.

Altogether, this work reveals how flexible the proteome of *V. parahaemolyticus* is according to different ecological niches and reports on the development of swarm colony populations and how the formation and release of a distinct cell type from swarm colonies facilitates the dissemination of an important human pathogen in the environment – thus, influencing the ecology of this marine bacterium.

Zusammennfassung

In der natürlichen Umgebung von Bakterien gibt es oft Veränderungen, und Bakterien haben verschiedene Strategien entwickelt um dementsprechend zu reagieren. Ein Mechanismus um sich an solche Veränderungen anzupassen ist die Differenzierung in Zellarten die für die jeweiligen Bedingungen spezialisiert sind. *Vibrio parahaemolyticus* kommt beispielsweise in Form von Schwimmerzellen vor, die an einen flüssigen Lebensraum angepasst sind, und in Form von Schwärmerzellen, die wiederum spezialisiert darauf sind auf festen Oberflächen zu wachsen. Schwärmer durchlaufen einen Differenzierungsprozess der zu Zellverlängerung und zur Produktion von vielen lateralen Flagellen entlang der Zelle führt, was notwendig zum Schwärmen ist. Individuelle *V. parahaemolyticus* Zellen können, je nachdem wo in einer Schwarmkolonie sie sich befinden, unterschiedliche Zellgrößen aufweisen. Insbesondere die langen Schwärmerzellen sind ausschließlich in der Kolonieperipherie zu finden, wohingegen das Zentrum der Kolonie aus wesentlich kürzeren Zellen besteht. Allerdings ist es nicht bekannt, wie sich die Koloniearchitektur im Laufe der Zeit oder als Reaktion auf Umweltschwankungen verändert. *V. parahaemolyticus* ist ein mariner Organismus und einer der Hauptverursacher von Gastroenteritis, hervorgerufen durch den Verzehr von Meeresfrüchten; darum ist es von besonderem Interesse die Faktoren zu verstehen, die an seiner Ausbreitung beteiligt sind.

Durch Charakterisierung der Architektur und Entwicklung der Schwarmkolonie zeigen wir, dass eine neuentdeckte spezifisch differenzierte Zellart von der Schwarmkolonie in die Umgebung abgegeben wird. Mit Hilfe von Massenspektrometrie und konfokalen Mikroskopiemethoden zeigen wir, dass diese Zellen sich von den bisher bekannten kurzen Zellen im Zentrum und den Zellen in der Kolonieperipherie unterscheiden.Überraschenderweise war die Länge der freigesetzten Zellen sehr homogen und es wurden kaum lange Zellen gefunden. Dies deutet darauf hin, dass lange Schwärmerzellen nicht in das flüssige Umgebungsmilieu abgegeben werden sondern mit der Oberfläche verbunden bleiben. Wir zeigen auch, dass die freigesetzten Zellen die Fähigkeit haben sich in flüssigem Milieu auszubreiten und sich dann an anderen Oberflächen festzusetzen. Darüberhinaus weisen unsere Ergebnisse darauf hin, dass die freigesetzten Zellen optimiert zum Schwimmen sind und sich mit Hilfe von Chemotaxis zur Chitinkomponente N-Acetylgucosamin hin bewegen können. Mit Hilfe von Fluoreszenzmikroskopie und Stereomikroskopie können wir die zeitliche Entwicklung der Schwarmkolonie beobachten und zeigen, wie die Koloniearchitektur

sich im Laufe der Zeit mit verändernden Umweltbedingungen auch ändert. Unsere Ergebnisse bekunden, dass Schwarmkolonien selbst als kontinuierliche Quelle von Zellen dienen, welche in die Umgebung abgegeben werden. Das bedeutet, dass die Freisetzung von spezialisierten Zelltypen die Ausbreitung von *V. parahaemolyticus* aktiv unterstützt, und damit wahrscheinlich die Ökologie dieses marinen Bakteriums mit beeinflusst.

Unsere Untersuchungen beinhalten außerdem den Grad der Veränderung des gesamten *V. parahaemolyticus* Proteoms im Hinblick auf verschiedene Umgebungsverhältnisse. Insbesondere stellen wir fest welche Proteine spezifisch in den *Flares* (fackelförmigen Ausbreitungen an der Schwarmperipherie), spezifisch im Schwarmzentrum, oder spezifisch unter plaktonischen Wachstumsbedingungen exprimiert werden. Durch Gendeletionen identifizieren wir potentielle Regulatoren der Schwärmerzelldifferenzierung. Weiterhin definieren wir welche Proteine in diesem Bakterium konstitutiv exprimiert werden.

Unsere Ergebnisse zeigen wie flexibel das Proteom von *V. parahaemolyticus* auf verschiedene ökologische Nischen reagiert und wie es sich bei den einzelnen Populationen einer Schwarmkolonie unterscheidet. Weiterhin zeigen wir wie die Bildung und Freisetzung von spezialisierten Zellen einer Schwarmkolonie zur Ausbreitung eines wichtigen Humanpathogens in der Umwelt und damit auch der Ökologie dieses marinen Organismus beiträgt

Chapter I - Introduction

1.1 Biofilm dispersal

Biofilms are surface associated communities of microbes encased in a self-produced polymeric matrix. Biofilm formation is a beneficial mode of life, where microorganisms are better adapted than free-swimming bacteria to withstand nutrient deprivation, pH changes, oxygen radicals, biocides and antimicrobial agents (Huang *et al.*, 1998; Cochran *et al.*, 2000; Maira-Litrán *et al.*, 2000). However, upon formation of a mature biofilm, cells may not have access to nutrients or may suffer from accumulation of toxic waste products. Such an unfavourable environment will persuade bacteria to leave the biofilm and colonize new environments. As bacteria must be able to detect and respond to such challenging situations, it is not surprising that biofilm dispersal is a highly regulated process involving many sensory circuits (Karatan and Watnick, 2009). Cell loss from the biofilm to the environment can also happen as a result of physical forces such as abrasion, erosion, and sloughing (Stoodley *et al.*, 2001). Yet, widespread acute release of cells is not attributed solely to the effect of physical impact or shear stress. The mechanisms, signals and regulatory networks that contribute to active dispersal of bacteria from biofilms will be presented next.

1.1.1 Signals and Regulatory Networks

The biofilm dispersal process occurs during the final stage of biofilm development and is a necessary step for bacteria to break their biofilm bonds and spread to new locations. This process allows the release of individual cells and multicellular aggregates (Guilhen *et al.*, 2017). This regulated process, which is triggered in response to various environmental and biological signals, can be observed in a wide variety of species (Thormann *et al.*, 2005; Morgan *et al.*, 2006; Barraud *et al.*, 2009b; Stacy *et al.*, 2014; Singh *et al.*, 2017). Studies have identified a large panel of signals, regulatory pathways and effectors but the connections between them are still incompletely understood (Sauer *et al.*, 2004; Thormann *et al.*, 2005; Gjermansen *et al.*, 2005; Boles and Horswill, 2008).

1.1.1.1 Nutritional cues

Biofilm dispersal can be induced by both decrease or increase in environmental nutrients. For example, *Pseudomonas putida* biofilms dissolved in response to carbon starvation (Gjermansen *et al.*, 2005) while *Pseudomonas aeruginosa* biofilms were

shown to disperse under increased concentrations of various carbon and nitrogen sources (Sauer *et al.*, 2004). This indicates that biofilm environment might be advantageous only within a window of nutrient concentrations.

1.1.1.2 Oxygen depletion, oxidative stress and nitric oxide

Bacteria residing at various layers of biofilms experience differences in oxygen tensions (Walters *et al.*, 2003). A sudden decrease in oxygen concentration led to detachment of *Shewanella oneidensis* biofilms (Thormann *et al.*, 2005). Biofilms of null mutants of genes *arcA* and *crp*, which encode for transcriptional regulators that mediate responses to changing oxygen levels, showed a severe decrease in the detachment response, suggesting a role for these genes in dispersal regulation (Thormann *et al.*, 2005). Nevertheless, how these oxygen-sensing circuits mediate or coordinate the detachment response is currently not known.

Oxidative stress results from either endogenous production of, or exposure to, reactive oxygen intermediates (ROI), which include superoxide (O_2^-), hydrogen peroxide (H_2O_2), and hydroxyl radical (HO·). When the production of ROI overwhelms the capacity of the cell to remove such molecules, damage to DNA, lipids and proteins may occur (Boehme *et al.*, 1976; Wallace *et al.*, 2004; Park *et al.*, 2005b; Boylan *et al.*, 2008). While the roles of ROI have been extensively studied in planktonic bacterial physiology in the context of protective mechanisms, there are still many questions to explore regarding their role in multicellular biofilm development and differentiation processes (Altuvia *et al.*, 1994; Touati *et al.*, 1995; Park *et al.*, 2005b; Liu *et al.*, 2011). ROI can accumulate inside *P. aeruginosa* biofilm microcolonies and they appear to have an indirect role in dispersal of this bacterium by inducing a phage-dependent cell death program (Webb *et al.*, 2003). Oxidative stress was also shown to induce biofilm dispersal in *Aggregatibacter actinomycetemcomitans*. In an infection site, this oral pathogen forms mixed-species biofilms with many microbes, including commensal *streptococci* such as *Streptococcus gordonii*. To overcome toxic levels of the antimicrobial, hydrogen peroxide (H_2O_2) produced by *S. gordonii*, *A. actinomycetemcomitans* responds in two ways. One being detoxification, which is achieved by inducing expression of a catalase (KatA), and the other being dispersion that is mediated by Dispersin B (DspB). DspB is an enzyme that dissolves *A. actinomycetemcomitans* biofilms (Stacy *et al.,* 2014) (section "1.1.2. Mechanisms of dispersal").

Another form of stress that can also lead to damage of DNA, lipids and proteins is termed nitrosative stress, which involves production of reactive nitrogen intermediates (RNI). Nitrosative stress, in particular, exposure to nitric oxide (NO) or reactive species resulting from NO, led to dispersal of mature *P. aeruginosa* biofilms (Barraud *et al.*, 2006) (section 1.1.3 "Effect of nitroxides on swarming motility and biofilm dispersal of *Bacillus subtilis* and *Pseudomonas aeruginosa*").

1.1.1.3 c-di-GMP

c-di-GMP is a global second messenger signalling molecule, which is involved in a wide variety of biological processes (Ross *et al.*, 1987; Chua *et al.*, 2014; Yang *et al.*, 2016; Fernandez *et al.*, 2018; Li *et al.*, 2018; McKee *et al.*, 2018; Waters *et al.*, 2018; Xue *et al.*, 2018; Zhang *et al.*, 2018; Wang *et al.*, 2019). One of these processes is regulation of biofilm formation and dispersal. In response to environmental cues, diguanylate cyclases synthesize and phosphodiesterases degrade c-di-GMP (Christen *et al.*, 2005; Al-Bassam *et al.*, 2018). The essential domains for such activity are the GGDEF and EAL domains, respectively (Simm *et al.*, 2004; Chan *et al.*, 2005; Ryjenkov *et al.*, 2005).

Induction of the EAL-domain containing protein (which leads to low c-di-GMP levels) in cells from *P. putida* biofilms led to their rapid dispersion (Gjermansen *et al.*, 2006). A similar effect was also seen in *S. oneidensis* biofilms, where transcriptional activation of the EAL-domain encoding gene from *Escherichia coli* (*yhjH*) led to a rapid cellular detachment from the biofilm (Thormann *et al.*, 2006). Dispersal of *P. aeruginosa* biofilms induced by addition of NO (Barraud *et al.*, 2009a) or increased glutamate levels (Morgan *et al.*, 2006), was shown to be regulated via a c-di-GMP-dependent regulatory network. Addition of NO stimulates phosphodiesterases that decrease c-di-GMP levels, which in turn triggers dispersal response (Barraud *et al.*, 2009a).

1.1.1.4 Quorum sensing and RpoS stress response

Quorum-sensing circuits allow bacteria to coordinate their gene expression in a cell density-dependent manner. Small molecules called autoinducers are secreted by bacteria and accumulate in the extracellular environment. When the autoinducer

concentration exceeds a requisite threshold, the quorum-sensing circuit is activated (Atkinson and Williams, 2009; Roy *et al.*, 2011). Autoinducers such as acyl-homoserine lactones (AHLs) are produced by Gram-negative bacteria and have been related to biofilm dispersal in several bacterial species, including *P. aeruginosa* and *Vibrio vulnificus* (Henke and Bassler, 2004; Thiel *et al.*, 2009; Ueda and Wood, 2009; Lee *et al.*, 2013). Moreover, *agr*, a quorum-sensing accessory gene regulator was shown to contribute to *Staphylococcus aureus* biofilm dispersal (Ji *et al.*, 2006; Boles and Horswill, 2008).

HapR is a transcription factor involved in *Vibrio cholerae´s* quorum sensing system. At high cell density, HapR is synthesized and it indirectly represses the expression of the exopolysaccharide biosynthesis operon and decreases intracellular levels of c-di-GMP, which consequently promotes dispersal of *V. cholerae* biofilms (Liu *et al.*, 2007; Srivastava and Waters, 2012). RpoS is a specialized sigma factor that leads to general stress resistance of cells and is induced, for instance, by a change in flow conditions or the removal of a nutrient source (Mandel and Silhavy, 2005; Ait-Ouazzou *et al.*, 2012). A recent paper demonstrates that in the case of *V. cholerae* biofilms with a diameter of ≈20 µm or more, high HapR levels *per se* were not enough to trigger dispersal response. In addition, cells also needed a stress signal that led to induction of the sigma factor, RpoS in order to disperse (Figure 1) (Singh *et al.*, 2017).
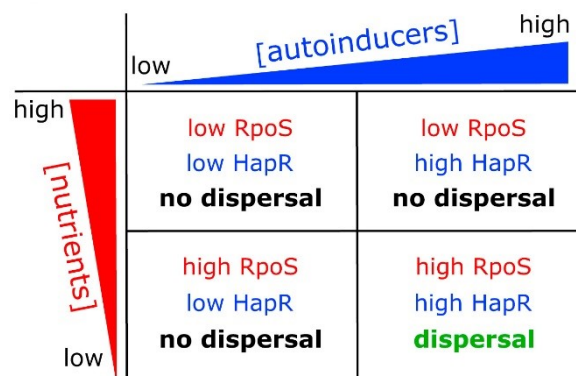
Figure 1. Biofilm dispersal decision by integrating nutrient and autoinducer sensing yields. *V. cholerae* biofilm cells can have four different combinations of HapR and RpoS levels. Dispersal only occurs when levels of both RpoS and HapR are high. Adapted from (Singh *et al.*, 2017).

1.1.2 Mechanisms of dispersal

Biofilm matrix is usually composed of polysaccharides, extracellular DNA and proteins (Steichen *et al.*, 2011; Foulston *et al.*, 2014; Cho *et al.*, 2015; Dengler *et al.*, 2015). Therefore, some already identified effectors important for biofilm dispersal include polysaccharide degrading enzymes and extracellular or periplasmic proteases- which process bacterial surface adhesins (Allison *et al.*, 1998; Baty *et al.*, 2000; Dow *et al.*, 2003; Boles and Horswill, 2008; Dean *et al.*, 2015). As mentioned above, dispersin B (or DspB) can dissolve *A. actinomycetemcomitans* biofilms in response to hydrogen peroxide and oxygen (Stacy *et al.*, 2014) (section "1.1.1.2 Oxygen depletion, oxidative stress and nitric oxide"). The mechanism by which this β-hexosaminidase DspB works is by hydrolysing the glycosidic linkages of the exopolysaccharide poly-GlcNAc, a major component of the extracellular matrix of *A. actinomycetemcomitans* biofilms (Kaplan *et al.*, 2004).

Although it has been long known that flagella function is vital for transport and initiation of cell-to-surface interactions, some studies suggest that it might also be important for cell detachment from biofilms (Magariyama *et al.*, 1995; Sauer and Camper, 2001; Sauer *et al.*, 2002; Sauer *et al.*, 2004; Utada *et al.*, 2014). For instance, studies on *P. aeruginosa* dispersal through a cell flow system revealed that cells evacuating cell clusters showed motility, while cells remaining in the walls of cell clusters were non-motile (Sauer *et al.*, 2002).

Biofilm dispersal of different species, such as *P. aeruginosa*, *Staphylococcus epidermidis* and *P. putida*, can also be caused by amphipathic molecules and surfactants that can disrupt noncovalent interactions between matrix components leading to reduced surface tension (Yao *et al.*, 2004; An *et al.*, 2010; Cárcamo-Oyarce *et al.*, 2015).

Another biological process that contributes to biofilm dispersal is cell autolysis, which leads to cavities formed in the biofilm matrix (Webb *et al.*, 2003; Barraud *et al.*, 2006). The formation of voids inside biofilm microcolonies is beneficial for the subpopulation of released cells, which can explore new niches but also for the remaining cells in the biofilm, which may consequently have greater access to nutrients.

1.1.3 Effect of nitroxides on swarming motility and biofilm dispersal of *Bacillus subtilis* and *Pseudomonas aeruginosa*

Swarming motility is a multicellular movement of bacteria that migrate above solid substrates (Harshey and Partridge, 2015). Although a lot of research has been done to understand the process of cells being released from biofilms there are, so far, no studies focusing on the dispersal of cells from swarming colonies. However, in two different studies, the effect of nitroxides on swarming motility as well as on biofilm dispersal was analysed.

Schreiber *et al.*, showed that a strongly enhanced biofilm dispersal in *Bacillus subtilis* was observed when nitric oxide (NO) bioavailability was supressed by the use of NOS inhibitors, NO scavengers or the use of NO-synthase mutant Δ*nos* (Schreiber *et al.*, 2011). NOS-derived NO might be involved in fine-tuning the cellular decision-making between dispersal from the biofilm or adaptation of the metabolism to (anoxic) conditions in the biofilm (Schreiber *et al.*, 2011)*.*

A study on the swarming bacterium *P. aeruginosa* showed contrary results as exogenous addition NO at low concentrations led to a marked dispersal of biofilm (Barraud *et al.*, 2006). Moreover, a Δ*nirS* mutant (a nitrite reductase mutant), which is unable to produce NO, forms biofilms that fail to disperse, whereas a Δ*norCB* (NO reductase) mutant, which produces large amounts of NO, shows enhanced biofilm dispersal (Barraud *et al.*, 2006). Moreover, addition of NO led to enhanced swimming and swarming motilities, while no differences were observed in the study, done in *B. subtilis* (Barraud *et al.*, 2006; Schreiber *et al.*, 2011).

The dissimilar effects of NO on dispersal and motility between species might be explained by the different types of dispersal assays used in the studies. Alternatively, the effect of NO on dispersal can be a species-specific phenomenon, in that different bacteria may use NO for opposing dispersal strategies.

1.1.4 Dispersed bacteria, a specific cell type

The active escape of bacterial cells from the biofilm matrix is referred to as dispersion and it involves a phenotypic switch dependent on the sensing of environmental cues. The external signals are transduced to final effectors that will allow the release of individual cells and/or multicellular aggregates to explore new habitats (Petrova and Sauer, 2016; Guilhen *et al.*, 2017).

Single cells dispersed from the biofilms of *P. aeruginosa* and *Klebsiella pneumoniae* display phenotypes that differ not only from those in biofilms but also from planktonic cultures (Sauer *et al.*, 2002; Sauer *et al.*, 2004; Guilhen *et al.*, 2016). Compared with planktonic cells, the dispersed cells of *Caenorhabditis elegans* are more sensitive towards iron stress but present higher virulence against macrophages (Chua *et al.*, 2014). Transcriptional profiling analysis of *P. aeruginosa* (Figure 2) and *Streptococcus pneumoniae* also defined dispersed cells as a unique state (Pettigrew *et al.*, 2014; Chua *et al.*, 2014). In the case of the dispersed cells of *P. aeruginosa*, the expression of the small regulatory RNAs is down-regulated, whereas secretion genes are induced.

Studies on *S. pneumoniae* revealed that genes involved in carbohydrate metabolism were upregulated in dispersed cells (Pettigrew *et al.*, 2014). Enzymatic measurements of ATP and lactate production in *S. pneumoniae* also showed that the metabolic activity of dispersed cells is higher compared to that of the biofilm and planktonic lifestyles (Pettigrew *et al.*, 2014). Such phenotypic adaptation might enable bacteria to actively escape the biofilm matrix. In this human pathogen, virulence factors were also overexpressed in biofilm-dispersed cells when compared to the planktonic or sessile states (Marks *et al.*, 2013). The dispersed cells of *S. pneumoniae* biofilms were shown to express virulence-specific genes, which allows them to invade and kill human respiratory epithelial cells more effectively and to induce high pro-inflammatory cytokine responses (Marks *et al.*, 2013). Considering the above data, it has been suggested that biofilm-related infections are the result of both the release of the bacterium from its biofilm and the enhanced virulence potencies of the dispersed cells.

Also in yeast, dispersed cells are transcriptionally distinct from the biofilm-associated cells. Dispersed cells from *Candida albicans* biofilms are reprogrammed to acquire specific nutrients and metabolize alternative carbon sources. Interestingly, these

dispersed cells also show enhanced virulence-associated gene expression, exhibiting greater adhesion, invasion, and biofilm formation compared to the planktonic cell state (Uppuluri *et al.*, 2018).
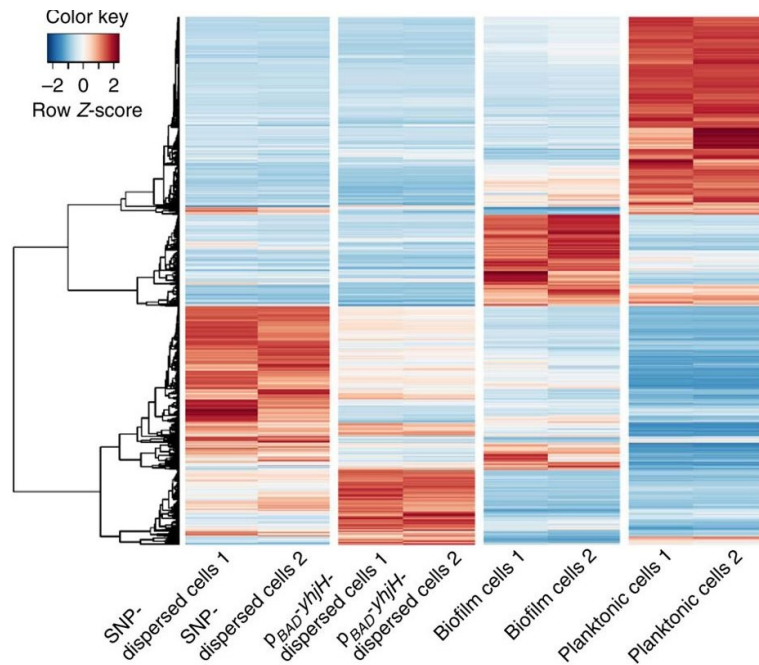
Figure 2. Hierarchical clustering analysis and heat map showing the differentially expressed genes specific to the dispersed cells of *P. aeruginosa* biofilms (induced by SNP and YhjH), biofilm cells and planktonic cells. Dispersal was induced by reduction of intracellular c-di-GMP using two methods: either chemically, by applying sodium nitroprusside (SNP), or enzymatically, by inducing the expression of a plasmid-encoded YhjH phosphodiesterase. Adapted from (Chua *et al.*, 2014).

Overall, biofilm-dispersed bacteria appear as a unique state in the bacterium's lifecycle, being transcriptionally and physiologically different from the other states. The highly regulated process of cell dispersal allows the release of bacteria with specific properties that make them fit for colonization of new niches. The astonishing ability to switch between planktonic, sessile and dispersal states provides plenteous solutions for the bacteria to adapt to a diverse range of environmental conditions.

Although dispersal of cells from a mature biofilm has been observed in many different bacteria, it is still a current challenge to identify all the players involved in this fascinating but also complex process. It is understandable that more than one signalling cascade/mechanism is needed to achieve the ultimate goal of freeing cells from a structure that has grown with the opposing purpose of keeping cells adhered to one another and/or to a substrate. Another question that remains to be answered is whether cells that are dispersed belong to a specific region or layer of the biofilms´ structure, before leaving this environmental niche, and if yes what are the features of those regions.

Some players within certain signal transduction cascades important for cell dispersal have been identified. However only very few effector proteins, among the aforementioned targets, were discovered so far. Additional research is required to understand the whole cascade, that is, from how environmental signals are detected by the cell to what signalling mechanisms are activated and subsequently, what effector targets are induced to ultimately lead to dispersal of cells.

1.2 Swarming motility

The ability to move on solid surfaces provides ecological advantages. Hence, many bacteria adapt varied methods to actively accomplish surface translocation, such as twitching, gliding, and swarming. Twitching motility uses type IV pili to pull the cells forward. This movement is powered by pilus retraction. This process involves the following steps: the pili first extends, then attaches to the surface and subsequently retracts, pulling the cell closer to the site of attachment (Harshey, 2003). In the case of gliding motility, there are no appendages or flagella and this translocation occurs along solid bodies or focal adhesion complexes. By using this mechanism, bacteria glide slowly over solid surfaces. Social bacteria such as myxobacteria use this type of motility to aggregate. *Myxococcus xanthus* uses both gliding and twitching motility, which are also called A and S motility respectively. In *M. xanthus*, gliding motile cells (A^-S^+) move best on firm surfaces (1.5% agar), whereas twitching motile cells (A^-S^+) moved best on relatively soft, wet surfaces (0.3% agar) (Mauriello *et al.*, 2010). Another major locomotion system used by bacteria to move over substrates is swarming motility (J Henrichsen, 1972).
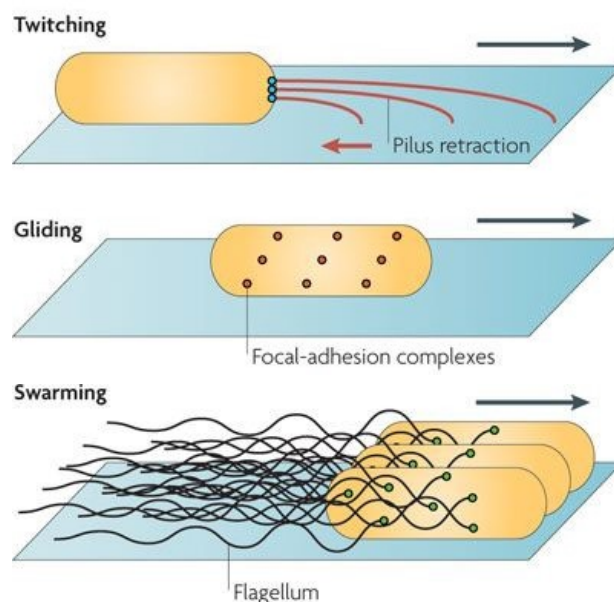
Figure 3. Different bacterial strategies for active surface translocation. Twitching motility is powered by pilus retraction. Gliding is a surface movement that does not require flagella or pili and involves focal-adhesion complexes. Swarming is a multicellular movement and is powered by rotating helical flagella. Adapted from (Kearns, 2010).

Swarming motility is a flagella-based motility and is used for fast migration over surfaces. It involves a differentiation process that results in an elongated and highly flagellated swarmer cell (Copeland & Weibel, 2009, Figure 3). In swarming, the movement of the microorganisms is achieved by rotation of the flagella. Swarming is often marked by numerous cells moving in a coordinated fashion while generating whirl and jet patterns, where cells move in circular and straight patterns, respectively (Rauprich *et al.*, 1996; Ingham and Jacob, 2008; Be'er *et al.*, 2013; Jeckel *et al.*, 2019). This process may provide a survival advantage, allowing bacteria to rapidly colonize a specific environment such as host tissues, thereby competing successfully with other microorganisms (Merino *et al.*, 2006). Swarming phenomena can also generate "moving ecosystems", as some swarms have been shown to transport other non-motile bacteria, with mutual benefits (Venturi *et al.*, 2010; Zhou *et al.*, 2011; Finkelshtein *et al.*, 2015). Swarming motility is represented by bacteria from three families so far: alpha-, gama-proteobacteria and firmicutes (Kearns, 2010). Swarming colonies can present diverse macroscopic patterns (Figure 4). Cell density, cell aspect ratio and cell rigidity, flagellar density, flagellar propulsion power and activity, interactions between flagella of adjutant cells and the ability to secrete biosurfactant are all factors that contribute to the formation of different swarming patterns (Ben-Jacob *et al.*, 1994; Gygi *et al.*, 1995; Tuson *et al.*, 2013; Ilkanaiv *et al.*, 2017; Hall *et al.*, 2018; Jeckel *et al.*, 2019). In addition, many environmental conditions can also greatly impact swarming, including temperature, nutrients, humidity, nearby interacting colonies, agar rigidity and stresses such as oxygen availability and presence of antimicrobial agents (Be'er *et al.*, 2009a; Be'er *et al.*, 2009b; Kamatkar and Shrout, 2011; Sokolov and Aranson, 2012; Benisty *et al.*, 2015).

Among the different swarmer species, only a limited number of bacteria express two entirely distinct flagella systems: a polar flagellum (used for swimming) and lateral flagella (for swarming). These organisms include *Vibrio parahaemolyticus, Vibrio alginolyticus*, *Aeromonas* spp., *Azospirillum brasilense*, *Rhodospirillum centenum*, *Helicobacter mustelae* and *Plesiomonas shigelloides* (Merino *et al.*, 2006). Other swarming species use either multiple polar flagella (as in the case of *P. aeruginosa*) or multiple petrichous flagella (as in the case of *E. coli*) (Rashid and Kornberg, 2000).

Swarming bacteria can be divided into two categories: robust swarmers, which can navigate across a hard agar surface (1.5% agar and above), and temperate swarmers, which can swarm only on a softer agar surface (0.5 to 0.8% agar). Both levels of hyperflagelation and elongation of a swarmer cell-type vary among species (Copeland

and Weibel, 2009). Robust swarmers include *Rhodospirillum* (McClain *et al.*, 2002), some *Vibrio* species (Ulitzur, 1974; Böttcher *et al.*, 2016) and *Proteus* species (Pearson *et al.*, 2010).

E. coli (Harshey and Matsuyama, 2006), *Bacillus* (Kearns and Losick, 2003), *Pseudomonas* (Rashid and Kornberg, 2000), *Rhizobium* (Tambalo *et al.*, 2010), *Salmonella* (Harshey and Matsuyama, 2006), *Serratia* (O'Rear *et al.*, 1992), and *Yersinia* species (Atkinson *et al.*, 2006) are temperate swarmers.

E. coli K12 (Harshey and Matsuyama, 2006), *P. aeruginosa* (Rashid and Kornberg, 2000), *Salmonella typhimurium* (Harshey and Matsuyama, 2006) and *Serratia liquefaciens* (Eberl *et al.*, 1996) show a 2 to 3 fold increase in flagella density, relative to planktonic cells. Cell lengths of *P. aeruginosa* and *B. subtilis* change from 1-2 µm to 2-3 or 3-6 µm in swarmer cell type, respectively (Rashid and Kornberg, 2000; Kearns and Losick, 2003).
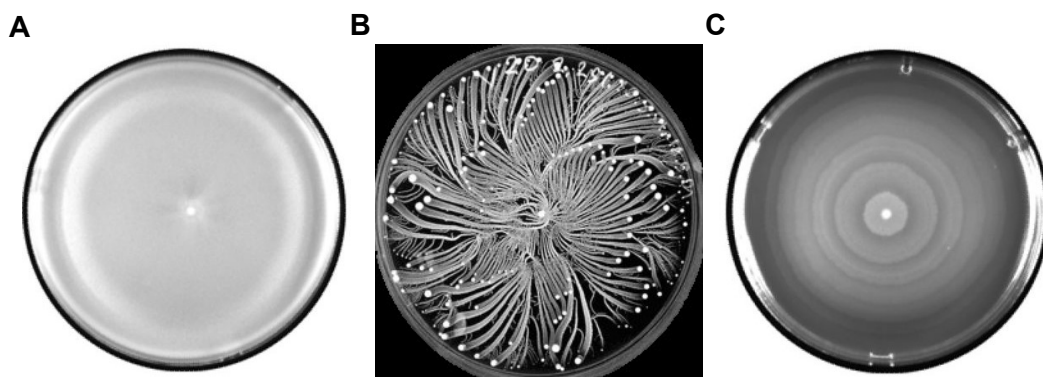
Figure 4. Diverse colony patterns formed by swarming bacteria. Uncolonized agar is black and bacterial biomass is white. A) *Bacillus subtilis* 3610: Featureless, B) *Paenibacillus vortex:* Vortex pattern. Each vortex (the bright dots) is composed of many cells that swarm collectively around their common center. C) *Proteus mirabilis* PM7002: Bull's eye pattern with periodic phases between swimmer cells (consolidate phase) and swarmer cells. Adapted from (Kearns, 2010).

The higher flagellar numbers in temperate swarmers allows them to swarm on harder agar and the increased flagella production in robust swarmers allows them to swim through a more viscous medium (Tuson *et al.*, 2013). Thus, one may infer that the higher flagellar numbers in robust swarmers function to provide more drive for moving on this surface. Moreover, an increase in cell size seems to be important for robust swarming. For instance, in the case of *Proteus mirabilis*, it was shown that the harder the surface, the more elongated the cells become (Little *et al.*, 2019).

The fact that so many bacterial species display this form of motility in the laboratory, and therefore possess mechanisms to overcome surface barriers, argues that swarming must be an important tactic to invade more territories in bacteria's natural habitats.

1.2.1 Gram-positive swarming bacteria

1.2.1.1 *Paenibacillus*

Species within the *Paenibacillus* genus comprise of Gram-positive, spore-forming facultative aerobes that were previously classified as *Bacillus* species. Some *Paenibacillus* species such as *Paenibacillus alvei*, *Paenibacillus denditiformis* and *Paenibacillus vortex*, exhibit complex patterns of collective migration behaviour (Cohen *et al.*, 2000; Ingham and Jacob, 2008; Be'er *et al.*, 2009a).

P. alvei and *P. dendritiformis* can move on semi-solid surfaces by producing a layer of lubricating fluid that enables movement on hard surfaces. Under different growth conditions, *P. alvei* develops distinct branching patterns (Cohen *et al.*, 2000). *P. dendritiformis* also forms different patterns, which are named accordingly to specific properties of colonial development. The categories include morphotype T (tip-splitting), morphotype C (chiral) and morphotype V (vortex) (Ben-Jacob *et al.*, 2002).

In liquid medium, *P. dendritiformis* possesses a single bundle of four flagella, located at one pole. The C morphotype of *P. dendritiformis* is formed by very long and rigid rods, that range from 5 µm to 40 µm in length. Each cell consists of many peritrichous flagella, which are uniformly distributed (Be'er *et al.*, 2013).
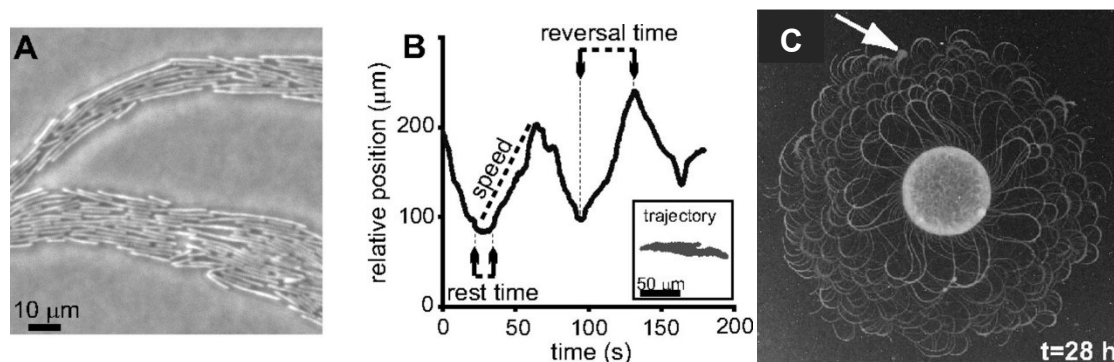
Figure 5. Swarming of *P. dendritiformis*, morphotype C. A) Microscopic picture of the outer parts of a colony. The cells form a monolayer in which roughly 10 bacteria lay one next to the other. Bacterial length distribution is broad-from 5 to 40 µm. B) Relative position of a single cell in a colony as a function of time. Reversal time is defined as the time between the point at which the bacterium begins moving and the point at which it stops changing direction. A trajectory of the bacterium is shown in the inset. C) Picture of swarm colony after 28h, of C morphotype. Growth conditions are 2 g/liter peptone, 1% (wt/vol) Difco agar, 30°C. The arrow indicates a small region of cells that spontaneously switched to morphotype T, exhibiting whirl and jet swarming patterns at the microscopic level. Adapted from (Be'er *et al.*, 2013).

Instead of the standard dynamic patterns of whirls and jets, observed in shorter species such as *B. subtilis* and, also in the shorter morphotype of *P. dendritiformis* (morphotype T), *P. dendritiformis* morphotype C forms long tracks in which individual bacteria repeatedly move back and forth along moderately curved lines (Figure 5A-B). Observed reversals present a typical time of around 20 s and seem to be spontaneous and independent of their neighbours, initial nutrient level, agar rigidity, surfactant additions, cell length, humidity level, temperature, food chemotaxis, and oxygen level (Be'er *et al.*, 2013). This observed autonomy of reversal times suggests a robust internal clock for reversal events. However, reversal periodicity is not correlated to colony expansion (Be'er *et al.*, 2013). Therefore, the evolutionary advantage of this unique back-and-forth swarming pattern remains unclear.

In *P. dendritiformis* type T, multiscale measurements for a variety of growth conditions have revealed that motion on the microscopic scale and colonial growth are largely independent. Increased microscopic bacterial motion (that is, increased average speed and increased collective motion in the whirls and jets) does not generally lead to an increase in the growth rate of a bacterial colony, at least in the case of *P. dendritiformis*. Instead, the growth of the colony is strongly affected by surfactant production, as increasing the surfactant concentration resulted in an increase in the colony growth speed, but had little effect on bacterial motion and speed (Be'er *et al.*, 2009a).

P. vortex swarming occurs on an extremely wide range of media and agar concentrations (0.3 to 2.2% w/v). Its name comes from the fact that at concentrations of agar above 1% (w/v), aggregates of hundreds to thousands of cells are able to detach from the central mass of cells to form rotating groups (vortices) (Ben-Jacob *et al.*, 1997) (Figure 5C). *P. vortex* cells in the vortices move outward as a unit, leaving behind a trail of motile but usually non-replicating cells – the vortex branch. The vortices vary in size, according to their location in the colony. The dynamics of the vortices is quite complicated and includes attraction, repulsion, merging and splitting of vortices. Cell shape, flagellation, the aversion of cell masses to fuse and temporary connections between proximate cells to form rafts are all features of this swarming pattern and also, play a role in rotation of the cell aggregates (Ingham and Jacob, 2008). Interestingly, in liquid growth, *P. vortex* cells lose both flagella and motility. Within a swarming population, elongated cells represent a consistently small fraction. At 37°C, 5% of the cells were above 16 µm long. Cell length increased dramatically with growth on agar at 42°C, where

33% of the population were above 16 µm long. All cells were hyperflagellated, presenting between 2 to 8 flagella per µm of cell length. When viewed by scanning electron microscopy, the flagella did not form helical bundles but rather they showed a tendency to entangle or associate with those of neighbouring cells. Similarly, swarming of *Aeromonas* spp. is characterized by lateral, entangling flagella that are important for rafting (Kirov *et al.*, 2002). The loose nature of the contacts could allow a dual role for flagella in motility and rafting, maintaining the cohesion of the mass but permitting a degree of rearrangement including the characteristic vortex motion.

1.2.1.2 *Bacillus subtilis*

Undomesticated strains of *B. subtilis*, but not laboratory strains, exhibit swarming motility on solid surfaces. The failure of laboratory strains to swarm is caused by a mutation in *sfp*, a gene involved in the synthesis of a lipopeptide surfactant, and another mutation that disrupts the putative master regulator of flagellar synthesis, *swrA* (Patrick and Kearns, 2009).

While the swarming motility in other Gram-positive bacteria such as *P. dendritiformis*, *Bacillus thuringiensis* and *Clostridium septicum* is associated with cells becoming very elongated and multinucleated, motile migrating cells of *B. subtilis* show a very slight increase in cell length when compared to swimmer cells (Kearns and Losick, 2003). Swarmer cells of *B. subtilis* have two nucleoids that appear unusually compact and well segregated, apparently in the absence of active cell division. The most noticeable morphological difference exhibited by this cell type is significantly enhanced flagellation.

Rafting appears to be necessary for surface movement as isolated cells were immobile but rapidly became motile when they joined a raft (Kearns and Losick, 2003). The edge of the swarm consisted of a narrow edge of poorly motile cells driven forward by vigorously motile cells behind the front (Kearns and Losick, 2003; Jeckel *et al.*, 2019).

During swarming development, while multicellular rafts of single hyperflagellated cells characterize the leading edge of the swarm, the center of the colony is enriched with long, unseparated chains of cells. Although there are also single cells present in the center, these are smaller and their nucleoids are less compact than the cells present in the swarm edge. Not only the cells in chains lacked flagella, but also many single cells

within the swarm centre were found to be aflagellated (Kearns and Losick, 2003). This suggests that as the swarm expands, a second internal population emerges that is non-motile and physiologically distinct from the highly motile progressive swarm edge. *B. subtilis* mutants that tumbled constitutively in liquid medium were severely impaired in both chemotaxis and surface motility (Kearns and Losick, 2003). As swarming involves the formation of rafts of cells, a simple explanation for the effects of these mutations could be that the increased tumbling of the cells interferes with the formation of stable rafts.

A long initial lag phase in which the swarm does not migrate outward for several hours is followed by an abrupt transition to an exponential expansion phase. (Kearns and Losick, 2003). An increase in surfactin production occurs just before the expansion phase (Jeckel *et al.*, 2019). However, addition of purified surfactin *per se*, is not enough to eliminate or even reduce the lag phase (Kearns and Losick, 2003). As swarming is associated with a dramatic increase in the density of flagella, the time required for flagellum production could contribute to the lag phase. Indeed transcription of the gene that encodes for flagellin monomer protein, *hag* strongly increases before the transition to the expansion phase (Jeckel et al., 2019). Overall, one can conclude that cell-density dependent physiological changes, such as surfactin and flagella production, are important to drive the transition to the expansion phase.

A recent study examines the microscopic dynamics of *B. subtilis* swarming using machine learning and as a result, five different swarming phases were determined (Figure 6A) (Jeckel et al., 2019). A single-cell phase (SC) characterized by low cell densities and little collective behaviour, a rafting phase (R) exhibiting high fractions of co-moving cells, and a biofilm phase (B) where cells are organized in non-motile structures, are the three pure phases. The two coexistence phases are a mixture of single-cell and rafting behaviour (SC + R), as well as a mixture of rafts and biofilm precursors (R + BP), which differ qualitatively and quantitatively from the pure phases (Figure 6B-C). By combining these experiments and particle-based active matter modelling with machine learning, this work revealed that hydrodynamic interactions are not a dominant effect, but rather steric interactions and motility are sufficient for explaining the observed dynamics within each phase (Jeckel et al., 2019).
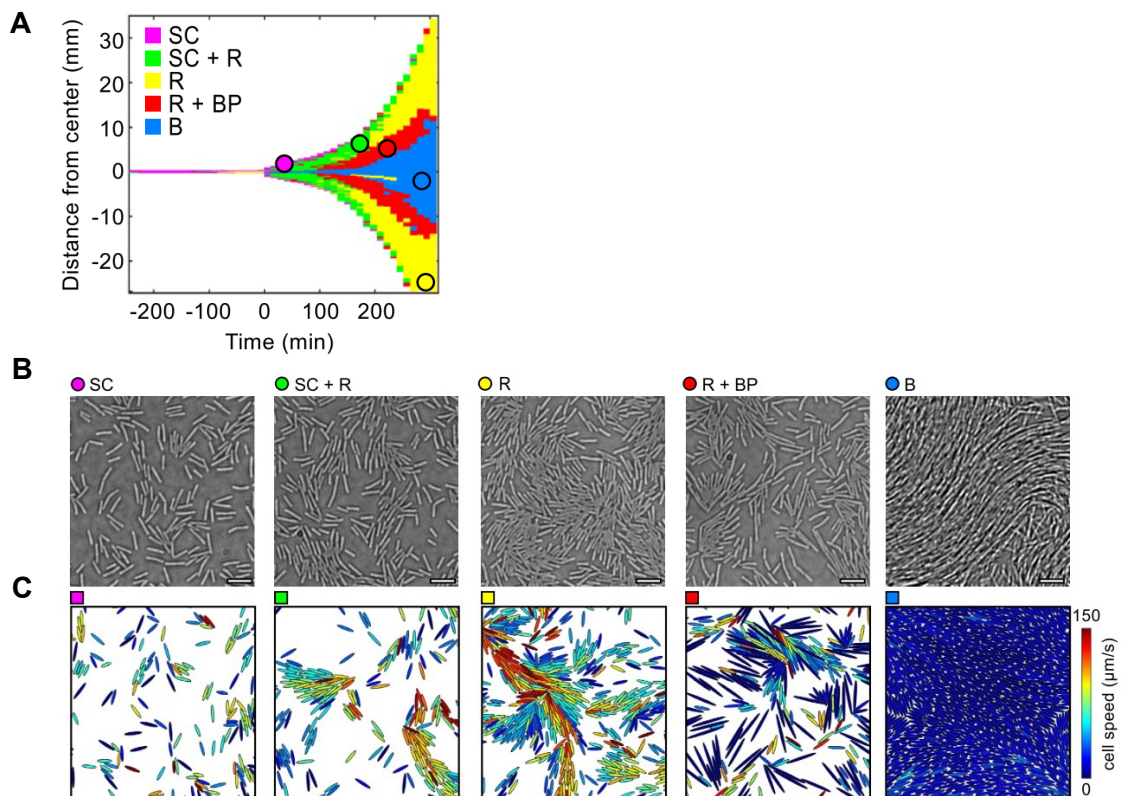
Figure 6. Different swarming phases from microscopic dynamics using machine learning. (*A*) The emergence of the different phases in time and space during swarm expansion using machine learning analyses. (*B*) Typical images for the phases identified in *A*: low-density single-cell phase (SC); high-density rafting phase (R) with a high percentage of co-moving cells; biofilm phase (B) characterized by long, unseparated cells; and coexistence phases that contain single cells and rafts (SC + R) or rafts and biofilm precursors (R + BP). (*C*) For each phase, simulations were run with the cell shape, motility, and density extracted from the particular phase as input parameters. Adapted from (Jeckel et al., 2019).

As already mentioned, swarming motility requires the production of the extracellular lipopeptide surfactant and flagellum biosynthesis. Therefore, several genes that directly or indirectly influence the presence of these components were shown to be essential for swarming (Kearns and Losick, 2003; Kearns *et al.*, 2004; Guttenplan *et al.*, 2013). These include, for instance, genes in the surfactin synthesis operon: *srfAA, srfAB, srfAC*. Flagellin mutant cells (Δ*hag* null deletion) were deficient in swimming and swarming, suggesting that the same flagellum drives both types of motility. Although neither the Δ*hag* mutant nor the Δ*srfAA* mutant could swarm separately, cells from a mixture of the two mutants were swarming proficient (Kearns and Losick, 2003). Four genes that were also found to have a role in swarming are *swrA, swrB, swrC* and *swrD*. SwrA is a transcriptional activator and its function is essential for swarming because it was found to determine the number of flagella in *B. subtilis* cells (Kearns and Losick, 2005; Guttenplan *et al.*, 2013). Mutation of *swrB* led to a reduction of late class flagellar

gene expression but the mechanism of its function is unknown. SwrC is an export pump that was found to contribute to the secretion of endogenously produced surfactin, and in a Δ*swrC* mutant, this intracellular accumulation was found to interfere with surface motility (Kearns *et al.*, 2004). Cells mutated for *swrD* were seem to move with reduced speed and all *swrD*-related phenotypes were restored when the stator subunits MotA and MotB were overexpressed. This data shows that SwrD is necessary for swarming because of its role in increasing flagellar torque (Hall *et al.*, 2018).

Translational regulation may also play a role in establishing the swarming state, as disruption of the gene *efp*, which is predicted to encode the elongation factor P (EF-P) was shown to abolish swarming (Kearns *et al.*, 2004). Furthermore, elevation of c-di-GMP levels in *B. subtilis* led to inhibition of swarming motility and it was shown to require the c-di-GMP receptor DgrA (Gao *et al.*, 2013). ATP-dependent proteases, ClpY-ClpQ, also contribute to regulation of *B. subtilis* swarming and swimming. The activity of these proteases was cumulative as the double mutant showed a much stronger defect swarming and swimming motility than the single mutants (Yu *et al.*, 2018). Sigma factor D, SigD, controls the expression of several motility-related genes, and proteomics results show that translation of many of these genes is reduced in a *clpYQ* deletion mutant. Therefore, the strongly reduced motility could possibly be due to reduced activities of SigD (Kearns and Losick, 2005).

To test the role of cell aspect ratio on bacterial swarming, several variants of *B. subtilis* differing only in aspect ratios (width/length) were compared. These experiments showed that the fastest motion was obtained for the wild-type and mutant cells of similar aspect ratios. This study demonstrated that the observed aspect ratio of 4.9 in wild-type cells of *B. subtilis* is optimal as it precisely allows for Gaussian statistics and effective swarming (Ilkanaiv *et al.*, 2017). Robust mechanisms to maintain aspect ratios may be important for efficient swarming motility. In agreement with the above presented data, deletion of the cell division gene *minJ*, which leads to the formation of longer cells, appears to be detrimental to swarming motility in *B. subtillis*. Instead of the classic spreading pattern formed by the wild-type, the mutant forms spiraling whirls on the surface of the medium (Patrick and Kearns, 2008).

Lévy walks are seen in dynamic organizations such as birds and fish and are characterized by trajectories composed of clusters of multiple short steps with longer

steps between them (Miramontes *et al.*, 2012; Humphries and Sims, 2014; Murakami *et al.*, 2015; Ariel *et al.*, 2017) . This type of motion is an optimized way to search for sparsely and randomly distributed targets in the absence of memory (Humphries and Sims, 2014; Ariel *et al.*, 2015). By tracking trajectories of fluorescently labelled bacteria within a *B. subtilis* swarm (and a *Serratia marcescens* swarm), it was shown that these bacteria perform super-diffusion, consistent with Lévy walks (Ariel *et al.*, 2015). It is possible that swarming bacteria use this random type of walk as a search strategy. If so, this mechanism would justify the high-energy cost required to maintain the swirling in the swarm, as it would help overcome the threat of death from starvation or environmental hazards.

1.2.2 Gram-negative swarming bacteria

There are Gram-negative bacteria that can swarm not only in soft agar (0.3-0.6%) such as *Rhizobium* (Tambalo *et al.*, 2010), *Salmonella* (Harshey and Matsuyama, 2006), *Azospirillum brasiliens* (Hall and Krieg, 2010)*, Serratia* (O'Rear *et al.*, 1992), and *Yersinia enterocolitica* (Atkinson *et al.*, 2006) but also in hard agar (0.8-2% agar)*,* such as *R. centenum* (McClain *et al.*, 2002)*, P. mirabilis* (Rauprich *et al.*, 1996)*, V. alginolyticus* (Böttcher *et al.*, 2016) and *V. parahaemolyticus* (Ulitzur, 1974)*.* The swarming motility of *P. mirabilis* and *V. alginolyticus*, two Gram-negative bacteria that can perform robust swarming in hard agar, will be described next.

1.2.2.1 *Proteus mirabilis*

P. mirabilis is a Gram-negative bacterium and a member of the family, Enterobacteriaceae. *P. mirabilis* can be found in soil, water and the intestinal tract of many mammals (Allison *et al.*, 1994). This bacterium causes a variety of human infections and is primarily associated with urinary-tract infections (Allison *et al.*, 1994; Mobley and Belas, 1995). In liquid culture, *P. mirabilis* cells are rod shaped, 2 µm in length and petrichously flagellated. Upon contact with a solid surface, swarmer cell differentiation is initiated by the inhibition of flagellar rotation and by cell–cell signalling. *P. mirabilis* differentiated swarmer cells are multinucleated, 20 to 50 fold elongated and express numerous flagella, representing the swarm-bacterium with the most striking morphological phenotype described so far (Copeland and Weibel, 2009). *P. mirabilis* is motile on high agar concentrations (1.5–2%), and unlike the straight *B. subtilis* cells, *P. mirabilis* cells are curved and bent during swarming (Rauprich *et al.*, 1996).

1.2.2.1.1 Bull´s eye pattern - consolidation-phase and swarm-phase

The swarming phenotype associated with this human pathogen shows a distinct periodicity between differentiation into swarmer cells followed by de-differentiation to swimmer cells in a process called consolidation (Fraser and Hughes, 1999). The cycle repeats multiple times and results in the characteristic concentric rings of growth seen on agar plates forming colonies that have a characteristic bull's eye appearance (Figure 4C). Higher agar concentrations leads to slower, shorter swarm phases and longer consolidation phases (Rauprich *et al.*, 1996).

Direct comparison of swarmer cells to consolidation-phase cells found that 541 genes were upregulated in the consolidated cells, but only nine genes were upregulated in swarmer cells (Pearson *et al.*, 2010). The consolidation phase appears to represent a time of preparation for the next phase of swarming, marked by the upregulation of nutrient uptake systems, central metabolism (TCA cycle, gluconeogenesis, and glycerol metabolism), respiration, cell wall synthetic enzymes and cell division proteins, such as MinC (4.61-fold increase) and MinD (2.36-fold increase) (Pearson *et al.*, 2010). An excess of MinCD can prevent cell division, thereby being a possible cause for the filamentation phenotype (Pearson *et al.*, 2010). These data suggest that the consolidation phase is a state in which *P. mirabilis* prepares for the next wave of swarming.

1.2.1.1.2 Environmental conditions that influence swarming

Swarmer cells of *P. mirabilis* contribute to the establishment of infection by migrating along the catheter (Mobley and Belas, 1995; Jones *et al.*, 2004). The decision to swarm appears to be influenced by the metabolic status of the cell and by the presence of specific amino acids, such as glutamine and histidine, which are two of the most concentrated amino acids in normal human urine (Mobley and Belas, 1995).

1.2.1.1.3 Importance of flagella and elongation for swarming motility

The elongated swarmer cells align themselves in multicellular rafts and are encased in an extracellular slime that facilitates movement (Stahl *et al.*, 1983). The flagellar filaments of *P. mirabilis* were found to be highly organized during raft migration and were interlaced in phase to form helical connections between adjacent swarmer cells. Mutants lacking these organized structures failed to swarm successfully, indicating that these structures are important for migration and formation of multicellular rafts (Jones *et al.*, 2004). There is still no clear explanation for the importance of elongation during swarming, especially for bacteria with a length/width ratio that is higher than 5. However, cell elongation is intimately connected to swarming response as *P. mirabilis* mutants defective in cell elongation show dramatically reduced swarming (and not swimming) motility (Belas *et al.*, 1995). In addition, under agar concentrations ranging from 0.75% to 2.5%, the length of swarmer cells was found to increase with increasing agar concentration, suggesting that elongation might aid cell motion on solid surfaces. However, elongation, *per se* is not sufficient to allow bacteria to swarm since on surfaces

where the concentration of agar is higher than 2.5%, although cells were found to elongate, they were not motile (Little *et al.*, 2019).

Experimental work on *P. mirabilis* in viscous fluids suggests that increase in surface density of flagella translates into a fast movement of cells through fluids of increasing viscosity. These results suggest that an increase in flagellum density is important for *P. mirabilis* motility in viscous fluids (Tuson *et al.*, 2013).

1.2.1.1.4 Genetic factors involved in *P.mirabilis* swarming

As expected for such a complex process, the ability to swarm is dependent on a large number of genes. Artificial overexpression of *flhDC*, the flagellar master regulatory operon led to premature differentiation, resulting in elongated swarmer cells, hyperflagellation and enhanced velocity during swarming (Furness *et al.*, 1997). The leucine-responsive protein, Lrp is a global regulator that according to amino acid availability performs diverse functions, including amino acid biosynthesis and degradation, peptide transport and pilin synthesis (Hart and Blumenthal, 2011). An *lrp* mutant was not able to swarm but overexpression of *flhDC* restores the swarming defect in this mutant. Therefore, Lrp is proposed to transmit signals for swarming through the *flhDC* operon (Hay *et al.*, 1997).

The *ppa* gene (Proteus p-type ATPase) encodes a putative P-type cation-transporting membrane ATPase. Such a mutant was impaired in swarmer cell differentiation and showed delayed migration of swarming. The fact that levels of *flhDC* and *lrp* transcripts are lower in *ppa* mutants might explain the reduction observed in differentiation to swarmer cells. This way, ion homeostasis might influence bacterial swarming differentiation (Lai *et al.*, 1998).

Null alleles in either *speA* or *speB* in *P. mirabilis* also resulted in a severe delay in swarmer cell differentiation (Sturgill and Rather, 2004). This delay results from the failure to produce the polyamine, putrescine. Addition of exogenous putrescine restored the normal timing of swarmer cell differentiation to both Δ*speA* and Δ*speB* mutants. Although there are no tested evidences, putrescine may act in a cell-to-cell signalling pathway that triggers swarmer cell differentiation at the appropriate cell density.

P. mirabilis swarmer differentiation might be induced via surface sensing in a so-called mechanosensing mechanism. In this case, mutations in flagellar structural proteins would mimic the scenario of a cell encountering a solid surface and so the mutant would differentiate even in liquid environments. (Cusick *et al.*, 2012). Indeed, mutations in *fliL*, a gene encoding for a flagellar structural protein, resulted in the production of differentiated swarmer cells under non-inducing conditions. Additionally, through transposon mutagenesis studies, many flagellar gene mutants were also found to have an elongation phenotype, which again might support the mechanosensing mechanism hypothesis (Belas *et al.*, 1991).

P. mirabilis is a social bacterium that is capable of self versus non-self recognition. Colonies of genetically distinct populations remain separate, while those of identical populations merge. Cell-cell communication is achieved via an identity-encoding protein (LdsD) that is exported, in a Type VI secretion system-dependent manner, from one cell and received by another. In the recipient cells, lack of interaction between LdsD with LdsE, a protein predicted to be an integral inner membrane protein, restricted swarm colony expansion but not viability. Although this intercellular exchange is not lethal, it does affect swarm colony expansion, indicating that social communication is important for regulation of swarming (Saak and Gibbs, 2016).

1.2.2.2 *Vibrio species*

Vibrio is a genus of Gram-negative bacteria and the species belonging to this genus possess a curved-rod shape (Thompson *et al.*, 2009). Typically found in salty waters, several species can cause foodborne infections (Newton *et al.*, 2012). All members of this genus are motile and have polar flagella with sheaths (McCarter, 2003). Some species such as *V. alginolyticus* and *V. parahaemolyticus* use a single polar flagellum for swimming motility in liquid medium, but on solid surfaces, they differentiate into elongated swarmer cells with multiple lateral flagella (McCarter and Silverman, 1990; Böttcher *et al.*, 2016). These two *Vibrio* species are robust swarmers, as they can swarm under surfaces with agar concentrations that are higher than 1% (McCarter, 2004; Böttcher *et al.*, 2016). Both species are among the most frequently encountered marine bacteria and can cause disease in marine animals and humans (Ma *et al.*, 2013; Mustapha *et al.*, 2013). In the latter, this specially occurs through food poisoning and wound infections (Di *et al.*, 2017). As *V. parahaemolyticus* will be the organism of study

in this doctoral work, the swarming motility of this bacterium will be presented in more detail later on, in a separate section. *V. alginolyticus* swarming will be described next.

1.2.2.2.1 *Vibrio alginolyticus*

Unlike the relatively stiff, rod-shaped swarmer cells of *B. subtilis*, *E. coli*, and *P. dendritiformis*, *V. alginolyticus* swarmer cells are highly flexible, and move in a snake-like fashion (Harshey and Partridge, 2015; Böttcher *et al.*, 2016).

The development of peritrichous flagella of *V. alginolyticus* depends on temperature and salt concentrations. At temperatures above 28ºC, *V. alginolyticus* did not develop peritrichous flagella unless minimal concentrations of NaCl were present, that is, the higher the temperature, the higher the NaCl concentration were required for peritrichous flagella synthesis (Ulitzur, 1975). By-products at certain concentrations accumulating in the colony area also induced flagella differentiation and swarming. These natural metabolic by-products are suggested to be volatile acids belonging to the valine and isoleucine pathway (Ulitzer, 1975).

One study reported temporal analysis on the highly flexible swarm cell type of *V. alginolyticus* in a strain isolated from a sample of red seaweed, namely *B522*. Carrageenan was used as an agar substitute to mimic the natural seaweed substrate, and *V. alginolyticus* exhibited vigorous swarming behaviour. The temporal variance analysis of the swarm revealed long-range coherence of bacterial motion that resulted in pattern formation with jets, swirls, and distinct areas with alternating high- and low-motion activities. In particular, the temporal analysis show that the surface monolayer consisted of three phases: 1) a rapidly swarming monolayer close to the swarming front; 2) a sharp decrease in velocity of cell motion within the first hundred microns from the swarming front; and 3) a recovery to the initial speed when swarmer cells begin occupying additional layers underneath the original monolayer (Böttcher and Clardy, 2014).

Although decrease of motion with distance from the front is usually observed, *V. alginolyticus* exhibits an additional phase showing recovery of the initial motility that has not been previously reported in swarming bacteria. This recovery phase originates from the cells starting to explore and occupy additional layers underneath the original surface monolayer.
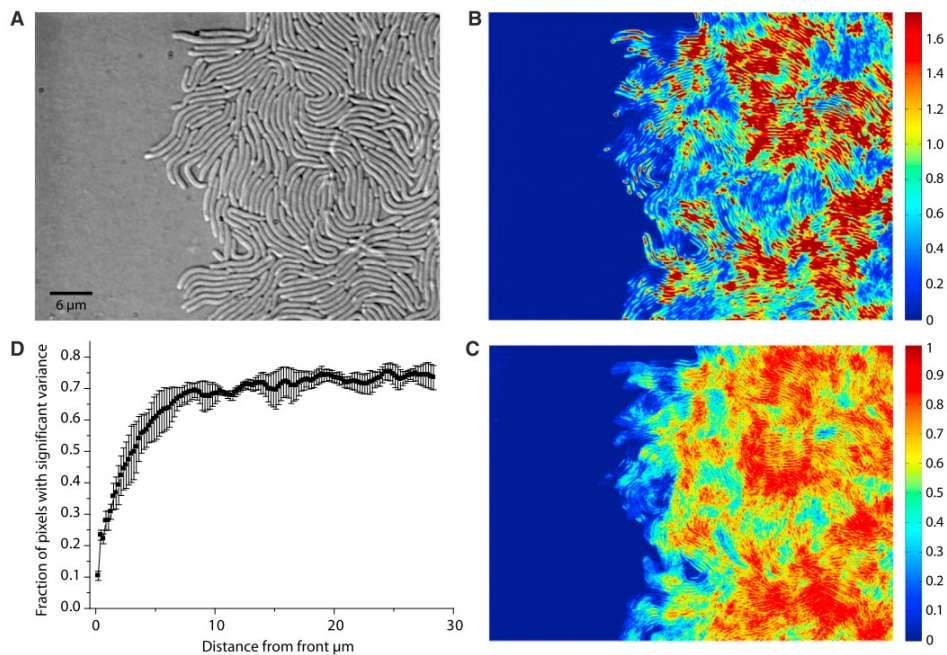
Figure 7. Motion analysis of the swarming front. A) Phase-contrast image of the swarming front. B) Whole-image-series temporal variance analysis indicates patches of different intense motion activity: high variance (red) and low variance (blue). C) The fraction of time with significant variance analysis reveals decreasing motion toward the swarming front: large fraction of time with significant variance (red) and small fraction of time with significant variance (blue). (D) The fraction of pixels with significant variance is plotted against the distance from the front, averaged from three independent replicates. Adapted from (Böttcher *et al.*, 2016).

The areas distant from the front showed a high degree of motion whereas the cells directly adjacent to the front showed less activity (Figure 7). The fact that *V. alginolyticus* cells directly at the swarming front were largely stalled are in line with earlier observations for *E. coli*, *B. subtilis* and *P. dendritiformis* (Be'er *et al.*, 2009a; Jeckel *et al.*, 2019). Therefore, this sharp decrease in bacterial motion at the swarming front may be a universal property of swarms. As the cells at the front may need to pump fluid outward to wet the agar to support swarm expansion, this may be a reason for the lower-motion activity at the swarming front.

1.3 *Vibrio parahaemolyticus* as model organism

In this thesis work, *V. parahaemolyticus* was employed as the model organism to study the architecture of a swarm colony and understand its influence on bacterial dissemination in the environment. Furthermore, this microorganism was used to analyze distinct proteomic landscapes according to different environments. Hence, an overview of this bacterium and its ecology, as well as, a detailed insight on its swarming differentiation process will follow.

V. parahaemolytycus is a Gram-negative motile bacterium that inhabits marine and estuarine environments throughout the world. It is also a human pathogen that can cause acute gastroenterites, after consumption of raw or undercooked contaminated seafood. Historically, *V. parahaemolyticus* was first isolated in 1950 from a major food poisoning outbreak traced to ingestion of "Shirasu" (partially boiled juvenile sardines) (Fujino, T et al., 1951).

To date, genomes of six strains of *V. parahaemolyticus* from different serotypes have been sequenced. The first fully sequenced and annotated genome strain RIMD221063 has been used as the reference sequence for analysis of numerous clinical and environmental *V. parahaemolyticus* strains (Makino et al., 2003). Once sequenced, the *V. parahaemolyticus* genome was compared with a genome from another diarrhoea-causing *Vibrio* species, namely *V. cholerae*. The results suggest these organisms use distinct mechanisms to establish infection. Genes for the type III secretion system (TIIISS) were present only in the *V. parahaemolyticus* genome. This explains the clinical features of *V. parahaemolyticus* infections, which commonly include inflammatory diarrhoea and in some cases, systemic manifestations, distinct from those of *V. cholerae* infections, which are generally associated with non-inflammatory diarrhoea (Makino et al., 2003).

To ensure its survival in varying environments, *V. parahaemolyticus* has two different types of flagellar systems, allowing it to adapt to constantly changing external conditions. A polar flagellum is required for swimming in liquid conditions and a lateral flagellum is used for swarm movement on solid surfaces.

The worldwide prevalence and distribution of gastroenteritis cases caused by *V. parahaemolyticus* emphasizes the need for understanding how this bacterium spreads in the environment and how its distinct life cycle influence its ecological dissemination.

1.3.1 Ecology of *Vibrio parahaemolyticus*

Vibrio species are widely distributed in warm estuarine and coastal environments, and they can infect humans through the consumption of raw and mishandled contaminated seafood. *V. parahaemolyticus* is a major food-borne pathogen worldwide and the U.S. Food and Drug Administration estimates infections caused by this organism at approximately 4,500 per year only in U.S.A. (FDA 2005). Over the past 15 years, outbreaks have been increasing in size and frequency. The most common symptoms of infection include gastroenteritis, acute diarrheal infection, headache, nausea and vomiting. *V. parahaemolyticus* infections are also disseminated through open wounds and in severe cases, can cause septicemia, which can be life threatening, specially for persons with a compromised immune system (Letchumanan *et al.*, 2014).

Although the mechanism underlying human infection by *V. parahaemolyticus* is not completely understood, there are two hemolysins that are commonly recognized as pathogenicity indicators: thermostable direct hemolysin (TDH) and TDH-related hemolysin (TRH). These proteins are involved in bacterium invasion by forming pores on the cells and cause a nonspecific efflux of divalent cations and influx of water molecules (Wang *et al.*, 2015). Most of the clinical isolates of *V. parahaemolyticus* possess *tdh* and/or *trh*. In many studies, a relatively low number of environmental isolates were found to carry these virulent genes, but this is somehow controversial. While some studies show percentages of detection of the *tdh* and *trh* genes as low as 4.3% and 0.3%, respectively (in South Carolina and Georgia coasts), analyses from intensive shrimp mariculture sites on the Pacific coast of Mexico revealed that 52% of environmental strains carry *tdh* and/or *trh* (Velazquez-Roman *et al.*, 2012). Detection of *tdh* at high rates has also been reported in the case of environmental strains found in the Pacific Northwest of the United States (Paranjpye *et al.*, 2012). An additional hemolysin gene, *tlh*, encodes the thermolabile hemolysin, a phospholipase A2. While the specific function of this gene in human infection is unknown, the gene is widely considered to be a marker for this organism, being expressed by all clinical and environmental strains *V. parahaemolyticus* (Letchumanan *et al.*, 2014).

The seasonal distribution of *Vibrio* populations can be species specific. A study conducted at 10 recreational beaches along the German North Sea over the course of two years found that *V. alginolyticus* and *V. parahaemolyticus* were ubiquitous all-year round, whereas *V. vulnificus* was limited to the summer months (Böer *et al.*, 2013). Similar results came from a study performed in South Korea, where *V. alginolyticus* and *V. parahaemolyticus* were detected in both tidal water and mud all year, while *V. cholerae* and *V. vulnificus* were seasonally specific to summer. Interestingly, although *V. parahaemolyticus* was isolated in all months, pathogenic strains were detected mostly in June (29 strains with *trh*) and September (14 strains with *tdh*, 36 strains with *trh*, and 12 strains with *tdh* and *trh*) (Di *et al.*, 2017). More seasonal studies are needed to understand why virulence factors were detected only during warm seasons but were absent during cold ones in the same location.

The fact that virulence traits of these enteropathogenic *Vibrio* spp. were restricted to warmer months suggests that the risk to the human population of contagion by these pathogens might accelerate as the temperature increases due to global warming. Indeed, in the past decade, incremental increases in seawater temperature along the shoreline have been linked to epidemic outbreaks of *Vibrio* associated illness caused by *V. parahaemolyticus* in parts of Chile, Peru, the United States, Europe, and Asia (González-Escalona *et al.*, 2005; Martinez-Urtaza *et al.*, 2008; Baker-Austin *et al.*, 2010; Ma *et al.*, 2013). In geographical areas with a tropical climate, infections can persist year-round (Deepanjali *et al.*, 2005). Studies have highlighted environmental factors that affect the abundance and distribution of *V. parahaemolyticus* and these include water salinity, temperature, turbidity, and the levels of chlorophyll and presence of organic matter in suspensions (López-Hernández *et al.*, 2015).

The incidence of *V. parahaemolyticus* is highest in estuarine or coastal areas of the world oceans rather than in offshore seas. Many workers have isolated *V. parahaemolyticus* and related organisms from seawater, sediment, fish, shellfish, and plankton. *V. parahaemolyticus* is commonly found in commensal relationships with shellfish (Kaneko and Colwell, 1975), free-living in the water column (Kaneko and Colwell, 1973), in sediments and mud (Kaneko and Colwell, 1973; Di *et al.*, 2017), and within in-faunal burrows (Gamble and Lovell, 2011).

The occurrence *of V. parahaemolyticus* in areas where rivers empty into the ocean suggests that the origin or source of *V. parahaemolyticus* might be terrestrial.

Interestingly, within isolates obtained from tidal water and mud samples over a 1-year period, the occurrence of *V. parahaemolyticus* was, in all months, higher and more stable in mud samples than in tidal water (Di *et al.*, 2017). This suggests that mud could serve as a reservoir for *V. parahaemolyticus*, especially in winter.
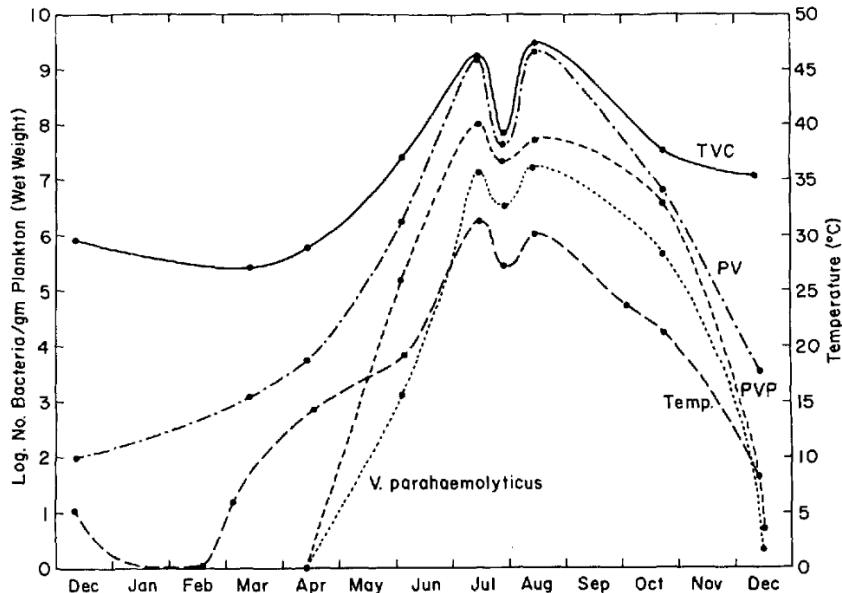
Figure 8. Seasonal change in the populations associated with plankton (per gram wet weight). TVC - total viable, aerobic, heterotrophic bacteria, PV- presumptive *Vibrios*, PVP - presumptive *V. parahaemolyticus*, and *V. parahaemolyticus* . The samples were collected in the Rhode River area (December 1970 to December 1971).Adapted from (Kaneko and Colwell, 1977)

The strong association of *V. parahaemolyticus* with zooplankton has been found to be important in the continuation of the annual cycle of this organism in the estuarine system (Figure 8). A population dynamics study in Chesapeake Bay shows that *Vibrio* spp. were not detected in the water column during the winter months, although they were present in sediments (Kaneko and Colwell, 1973). From late spring to early summer, when water temperatures were 14ºC, *Vibrio* spp. were released from the bottom communities and attached to zooplankton, proliferating as the temperature rose (Figure 8). More than 80% of *V. parahaemolyticus* were found associated with plankton or plankton detritus, while only around 20% existed as free cells in the water column or associated with sediments. In addition, the bacterial population associated with zooplankton was found predominantly on external surfaces of copepods. Interestingly, coliforms were not found to be associated with plankton or plankton detritus and almost all the total viable bacteria associated with plankton were composed of *Vibrio* species (Kaneko and Colwell, 1973). This study shows us not only that bacterial counts of zooplankton were found to be temperature dependent, but also that *V. parahaemolyticus*

survives in sediment at low temperatures. This, again, indicates an important role for sediments in *Vibrio* ecology.

If the association of *V. parahaemolyticus* with chitin or chitin-bearing copepods is considered necessary for the annual cycle of this organism in nature, then the adsorptive properties have a great ecological importance. Indeed, when natural estuarine water (0.42% salinity) was used, *V. parahaemolyticus* showed the second highest adsorption onto chitin, of the several strains tested. On the contrary, strains of *E. coli* and *Pseudomonas fluorescens* (isolated from the Chesapeake Bay) showed no adsorption. The efficiency of adsorption was found to be dependent on pH, concentration of NaCl and other ions found in seawater (Kaneko and Colwell, 1975). Since *V. parahaemolyticus* produces an active chitinase, chitinous materials provides a nutrient source, which it can then utilize. As pioneers in the initial colonization of copepods, this association implies an ecological significance, particularly in the recycling of organic matter of which those planktonic elements are composed.

The evidence for the distribution of *V. parahaemolyticus* in the open sea is contradictory. In a study done in the coastal regions of South Carolina and Georgia during the summer months, with regards to the distribution of *V. parahaemolyticus* in the open sea, this bacterium was not isolated from any water, plankton or sediment samples collected, even from those samples collected only 4 to 5 miles from shore (Kaneko and Colwell, 1974). However, another study indicates that non-virulent and virulent *V. parahaemolyticus* populations can survive in open sea conditions (Martinez-Urtaza *et al.*, 2012). Still, the occurrence of this bacterium in these natural systems has been found to be almost exclusively linked to the distribution and phenology of zooplankton. *V. parahaemolyticus* was found in only 12% of the seawater samples and occurred mostly during the summer and autumn months. The *trh* and *tdh*-positive samples were detected in 31% and 14% in zooplankton samples, respectively (Martinez-Urtaza *et al.*, 2012). In estuaries, temperature and salinity represent critical factors that influence the dynamics of *V. parahaemolyticus*. Yet, these variables showed no effect on the prevalence and seasonality of *V. parahaemolyticus* in offshore areas. The rias are subject to seasonal upwelling - downwelling sequences that determine the patterns of circulation and exchange of water in the inner areas of the rias. In offshore areas, the abundance and seasonality of *V. parahaemolyticus* associated with zooplankton was favoured by the concurrence of downwelling periods that promoted zooplankton patchiness (Martinez-Urtaza *et al.*, 2012).

The association of *Vibrio* spp. with zooplankton may provide protection from the stresses associated with cold saline environments and may represent a food source that ensures survival during prolonged journeys. These zooplankton may operate as a vehicle for dispersal of *V. parahaemolyticus* populations in the open sea drifting along with the ocean currents, connecting distant regions and habitats, and thereby producing impacts on bacterial community demography and epidemiology.

Furthermore, shellfish can also bio-accumulate *V. parahaemolyticus* through filter feeding. The amount of time this bacterium can remain inside an individual shellfish is not well defined and difficult to predict. The pili and flagellar systems of *V. parahaemolyticus* were found to contribute to bacterial persistence in naturally depurating Pacific oysters (Aagesen *et al.*, 2013).

Studies on oysters growing in the intertidal zone show that the concentration of total and potentially pathogenic (*tdh* and /or *trh* positive) *V. parahaemolyticus* increased when oysters were exposed to the sunny mudflats by a receding tide, then subsequently decreased when the tidal waters covered the shellfish and when filter-feeding recommenced (Jones et al., 2016). Another study revealed that *V. parahaemolyticus* is 4 to 8 times higher concentrated at maximal intertidal exposure than at the beginning (Nordstrom *et al.*, 2004). After re-immersion for one tidal cycle, it was shown that vibrio levels returned to background levels (Jones et al., 2016).

The decrease of bacteria once the tide comes up suggests that the cells attached to the oysters (and probably also to the sediment) are released into the liquid milieu. However, no work has been done to study what happens to these released cells. It is not known if these cells are actively being released and whether they can potentially contribute to the spread of this human pathogen into the marine milieu. Therefore, it is crucial to address such outstanding questions. Moreover, considering all the information described in this section concerning the prevalence and distribution of *V. parahaemolyticus*, it urges an understanding of the impact of the *V. parahaemolyticus* life cycle, namely the switch to surface motile cells and the consequent development of a swarm colony, in the dissemination of this microorganism in the environment.

1.3.2 Differentiation of *Vibrio parahaemolyticus*

V. parahaemolyticus can form two distint cell-types, which are adapted for locomotion in different circumstances: a 2-4 μm long swimmer cell with a single and polar sheathed flagellum for translocation in liquids and a swarmer cell that is up to 40 μm in length with multiple unsheathed lateral flagella positioned along the cell body for movement over surfaces (McCarter, 2003) (Figure 9). The polar flagellum has a constitutive expression and its rotation is driven by proton-motive force, whereas the synthesis of lateral flagella occurs under conditions that disturbed the polar flagellum rotation. Further, the motors of the lateral flagella rotate by sodium motive force. The polar flagellum of *V. parahaemolyticus* is encoded by 60 genes that are in turn distributed into five clusters located on chromosome I (Kim and McCarter, 2000). On the other hand, the lateral flagella is encoded by approximately 38 genes distributed within two clusters located on chromosome II (Stewart and McCarter, 2003). There are six polar flagellin subunits, whereas the lateral flagella are polymerized from a single flagellin subunit, LafA. (Macnab, 1999).

Recent work in our lab has shown that depending on their cell length, swarmer cells undergo two distinct types of cell division. Particularly, short swarmers divide at mid-cell, while long swarmers (longer than 8-10 μm) switch to a specific non-mid-cell placement of the division site (Figure 9). The position of the Z-ring at the non-mid-cell Length-Dependent division-site (LD-site) results in daughter cells of different sizes: a long and a short cell. Swarmer cells are only allowed to divide once per cell cycle independent of their length, as the level of FtsZ is regulated in swarmer cells to match the concentration of FtsZ in planktonic cells, restricting the number of Z-rings formed to one (Muraleedharan *et al.*, 2018). By limiting cell division-events to only one per cell at a non-mid-cell position, *V. parahaemolyticus* cells guarantee the preservation of long cells within a multiplying swarmer population that consequently permits cell division without diminishing the long swarmer cell population and the need for dedifferentiation.

During swarming morphogenesis, cell division seems to be supressed resulting in the formation of elongated and multinucleated cells (Copeland and Weibel, 2009). The fact that the elongated phenotype is usually more pronounced for species that navigate across hard agar surfaces (>1% agar), suggests that increase in cell length is needed for robust swarming (Be'er *et al.*, 2013) (Harshey and Partridge, 2015; Böttcher *et al.*, 2016) (Rauprich *et al.*, 1996). Nevertheless, the reasons for the importance of elongation

during swarming remain obscure. Likewise, very little is known about the regulation of the elongation process in any species. The known cell division regulators in *V. parahaemolyticus*, namely MinCDE and SlmA, were not found to be essential for the elongation phenotype of swarmer cells (Muraleedharan *et al.*, 2018). Hence, the mechanism for elongation during swarming differentiation remains an open question.

Developmental life-cycle of *Vibrio parahaemolyticus*
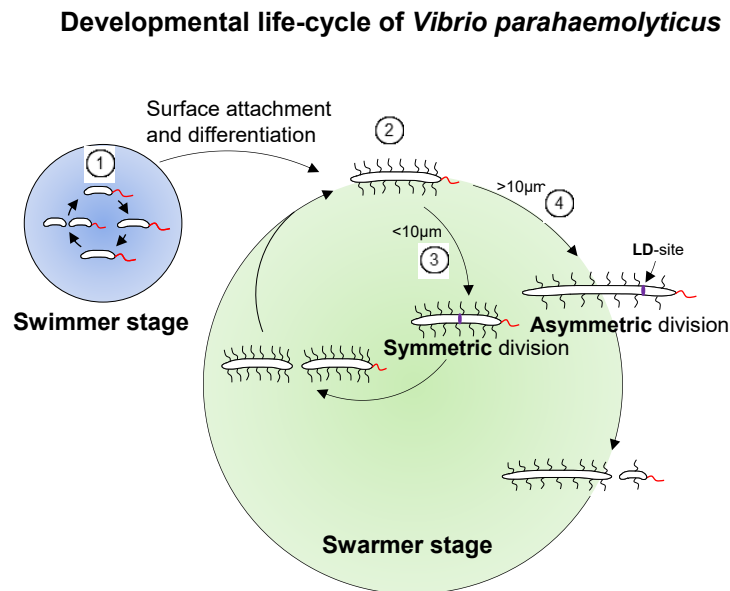
Figure 9. Developmental life-cycle of *Vibrio parahaemolyticus*. During the swimmer state, cells elongate and divide at mid-cell resulting in two progeny swimmer cells (#1*)*. Swimmer cells have a single polar sheathed flagellum (in red). Upon surface contact, swimmer cells can differentiate into the filamentous swarmer cells with multiple lateral flagella, in addition to the polar flagellum (#2). Depending on their cell length, swarmer cells undergo two distinct types of cell division: short swarmer cells position the Z-ring at mid-cell, resulting in swarmer progenies of equal sizes (#3); in long swarmer cells the Z-ring is positioned at the non-mid-cell LD-site, resulting in daughter cell of different sizes – a long and a short cell (#4). Adapted from (Muraleedharan *et al.*, 2018)

V. parahaemolyticus presents differences in cell size according to the position of cells within a swarm colony. In the periphery of the swarm colony, cells assemble into flares that extend outward from the colony and cells are stacked in a single layer or in a few layers. In the center of the swarm colony, cells are stacked in multiple layers and are generally considerably shorter than cells in the flares (Heering and Ringgaard, 2016; Heering *et al.*, 2017a). However, it is not known if the only difference between the cells in the center and in the periphery of *V. parahaemolyticus* swarm colony is their morphological appearance. Particularly, the temporal development and differentiation of swarm colonies is unknown. Moreover, it is not known how *V. parahaemolyticus* cells within swarm colony populations respond to changes in the external milieu – particularly

during fluctuations of flooding and non-flooding conditions, which is characteristic of the tidal rhythms found in estuarine areas – a common habitat for *V. parahaemolyticus*.

A particular feature of *V. parahaemolyticus* is the use of the polar flagellum as a tactile senser to induce the lateral flagella system. This idea is supported with evidence from different experiments showing that induction of lateral flagella can be stimulated in liquid-growing cells by: i) using antibodies that inhibit polar flagellum rotation (McCarter *et al.*, 1988) ii) growing mutants with polar flagella defects (McCarter *et al.*, 1988) or iii) blocking the sodium-channel with the drug, phenamil, which in turn slows rotation of the polar flagella (Kawagishi *et al.*, 1996). Together, these results suggest that the polar flagellum acts as a flagellar mechanosensor and when cells encounter a solid or viscous substrate, they sense and transfer the information to induce swarmer-cell-dependent gene expression.

Although mechano-inactivation of flagellar rotation induces the second motility system, this hyperflagelation phenotype requires an additional signal, iron-starvation (McCarter and Silverman, 1989). Other physiological stresses, such as the presence of volatile acids or excess of calcium, have also been shown to trigger the swarming differentiation program (Ulitzer, 1974,Gode-Potratz, Chodur, & McCarter, 2010). Regulators of swarming will be presented in the next section.

In terms of energy expenditure, it can be easily argued that requirement of multiple stimuli works as a strategy to avoid needless production of a very metabolically expensive hyperflagellated state, which is characteristic of the long swarmer cells. Another control of energy expenditure is achieved by careful transcription of flagella and motility genes in a sequential classes of gene expression (Figure 10). Such tuned regulation occurs in both the swarmer and the swimmer morphogenetic program within many bacteria in an almost universal cascade. Master regulators or Class 1 genes activate the Class 2 genes in a sigma 54 transcription factor (or RpoN) dependent manner. Class 2 genes (or early flagella genes) are composed of the assembly and functional components of the flagella apparatus, and are all master regulator(s)-dependent. Sigma 28 (or FliA) is required for expression of Class 3 genes (or late flagella genes), which encode for flagellin subunits and the haps, which are the adaptors for joining the propeller to the hook (McCarter, 2006).

Parts of the flagellum and order of *laf* expression
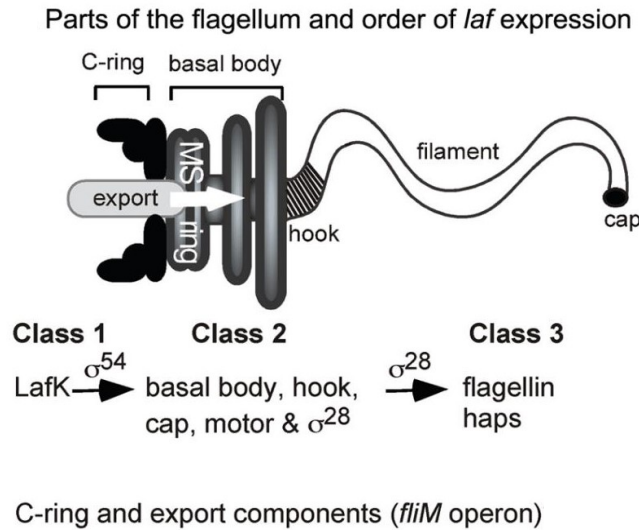
Figure 10. Schematic representation of the flagellar organelle and the hierarchy of lateral flagellar (*laf*) gene expression. LafK, a σ^{54}-dependent regulator, is required for the expression of Class 2 genes, which mostly encode for components of the basal body and hook, as well as a specialized sigma factor. This sigma factor (FliA or σ^{28}) is required for expression of Class 3 genes, which encode for the flagellin subunit and the haps. The *fliM* operon encodes for components of the C-ring and membrane-associated export components, and its expression is independent of the master regulator *lafK*. Adapted from (Gode-Potratz *et al.*, 2011).

Additional unknown regulators are most probably at the top of the hierarchy. In our model organism, the swimmer cells´ master regulator is FlaK. With respect to swarmer cells, LafK was initially thought to induce all the components of the lateral flagella system (Stewart and McCarter, 2003). However, in a study from 2011, synthesis of C-ring and export components (FliM operon) was demonstrated to be independent of LafK, suggesting the existence of a second lateral flagella master regulator (Gode-Potratz *et al.*, 2011).

Interestingly, it was shown that LafK can compensate FlaK, in terms of inducing the production of the polar flagella. On the other hand, loss of LafK is sufficient to eliminate swarming motility, suggesting the FlaK has no significant compensatory role in the lateral flagellar system (Kim and McCarter, 2004).

Swarming differentiation of *V. parahaemolyticus* is fine-tuned by environmental factors and a number of regulators, some of them already revealed. Nonetheless, the identity of the signal for sensing polar flagella inhibition and the signal-transducing pathway regulating lateral flagella and the expression of other swarming related genes remains unknown.

Although *V. parahaemolyticus* has a very complex life style with different cell types that seem to be adapted to specific conditions, no work has been done to analyse how much the proteome changes according to the environmental circumstances, namely growth in surface versus growth in liquid. Moreover, it would be interesting to know if there are proteins that are needed specifically to respond to a certain life style and also, if there are proteins whose levels are always unchanged and independent on the external context.

1.3.3 Regulation of swarming

As flagella synthesis and motility present a high metabolic cost for the bacterium, its activation is governed by a variety of specific conditions and regulators. Below are presented the swarming-related environmental factors, regulators and molecular mechanisms discovered so far.

1.3.3.1 Physiological conditions

In a 1974 study, *V. parahaemolyticus* was induced to swarm on solid media under three different conditions: growth in presence of 1% NaCl, growth in a sealed system and growth on an H_2O_2 treated medium (Ulitzer, 1974). The fact that alkali-saturated filter paper prevented swarming under all three conditions may indicate that one or more volatile acids are involved in induction of swarming. The identity of those volatile acids is not known, but it seems that the formation of a gradient of toxic metabolites is capable of triggering swarming.

As already mentioned, iron-starvation acts as another induction signal for swarming. This was first shown in a study where production of lateral flagella occurred only when polar flagellar function was perturbed and iron-limiting growth conditions were imposed (McCarter and Silverman, 1989).

More recently, it was shown that availability of calcium enhances swarming (but not swimming) gene expression and additionally, one of the organism's two type III secretion system regulons, TIIISS1 (Gode-Potratz *et al.*, 2010). TIIISS1 is a protein secretion system that delivers effector proteins directly into eukaryotic cells, that will alter or disrupt the normal cell signaling pathway. Interestingly, swarming and TIIISS1 gene expression were demonstrated to be linked by LafK. In the same study, iron limitation was found to play a role as a signal, this time responsible not only for inducing swarming but TIIISS1 as well, operating independently of calcium.

As far as these three swarming-triggering signals are concerned, the regulatory mechanism generated by these signals is understood only in the case of calcium. The calcium response was mediated by repression of LysR-type transcription factor CalR, an inhibitor of swarming motility, cytotoxicity, and TIIISS1 gene expression. Nonetheless, once swarming program is initiated, evidence suggests a capacity for a negative-

feedback loop on the swarming regulon, upon upregulation of *exsA* expression (Gode-Potratz *et al.*, 2010). Thus, calcium and iron play a signaling role with global consequences on the regulation of gene sets that are relevant for surface colonization and infection.

1.3.3.2 Quorum sensing and c-di-GMP

Many species of bacteria use quorum sensing, a chemical signalling system, to coordinate gene expression according to the density of their local population. Lateral flagella expression is modulated by quorum sensing (Jaques and McCarter, 2006; Trimble and McCarter, 2011).

The homologous quorum-sensing components OpaR, SwrT and SwrZ play different regulatory roles in swarming modulation. While the *V. parahaemolyticus* quorum sensing-master regulator OpaR was found to repress lateral flagella expression, SwrT positively influenced swarming by inhibiting a lateral flagella repressor, called SwrZ. Mutation of *swrT* abolished swarming motility. Interestingly, a ΔswrZ mutant did not produce constitutive lateral flagella, suggesting that SwrZ is not responsible for transmitting the signal that triggers the second motility system (Jaques and McCarter, 2006).

A three-gene operon (*scrABC*) appears to be involved in the regulation of *V. parahaemolyticus* swarming differentiation (Boles and McCarter, 2002) (Figure 11). This Scr system is induced upon surface growth and is transcribed independently of LafK (Gode-Potratz *et al.*, 2011). Mutants with defects in any of these three genes show decreased swarming motility and decreased *laf* gene expression (Boles and McCarter, 2002).

ScrA encodes a predicted pyridoxal-phosphate-dependent enzyme. It produces the autoinducer S-signal (as yet unidentified), which can exit the cell to communicate with neighboring cells via ScrB, a periplasmic solute-binding protein (Trimble and McCarter, 2011). ScrC is a bifunctional enzyme that has the ability to synthesize and degrade the second messenger, bis-(3'-5') cyclic dimeric GMP (c-di-GMP). In the presence of ScrA and ScrB, ScrC acts to degrade c-di-GMP. c-di-GMP levels inversely modulate lateral flagellar and CPS (capsular polysaccharide gene) expression, meaning that high concentrations of this nucleotide prevent swarming and promote adhesiveness

(Boles and McCarter, 2002) (Figure 11). Thus, the *V. parahaemolyticus* ScrABC system modulates decisions concerning swarming or sticking, via quorum control of c-di-GMP levels.
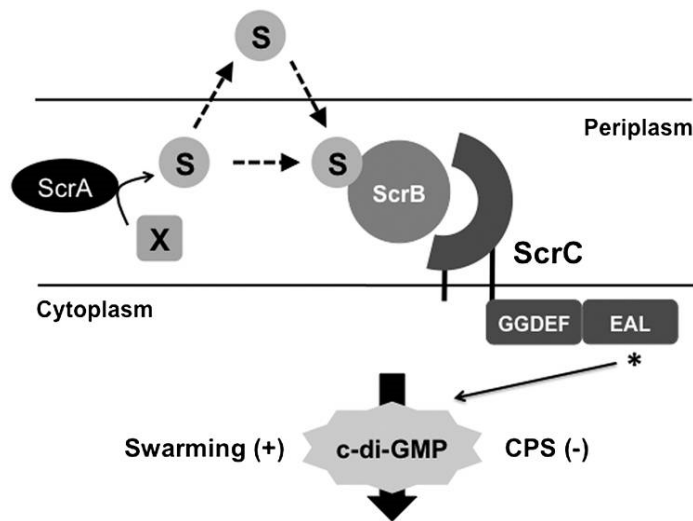
Figure 11. ScrABC circuit participates in directing quorum control of c-di-GMP-modulated swarming and sticking in *V. parahaemolyticus* . ScrC is a membrane-bound protein, with a periplasmic domain and cytoplasmic GGDEF and EAL domains. In the presence of ScrA and ScrB, ScrC displays phosphodiesterase (PDE) activity. Activation of the PDE reduces the amount of c-di-GMP in the cell, resulting in an increase in swarming and a decrease in CPS production. ScrA, a phosphate-dependent aminotransferase, produces the autoinducer S-signal, which can exit the cell to communicate with ScrB in neighboring cells. Cell-free supernatants prepared from a ScrA-overproducing strain or the wild-type activate swarming and repress capsule gene expression in an ScrBC-dependent manner. Adapted from (Trimble and McCarter, 2011).

Furthermore, another gene, *scrG*, was found to act as a phosphodiesterase (PDE), i.e involved in degradation of c-di-GMP. Overexpression of *scrG* was sufficient to induce lateral flagellar gene expression in liquid and also, decrease biofilm formation, *cps* gene expression, and suppress the *ΔscrABC* phenotype, consistent with a c-di-GMP modulated system, as described above (Kim and McCarter, 2007). These results are in agreement with the fact bacterial swarming motility is often oppositely regulated and is antagonistic to biofilm formation (Verstraeten *et al.*, 2008).

1.3.3.3 The autoinducer S-signal

In *V. parahaemolyticus*, the S signal is a quorum-sensing molecule that induces the swarming motility system (Trimble and McCarter, 2011). In addition to this function, the S signal also coordinates behaviour by promoting chemotaxis and acting as a recruitment molecule (Lamb *et al.*, 2019). Two methyl-accepting chemotaxis proteins participating in signal reception were identified: one being important for S signal

dependent chemotaxis during growth on a surface (SscS) and the other playing a key role in swimming (SscL). Rather than staying together, the MCP mutant (Δ*sscS)* appears to move with less coordination when they are unable to detect the S signal (Lamb *et al.*, 2019). Coordination of the advancing swarm aided by cell-cell recruitment might be of crucial importance in the environment.

1.3.4 Swarming and Virulence

There are only few studies that link swarming motility to biofilm formation and virulence. In *P. mirabilis* related urinary tract infections, swarming motility is reported to contribute to the infection process (Mobley and Belas, 1995). Swarmer cell differentiation of this organism is accompanied by a marked increase in the expression of several putative virulence factors (cell-bound haemolysin, urease, metalloprotease, ability to invade urothelial cells). Studies *in vivo* using mouse models of uropathogenicity have demonstrated that mortality rates are reduced when mice are infected with mutants that are defective in swarming (Allison *et al.*, 1994).

Lateral flagella of *Aeromonas spp.*, in addition to mediating swarming motility, appear to function as adhesins, contributing to microcolony formation and efficient biofilm formation on surfaces, and possibly facilitating host cell invasion (Gavín *et al.*, 2002).

In *V. parahaemolyticus*, lateral flagella play an important role in adherence to and colonization of the chitinaceous shells of crustaceans, probably by a mechanism distinct from that used by the polar flagellum (Belas & Colwell, 1982). Additionally, *V. parahaemolyticus* lateral flagella are involved in adhesion to HeLa cells (Park *et al.*, 2005a). An *in vitro* experiment demonstrated that cytoxicity levels (towards host tissue cells) were higher when *V. parahaemolyticus* was previously grown on a solid surface instead of liquid (Gode-Potratz *et al.*, 2011). This suggests that pre-growth on a surface condition prepares *V. parahaemolyticus* for virulence. *In vivo* studies showed that after injecting rabbits orally with liquid culture, Type III secretion and its effectors were highly up-regulated. However, majority of genes in the *lafK* and *scrABC* regulons were not differentially expressed (Livny *et al.*, 2014).

Although in some species, swarming has been shown to be important for human infection, in the case of *V. parahaemolyticus*, a clear link between swarming and virulence has not been directly demonstrated.

As mentioned before, *V. parahaemolyticus* is a prevalent worldwide marine bacteria that can cause disease outbreaks and therefore, it is essential to understand what factors influence the dissemination of this pathogen in the environment. It is known that the amount of cells grown on oysters decreases dramatically after one tide (Jones *et al.*, 2016). Yet, there are no studies that further investigate what happens to these released cells, that is, if they are actively being released and, more importantly, whether

these cells can potentially contribute to the spread of this human pathogen into the marine environment. Moreover, it is not known if the difference between the cells in the center and in the periphery of *V. parahaemolyticus* swarm colony is solely in regard to their morphological appearance or if the swarm colony consists of truly distinct regions. Particularly, to our knowledge, there have been no studies addressing the development of the swarm colony to understand how its architecture changes over time and also, when exposed to oscillations in external conditions such as flooding, which occurs in estuarine areas, namely *V. parahaemolyticus´* natural habitat.

Although there are some genes that have been identified as important or even essential for swarming motility of *V. parahaemolyticus,* there are still many pertinent players that have not been revealed yet. For intance, what key players participate in sensing the environmental signals or in the signal transduction or even in the elongation process remains to be discovered. Furthermore, there is not much data on how the proteome of *V. parahaemolyticus* changes according to its environmental circumstances, such as growth on a solid surface or in liquid conditions.

Considering all the current knowledge evidenced through this introduction, as well as, all the unknowns still to be revealed, the present work was conducted in order to address some of these outstanding questions.

Chapter II - Aim and scope

V. parahaemolyticus is a marine bacterium recognized as the leading cause of human seafood-borne gastroenteritis and its highest incidence is in coastal and estuarine areas. *V. parahaemolyticus* exists as swimmer and swarmer cells, specialized for growth in liquid and on solid environments, respectively. *V. parahaemolyticus* swarmer cells express a second motility system, resulting in the production of multiple lateral flagella, which are essential for swarming behavior and for surface and cell-cell contact in order to coordinate movement across surfaces. Swarmer cells are highly elongated by a probable regulated inhibition of cell division. (Baumann & Baumann, 1977; Böttcher et al., 2016; McCarter, 2004). The fact that many bacterial species display this form of surface motility in the laboratory and thus encode for a mechanism that enable for fast migrations and surface colonization, argues that swarming must be an important strategy in the bacteria's natural habitats.

According to the position of cells within a swarm colony of *V. parahaemolyticus*, there are differences in cell size. However, what are the proteome differences between the cells in the center and in the periphery of the colony and how the architecture of a swarm colony develops over time, are still questions to be answered. Moreover, it is not known how the swarm colony architecture responds to environmental fluctuations, such as flooding, which occurs commonly in *V. parahaemolyticus'* natural habitat. Indeed, there have been reports demonstrating that the level of *V. parahaemolyticus* in the water depends on the tide, thus, suggesting that cells could be released from surfaces into the liquid surroundings (Jones *et al.*, 2016; Nordstrom *et al.*, 2016). However, the release of surface-attached cells into liquid environments have been unexplored for *V. parahaemolyticus* – and for swarm colonies in general. Thus, the question of how swarm colonies contribute to the general occurrence of *V. parahaemolyticus* in the environment remains open. As this bacterial pathogen can cause serious disease outbreaks, it is essential to understand what factors influence its dissemination in the environment.

Although some swarm regulators are already revealed, there are still many important players and key mechanisms of this process that remain to be discovered. Furthermore, although *V. parahaemolyticus* has a very complex life cycle with different cell types that seem to be adapted to specific conditions, no work has been done to analyze how the proteome changes according to distinct environmental cues.

Therefore, the following aims of this work were defined:

1) Comprehend the architecture of swam-colonies and examine how it responds when exposed to fluctuations in its environment.

2) Understand the importance of the life cycle of *V. parahaemolyticus* for the dissemination of this bacterium in the liquid environment.

3) Determine a proteome that is specific to the swarmer cells and identify potential proteins involved in the swarming motility process.

4) Define the proteomic landscape of *V. parahaemolyticus* in swimming and solid conditions and use this data set to identify housekeeping proteins.

Chapter III - Release and dissemination of distinct cells from swarm-colonies

3.1 Results – Part I

3.1.1 Cells are released from flooded swarm colonies into their liquid surroundings

In order to understand how changing environments influence *V. parahaemolyticus* cells within swarm colonies we analyzed if cells are released from flooded swarm colonies into the environment. *V. parahaemolyticus* swarm colonies were very gently flooded with buffer for 90 minutes and the amount of bacteria in the liquid phase was analyzed (Figure 12A). Importantly, we could detect high amounts of bacteria in the liquid phase (Figure 12A), suggesting that *V. parahaemolyticus* cells are released from swarm colonies into the liquid surroundings. To make sure that cells present in the liquid phase did not only originate from the initial flooding of the swarm colony, we performed a time-course experiment, where we measured the amount bacteria present in the liquid phase as a function of time (Figure 12B). Indeed, there was a time-dependent accumulation of cells in the liquid surroundings (Figure 12B), showing that *V. parahaemolyticus* cells are released from flooded swarm colonies into their liquid surroundings.
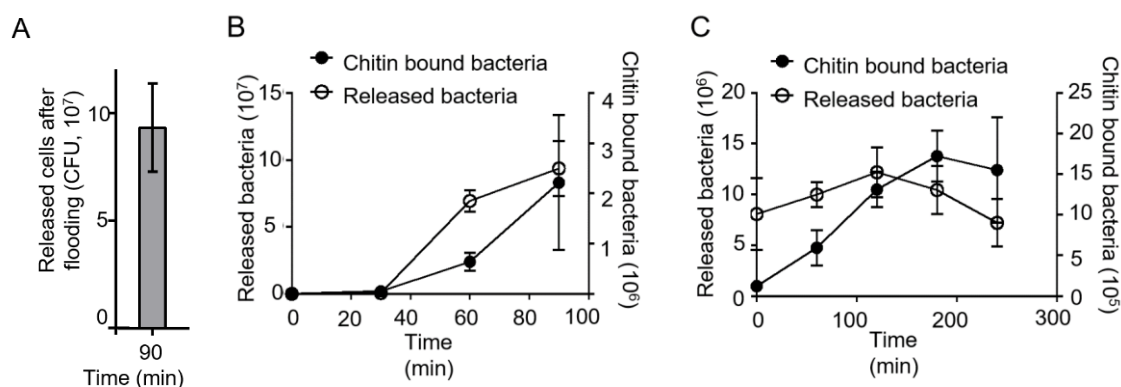
Figure 12. Cells are released from flooded swarm colonies into their liquid surroundings. (A) Schematic showing the developmental life-cycle of *V. parahaemolyticus*. Figure adapted and edited from (Muraleedharan *et al.*, 2018). (B) Bar graph showing the number of cells in the liquid phase after flooding of swarm colonies. (C) Graph showing the number (CFU/mL) of released cells into the liquid phase of flooded swarm colonies as a function of time (filled black circles). Graph showing number of cells (CFU/20 mg of chitin) that have attached to chitin surfaces as a function of time during flooding of swarm colonies (open circles). (D) Cells released from flooded swarm colonies were collected and their ability to attach to chitin was measured as a function of time. Graphs show the number of cells (CFU) in the liquid phase (open circles) and cells attached to chitin (filled circle) as a function of time. (B-D) Error bars indicate standard error of the mean (SEM) and is based on three independent biological replicates.

3.1.2 Release of cells from swarm colonies facilitates dissemination of *V. parahaemolyticus* in the environment and its re-attachment to new submerged surfaces

To test if cells released from the swarm colony into the liquid environment were able to spread and re-attach to surfaces, we measured the ability of released cells to attach to submerged chitin flakes over time. Indeed, there was a time-course dependent increase in chitin attached cells that correlated with the increase in released cells into the liquid surroundings (Figure 12B). To further analyze the efficiency by which released cells are able to spread in the environment and attach to chitin, we collected released cells and transferred them to a new test tube. We then added chitin flakes and followed attachment and presence of planktonic cells over time – this allowed us to assay for attachment efficiency of released cells without the continuous contribution from the release of cells from swarm colonies. Indeed, there was a time-dependent increase in the amount of chitin-attached cells over time (Figure 12C). These experiments further confirm that cells released from flooded swarm colonies have a high ability to spread in the environment and re-attach to new surfaces such as chitin.

3.1.3 Cells released from swarm colonies possess a length distinct from cells from the center and from the periphery of swarm colonies

As swarm colonies primarily consist of short cells in the center and fully differentiated highly elongated swarmer cells in the periphery one could expect a heterogeneous population of released cells. Thus, we analyzed the cell lengths and cell length distribution of released cells and compared them to cells from the center and periphery of swarm colonies and to that of planktonic cells. As expected cells in the center were short with little variance in size while cells from the periphery were highly elongated and showed a high variance in cell length distribution (Figure 13A-C). However, surprisingly, the cell length distribution of released cells was very homogenous and almost no long cells were detected. Thus, showing that long swarmer cells are not released into the liquid environment but stay surface attached during flooding. Importantly, released cells were on average also significantly different in their cell length distribution from cells found in the center of the swarm colony and they were most similar in size to planktonic cells (Figure 13A-C). To test if incubation in our release-buffer could influence the cell length during the course of the release-experiment, we analyzed the cell length of cells collected from the center and periphery of swarm colonies, after

incubation in our release buffer and compared with the cell length of released cells. Again, released cells were on average significantly different in their cell length from either the cells from the center or from the periphery of swarm colonies (Figure 13A-C). This shows that cells released from swarm colonies are significantly different in size from the two types of cells generally found in the center and periphery of swarm colonies, respectively, suggesting that released cells comprise a different cell type.
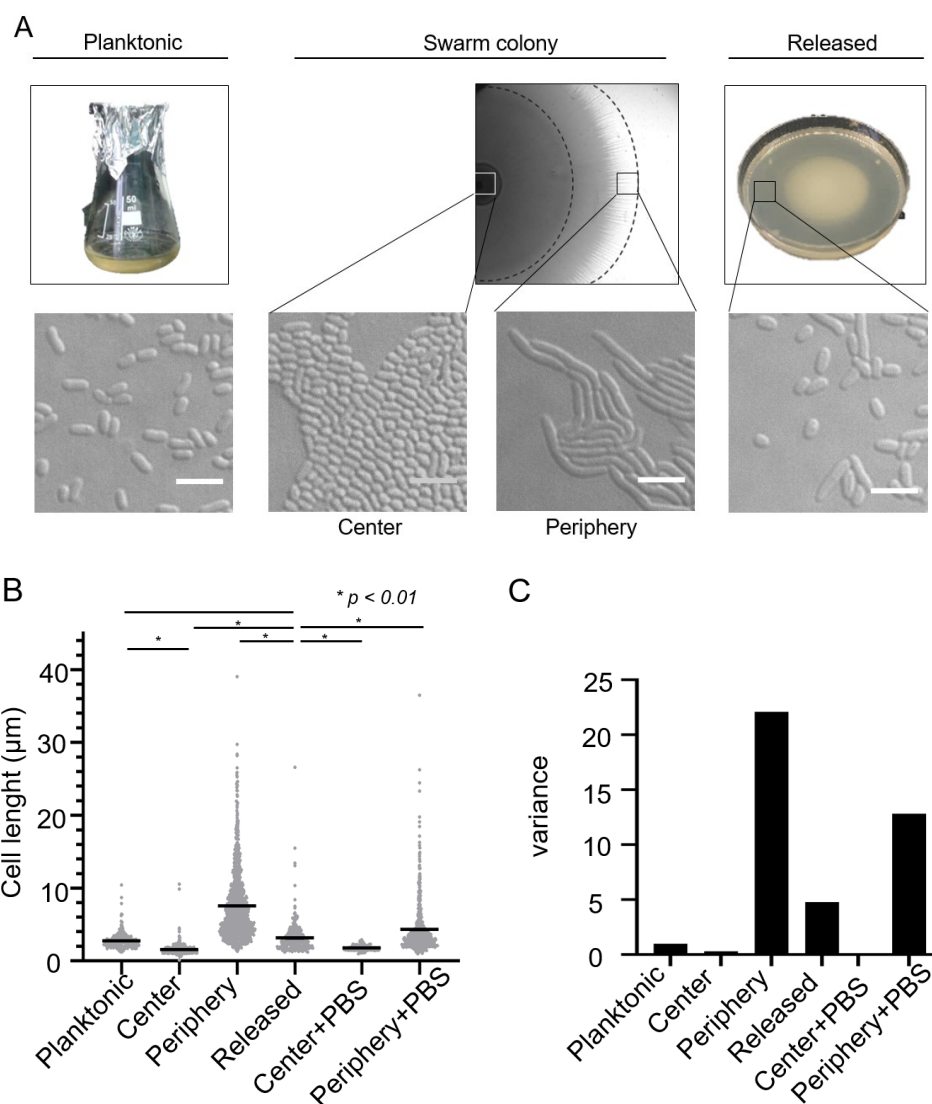
Figure 13.Cells released from swarm colonies have a distinct morphology. (A) DIC microscopy showing the morphology of planktonic cells, cells collected from the center and periphery of swarm colonies and cells released from flooded swarm colonies. (B) Graph showing the cell-length distribution of cells from indicated environments. Black bars indicate the mean value. P value was calculated using Student's t-test. (C) Bar-graph showing the variance in cell length of cells from indicated environments.

3.1.4 Cells released from swarm colonies comprise a distinct cell type

We next analyzed how cells released from swarm colonies into the liquid environment are related to the populations found within mature colonies. Particularly, we performed proteomic analysis of cells from the center (C) and cells from the flares in the periphery (P) of swarm colonies and compared these to that of cells released into the liquid environment (R) (Figure 14A-C).
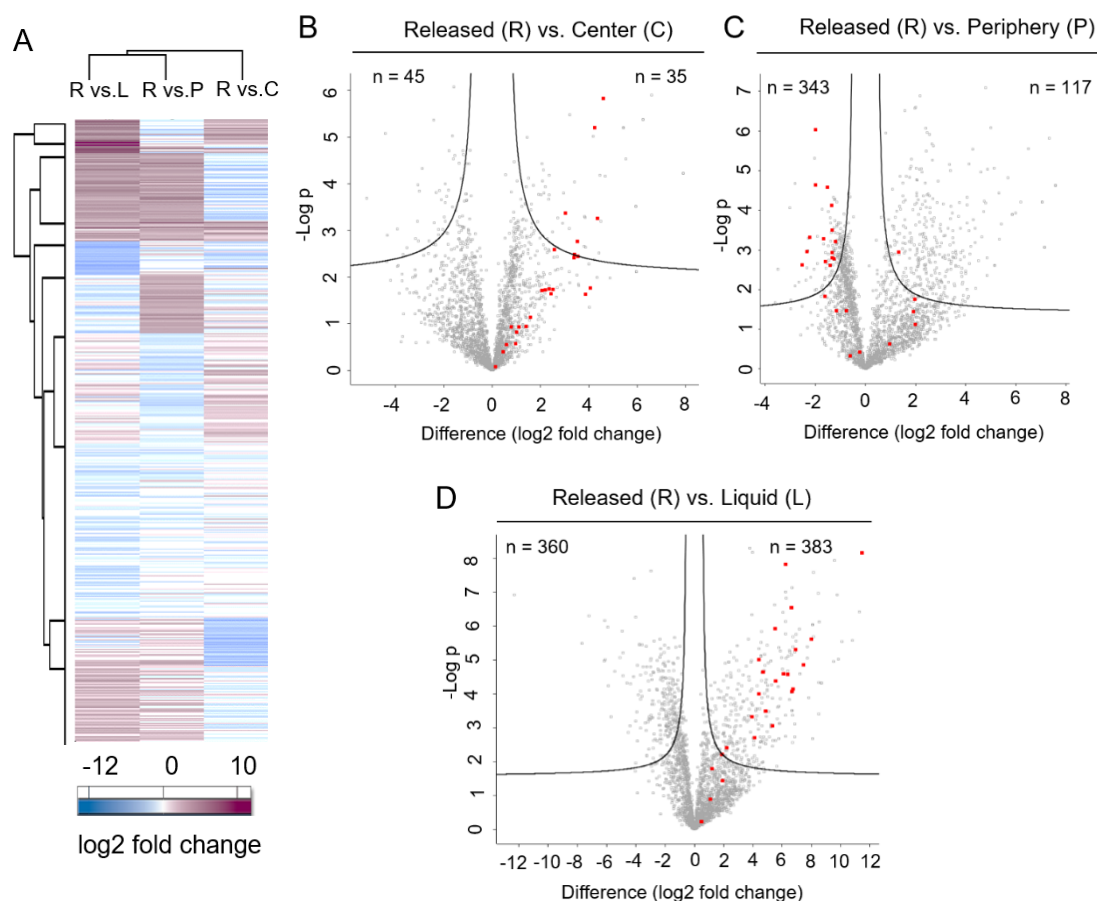
Figure 14. Cells released from swarm colonies comprise a distinct cell type. (A) Clustering map depicting changes in protein intensities in three sets of comparison: Comparison of Release vs. Liquid (R vs. L); Released vs. Periphery (R vs. P); Released vs. Center (R vs. L). The color code indicates the difference of fold change, in log2 of the intensities ratio. (B-D) Volcano plot depicting changes in protein intensities in a comparison of cells from (B) Released vs. Periphery (R vs. P) of swarm colonies, (C) Released vs. Center (R vs. C) of swarm colonies, (D) Released vs. Liquid (R vs. L). In B-D number "n" indicates the number of differentially expressed proteins that were significantly up- and down-regulated and highlights in red indicate lateral flagellum proteins.

Strikingly, the results showed that released cells have a proteomic profile distinct from both cells in the center (Figure 14A, B) and the swarm periphery (Figure 14A, C) of swarm colonies. Additionally, we compared released cells to planktonic cells continually

cultivated in liquid medium (L), and interestingly the results showed that released cells also are highly different from planktonic cells on the proteomic level (Figure 14A, D). Thus, showing that not only are released cells morphologically different from cells in the center and periphery of swarm flares (Figure 13A-C), but also display a distinct proteomic profile specific to this cell type and different from both center, periphery and planktonic cells. Interestingly, regarding the levels of proteins belonging to the type VI secretion system 1, released cells contain much higher expression of these proteins when compared to planktonic cells (Figure 15A).
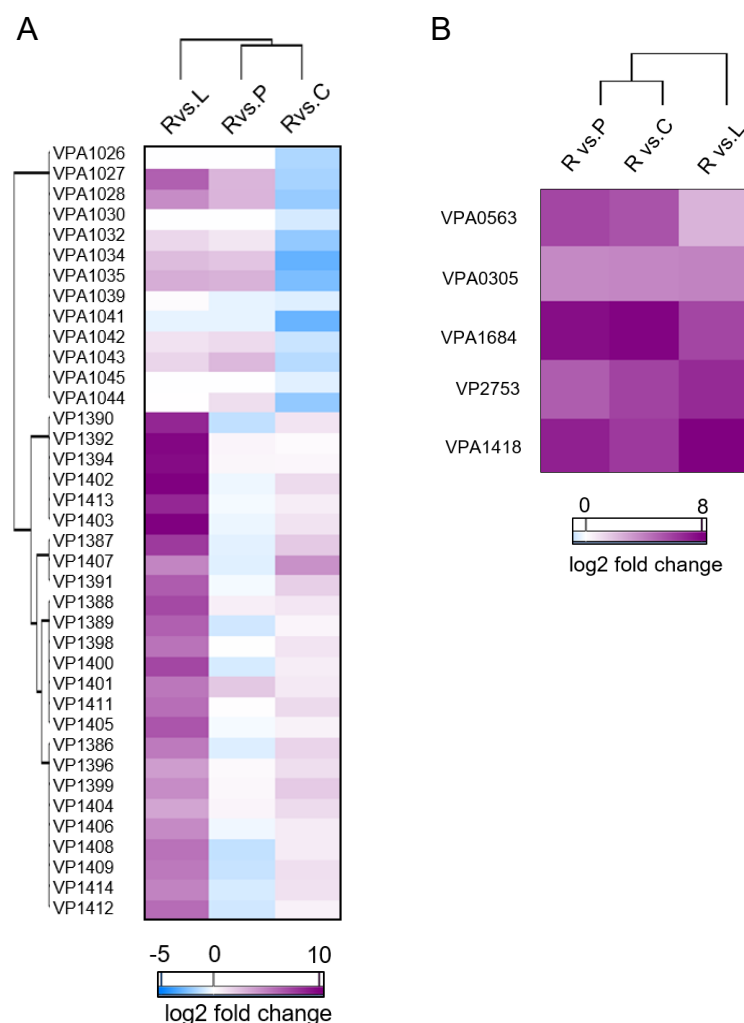
Figure 15. Clustering map depicting changes in intensities of specific proteins, in three sets of comparison: Release vs. Liquid (R vs. L); Released vs. Periphery (R vs. P); Released vs. Center (R vs. L).. (A) Clustering map showing intensities ratios of Type VI SS 1 and 2 proteins. All proteins from type VISS1 start with VP# while all proteins from type VISS2 start with VPA#. (B) Clustering map showing intensities ratios of five proteins related to oxidative stress. The color code indicates the difference of fold change, in log2 of the intensities ratio:

The fold change of the type VISS1 proteins is slightly positive when comparing to cells from the center. Furthermore, five proteins related to oxidative stress were always found to be upregulated in released cells (Figure 15B, Table 12). Altogether, this shows that cells released from the swarm colony into liquid environments are different both morphologically and proteome wise compared to cells from the center and colony periphery, respectively. Thus, indicating that released cells comprise a distinct cell type.

3.1.5 Cells released from swarm colonies are highly swimming proficient

Since our results show that released cells from swarm colonies are very proficient in spreading in liquid environments (Figure 16), we analyzed the swimming potential of released cells compared to that of cells obtained from the swarming colony periphery and planktonic cells. Particularly, we performed single cell analysis and measured the swimming speed and displacement of individual cells as a function of cell length. The results very clearly showed that the swimming proficiency was cell length dependent. Cells shorter than 5 µm in length were highly motile while cells longer than 5 µm in length almost showed no swimming behavior with significantly reduced speed and displacement compared to short cells – independent of the origin of the cell within the swarm colony (Figure 16). Importantly, cells released from the swarm colony almost all possessed a length that correlated with a high swimming proficiency resembled planktonic cells in respect of swimming ability – thus, showing that cells released from swarm colonies are highly swimming proficient (Figure 16).
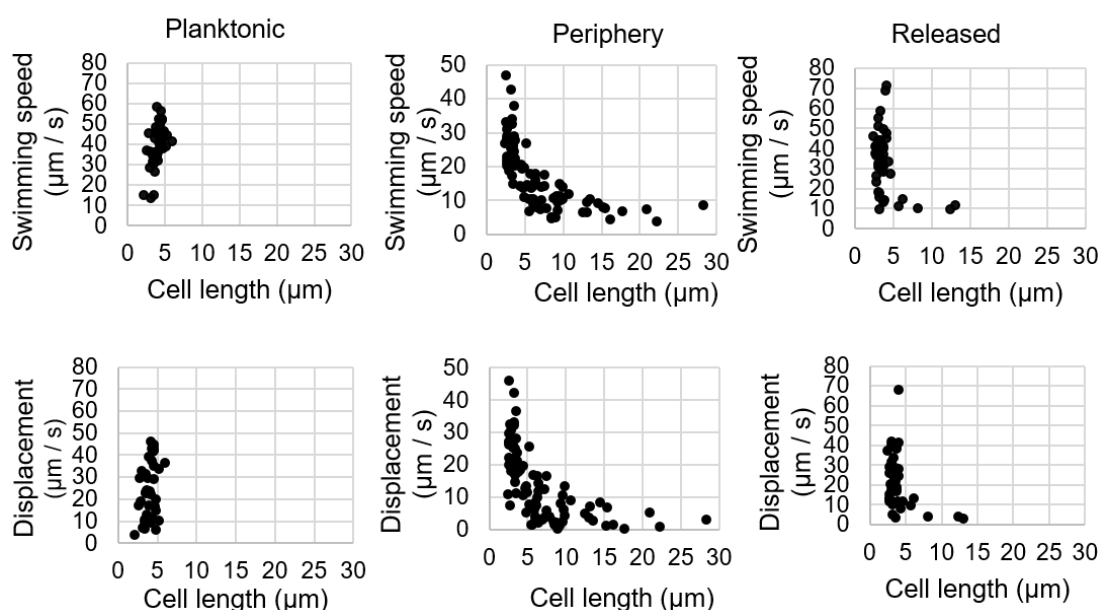
Figure 16. Cells released from swarm colonies are highly swimming proficient. Graphs showing the swimming speed and displacement as a function of cell length. Particularly of planktonic cells, cells collected from the periphery of swarm colonies and cells released from flooded swarm colonies.

3.1.6 Cells released from swarm colonies chemotax towards the chitin component N-acetylglucosamine.

Chitin, a derivative of glucose, is a long-chain polymer of the monosaccharide N-acetylglucosamine (GlcNAc). It is one of the primary components of the exoskeletons of crustaceans such as crabs, lobsters and shrimps and the scales of fish. Thus, as our results show that cells released from swarm colonies are able to spread in their new liquid surroundings and subsequently re-attach to chitin surfaces, we tested the ability of released cells to perform chemotaxis towards the chitin component GlcNAc, and compared it to that of planktonic cells. As a negative control we included a strain deleted for the chemotaxis protein CheW (*ΔcheW*), which is defective in chemotactic behavior (Heering and Ringgaard, 2016).
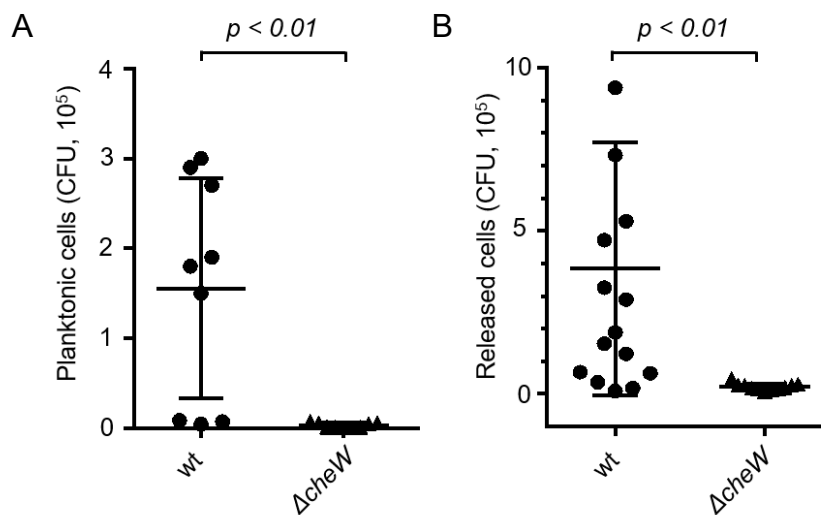
Figure 17. Cells released from swarm colonies chemotax towards the chitin component N-acetylglucosamine. (A) Chemotactic capillary experiment using planktonic wild-type *V. parahaemolyticus* and a *ΔcheW* strain. (B) Chemotactic capillary experiments using wild-type *V. parahaemolyticus* and *ΔcheW* cells released from flooded swarm colonies. (A-B) Strains assayed for chemotaxis against N-acetylglucosamine, the component of chitin polymers. Error bars indicate standard error of the mean and is based on, at least, three independent biological replicates. P value was calculated using Student's t-test.

Planktonic cells showed a clear positive chemotactic response towards GlcNAc while no chemotactic response was detected for strain *ΔcheW* (Figure 17A). Thus, showing that *V. parahaemolyticus* RIMD 2210633 is able to sense and elicit a chemotactic response towards GlcNAc, which thus serves as a chemotactic attractant. Importantly, similar to planktonic cells, released cells from flooded swarm colonies also displayed a positive chemotactic response towards GlcNAc (Figure 17B). Thus, not only are cells released from swarm colonies highly swimming proficient, but also possess the

ability to perform chemotaxis towards an important source of food and habitat of *V. parahaemolyticus* in its natural environment.

3.1.7 A distinct regional architecture of mature swarm colonies

To further understand the function that released cells have on the spread of *V. parahaemolyticus* in the environment, we set out to analyze swarm colony development and how swarm colony architecture depends on fluctuations in the external environment – *e.g.* such as flooding. To address this, we initially set-out to define the swarm colony architecture and development. Particularly, we performed proteomic analysis on cells collected from the center and periphery (Figure 18A).
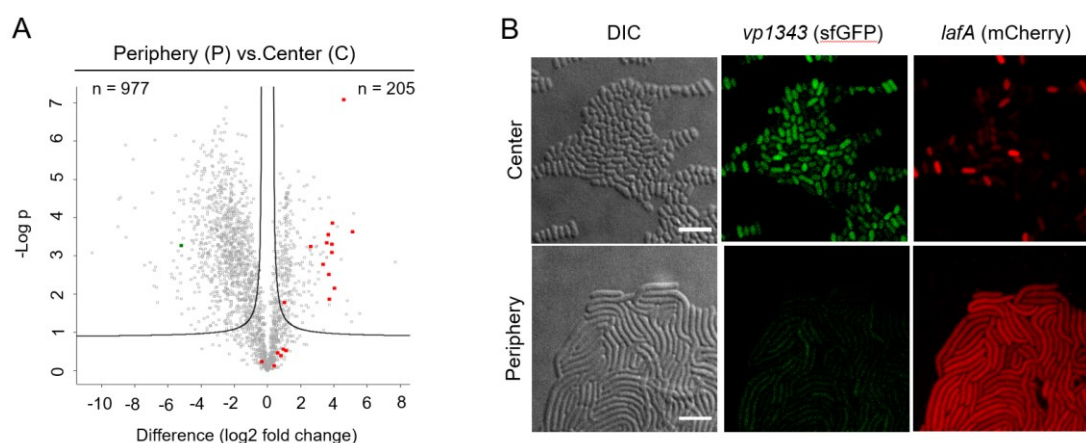
Figure 18. A distinct zonal architecture of mature swarm colonies. (A) Volcano plot depicting changes in protein intensities in a comparison of cell from the periphery vs. center of swarm colonies. X-axis indicates the difference (log2) of the intensities ratio. Y-axis indicates the -log of the p value. Number "n" indicates the number of differentially expressed proteins that were significantly up- and down-regulated. Highlights in red indicate lateral flagellum proteins. Highlight in green indicates the protein VP1343, which is significantly down-regulated in cells from the periphery. The promoter of *vp1343* was fused to T7 polimerase and the promotor of T7 polimerase was fused to *sfGFP* (P*vp1343::T7 and Pt7::sfGFP*) in order to monitor VP1343 expression. (B) Fluorescence and DIC microscopy of cells collected from the center and periphery of mature swarm colonies of CF36 strain.. In CF36 the promotor of *lafA* was fused to *mCherry* in order to monitor lafA expression, and the promoter of *vp1343* was fused to *T7 polimerase* and the promotor of *T7 polimerase* was fused to *sfGFP* (P*vp1343::T7 and Pt7::sfGFP*) in order to monitor *vp1343* expression.

From the 2077 identified proteins, 1186 were found differentially altered, including 977 down-regulated and 205 up-regulated in swarmer cells from the periphery compared to cells from the center of the colony (Figure 18A, Table 13). Interestingly, the majority of lateral flagella proteins were found to be significantly upregulated in the periphery cells, when compared to cells from the center consistent with periphery cells also

showing clear swarmer morphology (Figure 18A, in red, Table 13). These results show that not only are there morphological differences, but also significant changes in the protein expression profiles of cells depending on individual cells position within swarm colonies.

To further analyze how distinct these regions are within colonies, we took a microscopy approach. Particularly, we transcriptionally fused the two fluorescent proteins sfGFP and mCherry, respectively, to promoters of genes encoding proteins that based on our proteomics results were up regulated in the center (*vp1343*) and in the periphery (*lafA*) of the colony– strain CF36 (P$_{vp1343}$::*t7*, P$_{t7}$::*sfGFP*, P$_{lafA}$::*mCherry*). Consistent with the proteomics results, the fluorescence microscopy showed a clear and distinct difference in expression profiles between cells from the center and the periphery (Figure 18B). Particularly, sfGFP and mCherry expression was almost completely restricted to the center and periphery of the colony, respectively. Altogether, these results show that swarm colonies have a very structured architecture and are divided into specific regions of distinct cell types – not only on the morphological level, as has been previously reported, but also on the translational level. Particularly, it shows that fully differentiated swarmer cells – i.e. they are both morphologically differentiated and have initiated the LafK dependent swarm expression program – are found in the swarm flares of the periphery of the swarm colony, while cells in the center of the colony are distinctly different and do not have the swarm program activated. Thus, mature swarm colonies have a specific architecture and are comprised of regions of distinct cell types in different morphological and differential proteomic states.

3.1.8 Temporal architecture development of swarm colonies

To further understand how swarm colonies develop, we followed the progression of swarm colonies over time. Particularly, we took advantage of our double labeling strain that encodes sfGFP and mCherry expression from promoters that are specifically active in the center and periphery of fully developed swarm colonies, respectively. Additionally, in order to map the architectural development, swarm colony development was tracked using stereo-microscopy. Based on our analysis we could define four stages, stage I - IV, of swarm colony development, which ultimately results in a fully matured swarm colony with a defined architecture that is comprised of regions of specific cell types (Figure 19A): stage I, colony growth; stage II, differentiation initiation and swarm-flare formation; stage III, swarm-front expansion; and stage IV, swarm colony maturation and final architecture formation. Stage I was defined by a smooth colony periphery and the

absence of swarm flares (Figure 19A), all cells displayed a short-cell morphology throughout the colony and independent of their position in the center or the periphery of the colony (Figure 19A,B). Consistently, almost no cells had initiated the swarm specific gene program as only 1.6% were expressing mCherry from the PlafA promoter and ~90% were displaying sfGFP expression from the Pvp1343 promoter (Figure 19A,D). Stage II was defined by differentiation initiation and swarm-flare formation (Figure 19A). In the swarm flares, cells displayed an elongated-cell morphology (average of 6.5 µm in cell length) and a bigger variance in their cell sizes compared to the cells in the center of the colony that displayed an average of 3.3 µm in cell length and a small variance (Figure 19A-C).

A
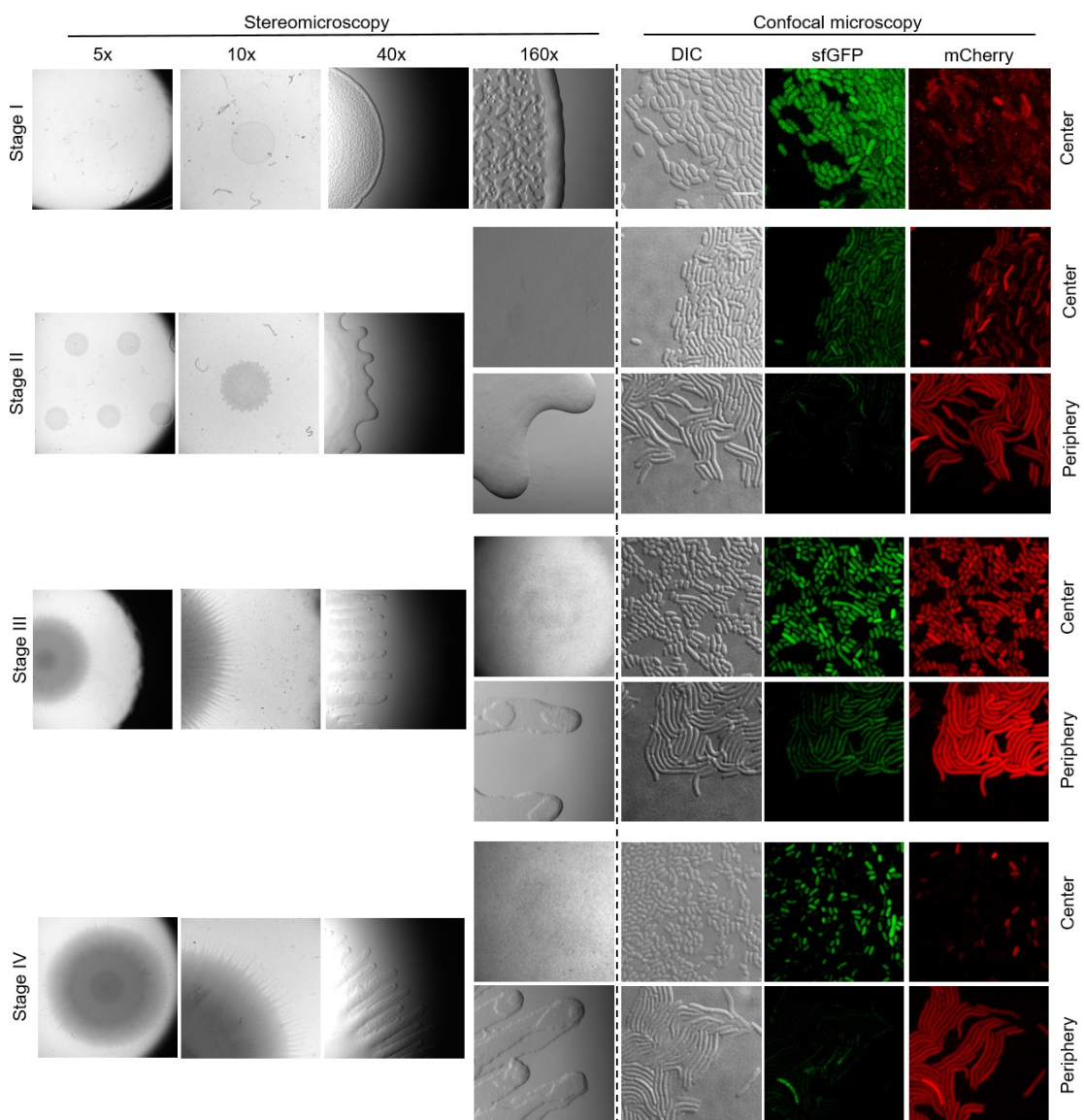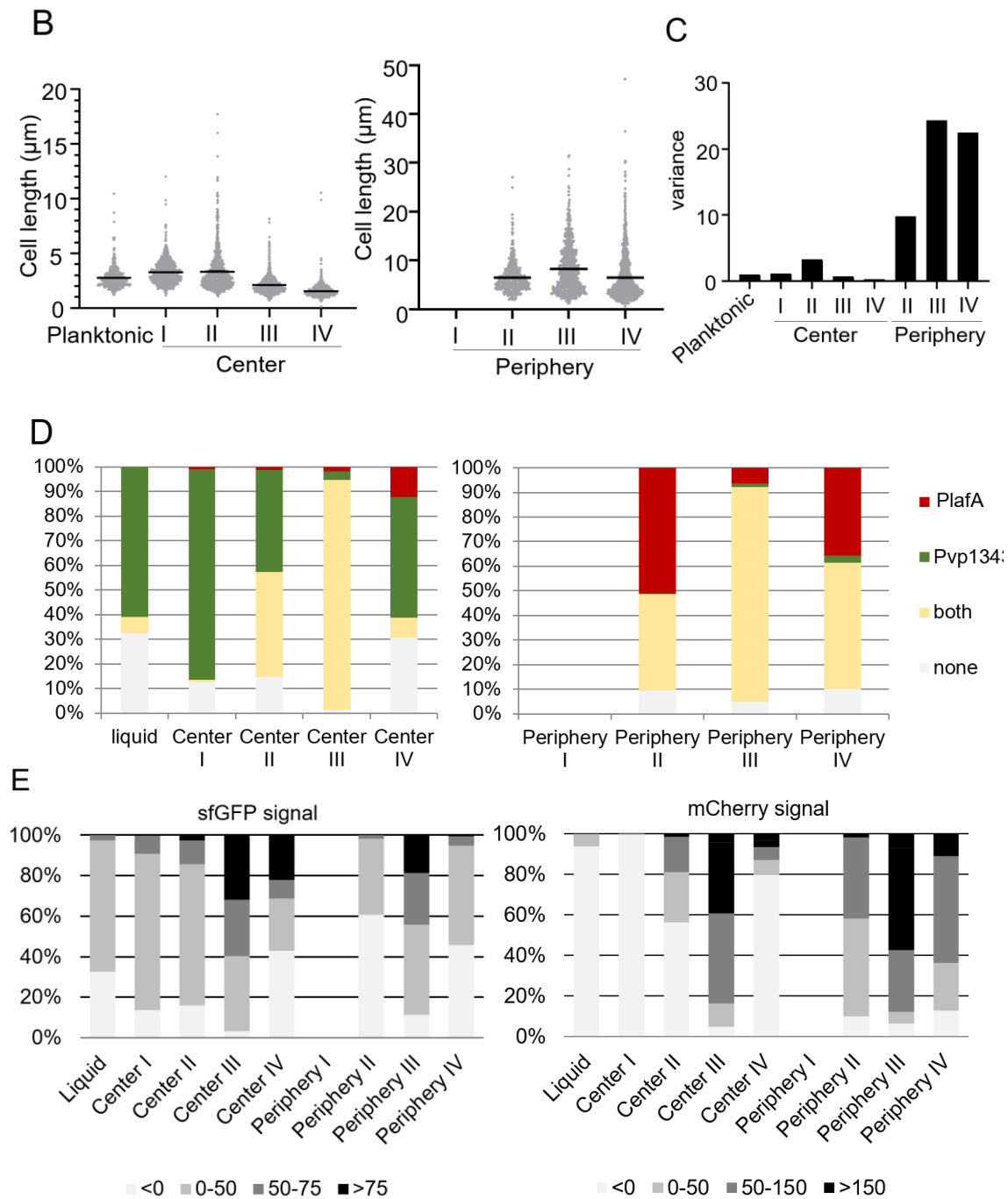
Figure 19. Temporal architectural development of swarm colonies. (A) Stereomicroscopy imaging of swarm colony architecture during the four stages (I-IV) of swarm colony development. Additionally, cells were collected from the center and periphery of swarm colonies and analyzed by DIC and fluorescence microscopy in order to evaluate cellular morphology and expression from the promoters P*vp1343* (sfGFP) and P*lafA* (mCherry), respectively. (B) Graph showing the cell length distribution of planktonic cells and cells from the center and periphery of swarm colonies during the four stages of swarm colony development. Black bars indicate the mean value. P value was calculated using Student's t-test. (C) Bar-graph showing the variance in cell length of cells from indicated environments. (D) Quantification of % of cells expressing mCherry and sfGFP proteins from indicated environments. Wild-type non-labelled cells from center, periphery and liquid were imaged with the same exposure time and laser power as CF36 strain to obtain values for autofluorescence. The 95 percentil of the autofluorescence intensity was calculated and this value was then subtracted to the fluorescence intensities of CF36 cells. As planktonic cells do not possess lateral flagella, the 95 percentil of the mCherry intensity from planktonic cells was calculated and this value was also subtracted to the fluorescence intensities of CF36 cells. (E)

Quantification of percentage of cells expressing different intensity levels of mCherry and sfGFP proteins from indicated environments. The 95 percentile of the wild-type auto fluorescence intensity was calculated for each environment and then subtracted to the fluorescence intensities of CF36 cells. The color code indicates the interval of fluorescent intensity values (A.U.).

Importantly, swarmer cell differentiation was initiated throughout the colony, with ~50% of cells expressing mCherry in the center of the colony and ~90% of cells expressing mCherry in the developing swarm flares. sfGFP expression from the Pvp1343 promoter was detected in ~85% of cells in the center and in only ~40% of cells from the periphery of the colony (Figure 19A,D). Stage III consisted of swarm-front expansion (Figure 19A). Interestingly, cell sizes were more segregated at this stage, with cells from the center displaying a decrease in average cell length (2.1 µm) and cells from the swarm flares displaying an increase in average cell length (8.2 µm), when comparing to the previous stage II. Additionally, cells in the swarm flares displayed a significantly bigger variance in their cell sizes when compared to cells from the center and cells from the periphery in stage II colonies (Figure 19C). Swarmer cell differentiation was present throughout the colony, with ~95% of cells expressing mCherry in both center and periphery regions of the colony. sfGFP expression from the Pvp1343 promoter was detected in ~100% of cells in the center and ~90% of cells in the expanding flares in the periphery of the colony (Figure 19A, D). Stage IV was characterized by swarm colony maturation and final architecture formation (Figure 19A), where cells from the center displayed the shortest cell length average of all stages (1.6 µm). Cells from the flares maintained their elongated cell morphology with an average of 6.5 µm in cell length and a significantly higher variance comparing to cells in the center (Figure 19A-C). Importantly, at this last stage there was a distinct difference in expression profiles between cells from the center and the periphery, with only ~20% of cells expressing mCherry in the center of the colony and ~90% expressing mCherry in the developing swarm flares in the periphery of the colony. Although the percentage of cells expressing sfGFP from the Pvp1343 promoter was similar between cells in the center (~60%) and in the periphery (~55%), the intensity of the sfGFP signal was stronger in the cells in the center compared to cells in the periphery (Figure 19E). Only 0.6% of cells from the periphery compared to 22% of cells from the center emit fluorescence intensity higher than 75 A.U (Figure 19E). Thus, these results show that during its development a swarm colony encompasses distinct regions of cells that display fluctuations in their expression profile, ultimately resulting in a final mature stage (stage IV) where the colony consists of two distinct regions with a clear difference between expression profiles and cellular morphology.
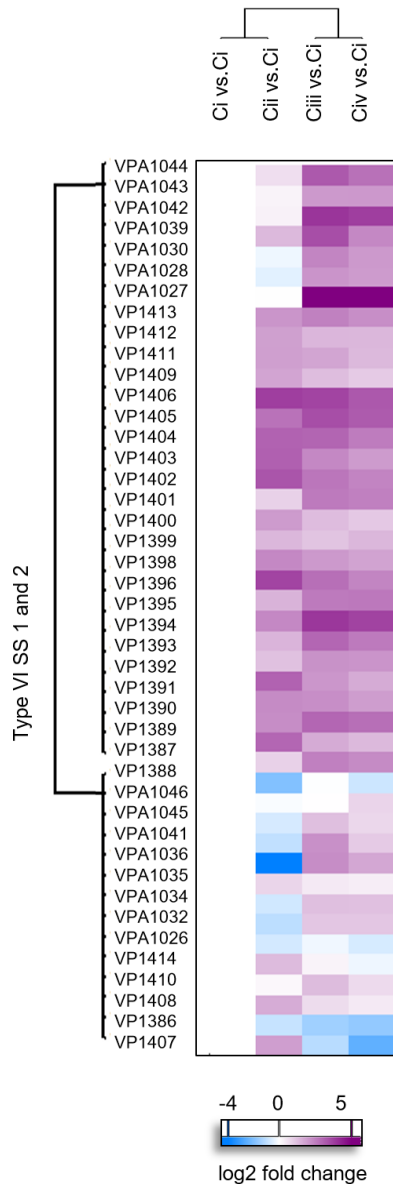
Figure 20. Clustering map depicting changes in intensities ratios of proteins of type secretion system 1 (Type VISS1) and 2 (Type VISS2). All proteins from type VISS1 start with VP# and all proteins from type VISS2 start with VPA#. Four sets of comparison were made: Center stage I vs.Center stage I (Ci vs. Ci), Center stage II vs.Center stage I (Cii vs. Ci), Center stage III vs.Center stage I (Ciii vs. Ci) and Center stage IV vs.Center stage I (Civ vs. Ci).

Additionally, we performed proteomics on cells in the center of the swarm colony in the four stages of swarm colony development. From the 2885 identified proteins, the number of differentially altered proteins increase with the progression of the colony development. Particularly, 319 proteins were differentially expressed when comparing stage II with stage I (Cii vs. Ci), but this number rose to 1321 and 1418 in stage III and IV in comparison with stage I (Ciii vs. Ci and Civ vs. Ci). Moreover, 81 proteins were up-regulated and 74 proteins were down-regulated in cells from the center of the colony

during stage II, III and IV when compared to stage I (Table 14). Interestingly, many of the proteins whose expression continuously increased during development were proteins of the Type VI secretion system 1 (Type VISS1) (Figure 20). As *V. parahaemolyticus* Type VISS1 conferes virulence against other Gram negative bacteria (Salomon *et al.*, 2013), our results suggest that cells under swarm induction conditions seem to be activated for an antibacterial program mechanism.

3.1.9 *V. parahaemolyticus* colonies act as recurrent sources of swarmer cells during fluctuations in the external environment

Next we asked what the consequence is on swarm colony development and architecture, if the colony fluctuates between distinct environments that either stimulate or suppress swarming behavior. To this end, swarming was first induced and after reaching stage IV of development, the colony was transferred to non-swarming conditions and imaged by stereo and confocal fluorescence microscopy 5h and 23h post-transfer. Subsequently, the colony was then transferred back to swarm-inducing environments and imaged after 24h. The experiments showed significant changes in colony architecture and in its composition of cell types as a consequence of the environmental changes (Figure 21A-D).Following transfer to non-swarming conditions there was a clear cessation to swarming expansion and an increase in cell density within swarm-flares produced during the initial swarm-colony expansion (Figure 21A). Furthermore, cells from flares experienced a change in their morphology from being highly elongated during the initial swarming and showing high expression from the PlafA promoter, to a short cell type similar in length to that of cells from the center of swarm colonies (Figure 21B,C) and did no longer express from the PlafA promoter (Figure 21B, D). When the colony once again was transferred to swarm stimulating conditions new swarm flares formed and spread from the periphery of the colony (Figure 21A) and cells from flares showed full morphological swarmer differentiation (Figure 21B,C) and had initiated the swarm program (Figure 21B,D).

Interestingly, a similar fluctuation between differentiation/dedifferentiation and corresponding swarm expansion/swarming cessation occurred when swarm colonies were subjected to flooding, and subsequent drying and transfer to swarm stimulating conditions (Figure 22A-D). Importantly, subsequent to flooding multiple satellite colonies formed at various distances from the mother colony. When transferred to swarm inducing conditions cells from all of these satellite colonies induced the swarm program and

differentiated into swarmer cells, resulting in swarming expansion of the colony (Figure 22A-D).
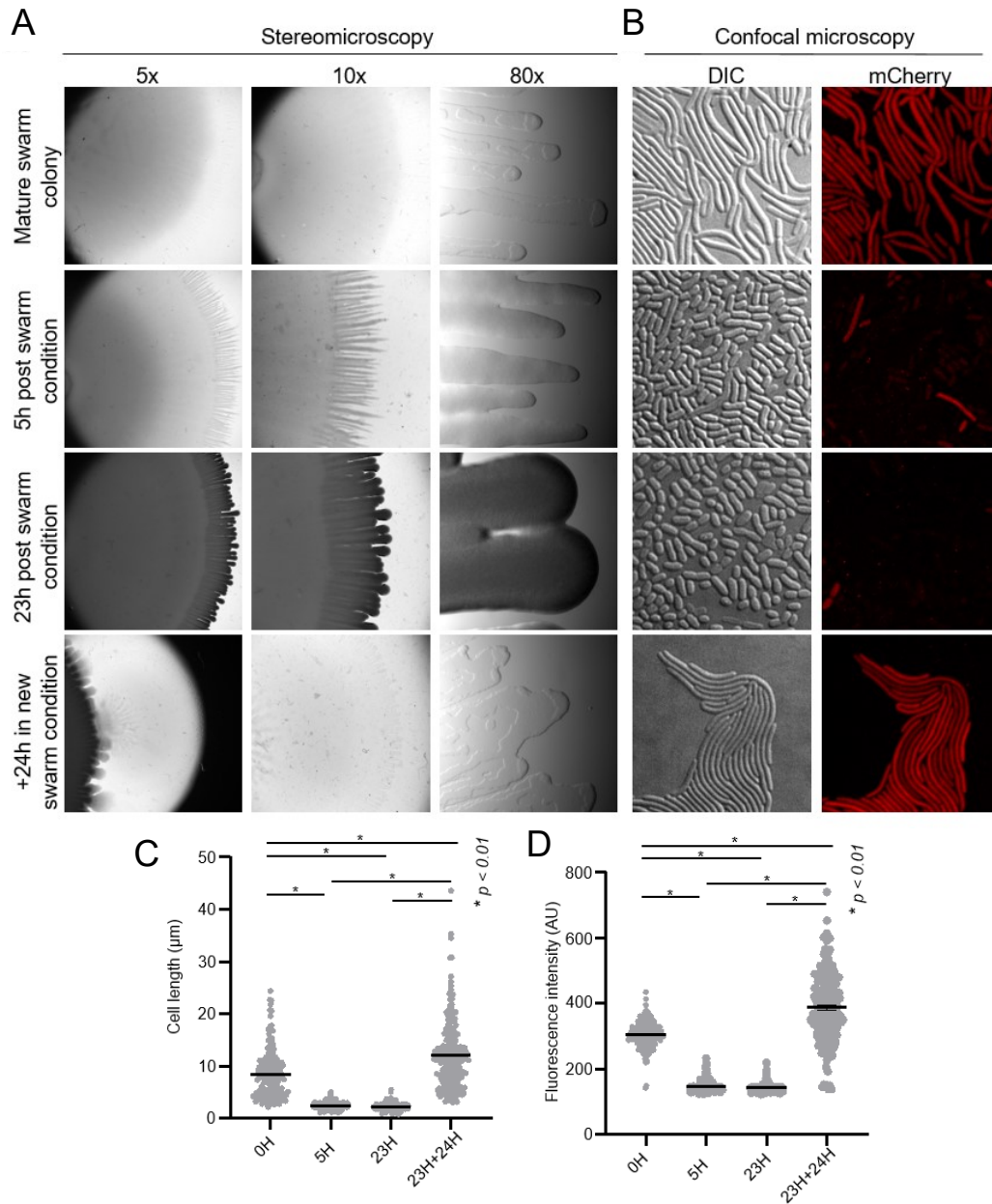
Figure 21. ***V. parahaemolyticus* colonies act as recurrent sources of swarmer cells during fluctuations in the external environment.** (A-B) Stereomicroscopy imaging of swarm colony architecture (A) and DIC and fluorescence microscopy (B) in order to evaluate cellular morphology and expression from the swarm-specific promoter P*lafA* (mCherry). (C) Graph showing the fluorescence intensity (A.U) distribution of cells from the periphery of colonies imaged in "B". (D) Graph showing the cell length distribution of cells from the periphery of colonies imaged in "A-B". In C, D black bars indicate the mean value, and P value was calculated using Student's t-test.
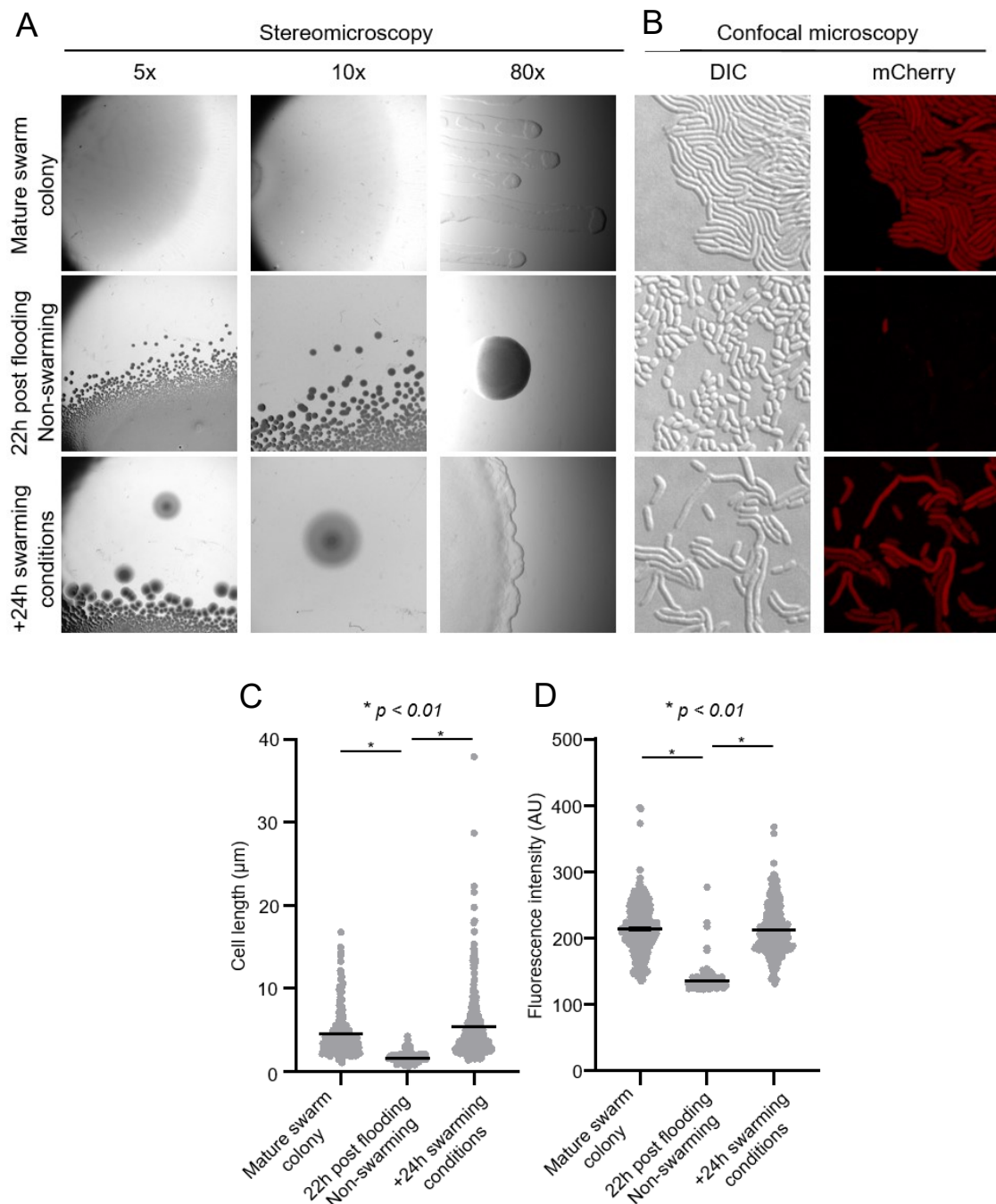
Figure 22. *V. parahaemolyticus* **colonies act as recurrent sources of swarmer cells after flooding conditions.** (A-D) Stereomicroscopy imaging of swarm colony architecture (A) and DIC and fluorescence microscopy (B) in order to evaluate cellular morphology and expression from the swarm-specific promoter P*lafA* (mCherry). (C) Cell length distribution of cells from the periphery of colonies imaged in "A-B". (D) Graph showing the fluorescence intensity (A.U) distribution of cells from the periphery of colonies imaged in "B". In C,D black bars indicate the mean value, and P value was calculated using Student's t-test.

Altogether, these results show that *V. parahaemolyticus* colonies act as recurrent sources of swarmer cells during fluctuations in the external environment and that the colony itself undergoes significant architectural changes with specific differentiation and dedifferentiation events within the colony flares.

3.2 Discussion

The incidence of *V. parahaemolyticus* is highest in estuarine areas than in offshore sea. In both natural environments, *V. parahaemolyticus* occurrence is almost exclusively linked to the distribution of zooplankton. Over an 18-month period only 12% of the water samples from offshore sea contain *V. parahaemolyticus* (Martinez-Urtaza *et al.*, 2012). In estuarine areas, during summer months, more than 80% of *V. parahaemolyticus* is found associated with plankton or plankton detritus, rather than in the water column (Kaneko and Colwell, 1973). Additionally, it was shown that oysters that are exposed on the sunny mudflats, accumulate high concentrations of this bacterium, followed by a striking decrease when the tidal waters covered the shellfish (Jones *et al.*, 2016). This occurrence led us to interrogate if the cells attached to the shelfish are released into the tidal water and if this is an active mechanism. Indeed our results verify that once swarm colonies are flooded, a specific cell type is actively released from the solid surface into the liquid environment. Additionally, we demonstrated that the released cells from the swarm colony are characterized by a sub-population of cells containing the correct size to swim efficiently and comprising the ability to re-attach to chitin surfaces. Thus, our results suggest the release of a distinct cell type from swarm colonies facilitates the dissemination of this important human pathogen in the environment. We defined cells belonging to this group as a population of "adventurer" cells.

Chitin is a polymer of *N*-acetylglucosamine (GlcNAc) and a structural polysaccharide found in zooplankton and the outer shells of crustaceans, being the most abundant polymer in the ocean. Therefore, it is not surprising that all sequenced *Vibrio* species encode genes for degradation of chitin (Brennan, 2013). The chitinases (EC 3.2.1.14) secrete by bacteria generate N,N´-diacetylchitobiose $(GlcNAc)_2$ as a final chitin hydrolysis product, which the bacteria can then use as a nutrient. It was previously showed that *V. parahaemolyticus* and *V. alginolyticus*, are chemotactic towards GlcNAc-GlcN and $(GlcNAc)_2$ (Hirano *et al.*, 2011). The chemotaxis assays presented in this study further clarified that released cells from *V. parahaemolyticus* swarm colony can sense the chitin derivative sugar GlcNAc and swim towards its highest concentration. As mentioned before, in offshore sea, *V. parahaemolyticus* is found mainly associated with zooplankton. As marine waters are limited in nutrients, the commensal relationship of *V. parahaemolyticus* with zooplankton represents a food source that ensures survival during prolonged journeys. Consequently, to sense and locate chitin via chemotaxis is

the extreme relevance for the ecological distribution and survival of these bacteria. We argued that bacteria attached to zooplankton can be transported along with the ocean current and migrate to distant regions and habitats, and thereby the ability of released cell to re-attach to chitin is pertinent for *V. parahaemolyticus* demography and epidemiology. Furthermore, chitin digestive bacteria slowly decompose non-living zooplankton and shellfish. Therefore, the ability to digest this polymer implies an ecological significance in the recycling of this organic matter.

The occurrence of *V. parahaemolyticus*, over a 1-year period study, was in all months, higher and more stable in mud samples than in tidal water (Di *et al.*, 2017). This suggests that mud can serve as a reservoir for *V. parahaemolyticus*, especially in winter. Interestingly, our results also show that once swarm colonies are flooded, cells released from swarm colonies are able to spread and spawn new daughter colonies that, when the conditions are favorable, are able to initiate swarmer differentiation – hereby facilitating the colonization and distribution of *V. parahaemolyticus* over new surfaces. Thus, our results indicate that *V. parahaemolyticus* colonies act as recurrent sources of swarmer cells during fluctuations in the external environment.

Based on all this information, we can summarize the swarm colony development and how its architecture allows for the release of a distinct cell type facilitating dissemination of *V. parahaemolyticus* in the liquid environment. Once a cell attaches to a solid surface (Figure 23 #1) and is under swarm inducing conditions, the cell can initiate the development of a swarm colony. Stage I of this development consists of growing and increasing of cell density (Figure 23 #2). Once the cell density has reached a certain threshold, the swarm colony enters stage II of development, where cells start differentiating and forming swarm-flares (Figure 23 #3). In stage III of development, the swarm-front starts expanding (Figure 23 #4) and subsequently, in stage IV of development, swarm colony maturation and final architecture formation is achieved. At this stage there are two distinct regions of the colony - the center containing cells expressing high levels of *vp1343* and the flares predominantly containing cells with the differentiation program active, expressing *lafA* (Figure 23 #5).

1.Attachment

2.Colony growth

3. Differentiation and swarm-flare formation

4. Swarm-front expansion

6. Chemotaxis + Chitin binding

5. Release of adventurer cells from a flooded mature swarm colony
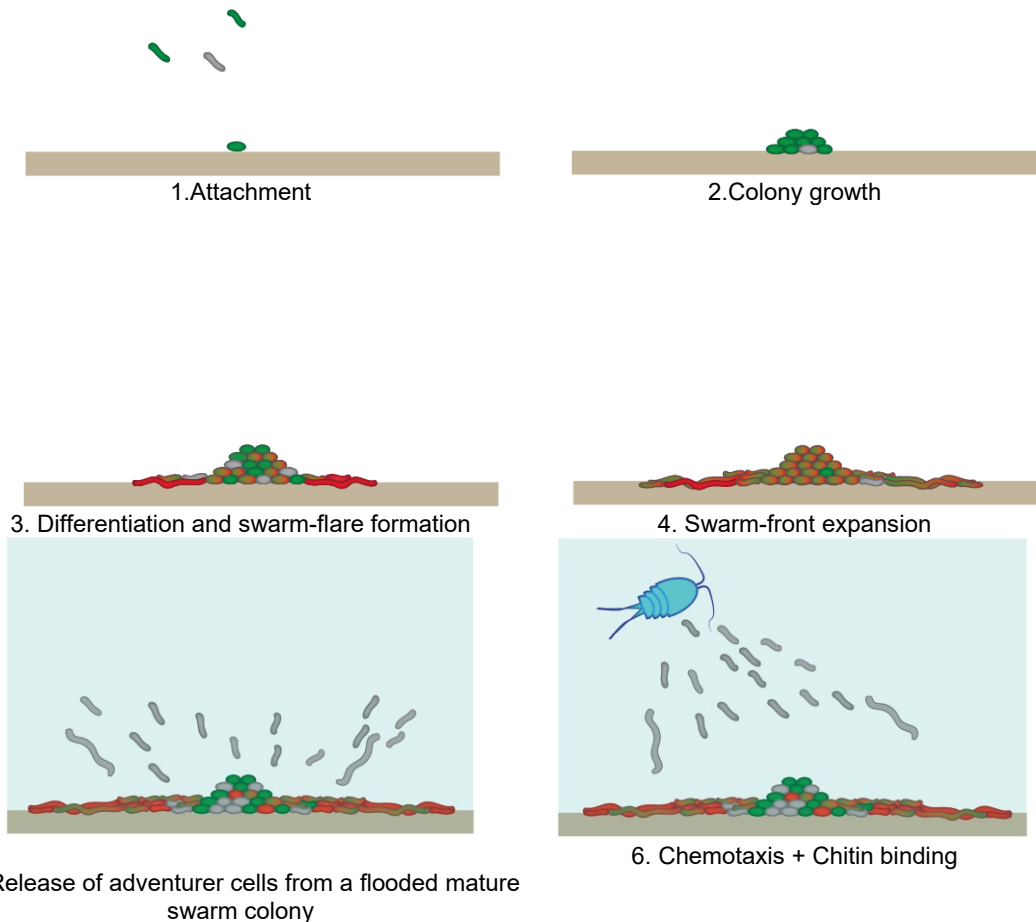
Figure 23. Schematic summarizing our current model. 1) Planktonic cell attaching to a solid surface; 2) Stage I of swarm colony development: colony growth. Under swarm inducing conditions, the cell will activate the swarming program; 3) Stage II of development: differentiation initiation and swarm-flare formation; 4) Stage III of development: swarm-front expansion; 5) Stage IV of development: swarm colony maturation and final architecture formation. Once the swarm colony is flooded, a morphologically short and specific cell type is released into the liquid – the adventurer cells; 6) Adventurer cells are highly swimming proficient and can chemotax towards an attractant such as, the GlcNA chitin component. When the tide goes down, adventurer cells can also reattach to the dry surface and, under swarm conditions, reinitiate development of the swarm colony. In developmental stages I,II,III and IV, the colour of cells in the center and periphery is in agreement with the values from our quantification analyses, that disclose the amount of cells expressing *vp1343* (green), *lafA* (red), both genes (green and red) or none (grey).

Once the swarm colony is flooded, a morphologically short and specific cell type is released into the liquid – the adventurer cells (Figure 23 #5). Adventurer cells are highly swimming proficient and can chemotax towards an attractant such as the GlcNAc chitin component. Released cells can re-attach to submerged surfaces, such as the zooplankton exoskeleton (Figure 23 #6). This zooplankton may operate as a vehicle for dispersal of *V. parahaemolyticus* populations in the open sea, drifting along with the

ocean currents, connecting distant regions and habitats, and thereby having an impact on the demography and epidemiology of the bacterial community. Based on our research, the cycle can continue and recommence (Figure 23 #1), since we have shown that released cells are capable of reattaching to new surfaces and spawn new colonies that depending on their environment also will result in the formation of swarm colonies and fast expansion of the colony over solid surfaces.

It is not clear where exactly the released bacterial cells are located within the swarm colony before they disperse. To address the question if released cells are coming from the center or from the periphery of the swarm colony, further studies have to be performed.

There are many example of bacterial species that actively release cells from submerged biofilms into the surroundings and this is dependent on specific trigger signals (Webb *et al.*, 2003; Thormann *et al.*, 2005; Morgan *et al.*, 2006; Barraud *et al.*, 2006; Singh *et al.*, 2017). Here we show that also in a swarm colony, cells are actively being released into the water environment. One remaining question is what are the mechanisms and signals to trigger the release of these cells within the swarm colony into the surroundings. According to our proteomic results, proteins related to oxidative stress such as presence hydroxide peroxide, namely VPA1418, VPA0350, VPA1684, VP2753, represented almost half of the specific up regulated proteins in released cells (Table 12, Figure 15B). Another hit was VPA0563 or Dps, an iron homeostasis related protein. In *E. coli*, Dps protein is induced after exposure to H_2O_2 stress and it strongly prevents DNA damage by sequestering iron (Altuvia *et al.*, 1994; Ilari *et al.*, 2002; Greco *et al.*, 2004; Park *et al.*, 2005). Interestingly, it has been shown that hydroxide peroxide induces biofilm dispersal, by activating transcription of the β-hexosaminidase *dspB* in *A. actinomycetemcomitans* (Stacy et al., 2014). The presence of hydroxide peroxide led to expression of a catalase (KatA) as a detoxification mechanism and to expression of Dispersin B (DspB) an enzyme that hydrolyses the exopolysaccharide poly-GlcNAc, a major component of the extracellular matrix of *A. actinomycetemcomitans* biofilms (Kaplan *et al.*, 2004; Stacy *et al.*, 2014). Overall our proteomics results show that released bacteria have a specific proteomic distinct from planktonic or sessile states. Additionally, our data shows that bacteria residing at various regions of the swarm colony might experience different levels of oxidative tensions which will induce the production of proteins that can react against reactive oxygen species in order to achieve cell redox homeostasis. The fact that these proteins were up regulated specifically in the released

cells strongly suggests that reactive oxygen species might be one of the signals involved in dispersal of cells from the swarm colony of *V. parahaemolyticus*.

V. parahaemolyticus differentiation into a swarmer cell would enable this bacterium to explore the surface faster than other competing bacteria, as many marine chitin colonizers species, are not able to swarm over surfaces. The type VI secretion system (TVISS) is recognized as an important virulence and interbacterial competition mechanism in several Gram-negative pathogens (Hood *et al.*, 2010; MacIntyre *et al.*, 2010; Schwarz *et al.*, 2010; Miyata *et al.*, 2011). *V. parahaemolyticus* TVISS1 is active under marine like conditions and it conferes anti-bacterial virulence against other Gram-negative bacteria, including the human pathogen *V. cholerae* (Salomon *et al.*, 2013). In our study, levels of TVISS1 proteins were continuously increasing in the cells from the center during swarm colony development (Table 14). Altogether, our data suggests that type VISS1 machinery is induced during swarming conditions, which could enable this bacterium to succeed in invading the solid territory by killing other colonizing bacteria. Interestingly, as the proteome of released cells is also enriched in TVISS proteins when compared to planktonic cells, released cells seem to be prepare to compete with other colonizers once they reach the next surface location. A parallel comparison can be made with *S. pneumoniae* biofilm dispersed cells that show a pattern of virulence gene expression that will help them in their next environmental context - the host - allowing them to invade and kill human respiratory epithelial cells more effectively and to induce high pro-inflammatory cytokine responses (Marks *et al.*, 2013). *P. mirabilis* is a swarm organism that uses TVISS to export an identity-encoding protein, IdsD important for cell-cell communication. The intercellular exchange of IdsD leads to separation of colonies of genetically distinct populations and allows the merging of identical populations (Wenren *et al.*, 2013; Saak and Gibbs, 2016). Maybe in *V. parahaemolyticus* TVISS1 also has an additional of social communication that will, in turn, regulate swarm colony expansion.

From the proteomics performed over time in cells from the center of a swarm colony, we can appreciate the fact that levels of both the master of quorum-sensing OpaR and the general stress resistant sigma factor RpoS were higher in stage IV when comparing to the previous stages of swarm development of cells in the center. These results are in agreement with the findings regardig dispersal of biofilms in *V. cholerae,* where the levels of HapR (OpaR homologue) are not enough to trigger dispersal response, as cells also need a stress signal that leads to RpoS induction, in order to disperse (Singh *et al.*, 2017).

The fact that many bacterial species display swarming motility in the laboratory and thus possess mechanisms to override surface obstructions, indicates that swarming behavior must be an important mean of invading and colonizing more surface area in their natural habitats (Alberti and Harshey, 1990; Sar *et al.*, 1990; Harshey, 1994; Kirov *et al.*, 2002; Rather, 2005)*. V. alginolyticus*, a close relative to *V. parahaemolyticus*, can also differentiate into elongated swarmer cells with multiple lateral flagella once it encounter solid surfaces (Böttcher *et al.*, 2016). These two species are among the most frequently encountered marine bacteria (Böer *et al.*, 2013). *V. alginolyticus* is an opportunistic pathogen causing ear infection and intestinal disease in humans and high-mortality vibriosis in marine animals (Hornstrup and Gahrn-Hansen, 1993; Mustapha *et al.*, 2013). Here we described how swarm colonies facilitate the dissemination of *V. parahaemolyticus* in the environment and its re-attachment to new surfaces. We argue that swarm colonies from other pathogenic bacteria living in estuarine areas, such as *V. alginolyticus*, might also present a similar spreading mechanism like *V. parahaemolyticus* based on the release of distinct swimming proficient cells from swarm colonies. Particularly, in fluctuating environments, where surfaces upon which the swarm colony is attached, experience periodic flooding. Thus, we speculate that the work presented here could represent a general mechanism that is utilized by other swarming proficient bacteria to allow for the release of swimming proficient cells from swarm colonies and the consequential dissemination of the bacterium in the liquid environment, whilst permitting rapid surface colonization.

Chapter IV - Potential swarm-regulators and distinct proteomic identities of *Vibrio parahaemolyticus*

4.1 Results – Part II

4.1.1 Set of periphery-specific proteins

The results presented in Chapter III of this work revealed that depending on the position of cells within swarm colonies, there are significant changes in their proteomic expression profile. Particularly, in swarmer cells from the periphery, 1186 out of the 2077 identified proteins were found to be differentially altered compared to cells from the center of the colony (Table 13). For instance, there was a significant increase in the levels of lateral flagella proteins in the cells from the flares of the swarm colony. This result nicely correlates with a clear swarmer cell-type morphology presented by these cells. Thus, here we further sought to unravel what proteins are specifically regulated in a swarmer cell-type. Therefore, we compared the proteome of cells located in the flares of a swarm colony with three other conditions, 1) cells from the center of the colony 2) planktonic cells grown in LB (liquid) medium and 3) cells grown on an LB-agar (solid, non-swarm inducing conditions) plate. Periphery condition was quite different not only from the center of the swarm colony as previously shown, but also from either liquid or solid conditions (Figure 24A). A total of 432 and 1256 proteins were differentially regulated between Periphery vs. Liquid and Periphery vs. Solid, respectively (Figure 24B).

In order to identify which proteins are swarmer cell specific, an overlap between the proteins differentially expressed in the cells from the periphery of the swarm colony compared to the cells in the center of the colony (P vs. C), cells grown in solid (P vs. S) and cells grown in liquid (P vs. L) was performed. Upon looking at the commonly and significantly up- and down-regulated proteins among the aforementioned three comparisons, we found 62 induced and 81 repressed proteins differentially expressed exclusively in the periphery (Figure 24B, Table 15). These 114 swarm specific proteins were further categorized in terms of their function. Fourteen categories represent all swarming specific proteins (Figure 24C). A detailed plot containing the name, functional domain and fold change of periphery specific proteins is available in the supplementary materials (Figure 30, Figure 31).

Lateral flagella genes and chemotaxis proteins comprised the largest fraction of up-regulated proteins with 27% and 18%, respectively (Figure 24C, left). Among the down-regulated targets, metabolic proteins constituted the largest fraction (52%),

followed by transcriptional regulators and DNA binding proteins (12%) (Figure 24C, right).

Figure 24. Comparative analyses of the proteome of *V. parahaemolyticus* in four different conditions to define a set of swarming periphery proteins. P-periphery, C-center, S-solid, L-liquid (A) Clustering map depicting changes in protein intensities in three sets of comparison: Periphery vs. Solid (P vs.S), Periphery vs. Center (P vs.C) and Periphery vs. Liquid (P vs. L) B). Venn diagrams showing intersection among the three aforementioned comparisons with enhanced (left) and reduced (right) protein intensities. Statistical analysis of all ratios were performed using unpaired Student´s t-test (FDR 0.01 and S_0=0.2) and a 2-fold regulation cutoff. C) Pie-charts for functional categories of up- and down- regulated swarming proteins. Classification of the molecular function and categories of the identified proteins was based on a UniProt KB search, Interpro analysis and gene ontology (GO) annotations.

There are groups that were found to be exclusive to either the up- or down-regulated set of proteins. Particularly, proteins involved in the lateral flagella, chemotaxis-related proteins and polar flagella proteins were found only among the up-regulated targets whereas cell division, chaperone and transcriptional regulator proteins were specific to the down-regulated group (Figure 24C).

Regarding proteins related to the bacterial secretion system, type VISS1 proteins were present in the up-regulated group (Figure 24C). As mentioned in Chapter III of this thesis, type VISS1 seems to be induced during swarm colony development, thereby likely enabling the swarmer cell type with an antibacterial machinery that is functional against potential competitors, during surface colonization. Some of the other categories displayed here will be discussed in detail in section "4.2 Discussion".

4.1.2 Potential swarm-regulators

From the obtained proteome specific to the swarmer cell type, we chose specific candidates to perform deletion strains of *V. parahaemolyticus* in order to find new potential swarm-regulators. Fifteen genes (which encode for 10 up- and 5 down-regulated proteins) were deleted in a wild-type *V. parahaemolyticus* strain and swarming assays were performed (Table 1).

The proteins presented in Table 1 were selected during the first run of mass spectrometry. The results obtained during our first run were values regarding peptide counts. Peptide counts constitute an estimate value of the protein levels, while intensity values obtained through label-free quantification (LFQ) represent a more accurate and precise measurement. After obtaining the corresponding LFQ values, the ratios between P vs. C, P vs. S and P vs. L, were updated and some of these ratios were found to differ from the initial first analysis– that is, the ones obtained through peptide counts. Therefore not all the targets chosen for deletion were found to belong to the final list of the swarm specific proteins (Table 15). Table 16 shows the fold change of these 15 proteins in P vs. C, P vs. S and P vs. L, based on the LFQ values.

Table 1. Name and function of the 15 genes that were selected for deletion based on proteomic analyses.

	Protein number	Description	Swarm phenotype of deletion mutant compared to wild-type
Up-regulated	VP0053	CinA Competence-damaged protein	=
	VP0649	Uncharacterized	+
	VP1391	Type VISS protein - transcriptional regulator	+
	VP2240	Polar flagella protein	-
	VP2972	Signal transduction c-di-GMP phosphodiesterase, EAL/HD-GYP	-
	VPA0584	DNA-binding protein VF530	=
	VPA0754	Endonuclease/Exonuclease/phosphatase family	+
	VPA1083	Ribokinase	-
	VPA1176	EAL _domain (cyclic-di-GMP)	+
	VPA1649	Metalloprotease, peptidase family M23	+
Down-regulated	VP0514	Sigma-54 dependent transcriptional regulator	=
	VP0764	Outer membrane protein OmpA	+
	VP1945	Transcriptional regulator, LuxR family- two-component system, NarL family, invasion response regulator UvrY	-
	VPA0662	Transcriptional regulator, MerR family	=
	VP2178	Nucleoid-associated protein	-

In order to perform the swarming assay, 1 µL of dense liquid culture was spotted in a petri dish containing a specialized medium (Heart Infusion-based 1% agar), and upon incubation at 24ºC for a period of at least 18 hours, cells grow radially forming a swarm colony with a circular shape. To check if the swarming efficiency of *V. parahaemolyticus* was affected by deletions of the above mentioned genes, both wild-type and the respective mutant strain were spotted far apart in the same petri dish, and after 18h of incubation at 24ºC the diameter of each swarm colony was measured.
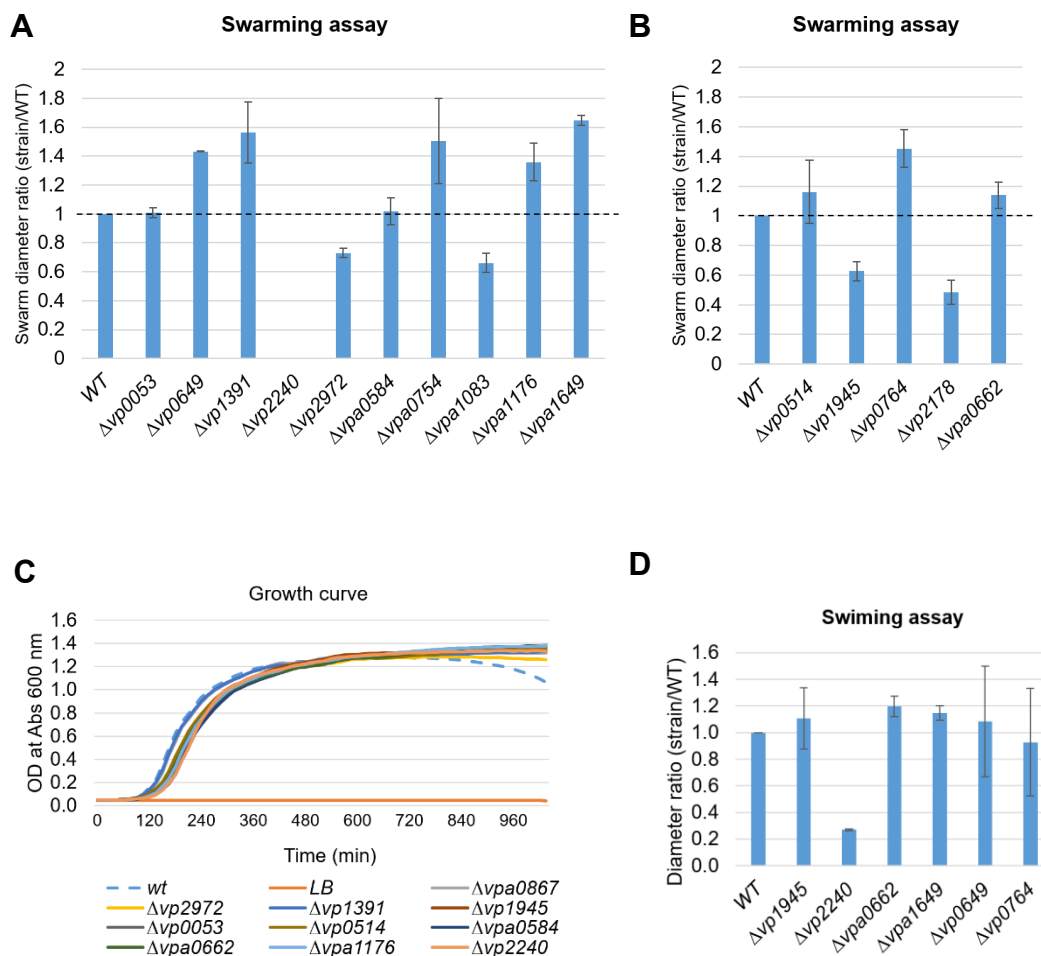
Figure 25. Phenotypical analyses of single deletion strains of *V. parahaemolyticus*. (A) Swarming assay with mutant strains whose deleted genes are up-regulated in cells from the periphery of a swarm colony (n=3 to 10). The x axis represents the ratio of the mutant diameter vs. the wild-type diameter of the swarming colonies. (B) Swarming assay with mutant strains whose deleted genes are down-regulated in cells from the periphery of a swarm colony (n=6 -10). The x axis represent the ratio of the mutant diameter vs. the wild-type diameter of the swarming colonies (C) Growth curve assay with mutants strains from up-regulated group and down-regulated groups. OD_{600} of each strain is plotted against time (in minutes). Non-inoculated LB medium was used as the negative control. (D) Swimming assay. The x axis represents the ratio of the mutant diameter vs. the wild-type diameter of the swimming colonies.

While deletion of some of the genes that were up-regulated in the swarmer cell type, namely Δ*vpa1083* and Δ*vp2972*, displayed around 30% reduced swarming, deletion of one candidate, namely Δ*vp2240* presented completely abolished swarming motility (Figure 25A) compared to wild-type. Interestingly, although *vp1945* and *vp2178* are genes whose proteins were down-regulated in the swarmer cell type, their deletions resulted in reduced swarming (Figure 25B). Additionally, six mutants were hyper-swarmers compared to wild-type, suggesting that these genes in wild-type cells might have a negative effect on swarm colony expansion (Figure 25A,B).

Importantly, all strains when propagated in liquid surroundings were indistinguishable from wild-type in regard to growth and cell morphology (Figure 25C). Thus, suggesting that the swarming phenotype observed it is not due to a deficiency in growth or in cellular morphology. Among the strains tested for swimming motility, only Δ*vp2240* displayed a clear swimming reduction, when compared to wild-type (Figure 25D). Δ*vp0649*, Δ*vp0764*, Δ*vp1945* and Δ*vpa1649* showed a swimming profile similar to the wild-type strain, which supported the hypothesis that such genes play a specific role in swarming motility (Figure 25D). Interestingly, a considerable number of genes that encode for up-regulated proteins showed hyper-swarming instead of reduced swarming. These proteins and their possible roles in swarming will be discussed in the section "4.2 Discussion".
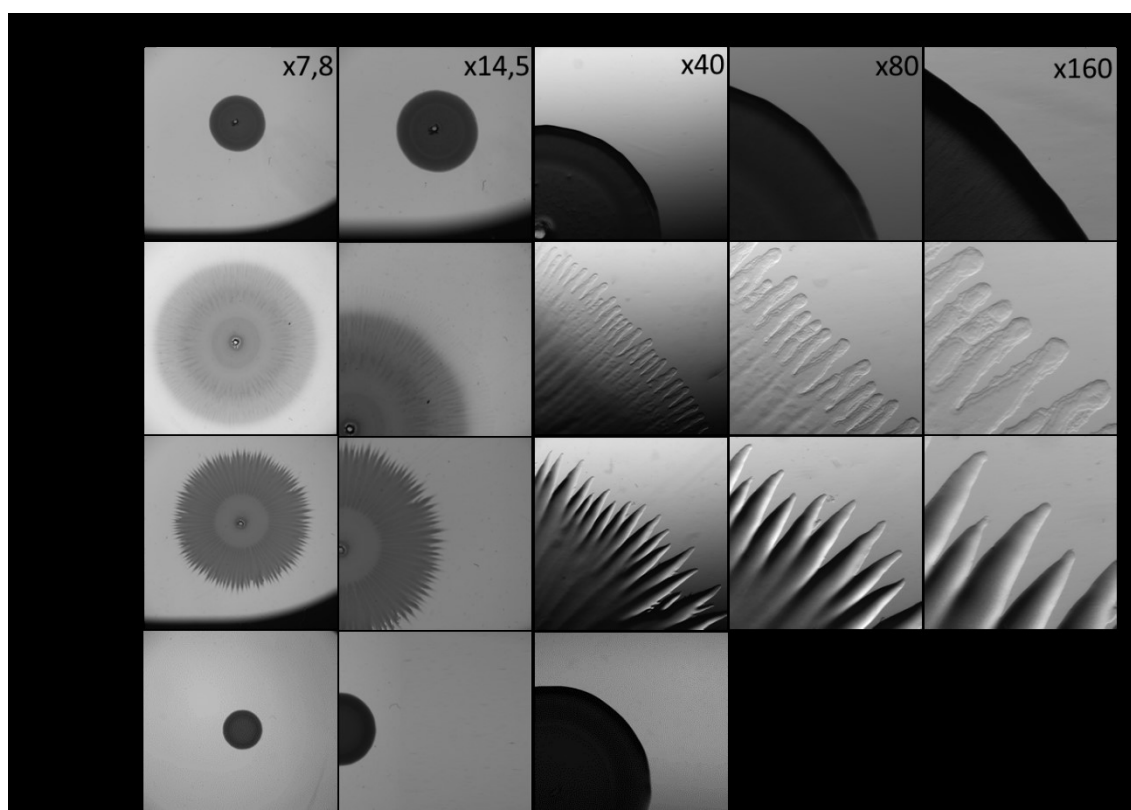
Figure 26. Morphological analyses of single deletion strains of *V. parahaemolyticus*. Swarming assays were performed by spotting the respective mutant strains in the same plate as wild-type and Δ*lafA* strain- as a negative control. The plates were then observed under a stereomicroscope and pictures were acquired at the specified magnifications. The images presented here are representative of at least three biological replicates.

Overall, two of the most striking swarming phenotypes were the deletion strains of *vp2240*, a polar flagella gene and *vp1945*, a putative transcriptional regulator. Hence,

we decided to observe if there were significant morphological differences in the swarm colony of these strains, by using stereomicroscopy techniques (

Figure **26**). The peripheral area of the swarm colony of the Δ*vp1945* mutant strain was significantly smaller compared to wild-type and the flares, characteristic of the periphery were more dense and spiked when compared to the periphery of wild-type. On the other hand, the Δ*vp2240* mutant strain displayed fully abolished swarming as it does not have any periphery, resembling our non-motile negative control, Δ*lafA.* This result suggests that the gene, *vp1945* is not required for the differentiation process considering that its mutant strain was still able to expand and move away from the central spot of inoculation.

Altogether, our findings show that 10 single deletions (out of 15) have an impact in swarming behavior, suggesting that they are important regulators. As cells of most mutant strains could swarm to some extent (except for Δ*vp2240*), these genes are not essential for swarming, but they are still relevant. Subsequent experiments on the target mutants are required to better understand the exact role of the specific proteins in the regulation of swarming behavior in *V. parahaemolyticus*. These targets and their possible roles in swarming will be addressed further in the section "4.2 Discussion".

4.1.3 Set of center-specific proteins

Our next aim was to examine the differences among cells in the center versus three other conditions: periphery of the swarm colony, liquid growth (LB) and solid growth in non-swarm inducing conditions (LB medium agar at 37°C). Therefore, the three comparisons were made: Center vs. Periphery (C vs. P), Center vs. Solid (C vs. S) and Center vs. Liquid (C vs. L) (Figure 27A). Interestingly, differences between Center and Periphery were so pronounced, that cells form the center were more similar to the ones in solid growth condition (LB plate) than to the ones in the periphery of the same swarm colony (Figure 27A). Particularly, only 526 proteins were differentially regulated between Center and Solid (yellow circles: 349 up + 177 down) while this number rises to 1190 and 1238 when comparing Center vs. Periphery (blue circles) and Center vs. Liquid (green circles), respectively (Figure 27B).

In order to identify the proteins specifically regulated in the cells from the center, an overlap of the targets obtained from the aforementioned comparisons was performed.

A

B

Up regulated proteins

Down regulated proteins

log2 fold change

-8   0   10

C vs. L   C vs. P   C vs. S

C

■ Chaperones and heat shock proteins
■ Chemotaxis
■ Cell wall biogenesis /degradation
■ Polar flagela
■ Metabolism
■ Membrane transport
■ Kinases
■ c-di-GMP regulation
■ Bacterial Secretion system (VI1, III2)
■ Transcriptional regulators and DNA binding proteins
■ Protein fate (proteases)
■ Others
■ Uncharacterized

Up regulated proteins

Down regulated proteins

■ Chaperones
■ Metabolism
■ Membrane transport
■ Kinases
■ Transcriptional regulators and DNA binding proteins
■ Protein fate and synthesis
■ Others
■ Uncharacterized

Figure 27. Comparative analyses of the proteome of *V. parahaemolyticus* in four different conditions to define a set of center specific proteins. P-periphery, C-center, S-solid, L-liquid (A) Clustering map depicting changes in protein intensities in three sets of comparison : Center vs. Solid (C vs.S),   Center vs. Liquid (C vs. L) and Center vs. Periphery (C vs.P). (B) Venn diagrams showing intersection among the   three aforementioned comparisons with enhanced (left) and reduced (right) protein intensities.Statistical analysis of all ratios were performed using unpaired Student´s t-test (FDR 0.01 and S0=0.2) and a 2-fold regulation cutoff. (C) Pie-charts for functional categories of up- and down- regulated proteins. Classification of the molecular function and categories of the identified proteins was based on a UniProt KB search, Interpro analysis and gene ontology (GO) annotations.

As a result of this overlap, 190 induced and 18 repressed proteins were common to all comparisons, meaning they were differentially expressed in Center compared with Periphery, Solid and Liquid growth (Figure 27B, Table 17). The three most abundant categories in both up- and down-regulated groups were found to be proteins involved in metabolism, membrane transport and those that were uncharacterized (Figure 27C). As previously revealed in Chapter III, expression of type VISS1 proteins increased continuously in the center during the four stages of swarm colony development. Here, we additionally clarify that this increase is specific to the center of the swarm colony, and does not occur on solid or in liquid growth conditions.

4.1.4 Set of liquid growth specific proteins

Now that we have obtained the total proteome of *V. parahaemolyticus* from four different conditions/states, we next tried to identify which proteins are solely regulated during liquid growth in rich medium (LB).

Therefore, to identify the core set of proteins that appear to be specific to a planktonic cell (grown in LB liquid media in exponential phase of OD_{600}=0.6), three comparisons were made: Liquid vs. Solid (L vs.S), Liquid vs. Center (L vs.C) and Liquid vs. Periphery (L vs.P). Liquid condition was, proteome wise, quite different from all other conditions (Figure 28A). A total of 1217, 1059 and 363 proteins were differentially regulated between Liquid vs. Center, Liquid vs. Solid and Liquid vs. Periphery, respectively (Figure 28B). Therefore, cells growing in liquid were most distinct from cells from the center and most similar to cells from the periphery (Figure 28A). One reason that could explain the fact that liquid grown cells were most similar to cells from the periphery is that in both scenarios, the cells are in an exponential growth-phase, in contrast to cells in the center and solid conditions, which experience a stationary phase in the presence of high cell density.

In Figure 28B, the intersection between the proteins present in these three comparisons is elucidated. As one can observe from the figure, 29 up-regulated and 101 down-regulated proteins were defined as being specific to planktonic (liquid) growth (Figure 28B, Table 18).

Figure 28C describes the different categories according to their abundance (in percentages).

A

L vs. C L vs. S L vs. P

-8   0   6
log2 fold change

B

Up regulated proteins

L vs. C   L vs. P

70   3   86
        29
    92   7
        63

L vs. S

Down regulated proteins

L vs. C   L vs. P

200   82   50
        101
    640   5
        122

L vs. S

C

Up regulated proteins

- Integral component of the membrane
- Chemotaxis related proteins
- Metabolism
- Membrane transport
- Kinases
- c-diGMP regulation
- Cell division
- Protein fate and synthesis
- Others
- Uncharacterized
- Transcriptional regulator and DNA binding proteins

7% 7% 4%
10%
10%
3%
3%
4%
7% 7%
38%

Down regulated proteins

- Lateral flagela
- Chemotaxis related proteins
- Metabolism
- Membrane transport
- Bacterial secretion system (II1,VI1)
- c-diGMP regulation
- Cell division
- Protein fate and synthesis
- Others
- Uncharacterized
- Transcriptional regulator and DNA binding proteins
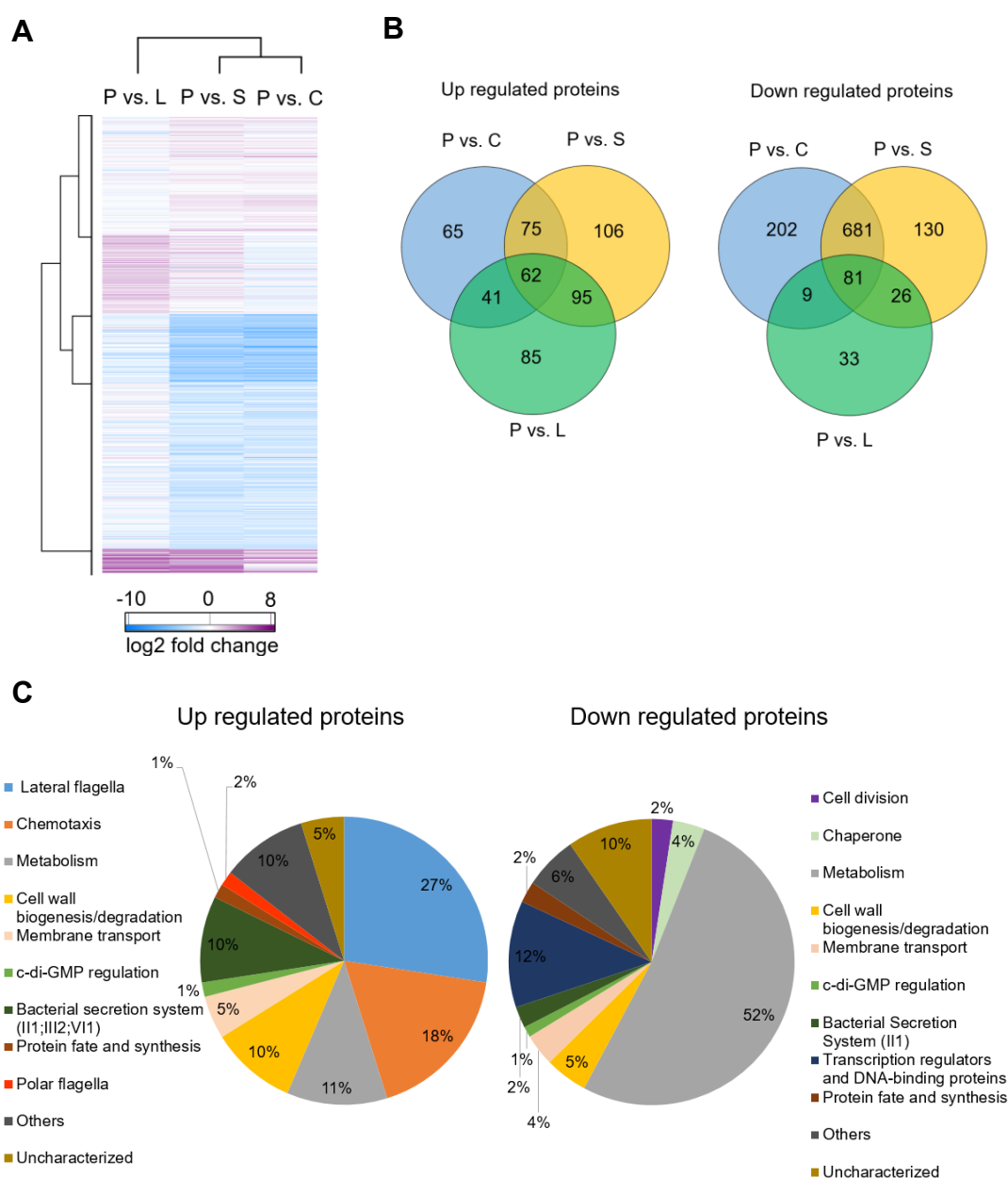- Polar flagela

3% 1%
4% 7%
13%
15%
30%
4%
1%
2%
5%
15%

Figure 28. Comparative analyses of the proteome of *V. parahaemolyticus* in four different conditions to define a set of liquid growth specific proteins. P-periphery, C-center, S-solid, L-liquid (A) Clustering map depicting changes in protein intensities in three sets of comparison Liquid vs. Solid (L vs.S), Liquid vs. Center (L vs.C) and Liquid vs. Periphery (L vs.P) B) Venn diagrams showing intersection among the three aforementioned comparisons with enhanced (left) and reduced (right) protein intensities .Statistical analysis of all ratios were performed using unpaired Student´s t-test (FDR 0.01 and S0=0.2) and a 2-fold regulation cutoff (C) Pie-charts for functional categories of up- (left) and down- (right) regulated proteins in LB liquid growth. Classification of the molecular function and categories of the identified proteins was based on a UniProt KB search, Interpro analysis and gene ontology (GO) annotations.

One can see that the 29 proteins with increased expression in liquid growth, when compared to all other growth conditions, are distributed between twelve different categories, while the 101 down-regulated proteins are represented by eleven functional categories (nine of these being shared by both groups) (Figure 28C). Among these targets, proteins that make up integral components of the cell membrane and kinases were specifically present in the up-regulated group, while some lateral flagella, polar flagella and secretion system-specific proteins are exclusive to the down-regulated group (Figure 28C). In terms of percentages of significantly regulated proteins, the more abundant category in both up and down-regulated groups was composed of proteins that are involved in metabolism (Figure 28C).

4.1.5 Housekeeping proteins

By taking advantage of our proteomics data, we sought to reveal proteins that were found to be housekeeping in nature. To achieve this aim, all possible comparisons between the 4 conditions were made (P vs. C, P vs. S, P vs. L, C vs. S, C vs. L, L vs. S). As a result of these comparisons, 231 proteins with fold changes between 0.5 and 2 within all six sets of comparisons were considered to be constitutively expressed in all tested conditions (Table 19).

The 231 housekeeping proteins were distributed among twelve different annotated groups, including being categorized as "uncharacterized" (if the function was unknown) (Figure 29). One can note that more than half of the housekeeping proteins had metabolic functions. Membrane transport proteins were the second biggest group of proteins that remained constant between all different conditions tested (Figure 29). It is not surprising that proteins from categories such as cell division, cell wall synthesis and chaperones were part of a set of proteins that needs to be expressed all the time, regardless of the physiological environment, working as a minimal survival baseline.
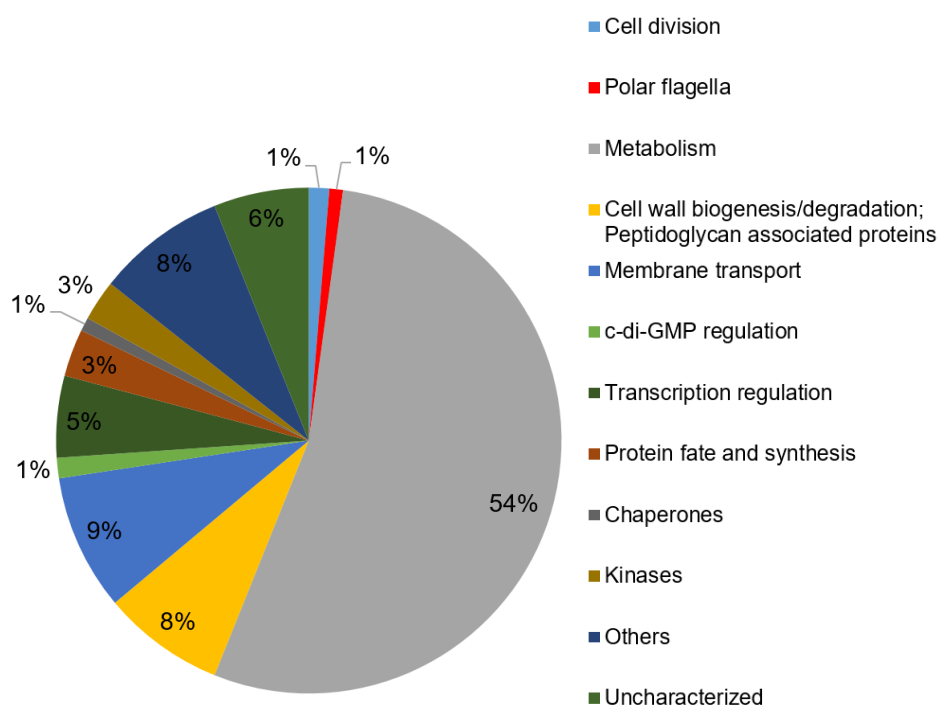
Figure 29. Pie-chart for functional categories of housekeeping proteins. This set of proteins were non-differentially regulated when all six combinations of the 4 different conditions were analyzed: S-solid, L-liquid C-center, P-periphery (P vs. C, P vs. S, P vs. L, C vs. S, C vs. L, L vs. S).

4.2 Discussion

Previous transcriptomic and proteomic studies that compare swimmers and swarmers were performed in *S. typhimurium* (Wang *et al.*, 2004), *S. enterica* (Kim and Surette, 2004), *P. aeruginosa* (Overhage *et al.*, 2008) and *P. mirabilis* (Pearson *et al.*, 2010). In total, these studies present a striking picture of how large the differences between life in liquid and life on a surface can be. However, it is impossible to discern from the studies cited above, which changes in gene expression reflect metabolic influences and which are the result of some intrinsic response to growth on surfaces or liquid. In this study, we overcame this problem by selecting proteins whose levels were exclusively up- or down-regulated in a certain condition (such as periphery), and not in the other physiological states - center of the swarm colony, cells grow in liquid medium or cells grown on (LB-agar) solid surface. It is worth mentioning a transcriptomic study in *V. parahaemolyticus* where they exclude the metabolic differences when comparing liquid condition with surface and pseudo-surface conditions (Gode-Potratz *et al.*, 2011). However, in their experimental approach, entire swarm colonies were collected. From the results of our research, we now know that swarm colonies include cells that stopped the swarm program and do not express *lafA* anymore – that is, the big majority of the cells from the center of the colony. Therefore, the aforementioned study, did define proteins responsive to surface sensing, but could not discern proteins that belong to a swarmer cell type.

In this thesis work, by performing an overlap of all our comparisons, we were able to define and examine not only the set of proteins specific to a swarmer cell type, but also to the cells from the center of the swarm colony and planktonic cells.

4.2.1 Set of periphery-specific proteins

So far, it was only known that *V. parahaemolyticus* swarmer cells produce numerous lateral flagella and have an increased length compared to both planktonic cells and to cells from the center of the swarm colony (Stewart and McCarter, 2003; Heering *et al.*, 2017). However, whether they differ more extensively in terms of their proteome compared to cells in the center of the swarm colonies and to cells from other growth conditions, was unknown. In this study, we have shown that the cells in the periphery of a swarm colony are highly different from cells from the center of the colony and those from the other growth conditions tested. Particularly, we identify 157 proteins as being

exclusively induced and repressed in cells from the swarm periphery, suggesting they are important players involved in proper differentiation and swarming behavior of *V. parahaemolyticus*. Indeed, this was confirmed to be the case for several candidates, deletion of which resulted in either reduced swarming or hyper-swarming behavior.

Upon deletion of genes that were up-regulated during swarming, we hypothesized that the corresponding mutant strains would present a defect in swarming rather than an increase. Yet, an enhanced swarming phenotype was observed in five mutant strains, namely *Δvp1391, Δvp0649, Δvpa0754, Δvpa1176* and *Δvpa1649*. One can assume they might work as negative regulators of swarming. Given that swarming is an energetically expensive process for the cell, fine-tuning is required. One of the ways that this could be achieved is through negative regulators, such as the above, whose role is to keep swarming under control, once the process has already been activated.

Since it is known that lateral flagella genes are essential for swarming motility (Stewart & McCarter, 2003), these proteins were expected to be specific to the cells from the swarm flares. Indeed, lateral flagella-specific proteins were identified in our proteomic data set, representing the highest fraction of proteins, which were exclusively up-regulated in the cells from the periphery of the swarm colony. However, the identification of two polar flagella proteins VP2243 (FliL) and VP2240 (FliO) as up-regulated hits in swarmer cells was more intriguing. Polar flagella proteins are known to be constitutively expressed (McCarter, 1999). However, a transposon mutagenesis study in *R. centenum* indicated that some polar flagella genes are essential not only for swimming but also for swarming motility (Jiang *et al.*, 1998). Indeed, here we show that deletion of the gene, *fliO*, which is involved in the export and assembly of the polar flagella (Ohnishi *et al.*, 1997; Macnab and Minamino, 1999), resulted in complete abolishment of swarming behavior – a phenotype identical to cells lacking the major lateral flagellin, LafA. Interestingly, the lateral flagellar gene cluster in *V. parahaemolyticus, V. alginolyticus or R. centenum* do not encode for a homolog of *fliO* (Merino et al., 2006). Therefore, as swarming expansion of the *Δvp2240* mutant is not merely reduced but completely abolished, one explanation for the impairment observed in the swarming motility of the *Δvp2240* (*ΔfliO*) mutant is that these cells do not produce or export any lateral flagella, due to lack of the flagellar export-assembly gene, *fliO*.

Deletion of the swarm-specific up-regulated *vp2243* (*fliL*), which encodes for a flagellar basal body protein, might likewise cause an impairment in swarming. For instance, a FliL homolog in *Caulobacter crescentus* was found to be required for flagellar gene expression and normal cell division (Stephens and Shapiro, 1993). Interestingly, in

P. mirabilis, a transposon mutant containing an insertion in *fliL* presented a constitutive elongation phenotype (Belas *et al.*, 1995). Cell division seems to be suppressed during swarming differentiation leading to an elongation phenotype (McCarter, 2004; Böttcher *et al.*, 2016). Therefore, in *V. parahaemolyticus*, FliL may also be involved in some aspect of division or septation, which can in turn influence swarming behavior. Moreover, cell division proteins, namely ZapB and FtsY, as well as six other proteins related to cell wall biogenesis and degradation, whose levels were exclusively enhanced in the swarmer cell type (Figure 30), might play an important role in negatively regulating cell division. However, future works needs to be done to determine the exact role of these proteins during swarming differentiation.

Low levels of c-di-GMP have been shown to induce active forms of motility such as swarming (Gode-Potratz, Kustusch, Breheny, Weiss, & McCarter, 2011; Boles & McCarter, 2002; Stewart, Enos-Berlage, & McCarter, 1997). Two proteins participating in c-di-GMP regulation, namely VP2972 and VPA1176, were found to be part of the swarm-specific set of proteins. As these two proteins have been predicted to comprise an EAL domain (whose activity results in degradation of c-di-GMP), they can be relevant players in the swarm differentiation process. Indeed, we show that deletion of *vp2972* and *vpa1176* did affect swarming behavior. Both deletion strains were still capable of swarming, suggesting that VP2972 and VPA1176 are not required for the differentiation process. Interestingly, the effect of the absence of VPA1176 was opposite to that of VP2972, the latter of which showed reduced swarming, while the former swarmed faster over surfaces compared to wild-type. Nevertheless, the result suggests that c-di-GMP levels might not only be involved in regulation of differentiation *per se*, but also might also contribute to surface colonization, subsequent to the establishment of a swarm colony.

Deletion of some chemotaxis proteins have been shown to be detrimental for swarming not only in *V. parahaemolyticus,* but also in other bacterial species that exhibit swarming behavior (Jiang *et al.*, 1997; Senesi *et al.*, 2002; Kearns *et al.*, 2004; Mariconda *et al.*, 2006; Ringgaard *et al.*, 2014). Still, the exact mechanism by which these chemotaxis proteins influence swarming remains to be elucidated. For instance, *R. centenum* utilizes a *che*-like signal transduction pathway (*che2*) for regulating flagellum synthesis. *che2* mutants are non-motile and this phenotype results from reduced polar and lateral flagella synthesis (Jiang *et al.*, 1997). Yet another example is the *fliY* gene of *B. cereus*, which encodes for an essential component of the flagellar motor-switch complex. Although Δ*fliY* mutant cells do possess flagella, their swarming

motility is compromised, probably due to an impairment in the motor switch (Senesi *et al.*, 2002). In our work, we have detected chemotaxis related proteins as being up-regulated in the periphery of a swarm colony. It would be interesting to analyse the importance of these proteins in swarming behavior, and investigate whether it would be due to reduced lateral flagella synthesis or impairment in the motor switch, as seen for the other swarming bacteria mentioned above.

Some studies have shown that swarmer cells are more resistant to antibiotics than swimmer cells (Overhage *et al.*, 2008; Pearson *et al.*, 2010). Our proteomics data set shows that a putative multidrug resistance protein, VP0038 was increased by two fold in the periphery, when compared to the center of the swarm colony (Table 13). Additionally, a putative Lipid A ethanolaminephosphotransferase, VPA1280, was found to be up-regulated by almost 7 fold in the periphery and belongs to the cluster of swarm-specific proteins (Table 15). This protein shares a 90% homology with the protein EptA of *E. coli*. EptA contributes to cationic antimicrobial peptide (CAMP) resistance by modifying lipid A in order to increase the membrane's positive charge (Herrera *et al.*, 2010). Moreover, production of the Lipid A protein LpxL (VP0179) was also found to be increased in the periphery by 2.5 fold (Table 13). One can assume that up-regulation of these proteins might confer antibiotic resistance to the swarmer cells of *V. parahaemolytcius.*

Proteins that participate in the phosphotransferase system (PTS) were also found to be differentially regulated during swarming. PTS proteins provide a major carbohydrate driven transport system in bacteria by catalyzing the phosphorylation of incoming sugar substrates, concomitantly with their translocation across the cell membrane (Deutscher *et al.*, 2006). Three PTS-fructose component-specific proteins, namely VPA0297 (IIBC), VPA0811 (IIBC) and VPA1424 (IIABC) were found to be among the most up-regulated proteomic targets in the periphery when compared to the center of the swarm colony (Table 13). Interestingly, mutations in the phosphotransferase system (PTS) were shown to abolish swarming motility in *S. serovar Typhimurium*, and swarming was restored when the medium was supplemented with non-PTS sugars such as *N*-acetylglucosamine or arabinose (Kim and Surette, 2005). This suggests that the sugar substrate for the PTS can be used to produce an extracellular polysaccharide, which in turn can aid to wet the surface, thereby enabling swarming motility (Toguchi *et al.*, 2000). We surmise that the PTS system in *V. parahaemolyticus* might play a similar role in swarming motility*.*

Quorum sensing has also been shown to influence swarming development. The transcription factor, AphA is a master regulator of quorum sensing that operates at low cell density (LCD) in *Vibrio harveyi, V. cholerae* and *V. parahaemolytcius* (Rutherford *et al.*, 2011). In contrast, OpaR is the master regulator that operates at high cell density (HCD) (Gode-Potratz and McCarter, 2011). In our proteomics results, we observed a 6-fold up-regulation of the protein AphA (VP2762) and 2-fold down-regulation of OpaR (VP2516) in cells from the periphery when compared to the cells from the center (Table 13). This observation makes sense as the peripheral area within the colony is where the swarmer cells are organized from a few layers up to a single cell layer, and so the cell-density is much lower in this area when compared to the cells in the center. Furthermore, AphA induces motility and expression of type III SS 1 proteins, consequently being important for cytotoxicity of *V. parahaemolyticus* in host cells (Ono *et al.*, 2006). In our analysis, the type III export protein YscF and type III secretion protein YscC were the only two Type IIISS1 proteins that were found to be up-regulated in swarmer cells (Table 13). The reasons why other proteins from this secretion system were not present remains elusive. *V. parahaemolyticus* encodes for an additional Type III secretion system, TIIISS2, which was shown to be the one required for colonization and disease formation in animal models (Gode-Potratz *et al.*, 2011; Livny *et al.*, 2014). Interestingly, only 3 among the 17 Type IIISS2 proteins detected showed an increased expression in cells from the periphery compared to the cells from the center of the colony. These proteins are the targeted effector protein YopP (VPA1346), an uncharacterized protein containing an exonuclease domain VPA1356 and the putative type III secretion system translocon protein VopD2 (VPA1361). Previous results show that cells originating from surface colonization are hyper-infectious (Gode-Potratz *et al.*, 2011). Our results suggest that either few effector proteins are enough to confer virulence, or that the hyper-infectious phenotype observed in surface grown cells might not be due to TIIISS2, but an additional and as yet uncharacterized factor.

Among the proteins that were down-regulated, one of the mutants that was found to be impaired in swarming motility was *Δvp1945*. The homologous gene in *V. cholerae* is called VarA. VarA, together with VarS, create a two component-system that modulates the activity of HapR, the homolog of the quorum sensing transcriptional regulator OpaR (Tsou, Liu, Cai, & Zhu, 2011). VarA is the response regulator and lies downstream of VarS. The effect of VarS and VarA on quorum sensing is dependent on the Csr small RNAs, which regulate carbon metabolism, suggesting that *V. cholerae* may integrate nutrient status and cell density sensory inputs (Tsou, Liu, Cai, & Zhu, 2011). In *V.*

parahaemolyticus, VP1945 may play a similar role in integrating sensory inputs regarding carbon availability and cell density in cells from the swarm flares. Further experiments need to be done in order to verify this hypothesis. By performing proteomics in *Δvp1945*, one could may be determine which pathways are significantly affected by the deletion of this gene.

4.2.2 Set of center-specific proteins

By identifying proteins specific to cells within the center, we can understand how different the cells are in this region of the swarm colony and speculate about the environmental surroundings that lead to such changes in their proteomic profile.

Iron limitation is a key signal mediating *V. parahaemolyticus* swarmer cell differentiation (McCarter and Silverman, 1989; Glick *et al.*, 2010). Iron acquisition and storage via siderophore production is critical for successful colonization and for providing the bacterium with a distinct competitive advantage over other pathogens (Tremblay and Déziel, 2010; Watts *et al.*, 2012; Deriu *et al.*, 2013). The analysis presented here shows that certain proteins involved in iron storage were up-regulated in the cells from the center of the swarm colony (Table 13). These include the putative siderophore utilization protein VPA0089, the Fe-regulated protein B (VPA0664), the HesB family protein (VP0598) and the ferric iron reductase Fhuf (VPA1659). Moreover, two ferric siderophore receptors revealed increase expression in the cells from the center during the swarm colony development, namely the ferric vibrioferrin receptor (VPA1656) and the ferric siderophore receptor-like protein (VPA1657) (Table 14). The ferric uptake regulatory protein, Fur (VPA0833) is a master regulator (repressor) of iron acquisition proteins and its translation was found to be decreased in the periphery compared to the center of the colony (Table 13), meaning that production of iron acquisition proteins in the periphery is increased. Altogether, our analyses suggest that cells from the periphery show a higher iron uptake while cells from the center of a swarm colony have lesser iron uptake but higher iron storage to compensate for the depletion of this element in the microenvironment of the center of a swarm colony.

OpaR in *V. parahaemolyticus* represses lateral flagella expression and in our proteomics experiments, OpaR was found to be increased in the center compared to the periphery (Table 13). This is in agreement with our fluorescence microscopy results,

which show that almost no cells in the center of a swarm colony express P_{lafA}, meaning that they are non-motile on solid surface.

As cells in the center are usually stacked in many layers, it is assumed that they will, over time, start entering stationary phase. Indeed, we identify a very high amount of proteins involved in translation being down-regulated in the center compared to cells in the swarm colony periphery (Table 13). Moreover, specialized sigma factors that lead to general stress or heat resistance of cells, such as RpoS and RpoH, respectively, were highly induced in cells from the center (Cochran *et al.*, 2000; Mandel and Silhavy, 2005; Ait-Ouazzou *et al.*, 2012; Fiebig *et al.*, 2019) (Table 13). Furthermore, oxidative stress response proteins including superoxide dismutase, dehydrogenases and oxidase oxireductases, are all components that were up-regulated exclusively in the center (Table 17). Altogether, these analyses suggest that the center of a mature swarm colony seems to be a microenvironment comprising of multiple stresses, to which cells have to adapt by expressing the respective response regulatory proteins.

4.2.3 Set of liquid growth specific proteins

In this study, we analysed which proteins were exclusively up or down-regulated in cells from liquid growing conditions. Although there were many proteomic differences between cells in liquid condition compared to cells in solid conditions, only few proteins were specifically induced, when comparing liquid growth to all conditions. One possible explanation for why growth in LB liquid medium was not a very specific condition could be the fact that, since LB is a rich medium, all nutrients are readily available. Therefore, planktonic free cells growing in a rich medium may not require such specific machinery when compared to cells that are attached to a surface either exploring the surroundings (by motile means) or creating complex multicellular structure, such as biofilms. However, we speculate that when planktonic cells are grown in minimal medium (liquid) rather than in a rich medium such as LB, more drastic proteome changes would, most likely, appear.

Polar flagella genes are expected to be constitutively expressed and they are essential for swimming behavior (McCarter, 1999; McCarter, 2006). Therefore it is unclear why polar proteins such as flagellin A, polar flagellin B, flagellar motor switch protein FliG and polar flagellar sheath protein A were down-regulated in liquid, when compared to solid and swarming-specific conditions (Table 18). In contrast, it is comprehensible that lateral flagella proteins, such as FliDL were repressed during growth

in liquid environment, as induction of lateral flagella occurs only when a cell encounters a solid surface (McCarter *et al.*, 1988).

It would be interesting to analyse, in more detail, the role of the kinases and transcriptional regulators that were part of the set of up-regulated liquid-specific proteins. Particularly, it remains to be elucidated whether these kinases are important players for sensing certain environmental stimuli and eventually, transducing it to the cell. Consequently, analyses of their role in regulating the activity of transcriptional regulators, in order to ultimately activate pathways important for the life-style as a free planktonic cell, would be interesting to study.

4.2.4 Housekeeping proteins

As a last step, we analyzed which proteins did not change significantly between all of the different conditions studied. This analysis was performed in order to identify the set of *V. parahaemolyticus* housekeeping proteins that are required for all growth conditions. If housekeeping proteins are important to fulfill the basic needs of a cell, one would expect that many of these proteins hold functions that are essential for the survival of the bacterium. Indeed, by comparing our list of proteins with the data from a transposon mutagenesis study - where they detected proteins essential for growth of *V. parahaemolyticus* in LB liquid culture (Hubbard *et al.*, 2016)- around 40% of the proteomics data set were found to be essential or contain essential domains (Table 19 - essential proteins marked in green, proteins with essential domains marked in orange). Although the other 60% of proteins belonging to our housekeeping set do not contain any essential domains, they might still be required for optimal growth.

Chapter V - Conclusions and future prospects

Multiple species of bacteria inhabit the world's oceans and estuarine areas and their population size and spreading in the environment depend on many different variables and is highly influenced by fluctuations in the external milieu – and thus in the case of human pathogens, changing the likelihood of human infections. Consequently, it is essential to understand how bacteria adapt to changes in their environment and what strategies they employ to ensure their dissemination.

One mechanism, employed by many different species of bacteria to accommodate changes in the environment involves the differentiation into specialized cell types suitable for the particular conditions they encounter. A distinct type of differentiation utilized by many bacteria, including species of *Serratia*, *Aeromonas*, *Salmonella*, *Proteus* and *Vibrio*, is the differentiation between a planktonic swimmer cell and a swarmer cell that is specialized for movement over solid surfaces. Here we have anlyzed one such example, *V. parahaemolyticus*, which is a marine bacterium and a worldwide human pathogen, being the leading agent of seafood borne gastroenteritis in the world. As outlined here, it has an intricate life-cycle that depends on its environmental conditions. Particularly, in liquid environments it exits as a short motile cell that is propelled by a single polar flagellum. However, when it attaches to solid surfaces it induces a distinct differentiation program, which allows it to adapt to changes in its environment and colonize solid surfaces by means of swarm motility. Reports based on *V. parahaemolyticus* levels in estuarine environments have suggested that the level of bacteria in the water is tide dependent. Thus, suggesting that *V. parahaemolyticus* cells could be released from surfaces into the liquid surroundings. Nonetheless, the release of surface attached cells into liquid environments have remained unexplored for *V. parahaemolyticus* as well as for swarm colonies in general.

In Chapter III of this study we revealed a new distinct cell type, which is released from swarm colonies into the liquid environment upon swarm colony flooding. Furthermore, our results show how the swarm colony architecture fluctuates with changing environmental conditions with responses of differentiation and dedifferentiation within zonal regions of the colony. Importantly, our data shows that cells are continuously released from flooded swarm colonies, thus indicating that swarm colonies function as a continuous source of cells that can be released into the environment upon colony flooding. Surprisingly, our results indicate that long swarmer cells are not released into the liquid environment. Instead, released cells comprise of a distinct cell type that is morphologically optimized for swimming behavior and capable of spreading and exploring their new liquid environment and eventually attach to new solid surfaces where

they can initiate new swarm colonies. Importantly, our data indicates that release of this distinct cell type facilitates the dissemination of *V. parahaemolyticus* in the environment.

At this point, more experiments are required to understand where exactly the released bacterial cells are located within the swarm colony before they disperse. One possible experiment would be to label the cells with a fluorescence protein fused to the promoter of a gene specifically up-regulated in released cells. This way one could see where the released cells are located during development of the colony. More importantly, it would be possible to analyse their location within the swarm colony, before being released into the liquid environment. Further work is needed to test the capacity of the released cells (once re-attached) and of cells within a swarm colony to utilize the type VISS1 machinery to successfully compete with and neutralize other surface colonizers.

Moreover, further studies are needed to understand the exact environmental circumstances within the bacterium´s natural habitat that induce swarming. We argue that swarm colonies from other pathogenic bacteria living in estuarine areas, such as *V. alginolyticus*, might also present a similar spreading mechanism like *V. parahaemolyticus* based on the release of distinct swimming proficient cells from swarm colonies. Thereby, more research is required to determine if other swarming proficient bacteria species also allow for the release of swimming proficient cells from swarm colonies, whilst permitting rapid swarming surface colonization.

In Chapter IV of this thesis, we demonstrated how elastic the proteome profile of *V. parahaemolyticus* can be in response and in adaptation to different conditions. We also revealed which proteins are specifically regulated in cells exposed to distinct environmental scenarios, namely, center and periphery of a swarm colony and liquid medium.

Our results show that deletion of genes that encode for proteins specifically regulated in cells within the swarm flares (periphery) have a significant impact in swarm motility. However, more work is still required to understand if these targets participate directly or indirectly in swarming motility and to unravel their specific role for this biological differentiation process. As topic for further research in the swarming motility field, it is still to be discovered which players are involved in the signal transduction mechanism and in the elongation of cell morphology. It would be interesting to see if the cell division and cell wall membrane proteins detected in our proteomics studies are also up-regulated in swarmer cells of other organisms and if they play a role in the elongation

phenotype. Moreover, further work is required to analyse if the cell wall composition of lipopolysaccharides is different between cells from the swarm flares and from the center of a swarm colony. Additional research is still needed to verify if *V. parahaemolyticus*, as in the case of other swarming species, also requires the production of amphipathic molecules that enable surface wettability and consequently, aid in motility upon solid surfaces.

Overall, this work shows how flexible the proteomic expression profiles are in order to greatly adapt to different environmental stresses and habitats. This would permit *V. parahaemolyticus* to colonize many different hosts and surfaces, and might be an explanation for the high worldwide prevalence of this bacterium.

Chapter VI - Materials and methods

6.1 Chemicals, equipment and software

Essential resources used during this thesis work, such as reagents (Table 2), kits (Table 3), software (Table 4) and equipment (Table 5) are listed below. Information regarding their supplier/source is provided, as well as an identifier number, when available.

Table 2. Reagents

Reagents	Supplier	Identifier
Genetic reagents		
Restriction enzymes	New England Biolabs (NEB) (Frankfurt a.M.)	
2-Log DNA Ladder (0.1-10.0KB)	New England Biolabs (NEB) (Frankfurt a.M.)	NEB Cat#: N3200S
Color Pre-stained Protein Standard Broad Range (11-245 KDA)	New England Biolabs (NEB) (Frankfurt a.M.)	NEB Cat#: P7712S
T4 Ligase	New England Biolabs (NEB) (Frankfurt a.M.)	NEB Cat#: M0202L
10X Buffer for T4 DNA Ligase with 10mM ATP	New England Biolabs (NEB) (Frankfurt a.M.)	NEB Cat#: B0202S
Q5 Hot Start High Fidelity DNA Polymerase	New England Biolabs (NEB) (Frankfurt a.M.)	NEB Cat#: M0493S
Q5 High GC Enhancer	New England Biolabs (NEB) (Frankfurt a.M.)	NEB Cat#: B9028A
Q5 Reaction buffer	New England Biolabs (NEB) (Frankfurt a.M.)	NEB Cat#: B9027S
Desoxyribonucleotide (dNTP) Solution Mix	New England Biolabs (NEB) (Frankfurt a.M.)	NEB Cat#: N04475
SyBR Green Master Mix Thermo Fisher	(Waltham, USA)	Cat #: 4309155
Alkaline Phosphatase Calf Intestinal (CIP)	New England Biolabs (NEB) (Frankfurt a.M.)	NEB Cat#: M0290L
Chemical compound, drug		
Antibiotics: Chloramphenicol; Ampicillin sodium salt; Streptomycin sulfate; kanamycin sulfate	Carl Roth GmbH + Co KG (Karlsruhe)	Art.-Nr: 3886.3; k029.3; 0236.2
Isopropyl β-D-1 thiogalactopyranoside (IPTG)	Peqlab (Erlangen)	Nr.: 35-2030
Difco Agar, Granulated	BD	Ref#: 214510
LB-Medium (Luria/Miller)	Carl Roth GmbH + Co KG (Karlsruhe)	Art.-Nr: X968,3
N-acetyl D- glucosamine (D-GlcNAc)	Sigma-Aldrich (Steinheim)	Art-Nr: A8625
L(+)-Arabinose	Carl Roth GmbH + Co KG (Karlsruhe)	Art.-Nr: 5118.3

peqGOLD Universal Agarose	Peqlab (Erlangen)	Nr.: 35-1020
Agarose NEEP Ultra-Quality	Carl Roth GmbH + Co KG (Karlsruhe)	Art.-Nr: 2267.3
D(+) Saccharose	Carl Roth GmbH + Co KG (Karlsruhe)	Art.-Nr: 4621.1
Bacto Yeast Extract	BD	Ref#: 212750
Difco HI agar	Beckton Dickinson GmBH (Heidelberg)	Ref#: 244400
Crystal Violet	Carl Roth GmbH + Co KG (Karlsruhe)	Nr.: 548-62-9
2,2′-bipyridyl	Sigma-Aldrich (Steinheim)	Lot#: STBD3612V
Ethidium bromide	Carl Roth GmbH + Co KG (Karlsruhe)	Nr.: 1239-45-8
Red-gal	Sigma-Aldrich (Steinheim)	Nr.:1364C-A103X
Instant Blue	Expedeon (United Kingdom)	
Gel loading dye purple 6X	New England Biolabs (NEB) (Frankfurt a.M.)	#B7025S
5-Bromo-4-Chloro-3-Indolyl-ß-D-Galactopyranoside (X-Gal)	Carl Roth GmbH + Co KG (Karlsruhe)	Art.-Nr: 2315.4
Materials		
96-well plates	Greiner Bio-One GmbH, Frickenhausen	
Microscopy slides	Carl Roth GmbH + Co KG (Karlsruhe)	Art.-Nr: 0656
Cover slips	Carl Roth GmbH + Co KG (Karlsruhe)	Art.-Nr: H875
Petri dish (round) 92x16mm	Sarstedt AG (Nümbrecht)	Cat#: 82.1472.001
Petri dish (round) 150x20mm	Sarstedt AG (Nümbrecht)	Cat#: 82.1184.500
Microcaps - disposable micropipettes 1 µL volume, 64 mm lenght	Drummond Scientific Company (USA)	Cat#: 1-000-0010-64
Microspin C18 columns	The Nest Group Inc. (USA)	Cat#: NC9270379

Table 3. Commercial kits and assays

Name	Manufacturer	Identifier
NucleoSpin Gel and PCR Clean-up kit	Macherey-Nagel (Düren)	Ref.: 740609.250
NucleoSpin Plasmid Kit	Macherey-Nagel (Düren)	Ref.: 740588.250

NucleoSpin RNA	Macherey-Nagel (Duren)	Ref.: 740955.50
Pierce™ BCA Protein Assay Kit	Thermo Fisher (Waltham, USA)	Ref.: 23227
High-Capacity cDNA Reverse Transcription Kit	Thermo Fisher (Waltham, USA)	Ref.: 4368813

Table 4. Software and on-line resources

Name	Source/Reference	Additional information
MetaMorph v7.5	Molecular Devices (Union City, CA)	
SeqBuilder v12.3.1	DNASTAR Software for Life Scientists (Madison, WI)	
SeqMan Pro v12.3.1	DNASTAR Software for Life Scientists (Madison, WI)	
ImageJ-Fiji	(Schindelin *et al.*, 2012)	http://rsbweb.nih.gov/ij
GraphPad Prism version 6.07	GraphPad Software (La Jolla CA)	https://www.graphpad.com/
ggplot2 version 0.9.3.1	Hadley Wickham, Department of Statistics, Rice University	http://ggplot2.org
UniProt sequence database	(Apweiler *et al.* 2004)	http://www.uniprot.org/
KEGG sequence database	(Ogata *et al.* 1999)	http://www.genome.jp/kegg/kegg2.html
NIS-Elements Software AR 4.60.00 (Nikon)	NIS-Elements Software AR 4.60.00 (Nikon)	
STRING-known and predicted protein-protein interactions	(Jensen *et al.*, 2009)	http://string-db.org/
Phyre: Protein Homology/analogY Recognition Engine V 2.0	(Kelley and Sternberg, 2009)	http://www.sbg.bio.ic.ac.uk/phyre/html/
Oligo Calc: Oligonucleotide Properties Calculator	(Kibbe, 2007)	http://biotools.nubic.northwestern.edu /OligoCalc.html
MaxQuant v 1.5.3.17	(Cox and Mann, 2008)	
Perseus Computational platform	(Tyanova *et al.*, 2016)	
Scaffold v4.8.9	Proteome Software (Oregon, USA)	http://www.proteomesoftware.com /products/scaffold/

NCBI (February 2019)	National Library of Medicine (USA)	https://www.ncbi.nlm.nih.gov/

Table 5. Essential equipment

Application	Device	Manufacturer
PCR	Mastercycler nexus PCR System	Eppendorf (Hamburg)
Centrifugation	Centrifuge 5424 and 5424R. Multifuge 1 S-R, Biofuge Pico17, multifuge X1R	Eppendorf (Hamburg) Heraeus/Thermo Scientific (Dreieeich)
Thermomixing	Thermomixer compact	Eppendorf (Hamburg)
Stereomicroscopy	Nikon H600L	Nikon (Düsseldorf)
Speed vacuum concentrator	Sovant SPD131DDA	Thermo Scientific (Dreieeich)
Mass spectrometry	Q Exactive Plus Hybrid Quadrupole-Orbitrap Mass Spectrometer	Thermo Scientific (Dreieeich)
Plate reader for absorbance measurements	Infinite M200 Pro	Tecan (Crailsheim)
Nanodrop for concentrations and purity of DNA/ RNA	ND-1000 Spectrophotometer	PeqLab (Eberhardzell)
Ultrasonicator	Sonopuls mini20	Bandelin (Berlin)
	UP200st Ultrasonic Processor	Hielscher (Teltow)
Microscopy*	Ziess Axio Imager M1 fluorescence microscope, Zeiss Axioplan 2 fluorescence microscope, Nikon eclipse Ti inverted microscope, Talos L120C transmission electron microscope.	

*for details of the microscopes set-up see section "Microscopy methods"

6.2 Media, buffers and solutions

The medium used to grow cells was LB or LB agar, except when performing swarming assays, in which case HI agar was used. Table 6 contains the list of growth media and buffers employed in this work.

Table 6. Media, buffers and solutions

Media/Buffer	Composition
Luria-Bertani (LB)	1% (w/v) tryptone; 0.5% (w/v) yeast extract; 1% (w/v) NaCl For solid plates: add 1.5%(w/v) agar For swimming plates: add 0.3%(w/v) agar
Difco Heart Infusion Agar	1%(w/v) beef-heart infusion; 1%(w/v) tryptone; 0.5%(w/v) NaCl; 1.5%(w/v) agar
HI additives	4 mM CaCl2 50 µM 2,2′-bipyridyl (solution in 100 % ethanol)
Phosphate buffered saline (PBS)	For 10x solution: 25.6 g $Na_2HPO_4 \cdot 7H_2O$ 80 g NaCl 2 g KCl 2 g KH_2PO_4 Bring to 1 liter with H_2O. Autoclave for 40 minutes at 121°C. For PBS 1.5% NaCl (10x): use 150g of NaCl instead of 80 g NaCl
TSS buffer (Transformation and Storage Solution)	1%(w/v) tryptone; 0.5%(w/v) yeast extract; 1%(w/v) NaCl; 10%(w/v) PEG; 5%(v/v) DMSO; 50 mM MgCl2 or MgSO4 adjust pH to 6.5 (Chung *et al.*, 1989)

6.3 Microbiological methods

6.3.1 Growth conditions

In all experiments, unless otherwise stated, *V. parahaemolyticus*, and *E. coli* were grown in LB medium or on LB agar plates at 37°C containing antibiotics in the following concentrations: 100 µg ml⁻¹ ampicillin, 5 µg ml⁻1 chloramphenicol for *V. parahaemolyticus* and 20 µg ml⁻¹ chloramphenicol for *E. coli*.

6.3.2. Strain storage

For the long-term storage of strains, glycerol stocks were made. 1 mL of densely grown bacterial cultures were stored, supplemented with 16% (v/v) glycerol, at - 80 °C.

6.3.3. Swarming assay

To perform swarming assay, a liquid culture of *V. parahaemolyticus* was grown in LB to an OD_{600} between 0.1-0.5 and subsequently spotted on swarm agar (40 g L^{-1} Difco Heart Infusion Agar (BD) supplemented with 4 mM CaCl2 and 50 mM 2,2′-bipyridyl (Sigma Aldrich). The swarm agar plates were dried 10 min at 37ºC before spotting the liquid culture. After letting the spot of liquid culture dry for 4 min at RT, plates were sealed with clear plastic tape and subsequently incubated overnight at 24ºC. The diameter of the swarming colony was then manually measured.

6.3.4. Swimming assay

For swimming assay, a liquid culture of *V. parahaemolyticus* was grown in LB to an $OD_{600} \approx 1$ and subsequently spotted on LB agar 0.3%, with a toothpick. The plates were incubated overnight at 30ºC for 15h. The diameter of the swimming colony was then manually measured.

6.3.5. Growth curve

All strains were grown to stationary phase and then their OD_{600} was normalized to 1. Samples were diluted 1/1000 and triplicates of 200 μL were placed in a 96 well plate. OD_{600} was measured in a TECAN Microplate Reader (Infinite 200 PRO) every 15 min for 18h, at 37°C. The average values of the replicates was plotted against time.

6.3.6. Release assay

In this assay, three individual swarming plates (round petri dish 92x16mm) were used for each time point. Swarming colonies were prepared from the same liquid culture and presented the same size. Chitin flakes ≈ 20 mg were added around a swarming colony and 10 mL PBS 1.5% NaCl were poured gently into each swarm agar plate. Cells released into the PBS and cells bounded to the chitin flakes were collected at 0, 30, 60 and 90 minutes after adding PBS to the swarm agar plates. To calculate the number of free-cells 100 μL was collected from the plate, and serial dilutions were plated for CFU

(per mL) determination. To calculate cells bounded to chitin, chitin flakes were collected in a 2 mL tube and washed 3 times with 1 mL of PBS 1.5% NaCl. Chitin flakes were then ressuspended in 100 µL of PBS 1.5% NaCl and serial dilutions were plated for CFU (per 20 mg of chitin) determination.

6.3.7 Chitin binding assay

10 mL of PBS 1.5% NaCl were gently pour into a swarming plate and after 30 min the liquid was collected using a pipette. The collected cells were harvest by centrifugation and washed 3 times in PBS 1.5% NaCl. Cells were ressuspended to an OD600 ≈ 0.03 and 1 mL was added to sterilized cryo-tubes containing ≈ 20 mg of chitin. The tubes were placed in a rotation shaker at 4 RPM at 24ºC. A time course assay was performed during 250 min and samples were collected at six time points. To calculate the number of free-cells for each time point, 100 µL was collected from the respective tube, and serial dilutions were plated for CFU determination (per mL). To calculate cells bounded to chitin the remaining liquid from the tube was discarded, and chitin flakes were washed 3 times with 1 mL of PBS 1.5% NaCl. Finally, the chitin flakes were re-suspended in 100 µL of PBS 1.5% NaCl and serial dilutions were plated for CFU determination (per 20 mg of chitin). This experiment was done in triplicates, using three swarming plates prepared in the same day.

6.3.8 Flooding assay

25 mL of PBS 1.5% NaCl were gently pour into a swarming plate (Round petri dish 150x20mm) and after 30 min the liquid was collected using a pipette. After letting the plates open to dry for 4h at RT, the plates were kept at non-swarming conditions - kept open at 24ºC. After another 5 h or 23 h the plates were sealed again and kept at 24ºC for another 24 h for obtaining swarming conditions. At least three biological replicates were performed.

6.3.9 Chemotaxis assay

Cells collected either from liquid culture or from release assay, were washed two times in PBS 1.5% NaCl. The final OD_{600} was normalized between the two strains used, wild-type and Δ*cheW*, and samples were distributed in triplicates in a 96 well plate. Cappilaries containing 2 mM of D-GlcNAc were introduced in the wells for 30 min at RT.

The volume of each cappilary was transfered into 250 μL of PBS 1.5% NaCl and serial dilutions were performed to determine CFU.

6.4 Molecular cloning

6.4.1 Isolation of genomic DNA from *V. parahaemolyticus*

A small portion of cells grown overnight in a LB plate containing amphicilin, was resuspended in distilled water and boiled for 10-12 minutes in a Thermomixer (Eppendorf Thermomixer C). After centrifugation at 10,000 rpm for 10 minutes, the supernatant was then transferred to a fresh Eppendorf tube.

6.4.2 Isolation of plasmid DNA from E. coli

For plasmid isolation, *E. coli* strain containing plasmid was grown in 5 mL of LB supplemented with chloramphenicol overnight at 37 °C with shaking. Plasmid DNA was extracted by using the NucleoSpin Plasmid kit (Macherey-Nagel). The plasmid DNA concentration was measured using a Nanodrop spectrophotometer.

6.4.3 Polymerase chain reaction (PCR)

Amplification of DNA fragment was carried out either with Q5 Hot Start High Fidelity DNA Polymerase or Phusion High-Fidelity DNA Polymerase. In case of colony PCR, the total reaction volume used was 20 μL, otherwise the volume used was 50 μL . The composition of the PCR mixtures for Q5 Hot Start Polymerase and Phusion Polymerase are shown in Table 7 and Table 8, respectively. The temperature of annealing was choosen according to the primer meting temperature, and the extension time was choosen according to the size of the fragment to be amplified (usually 1 minute per kilobase). For colony PCR with *E. coli*, the colony of interest was suspended in the PCR reaction mixture. For *V. parahaemolyticus*, genomic DNA was obtained by the method described above and used as template.

Table 7. Components of the Q5 PCR reaction mix

Reagents	Volumes (µl)
10mM dNTPs	1
5X Q5 reaction buffer	10
5X Q5 High GC enhancer	10
0.5 µM forward primer	2
0.5 µM reverse primer	2
Polymerase	0.5
Template DNA	1
Nuclease-free water	Up to 50 µl

Table 8. Components of the Phusion PCR reaction mix

Reagents	Volumes (µl)
10mM dNTPs	1
10X Buffer	5
0.5 µM forward primer	2
0.5 µM reverse primer	2
Polymerase	1
Template DNA	1
Nuclease-free water	Up to 50 µl

6.4.4   Separation and detection of DNA using agarose gel electrophoresis

1% agarose gels prepared with 0.5X TAE buffer and supplemented with 0.005% (v/v) of ethidium bromide were used to separate the DNA fragments by agarose gel electrophoresis. 6X Gel loading dye purple (New England Biolabs) was added to DNA samples before loading the samples into the agarose gel wells. To be able to estimate the size of the DNA fragment, a 2-log DNA ladder (New England Biolabs) was loaded in the gel along with the samples of interest. Detection of DNA bands was obtain using the E-BOX VX2 imaging system (PeqLab). If needed, DNA fragments of interest were cutted and removed for further use.

6.4.5 Restriction digestion and ligation of DNA

Restriction of DNA fragments was performed using the appropriate restriction endonuclease (1µL/ µg of DNA fragment) and the corresponding buffer. Reaction was carried out at 37°C for at least 1 h. Next, in the case of the vector, to avoid sef-ligation, 1 µL of calf intestine alkaline phosphatase (CIP) was added and the reaction was carried out for at least 1 more hour at 37°C. Restricted DNA was directly purified by using the NucleoSpin Gel and PCR Clean-up kit (Machenery-Nagel).

Ligation reactions were performed in 20 µL total volume, using 1 µL T4 DNA ligase and the corresponding buffer (New England Biolabs). Approximately 1:5 ratio of the digested vector DNA and of insert DNA were added and the reaction was kept at 16°C between 2-3 h. Ligation mixtures were then transform into *E. coli* strains DH5αλpir.

6.4.6 Preparation of chemically competent *E. coli* cells

Cells growing in a 20 mL LB culture were harvested at OD_{600}=0.6 by centrifugation. The cell pellet was resuspended in ice-cold TSS buffer (Table 6), in 1/10 of the original cell culture volume. The culture was aliquoted, the tubes frozen with liquid nitrogen and and stored at -80°C.

6.4.7 Transformation of chemically competent *E. coli* cells

1-2 µL of the corresponding plasmid was added to 50 µL of the (above-obtained) chemically competent *E. coli* cells. After approximately 30 minutes on ice, the cells were heat-shock, placed at 42°C for 1 minute and immediatly transferred back to ice and resuspended in 500 µl of LB medium. The cells were then shaken for 1 h at 37°C followed by centrifugation. The pelletized cells were ressupended in 100 µL of LB and plated onto LB-agar plates containing the relevant antibiotic.

6.4.8 Preparation of electro-competent *V. parahaemolyticus* cells

To prepare electro-competent cells of *V. parahaemolyticus,* 200 mL of inoculated LB liquid culture were incubated at 37° C until it reached OD_{600}=1. After centrifugation for 10 min at 4700 rpm at 4° C, cells were kept on ice. The pellet was washed twice with ice-cold freshly prepared 273mM sucrose solution. The sucrose solution was buffered using KOH to keep pH at 7.2-7.4. After the two washes, the cells were re-suspended in sucrose solution with glycerol added to 1/10 of the original cell culture volume. Aliquots of 50µl were frozen in liquid nitrogen and then at -80° C.

6.4.9 Transformation of electro-competent *V. parahaemolyticus* cells

5 µL of the corresponding plasmid was added to 100 µL of the (above-obtained) electro-competent *V. parahaemolyticus* cells. After approximately 1 h on ice, the cells were transferred into a pre-chilled electroporation cuvette. Electroporation was carried out using a MicroPulser electroporator (Bio-Rad) at the following conditions: voltage 2200, µF 25 and 200 Ω and immediately after cells were resuspended in 1 mL of LB medium. The cells were then transferred back into a 1.5 mL Eppendorf tube and shaken for at least 2 hours at 37 °C, followed by centrifugation. The pelletized cells were ressupended in 100 µL of LB and plated onto LB-agar plates containing the relevant antibiotic.

6.4.10 Construction of strains

V. parahaemolyticus strains used in this study are derivatives of strain RIMD 2210633. Construction of *V. parahaemolyticus* deletions or insertions, was performed with standard allele exchange techniques using derivatives of plasmid pDM4 (Donnenberg and Kaper, 1991). *E. coli* strain SM10λ*pir* was used to transfer DNA into *V. parahaemolyticus* by conjugation (Miller and Mekalanos, 1988). DH5αλpir chemically competent cells were used for general cloning purposes.

A comprehensive list of all strains used for this work can be found in Table 9.

6.4.10.1 Construction of double-fluorescence strain

In order to measure expression from the *lafA* promoter and from the *vp1343* promotor, in the cells during development of the swarm colony, a double labeling strain was generated. In order to measure expression of sfGFP from the *vp1343* promotor, the gene encoding *sfGFP* was translationally fused to P_{T7} and the gene encoding *T7* was translationally fused to P_{vp1343}. The first fusion construct was integrated into the intergenic region between *vp2408* and *vp2409*, while the second fusion construct was integrated into the intergenic region between *vp2488* and *vp2489* on the *V. parahaemolyticus* chromosome. In order to measure expression of mCherry from the *lafA* promoter (P_{lafA}), the gene encoding *mCherry* was translationally fused to P_{lafA}. The fusion construct was then integrated into the intergenic region between *vp0984* and *vp0985* on the *V. parahaemolyticus* chromosome. The resulting strain from these three integrations is CF36 (P_{lafA}-mCherry; P_{t7}-sfGFP; P_{vp1343}-T7).

Table 9. Strains

Strain name	Genotype	Reference
Vibrio parahaemolyticus RIMD 2210633	Clinical Isolate, wild-type	(Makino *et al.*, 2003)
E. coli SM10 λ pir	*KmR, thi-1, thr, leu, tonA, lacY, supE, recA::RP4-2-Tc::Mu, λpir*	
E. coli DH5a λ pir	*sup E44, ΔlacU169 (ΦlacZΔM15), recA1, endA1, hsdR17, thi-1, gyrA96, relA1, λpir phage lysogen*	
SR58	*Δvp2225 (cheW)*	(Ringgaard *et al.*, 2014)
JH2	*Δvpa1548 (lafA)*	J. Heering
CF2	*Δvp0764*	This work
CF5	*Δvp0649*	This work
CF6	*Δvpa1649*	This work
CF10	*Δvp1391*	This work
CF12	*Δvp0053*	This work
CF13	*Δvpa0584*	This work
CF14	*Δvpa1176*	This work
CF15	*Δvp2240*	This work
CF16	*Δvp2972*	This work
CF18	*Δvpa0754*	This work
CF19	*Δvp1945*	This work
CF21	*Δvp0514*	This work
CF22	*Δvpa0662*	This work
CF26	*Δvp2178*	This work
CF36	*ΩPlafA-mCherry;ΩPt7-ΩPvp1343-T7* in wildtype	This work
CF39	*Δvpa1083*	This work

6.4.12 Plasmids and primers

All plasmids and primers used in this work are listed in Table 10 and Table 11, respectively. A descriptive information regarding construction of each plasmids is also provided in this section.

Table 10. Plasmids

Plasmid name	Relevant genotype/description	Reference
pDM4	Suicide vector for gene deletions and insertions	(Donnenberg and Kaper, 1991)
pCF002	plasmid for deletion of *vp0764*	This work
pCF007	plasmid for deletion of *vp0649*	This work
pCF010	plasmid for deletion of *vpa1649*	This work
pCF012	plasmid for deletion of *vp1391*	This work
pCF015	plasmid for deletion of *vp0053*	This work
pCF016	plasmid for deletion of *vpa0584*	This work
pCF017	plasmid for deletion of *vpa1176*	This work
pCF018	plasmid for deletion of *vp2240*	This work
pCF020	plasmid for deletion of *vp2972*	This work
pCF021	plasmid for deletion of *vpa0754*	This work
pCF022	plasmid for deletion of *vp1945*	This work
pCF023	plasmid for deletion of *vp2178*	This work
pCF025	plasmid for deletion of *vpa0514*	This work
pCF026	plasmid for deletion of *vpa0662*	This work
pJH047	plasmid for integration of P_{t7}-*sfGFP* on the chromosome	J. Heering
pCF048	plasmid for integration of P_{lafA}-*mCherry* on the chromosome	(Muraleedharan *et al.*, 2018)
pCF050	plasmid for integration of P_{vp1343}-*T7* on the chromosome	This work
pCF054	plasmid for deletion of *vpa1083*	This work

Table 11. Primers

Primer name	Primer sequence
VP0984-ins-CHK	AAGCTCGCACCATGAGTATGG
VP0984-ins-Prom AQUA cw-a	AAGCTTGCATGCCTGCAGGTCGACTAGCCGTTTACCAGGTAAACC
ins-Pvpa1548-VP0984 Ccw-b	TTTTAGCGTTAGTTTCCGATGTGCTAAAGGAGCCTTTTTATTAACTGC
VP0984-ins-Pvpa1548-cw-c	TGCAGTTAATAAAAAGGCTCCTTTAGCACATCGGAAACTAACGC
Pvpa1548-mCherry-Ccw-d	AGTGATAAACTAAGGAGACTAAG
mCherry cw	ATGGTTTCTAAAGGTGAAGAAG
mCherry-VP-STOP-ccw	TTATTTGTATAGTTCGTCCATA
VP0985-mCherry-STOP-cw-g	TGGTGGTATGGACGAACTATACAAATAACATGGAGCCTTTGGCTTTAAGG
VP0985-ins Prom AQUA Ccw-h	AGCTCGGTACCCGGGGATCCTCTAGGATGGGCAACGTTCTGGCA
VP2408-ins-Prom AQUA cw-a	AAGCTTGCATGCCTGCAGGTCGACTTGTTGATCAGAGCTTGATTGAAC
ins-Pvp1343-VP2408 Ccw-b	CTCGGTGGATTGCCAGGGATAGTTGCCGCTGCTATGGCGAGAGT
VP2408-ins-P-vp1343-cw-c	AAGCCACTCTCGCCATAGCAGCGGCAACTATCCCTGGCAATCC
Pvp1343-T7-Ccw-d	AGCGATGTTAATCGTGTTCATAACGTCTCCTTAAGCCGAC
T7 cw	ATGAACACGATTAACATCGCT
T7 Ccw	TTACGCGAACGCGAAGTC
VP2409-T7-cw-g	GAGTCGGACTTCGCGTTCGCGTAAAGTGTCTTTTTCATTGAATATTTACT
VP2409-ins Prom AQUA Ccw-h	AGCTCGGTACCCGGGGATCCTCTAGAGCCTTTCGTGCATCGCTTG
ins-VP2488-cw	ACCCGCATGCAAGATCTATCGAGCAAGAAGGCTACGA
ins-T7sfGFP-VP2488-ccw	TTCCCCTATAGTGAGTCGTATTAGAGCGCCTTTTCAGACAGC
ins-T7-prom.+sfGFP-cw	TAATACGACTCACTATAGGGGAATTGTGAGCGGATAACAATTCCCCATCTTAGTATATTAGTTAAGTATAAGAAGGAGCCCATGAGCAAAGGAGAAGAACTTTTCAC
ins-sfGFP+STOP-ccw	TTATTTGTAGAGCTCATCCATGC
ins-T7sfGFP-VP2489-cw	TGGATGAGCTCTACAAATAATCAACAGGAGAAGAGCACTTG
ins-VP2489-ccw	TAGTGGGGCCCTTCTAGGAAATGCTAGAACTCGTGC
200vp0764-del-a	CAGGTTACCCGCATGCAAGATCTATAAATTGGCATGGGTAAAATCGG

1096vp0764-del-b	TTGATGCGATTGGGTTGTTTTCACCCCAAGATTTACCCATTTTACCGCC
1856vp0764-del-c	GGTGAAAACAACCCAATCGCATCAA
2760vp0764-del-d	CGCGTCACTAGTGGGGCCCTTCTAGCACCGCTTTATTTCGAAAGGC
Chk_vp0764-del	TACACCAAATGATCGCTGACG
221vpa1649-del-a	CAGGTTACCCGCATGCAAGATCTATATCGCCTGTACCTAAGTACGC
1001vpa1649-del-b	CCACGGTTTTTATCAAAGATTCCCATCAT GTC GTA ATG ATC GTA TTC TGG
1858vpa1649-del-c	ATGGGAATCTTTGATAAAAACCGTGG
2642vpa1649-del-d	CGCGTCACTAGTGGGGCCCTTCTAGATA AGG TTT TCG ACG ATC TCG CG
Chk_vpa1649-del	ACTGGCACCATACCGAGCG
204vp0649-del-a	CAGGTTACCCGCATGCAAGATCTATTGTGATTGGCGTAAACCGTGGC
1006vp0649-del-b	CGACTCATTGAAATTGAAAGGGTTACGA CAT ACT CCA TTC AAT TTG C
2258vp0649-del-c	TAACCCTTTCAATTTCAATGAGTCG
3068vp0649-del-d	CGCGTCACTAGTGGGGCCCTTCTAGTGC TCT TGC TCG AGT TCT GCG
Chk_vpa0649-del	TAGTTGTCGGTGGTGATGGC
219vp1391-del-a	CAGGTTACCCGCATGCAAGATCTATCGTATTCCTGCTAGTTGGCC
1014vp1391-del-b	GAA TTT TCT TTT TAA GCC CCA TCA ATTAGCTGAACGCATAGGTCA
2629vp1391-del-c	TTGATGGGGCTTAAAAAGAAAATTC
3442vp1391-del-d	CGCGTCACTAGTGGGGCCCTTCTAGAGTATTTATGTGCTGATTTCGGG
Chk_vp1391-del	CCGCAAAAGCTGGCTTGGG
VP0053-del-a	AAGCTTGCATGCCTGCAGGTCGACTTTGACTATTTGCTACCTCGCC
VP0053-del-b	GGGTTGACGATGGTTGCTTTA TATTCATTTGTCCTTGTTCGTTTCC
VP0053-del-c	TAAAGCAACCATCGTCAACCC

VP0053-del-d	AGCTCGGTACCCGGGGATCCTCTAGTCAAAACCTTGT CGAACTATCGC
Chk_vp0053	ACAAGCAATCGATGGAAAAACGG
VPA0584-del-a	AAGCTTGCATGCCTGCAGGTCGACTTTGCCGAACAAT CTTGTCGC
VPA0584-del-b	CTATTGTTTTCCAAGATAGTATACTA CATTTTAGGGGCCTTACTCATC
VPA0584-del-c	TAG TAT ACT ATC TTG GAA AAC AAT AG
VPA0584-del-d	AGCTCGGTACCCGGGGATCCTCTAGAGC ACT TAC TTA ACG ATC CCG
Chk_vp0584	ATCCATCATCGGGAACGAAGC
VP2240-del-a	AAGCTTGCATGCCTGCAGGTCGACTAAAAGACATAT CGTTGCGCG
VP2240-del-b	CGGATTGGATTACCCTTTGTCAT ATTAACGCAGCTTTTTGATGCG
VP2240-del-c	ATGACAAAGGGTAATCCAATCCG
VP2240-del-d	AGCTCGGTACCCGGGGATCCTCTAGATTGGCGATAG CATCATCATACC
Chk_vp2240	AAGAGATCATGGACTGTCCGG
VPA1176-del-a	AAGCTTGCATGCCTGCAGGTCGACTTGCCTGATACCT CTTTGCCG
VPA1176-del-b	CCGACATCACTAAAGCCATCGATTGTTTTGATAACCCC TAGC
VPA1176-del-c	CGATGGCTTTAGTGATGTCGG
VPA1176-del-d	AGCTCGGTACCCGGGGATCCTCTAGAAAAGCGTCTGA GCGTGAGG
Chk_vpa1176	TTCTGAAAGCAAAAAAATCACCG
VP2972-del-a	AAGCTTGCATGCCTGCAGGTCGACTAAAGTGCTGCGA TCGGACC
VP2972-del-b	CTAATAGAGAGAATTAGACCGTG TGT ATT CAT GCG ATA GAA CTA CC
VP2972-del-c	CACGGTCTAATTCTCTCTATTAG
VP2972-del-d	AGCTCGGTACCCGGGGATCCTCTAGAATTCACTGCAT CGATGTCGCG
Chk_vp2972	TCTGTCCCTTTAACAAAGCCC

VPA0053-del-a	AAGCTTGCATGCCTGCAGGTCGACTATCGGTGAGAGGTGCATAGC
VPA0053-del-b	CGTTACCCGTAGACGGTGTTAAACTGTAGTTTTAGCACGATCGTTC
VPA0053-del-c	TAACACCGTCTACGGGTAACG
VPA0053-del-d	AGCTCGGTACCCGGGGATCCTCTAGATAGCCAGAACGCGCAATGC
Chk_vpa0053	TAA GGT ACT GAA AAA TGG CCC
VP1945-del-a	AAGCTTGCATGCCTGCAGGTCGACTTTTCGTATAGCAAGCTGCGAG
VP1945-del-b	GAATCGAAAGGAGGATTCACACTAACTTGTATCTCCACACTTTTTATTGG
VP1945-del-c	TAGTGTGAATCCTCCTTTCGATTC
VP1945-del-d	AGCTCGGTACCCGGGGATCCTCTAGACATATTGCTGTTCTTGGACTCG
Chk_vp1945	AGATCTTGTAATACGAGTGCTTC
VP2178-del-a	AAGCTTGCATGCCTGCAGGTCGACTTCATCAGTTACGTTCACAGCG
VP2178-del-b	CCG CTT AAT TAG ATG TCA GCA GAGTTTATCTCTCTGGTTTAATTGGG
VP2178-del-c	TCTGCTGACATCTAATTAAGCGG
VP2178-del-d	AGCTCGGTACCCGGGGATCCTCTAGTATTGTGGGTGGCGTACTTGG
Chk_vp2178	AACCTCAGCAAGAAAGCGCG
VPA0062-del-a	AAGCTTGCATGCCTGCAGGTCGACTATCGTTTCCAAGACAAGCTCG
VPA0062-del-b	GAA CTG CAA TAG ATA GGC GAG CTTTGTCTTCATACAAACGAATCGAC
VPA0062-del-c	GCTCGCCTATCTATTGCAGTTC
VPA0062-del-d	AGCTCGGTACCCGGGGATCCTCTAGAAAGTGACGTCGATCATTGGC
Chk_vpa0062	AACTTGCCACCGAACTCACC
VPA0514-del-a	AAGCTTGCATGCCTGCAGGTCGACTAAGAAGATCTACAAAACCGCG

VPA0514-del-b	CTC TTT CAA TTC GAT TCA CTC ATTTCTCTAACCCTTATTCTTTTGTTG
VPA0514-del-c	AAT GAG TGA ATC GAA TTG AAA GAG
VPA0514-del-d	AGCTCGGTACCCGGGGATCCTCTAGTTA GCA CTC GAC GAA GAT GAC
Chk_vpa0514	AAC ACT ACA ACC CAG ACC ACG
vpa1083-del-a	AAGCTTGCATGCCTGCAGGTCGACTTGCTGGTACGTC TGCGGC
vpa1083-del-b	TAT TTT AAG AGG CCT TGT GCG CT ACG GTT ATC CTC GGT TCT GAA
vpa1083-del-c	AGC GCA CAA GGC CTC TTA AAA TA
vpa1083-del-d	AGCTCGGTACCCGGGGATCCTCTAGATT AAA TTC CAA GCC AGC TTC G
Chk_vpa1083	TCT GAC AAC GTT GTA GGC GG

6.4.12.1 Construction of plasmids

Plasmid pCF002
    The upstream and downstream flanking regions of the gene *vp0764* were amplified using the primers vp0764-del-a/vp0764-del-b and vp0764-del-c/vp0764-del-d and chromosomal DNA from *V. parahaemolyticus* RIMD2210633 as template. The resulting fragments were then fused together in a third PCR reaction by using primers vp0764-del-a/vp0764-del-d. The PCR product was mix with plasmid pDM4 digested by XbaI, resulting in plasmid pCF002, through Gibson assembly.

Plasmid pCF007
    The upstream and downstream flanking regions of the gene *vp0649* were amplified using the primers vp0649-del-a/vp0649-del-b and vp0649-del-c/vp0649-del-d and chromosomal DNA from *V. parahaemolyticus* RIMD2210633 as template. The resulting fragments were then fused together in a third PCR reaction by using primers vp0649-del-a/vp0649-del-d. The PCR product was mix with plasmid pDM4 digested by XbaI, resulting in plasmid pCF007, through Gibson assembly.

Plasmid pCF010
    The upstream and downstream flanking regions of the gene *vpa1649* were amplified using the primers vpa1649-del-a/vpa1649-del-b and vpa1649-del-c/vpa1649-del-d and chromosomal DNA from *V. parahaemolyticus* RIMD2210633 as template. The resulting fragments were then fused together in a third PCR reaction by using primers vpa1649-del-a/vpa1649-del-d. The PCR product was mix with plasmid pDM4 digested by XbaI, resulting in plasmid pCF010, through Gibson assembly.

Plasmid pCF012
    The upstream and downstream flanking regions of the gene *vp1391* were amplified using the primers vp1391-del-a/vp1391-del-b and vp1391-del-c/vp1391-del-d and chromosomal DNA from *V. parahaemolyticus* RIMD2210633 as template. The resulting fragments were then fused

together in a third PCR reaction by using primers vp1391-del-a/vp1391-del-d. The PCR product was mix with plasmid pDM4 digested by XbaI, resulting in plasmid pCF012, through Gibson assembly.

Plasmid pCF015

The upstream and downstream flanking regions of the gene *vp0053* were amplified using the primers vp0053-del-a/vp0053-del-b and vp0053-del-c/vp0053-del-d and chromosomal DNA from *V. parahaemolyticus* RIMD2210633 as template. The resulting fragments were then fused together in a third PCR reaction by using primers vp0053-del-a/vp0053-del-d. The PCR product was mix with plasmid pDM4 digested by XbaI, resulting in plasmid pCF015, through Gibson assembly.

Plasmid pCF016

The upstream and downstream flanking regions of the gene *vpa0584* were amplified using the primers vpa0584-del-a/vpa0584-del-b and vpa0584-del-c/vpa0584-del-d and chromosomal DNA from *V. parahaemolyticus* RIMD2210633 as template. The resulting fragments were then fused together in a third PCR reaction by using primers vpa0584-del-a/vpa0584-del-d. The PCR product was mix with plasmid pDM4 digested by XbaI, resulting in plasmid pCF016, through Gibson assembly.

Plasmid pCF017

The upstream and downstream flanking regions of the gene *vpa1176* were amplified using the primers vpa1176-del-a/vpa1176-del-b and vpa1176-del-c/vpa1176-del-d and chromosomal DNA from *V. parahaemolyticus* RIMD2210633 as template. The resulting fragments were then fused together in a third PCR reaction by using primers vpa1176-del-a/vpa1176-del-d. The PCR product was mix with plasmid pDM4 digested by XbaI, resulting in plasmid pCF017, through Gibson assembly.

Plasmid pCF018

The upstream and downstream flanking regions of the gene *vp2240* were amplified using the primers vp2240-del-a/vp2240-del-b and vp2240-del-c/vp2240-del-d and chromosomal DNA from *V. parahaemolyticus* RIMD2210633 as template. The resulting fragments were then fused together in a third PCR reaction by using primers vp2240-del-a/vp2240-del-d. The PCR product was mix with plasmid pDM4 digested by XbaI, resulting in plasmid pCF018, through Gibson assembly.

Plasmid pCF020

The upstream and downstream flanking regions of the gene *vp2972* were amplified using the primers vp2972-del-a/vp2972-del-b and vp2972-del-c/vp2972-del-d and chromosomal DNA from *V. parahaemolyticus* RIMD2210633 as template. The resulting fragments were then fused together in a third PCR reaction by using primers vp2972-del-a/vp2972-del-d. The PCR product was mix with plasmid pDM4 digested by XbaI, resulting in plasmid pCF020, through Gibson assembly.

Plasmid pCF021

The upstream and downstream flanking regions of the gene *vpa0754* were amplified using the primers vpa0754-del-a/vpa0754-del-b and vpa0754-del-c/vpa0754-del-d and chromosomal DNA from *V. parahaemolyticus* RIMD2210633 as template. The resulting fragments were then fused together in a third PCR reaction by using primers vpa0754-del-a/vpa0754-del-d. The PCR product was mix with plasmid pDM4 digested by XbaI, resulting in plasmid pCF021, through Gibson assembly.

Plasmid pCF022

The upstream and downstream flanking regions of the gene *vp1945* were amplified using the primers vp1945-del-a/vp1945-del-b and vp1945-del-c/vp1945-del-d and chromosomal DNA from *V. parahaemolyticus* RIMD2210633 as template. The resulting fragments were then fused together in a third PCR reaction by using primers vp1945-del-a/vp1945-del-d. The PCR product was mix with plasmid pDM4 digested by XbaI, resulting in plasmid pCF022, through Gibson assembly.

Plasmid pCF023

        The upstream and downstream flanking regions of the gene *vp2178* were amplified using the primers vp2178-del-a/vp2178-del-b and vp2178-del-c/vp2178-del-d and chromosomal DNA from *V. parahaemolyticus* RIMD2210633 as template. The resulting fragments were then fused together in a third PCR reaction by using primers vp2178-del-a/vp2178-del-d. The PCR product was mix with plasmid pDM4 digested by XbaI, resulting in plasmid pCF023, through Gibson assembly.

Plasmid pCF025

        The upstream and downstream flanking regions of the gene *vpa0514* were amplified using the primers vpa0514-del-a/vpa0514-del-b and vpa0514-del-c/vpa0514-del-d and chromosomal DNA from *V. parahaemolyticus* RIMD2210633 as template. The resulting fragments were then fused together in a third PCR reaction by using primers vpa0514-del-a/vpa0514-del-d. The PCR product was mix with plasmid pDM4 digested by XbaI, resulting in plasmid pCF025, through Gibson assembly.

Plasmid pCF026

        The upstream and downstream flanking regions of the gene *vpa0662* were amplified using the primers vpa0662-del-a/vpa0662-del-b and vpa0662-del-c/vpa0662-del-d and chromosomal DNA from *V. parahaemolyticus* RIMD2210633 as template. The resulting fragments were then fused together in a third PCR reaction by using primers vpa0662-del-a/vpa0662-del-d. The PCR product was mix with plasmid pDM4 digested by XbaI, resulting in plasmid pCF026, through Gibson assembly.

Plasmid pJH047

        Plasmid pJH047 was constructed by amplification of the intergenic region between genes *vp2488* and *vp2489*, amplification of the promotor region of T7 polimerase and amplification of *sfGFP* sequence. Amplification of the intergenic region between gene *vp2488* and *vp2489* was performed using the pair of primers ins-VP2488-cw /ins-T7sfGFP-VP2488-ccw and ins-T7sfGFP-VP2489-cw/ ins-VP2489-ccw and chromosomal DNA from *V. parahaemolyticus* RIMD2210633 as template. The promotor region of T7 polimerase was included in the primer ins-T7-prom.+sfGFP-cw. Amplification of *sfGFP* sequence was performed using primers ins-T7-prom.+sfGFP-cw/ ins-sfGFP+STOP-ccw and plasmid pJH036 as template. In a fourth PCR reaction the first product from intergenic region of vp2488/vp2489 was fused to the promotor of T7 and sfGFP product, using primers ins-VP2488-cw / ins-sfGFP+STOP-ccw and the products of the PCR reactions as template. In a final PCR reaction the products of both second and fourth PCR reactions were fused using primers ins-VP2488-cw /ins-VP2489-ccw and the products of PCR reactions as template. The final PCR product was inserted into plasmid pJH081 (pDM4 derivative) resulting in plasmid pJH047.

Plasmid pCF048

        Plasmid pCF048 was constructed by amplification of the intergenic region of gene *vp0984* and *vp0985*, amplification of the promotor region of *vpa1548* (*lafA*) and amplification of mCherry *V. parahaemolyticus* codon optimized sequence. Amplification of the intergenic region between gene vp0984 and vp0985 was performed using the pair of primers VP0984-ins-Prom AQUA cw-a/ ins-Pvpa1548-VP0984 ccw-b and VP0985-mCherry-STOP-cw-g/VP0985-insProm-AQUA-ccw-h, and chromosomal DNA from *V. parahaemolyticus* RIMD2210633 as template. Amplification of the promotor region of vpa1548 (lafA) was obtained using the pair of primers VP0984-ins-Pvpa1548-cw-c / Pvpa1548-mCherry-Ccw-d and chromosomal DNA RIMD2210633 as template. Amplification of mCherry *V. parahaemolyticus* codon optimized sequence was performed using primers mCherry cw-e / mCherry-VP-STOP-ccw-f. In a fifth PCR reaction the first product from intergenic region of vp0984/vp0985 was fused to the promotor of vpa1548, using primers VP0984-ins-Prom AQUA cw-a / Pvpa1548-mCherry-Ccw-d and the products of the PCR reactions as template. In a sixth PCR reaction the mCherry product was fused to the second product from intergenic region of vp0984/vp0985, using primers mCherry cw-e / VP0985-insProm-AQUA-ccw-h and the products of the PCR reactions as template. In a final PCR reaction the products of both fifth and sixth PCR reactions were fused using primers VP0984-ins-Prom AQUA cw-a VP0985-ins-Prom-AQUA-ccw-h and the products of the fifth and sixth PCR reactions as template. The final PCR product was inserted into plasmid pJH081 (pDM4 derivative) resulting in plasmid pCF048.

Plasmid pCF050

Plasmid pCF050 was constructed by amplification of the intergenic region of gene vp2408 and vp2409, amplification of the promotor region of *vp1343* and amplification of T7 polimerase sequence. Amplification of the intergenic region between gene *vp2408* and *vp2409* was performed using the pair of primers VP2408-ins-Prom AQUA cw-a/ ins-Pvp1343-VP2408 Ccw-b and VP2409-T7-cw-g/VP2409-ins Prom AQUA Ccw-h, and chromosomal DNA from *V. parahaemolyticus* RIMD2210633 as template. Amplification of the promotor region of *vp1343* was obtained using the pair of primers VP2408-ins-P-vp1343-cw-c/Pvp1343-T7-Ccw-d and chromosomal DNA RIMD2210633 as template. Amplification of T7 polimerase sequence was performed using primers T7 cw/ T7 Ccw. In a fifth PCR reaction the first product from intergenic region of vp2408/vp2409 was fused to the promotor of *vp1343*, using primers VP2408-ins-Prom AQUA cw-a/ Pvp1343-T7-Ccw-d and the products of the PCR reactions as template. In a sixth PCR reaction the T7 polimerase product was fused to the second product from intergenic region of vp2408/vp2409, using primers T7 cw/ VP2409-ins Prom AQUA Ccw-h and the products of the PCR reactions as template. In a final PCR reaction the products of both fifth and sixth PCR reactions were fused using primers VP2408-ins-Prom AQUA cw-a/ VP2409-ins Prom AQUA Ccw-h and the products of the fifth and sixth PCR reactions as template. The final PCR product was inserted into plasmid pJH081 (pDM4 derivative) resulting in plasmid pCF050.

Plasmid pCF054

The upstream and downstream flanking regions of the gene *vpa1083* were amplified using the primers vpa1083-del-a/vpa1083-del-b and vpa1083-del-c/vpa1083-del-d and chromosomal DNA from *V. parahaemolyticus* RIMD2210633 as template. The resulting fragments were then fused together in a third PCR reaction by using primers vpa1083-del-a/vpa1083-del-d. The PCR product was mix with plasmid pDM4 digested by XbaI, resulting in plasmid pCF054, through Gibson assembly.

6.5 Proteomics methods

6.5.1 Targeted Liquid chromatography-mass spectrometry (LC-MS)

To collect cells from different regions of the swarm colony, two regions were manually separated: center and periphery of the swarm colony. Cells were collected by flushing these regions with water. To collect released cells, PBS 1.5% NaCl was gently pour into a swarming plate and after 10 min the liquid was collected using a pipette. To collect cells from liquid growth, overnight cultures of *V. parahaemolyticus* were sub-cultured to an initial OD_{600} of approximately 0.05 in 20 mL of LB and were grown at 37°C until they reach an OD_{600} of around 0.6. To collect cells from solid growth, in non-swarm inducing conditions, liquid culture were grown until they reach an OD_{600} of around 0.1. In an 1.5 mL Eppendorf tube, a 10^{-2} dilution was prepared and 100 μL of that dilution were plated of LB plain agar plates and incubated at 37°C for 18h. Cells were collected by flushing the plates with water.

All collected cells were harvested by centrifugation and washed with water. The final pellet was then resuspended in lysis buffer (1 % Sodium lauryl sulphate in 0.1 M

NH4HCO3) and boiled for 5 min. Following ultrasonication (2x20 seconds) and a short centrifugation spin, the samples were incubated at 90°C and shaking for 15 min. A 40X dilution of Tris carboxyethyl phosphine (TCEP) (Thermo Scientific) was added to the sample and incubated again at 90°C and shaking for 15 min. After cooling down, a 40X dilution of 0.1M Iodoacetamide was added to the sample followed by incubation in dark for 40 min. The protein concentration of the samples was then determined by performing a BCA assay (Thermo Scientific Pierce BCA Protein Assay Kit). Samples equivalent to 50 µg of protein were digested with trypsin in presence of 1 % SLS overnight at 30ºC. Following digestion, the SLS was precipitated out adding TFA (Trifluroacetic acid) to a final concentration of 1.5 % and C-18 purification of peptides was performed to concentrate and desalt the samples. The C18 columns were equilibrated in 300 µl 100 % Acetonitrile, followed by 300 µl 0.1 % TFA. The samples were then loaded and bound to these columns. Following two washes with wash buffer (5 % acetonitrile (v/v), 0.1 % TFA (v/v)), the peptides were eluted in 300 µL elution buffer 4 (50 % acetonitrile (v/v), 0.1 % TFA (v/v)) and concentrated in a vacuum press. Finally, the peptides were dissolved in 100 µL 0.1 % TFA. These peptide samples were then analyzed by LC-MS.

6.5.2 Label-free quantification of total cell lysates using LC-MS-based proteomics

For each condition three or four biological samples were analyzed. Purified peptides were analyzed using liquid-chromatography-mass spectrometry (LC-MS) carried out on a Q-Exactive Plus instrument connected to an Ultimate 3000 RSLC nano and a nanospray flex ion source (all Thermo Scientific). Peptide separation was performed on a reverse phase HPLC column (75 µm × 42 cm) packed in-house with C18 resin (2.4 µm; Dr. Maisch). The following separating gradient was used: 98 % solvent A (0.15 % formic acid) and 2 % solvent B (99.85 % acetonitrile, 0.15 % formic acid) to 32 % solvent B over 60 min at a flow rate of 300 nl min–1. For label-free quantification (LFQ) the raw data was loaded into Progenesis (Version 2.0, Nonlinear Dynamics) and exported mgf files searched by MASCOT (Version 2.5, Matrix Science) using the uniprot database for *V. parahaemolyticus*. Progenesis peptide measurement exports were then further evaluated using SafeQuant (SQ) and LFQ values from the SQ output were used to determine protein abundance changes.

6.5.3 Differential expression analyses

To determine differentially regulated proteins in a comparison set between two conditions, student t-test was performed (FDR 0.1% and S0=0.2) and a 2-fold regulation cut off was further applied. Ratio of the protein intensities between two conditions was

shown in log2. Clustering of individual protein sets was performed using between 5-15 clusters and Euclidean distance. Heat maps and clustering were generated using Perseus computational platform.

6.6 Microscopy methods

6.6.1 Stereomicroscopy

Swarm colonies for stereomicroscopy were prepared as described above in section "6.3.3. Swarming assay". Stereomicroscopy was carried out using a Nikon H600L stereomicroscope equipped with a Q2 digital camera. The images were analyzed and captured using the NIS Elements AR (v 5.02.00) tool. The magnification of the lens used is indicated in the respective pictures.

6.6.2 Fluorescence microscopy

6.6.2.1 Sample preparation

CF36 cells from the center and the periphery of swarm-colony were analyzed by fluorescence microscopy to test for expression of mCherry and sfGFP proteins. Three independent experiments were performed for each condition and the intensity of cells was measured as well as the cell length. For imaging of swarmer cells from the periphery, a swarming assay was performed and the edge of the swarm colony was excised from the swarm agar, imprinted on 1 % agarose in PBS on the microscopy slide and mounted with the cover slip, as described previously (Heering and Ringgaard, 2016; Heering *et al.*, 2017). For imaging cells from the center of the swarming colony, cells were also imprinting but had to be spread into the agarose in order to get a single layer of cells before mounted the microscopy slide with the cover slip. For imaging cells from a swarming colony after being in contact with liquid, cells from center and periphery were scrapped off with an inoculation loop and ressuspended into 100 µL of PBS. After 30 minutes 1 µL was spotted on 1 % agarose in PBS on the microscopy slide and mounted with the cover slip. To study the development of the swarming colony the swarming colonies were analyzed at different time points correspondent to stages I, II, III, IV of development. For wild-type non labelled strain these correspond to time points 3h, 6h, 15h, 18h after incubation at 24ºC. Because CF36 strain grows slower the time points for this strain were determined not by the hours after inoculation but by the diameter of CF36

colonies, which had to be correspondent to wild-type non labelled strain for each time point.

6.6.2.2 Image acquisition

All the fluorescence microscopy was performed using a Nikon eclipse Ti inverted Andor spinning-disc confocal microscope equipped with a 100x lens and an Andor Zyla sCMOS cooled camera and an Andor FRAPPA system. Microscopy images were analyzed using ImageJ imaging software (https://rsbweb.nih.gov/ij) and Metamorph Offline (version 7.7.5.0, Molecular Devices).

Wild-type non-labelled cells from center, periphery and liquid were imaged with the same exposure time and laser power as CF36 strain to obtain values for auto fluorescence. The 95 percentile of the auto fluorescence intensity was calculated and this value was then subtracted from the fluorescence intensities of CF36 cells.

6.6.2.3 Sample size and image analysis

Image analysis was carried out essentially as described by (Heering and Ringgaard, 2016; Alvarado *et al.*, 2017; Heering *et al.*, 2017). Images generated using Nikon NIS-Elements AR were first separated into single channels using Fiji/ImageJ 1.49j10 and saved as tiff images. DIC and the corresponding fluorescent channel were loaded in MetaMorph Offline (Molecular Devices) for analysis. Cells were marked using the Multi-line tool. The regions were then transferred to the fluorescent channel image. Distances of cell length were then enumerated by hand. The intensity of all cells was plotted in GraphPad Prism with bars indicating the mean (SEM). At least 300 cells were analyzed. All images´ scale bar corresponds to 5 µm. Statistical analyses and plots were generated using GraphPad Prism, v6.07, software (Prism Software, Irvine, CA).

Chapter VII - Supplementary materials

7.1 Supplementary tables

Table 12. Set of proteins specific to Released cells. Proteins differentially expressed (log2 fold change (FC ≥1 or ≤-1) and statistically significant (FDR=0.01 S_0=0.2) between pairs of i) Release vs. Periphery ii) Release vs. Center, iii) Release vs. Liquid.

Protein number	Gene name	R vs. P (FC)	R vs. C (FC)	R vs. L (FC)	Description
VP0391		3.1	3.8	2.9	Uncharacterized protein
VP1533	*ttcA*	2.4	2.3	1.2	tRNA 2-thiocytidine biosynthesis protein TtcA
VP1889		3.8	4.2	4.0	Cold shock transcriptional regulator CspA
VP2753		5.1	5.9	6.7	Peroxiredoxin family protein/glutaredoxin
VPA0305		3.7	3.8	3.9	Catalase
VPA0563		5.8	5.4	2.4	DPS family protein
VPA0835		3.8	2.9	3.7	Inosine-guanosine kinase
VPA1289		3.8	4.5	8.1	Cold shock transcriptional regulator CspA
VPA1418		7.0	6.2	8.1	Catalase
VPA1552		1.3	4.6	3.9	LafD
VPA1684		7.6	7.9	5.8	Alkyl hydroperoxide reductase, subunit F

Table 13. Proteins differentially expressed (log2 fold change (FC ≥1 or ≤-1) and statistically significant (FDR=0.01 S_0=0.2) between Periphery vs. Center.

Protein number	Gene name	P vs. C (FC)	Description
NT01vpa1551	*NT01*	5.2	NT01vpa1551
VP0003	*yidC*	0.9	Membrane protein insertase YidC
VP0005	*rpmH*	1.4	50S ribosomal protein L34
VP0038		1.0	Putative multidrug resistance protein
VP0069	*rlmJ*	0.7	Ribosomal RNA large subunit methyltransferase J
VP0109	*engB*	0.7	Probable GTP-binding protein EngB
VP0113	*yihI*	0.8	Der GTPase-activating protein YihI
VP0133		0.6	General secretion pathway protein D
VP0135		1.0	General secretion pathway protein F
VP0141		0.7	Type II secretion system protein L
VP0179	*lpxL*	1.3	Lipid A biosynthesis lauroyltransferase
VP0180	*slmA*	2.5	Nucleoid occlusion factor SlmA
VP0185	*rpmB*	1.1	50S ribosomal protein L28
VP0186	*rpmG*	1.3	50S ribosomal protein L33
VP0187		1.1	Putative Dca
VP0208		1.0	Putative integral membrane protein

VP0209		0.8	Putative citrate synthase
VP0215		0.9	Putative OtnG protein
VP0216		0.8	Uncharacterized protein
VP0226		0.9	Putative rhamnosyl transferase
VP0230		0.9	Putative glycosyltransferase
VP0255	*rpmE*	1.2	50S ribosomal protein L31
VP0256	*rpsJ*	1.2	30S ribosomal protein S10
VP0257	*rplC*	1.3	50S ribosomal protein L3
VP0258	*rplD*	1.4	50S ribosomal protein L4
VP0259	*rplW*	1.5	50S ribosomal protein L23
VP0260	*rplB*	1.1	50S ribosomal protein L2
VP0261	*rpsS*	1.0	30S ribosomal protein S19
VP0262	*rplV*	1.6	50S ribosomal protein L22
VP0263	*rpsC*	1.1	30S ribosomal protein S3
VP0264	*rplP*	1.2	50S ribosomal protein L16
VP0265	*rpmC*	1.9	50S ribosomal protein L29
VP0266	*rpsQ*	1.3	30S ribosomal protein S17
VP0267	*rplN*	1.2	50S ribosomal protein L14
VP0268	*rplX*	0.9	50S ribosomal protein L24
VP0269	*rplE*	1.1	50S ribosomal protein L5
VP0270	*rpsN*	0.8	30S ribosomal protein S14
VP0271	*rpsH*	1.1	30S ribosomal protein S8
VP0272	*rplF*	1.0	50S ribosomal protein L6
VP0273	*rplR*	1.2	50S ribosomal protein L18
VP0274	*rpsE*	1.2	30S ribosomal protein S5
VP0276	*rplO*	1.0	50S ribosomal protein L15
VP0277	*secY*	0.6	Protein translocase subunit SecY
VP0279	*rpsM*	1.1	30S ribosomal protein S13
VP0280	*rpsK*	1.0	30S ribosomal protein S11
VP0281	*rpsD*	1.1	30S ribosomal protein S4
VP0282	*rpoA*	0.9	DNA-directed RNA polymerase subunit alpha
VP0283	*rplQ*	1.2	50S ribosomal protein L17
VP0288		1.6	ATP-dependent RNA helicase DbpA
VP0328	*rplU*	1.2	50S ribosomal protein L21
VP0329	*rpmA*	0.8	50S ribosomal protein L27
VP0330	*obg*	1.4	GTPase Obg
VP0336	*rsmA*	0.8	Ribosomal RNA small subunit methyltransferase A
VP0350		1.3	Transcriptional regulator, LysR family
VP0375		1.3	Putative lipoprotein
VP0386		1.3	Putative inner membrane protein
VP0388		1.2	Type I restriction enzyme M protein
VP0407	*rpsU*	1.2	30S ribosomal protein S21
VP0413	*uppP*	2.2	Undecaprenyl-diphosphatase
VP0417		0.7	Uncharacterized protein
VP0431	*parC*	0.8	DNA topoisomerase 4 subunit A
VP0438	*rplM*	1.1	50S ribosomal protein L13

VP0439	*rpsI*	1.1	30S ribosomal protein S9
VP0484		2.2	Glutamate synthase, large subunit
VP0505	*srmB*	0.9	ATP-dependent RNA helicase SrmB
VP0531	*rpsT*	1.4	30S ribosomal protein S20
VP0533		1.3	Riboflavin biosynthesis protein
VP0566		1.5	Ferredoxin
VP0590	*secD*	0.5	Protein translocase subunit SecD
VP0593		1.0	Inositol monophosphate family protein
VP0605	*rlmN*	2.5	Dual-specificity RNA methyltransferase RlmN
VP0616	*guaB*	0.6	Inosine-5'-monophosphate dehydrogenase
VP0647	*bamE*	0.9	Outer membrane protein assembly factor BamE
VP0649		2.5	Uncharacterized protein
VP0654	*dnaJ*	0.8	Chaperone protein DnaJ
VP0665	*mltF*	0.9	Membrane-bound lytic murein transglycosylase F
VP0679		1.2	Riboflavin biosynthesis protein RibD
VP0692		0.6	Transcriptional regulator, LysR family
VP0695	*rlmM*	1.5	Ribosomal RNA large subunit methyltransferase M
VP0699		1.2	GGDEF family protein
VP0710		1.0	PTS system, trehalose-specific IIBC component
VP0719		1.2	D-alanyl-D-alanine carboxypeptidase
VP0729	*lnt*	0.8	Apolipoprotein N-acyltransferase
VP0733	*miaB*	0.6	tRNA-2-methylthio-N(6)-dimethylallyladenosine synthase
VP0738	*pth*	1.1	Peptidyl-tRNA hydrolase
VP0750		1.1	Pseudouridine synthase
VP0819	*toxS*	1.1	Transmembrane regulatory protein ToxS
VP0820	*toxR*	0.6	Cholera toxin homolog transcriptional activator
VP0852	*znuC*	2.2	Zinc import ATP-binding protein ZnuC
VP0871	*rnd*	1.8	Ribonuclease D
VP0882		0.6	Putative beta-ketoacyl-ACP reductase
VP0903		1.1	RhlE
VP0907		0.8	Uncharacterized protein
VP0948		7.7	Uncharacterized protein
VP0956		1.3	Uncharacterized protein
VP0995		1.6	Uncharacterized protein
VP1002		1.0	Uncharacterized protein
VP1016	*infA*	0.5	Translation initiation factor IF-1
VP1036	*mukE*	1.0	Chromosome partition protein MukE
VP1037	*mukB*	0.9	Chromosome partition protein MukB
VP1053		0.8	Cytochrome d ubiquinol oxidase, subunit I
VP1061		0.9	Peptidoglycan-associated lipoprotein
VP1092		0.9	Acridine efflux pump
VP1105	*ftsK*	1.4	DNA translocase FtsK
VP1168		0.9	Peptide ABC transporter, ATP-binding protein
VP1185		1.4	Putative chemotaxis transducer
VP1186		4.7	Pseudouridine synthase Rlu family protein
VP1235		1.3	Iron-containing alcohol dehydrogenase

VP1243		1.1	Uncharacterized protein
VP1267		1.1	Putative lipoprotein
VP1268		1.2	Uncharacterized protein
VP1270		1.4	Uncharacterized protein
VP1281	rpmI	1.1	50S ribosomal protein L35
VP1282	rplT	1.7	50S ribosomal protein L20
VP1386		1.2	Type VI secretion system 1 protein
VP1387		1.4	Type VI secretion system 1 protein
VP1390		1.1	Type VI secretion system 1 protein
VP1407		1.9	Transcriptional regulator of type VI secretion system 1
VP1408		0.9	Type VI secretion system 1, Putative IcmF-related protein
VP1432		1.1	ATP-binding component of a transport system
VP1454		1.4	Uncharacterized protein
VP1506	fdhD	3.0	Formate dehydrogenase accessory protein
VP1513		1.2	Putative formate dehydrogenase large subunit
VP1514		5.6	Formate dehydrogenase, iron-sulfur subunit
VP1609		1.3	ABC transporter, ATP-binding protein
VP1694		5.1	Type III export protein YscF
VP1696		3.4	Putative type III secretion protein YscC
VP1698		1.8	Uncharacterized protein
VP1736		1.8	Uncharacterized protein
VP1777		2.7	Putative aldehyde dehydrogenase
VP1879		2.0	Serine transporter
VP1904		0.9	Methyl-accepting chemotaxis protein
VP1912		2.0	Uncharacterized protein
VP1917		1.6	Uncharacterized protein
VP1942		1.0	Diaminobutyrate-pyruvate transaminase & L-2,4-diaminobutyrate decarboxylase
VP1951	rluB	1.4	Ribosomal large subunit pseudouridine synthase B
VP1980		3.1	UPF0313 protein VP1980
VP1998		1.0	Putative outer membrane protein TolC
VP2030		1.2	30S ribosomal protein S1
VP2050		0.6	Uncharacterized protein
VP2058	rpmF	1.1	50S ribosomal protein L32
VP2062	rne	0.8	Ribonuclease E
VP2063		2.2	Sulfate permease family protein
VP2087		2.2	Oligopeptide ABC transporter, ATP-binding protein
VP2088		2.2	Oligopeptide ABC transporter, ATP-binding protein
VP2104		1.3	Electron transport complex subunit C
VP2159		2.1	Putative methyl-accepting chemotaxis transmembrane protein
VP2179		0.8	DNA polymerase III, subunits gamma and tau
VP2191		0.6	Uncharacterized protein
VP2211		2.1	Uncharacterized protein
VP2212		1.2	Long-chain fatty acid transport protein
VP2224		2.0	Uncharacterized protein
VP2227		1.0	Soj-like protein

VP2228	cheB	1.2	Chemotaxis response regulator protein-glutamate methylesterase of group 1 operon
VP2243		2.5	Polar flagellar protein FliL
VP2248		0.8	Flagellar motor switch protein FliG
VP2314	uppS	1.1	Ditrans,polycis-undecaprenyl-diphosphate synthase ((2E,6E)-farnesyl-diphosphate specific)
VP2318	rpsB	1.2	30S ribosomal protein S2
VP2329		3.1	Efflux pump component MtrF
VP2346	nqrF	0.9	Na(+)-translocating NADH-quinone reductase subunit F
VP2349	nqrC	1.1	Na(+)-translocating NADH-quinone reductase subunit C
VP2351	nqrA	1.2	Na(+)-translocating NADH-quinone reductase subunit A
VP2379		2.7	DNA damage-inducible gene in SOS regulon, dependent on cyclic AMP and H-NS
VP2430		0.7	Uncharacterized protein
VP2455	rbfA	0.9	Ribosome-binding factor A
VP2456	infB	0.7	Translation initiation factor IF-2
VP2464	rlmE	1.5	Ribosomal RNA large subunit methyltransferase E
VP2467	ompU	0.9	Outer membrane protein U
VP2497		2.2	Penicillin-binding protein 1B
VP2504	pcnB	1.5	Poly(A) polymerase I
VP2518		1.3	Acetyltransferase component of pyruvate dehydrogenase complex
VP2519		1.1	Pyruvate dehydrogenase E1 component
VP2530	rplS	1.1	50S ribosomal protein L19
VP2533	rpsP	1.1	30S ribosomal protein S16
VP2547		1.3	Aspartokinase
VP2572	rnc	0.9	Ribonuclease 3
VP2628		2.9	Membrane-bound lytic murein transglycosylase C
VP2629		1.8	Methyl-accepting chemotaxis protein
VP2662		0.8	Putative ABC superfamily transport protein
VP2664		1.3	ABC transporter, ATP-binding protein
VP2677		0.5	UPF0307 protein VP2677
VP2686		1.1	Uncharacterized protein
VP2737	rplI	1.1	50S ribosomal protein L9
VP2738	rpsR	1.0	30S ribosomal protein S18
VP2739	priB	2.6	Primosomal replication protein n
VP2740	rpsF	1.3	30S ribosomal protein S6
VP2762		2.7	Uncharacterized protein
VP2772	rpsG	1.2	30S ribosomal protein S7
VP2773	rpsL	1.0	30S ribosomal protein S12
VP2824	rsgA1	1.5	Putative ribosome biogenesis GTPase RsgA 1
VP2825	psd	0.9	Phosphatidylserine decarboxylase proenzyme
VP2827		1.3	Methyl-accepting chemotaxis protein
VP2885	fis	3.2	DNA-binding protein Fis
VP2902		0.8	Uncharacterized protein
VP2912		0.9	Uncharacterized protein

VP2921	*rpoC*	0.7	DNA-directed RNA polymerase subunit beta'
VP2922	*rpoB*	0.7	DNA-directed RNA polymerase subunit beta
VP2923	*rplL*	0.8	50S ribosomal protein L7/L12
VP2924	*rplJ*	1.4	50S ribosomal protein L10
VP2925	*rplA*	1.4	50S ribosomal protein L1
VP2926	*rplK*	1.1	50S ribosomal protein L11
VP2934		0.9	CDP-diacylglycerol--serine O-phosphatidyltransferase
VP2941		1.2	Transcriptional regulator, TetR family
VP3000	*rho*	0.6	Transcription termination factor Rho
VP3007		4.2	ATP-dependent DNA helicase RecQ
VP3051		1.3	Uncharacterized protein
VPA0054		1.1	Uncharacterized protein
VPA0173	*rimK*	1.3	Probable alpha-L-glutamate ligase
VPA0243		0.8	Putative virK protein
VPA0262		1.0	LfgM
VPA0264		4.6	Flagellar basal body rod protein FlgB
VPA0267		3.6	Flagellar hook protein FlgE
VPA0268		5.1	Flagellar basal body protein
VPA0269		3.9	Flagellar basal-body rod protein FlgG
VPA0273	*flgK*	3.6	Flagellar hook-associated protein 1
VPA0274		3.7	Putative flagellar hook-associated protein
VPA0275		2.6	Putative flagellin
VPA0286	*groS2*	1.2	10 kDa chaperonin 2
VPA0288		4.8	Uncharacterized protein
VPA0297		2.6	PTS system, fructose-specific IIBC component
VPA0318		1.6	Putative outer membrane protein OmpV
VPA0341		1.6	Uncharacterized protein
VPA0390	*rhlE*	1.9	ATP-dependent RNA helicase RhlE
VPA0394		2.4	Uncharacterized protein
VPA0491		1.7	Methyl-accepting chemotaxis protein
VPA0519		1.4	Transcriptional regulator, LysR family
VPA0583		2.4	Putative ATP-dependent RNA helicase
VPA0590		1.1	Putative ATP-dependent RNA helicase
VPA0608	*deaD*	2.2	ATP-dependent RNA helicase DeaD
VPA0627		1.8	Cytochrome o ubiquinol oxidase, subunit II
VPA0754		2.3	Uncharacterized protein
VPA0811		2.0	PTS system, fructose-specific IIBC component
VPA0845		1.0	ATP-dependent RNA helicase, DEAD box family
VPA0917		1.7	Uncharacterized protein
VPA1000		2.8	Methyl-accepting chemotaxis protein
VPA1067		1.1	Serine transporter
VPA1083	*rbsK*	1.1	Ribokinase
VPA1086	*rbsA*	3.0	Ribose import ATP-binding protein RbsA
VPA1176		1.4	Uncharacterized protein
VPA1182		1.1	Methyl-accepting chemotaxis protein
VPA1189		2.8	Methyl-accepting chemotaxis protein

VPA1209	*secD*	2.1	Protein translocase subunit SecD
VPA1280		2.7	Uncharacterized protein
VPA1294		3.1	Putative DamX-related protein
VPA1346		2.5	Putative targeted effector protein YopP, type III secretion system 2 protein
VPA1356		3.7	Type III secretion system 2 protein
VPA1361		1.4	Putative type III secretion system translocon protein VopD2
VPA1406		1.5	Putative exopolysaccharide biosynthesis protein
VPA1424		3.7	PTS system, fructose-specific IIABC component
VPA1434		0.8	Putative hemolysin secretion ATP-binding protein
VPA1435		1.2	Putative iron(III) compound receptor
VPA1436		1.1	Iron(III) ABC transporter, ATP-binding protein
VPA1437		2.8	Iron(III) ABC transporter, periplasmic iron-compound-binding protein
VPA1449		1.5	Methyl-accepting chemotaxis protein
VPA1452		1.6	Uncharacterized protein
VPA1468		0.8	ATP-dependent RNA helicase, DEAD box family
VPA1492		2.5	Methyl-accepting chemotaxis protein
VPA1527		1.4	Probable phosphatase VPA1527
VPA1535		3.7	Putative flagellar motor switch protein
VPA1536		3.6	Flagellar M-ring protein
VPA1539		3.9	Putative sodium-type flagellar protein MotY
VPA1546		2.6	Flagellar biosynthesis protein
VPA1548	*lafA*	3.3	Lateral flagellin
VPA1550	*fliDL,lafB*	3.4	Lateral flagellar hook-associated protein 2
VPA1554	*lafL*	4.0	Flagellar protein LafL
VPA1556	*lafT*	3.7	Chemotaxis protein LafT
VPA1557	*lafU*	3.9	Chemotaxis protein LafU
VPA1570		2.0	Uncharacterized protein
VPA1609		1.2	Proton/glutamate symporter
VPA1639		4.4	Putative secreted ribonuclease
VPA1649		3.2	Putative TagE protein
VPA1651		1.6	Putative methyl-accepting chemotaxis protein
VPA1652		1.1	ATP-binding component of citrate-dependent iron(III) transport protein
VPA1699		2.7	ATP-dependent RNA helicase, DEAD box family
VP0002	*mnmE*	-1.2	tRNA modification GTPase MnmE
VP0018		-1.2	16 kDa heat shock protein A
VP0019		-1.0	Valine-pyruvate aminotransferase
VP0020		-2.7	Alpha-amylase
VP0022	*glyQ*	-1.5	Glycine--tRNA ligase alpha subunit
VP0025	*tusA*	-2.7	Sulfurtransferase TusA homolog
VP0028		-2.8	Zinc-binding alcohol dehydrogenase
VP0029	*fadA*	-2.5	3-ketoacyl-CoA thiolase
VP0030	*fadB*	-2.2	Fatty acid oxidation complex subunit alpha
VP0035	*ilvC*	-2.0	Ketol-acid reductoisomerase

VP0048		-2.5	Peptide ABC transporter, periplasmic peptide-binding protein
VP0051		-1.2	Uncharacterized protein
VP0058		-1.0	Gluconate utilization system Gnt-I transcriptional repressor
VP0066		-2.9	Purine nucleoside phosphorylase
VP0068		-2.3	Glutathione reductase
VP0070		-2.2	Oligopeptidase A
VP0076		-2.3	Universal stress protein
VP0080		-4.7	Putative sigma-54 interacting response regulator transcription regulator protein
VP0092		-4.8	Uncharacterized protein
VP0094		-1.2	Uncharacterized protein
VP0104		-1.2	Delta-aminolevulinic acid dehydratase
VP0115		-2.2	Coproporphyrinogen-III oxidase
VP0122		-1.5	BipA protein
VP0124		-1.4	Uncharacterized protein
VP0126	*dtd*	-1.7	D-aminoacyl-tRNA deacylase
VP0127		-2.6	Uncharacterized protein
VP0129	*pckA*	-3.4	Phosphoenolpyruvate carboxykinase [ATP]
VP0130	*hslO*	-1.7	33 kDa chaperonin
VP0145		-3.3	MutT/nudix family protein
VP0146	*nfuA*	-2.1	Fe/S biogenesis protein NfuA
VP0154		-2.8	Transcriptional regulator OmpR
VP0155		-1.3	Osmolarity sensor protein EnvZ
VP0157	*recG*	-1.7	ATP-dependent DNA helicase RecG
VP0166		-1.5	Putative TolR
VP0171		-1.4	Putative peptide ABC transporter, permease protein
VP0173		-1.8	Oligopeptide ABC transporter, ATP-binding protein
VP0176		-1.2	Putative alpha helix protein
VP0178	*pyrE*	-2.6	Orotate phosphoribosyltransferase
VP0183		-2.2	Methyl-accepting chemotaxis protein
VP0189	*mutM*	-1.0	Formamidopyrimidine-DNA glycosylase
VP0190	*coaD*	-2.8	Phosphopantetheine adenylyltransferase
VP0191		-1.0	Putative lipopolysaccharide A protein
VP0197		-2.1	Putative capsular polysaccharide biosynthesis protein D
VP0198		-1.0	Putative aminotransferase
VP0202		-2.8	Putative sugar-phosphate nucleotide transferase
VP0203		-1.3	Putative CMP-N-acetlyneuraminic acid synthetase
VP0204		-1.7	Putative 3-chlorobenzoate-3,4-dioxygenase dyhydrogenase related protein
VP0205		-1.7	Putative glutamate-1-semialdehyde 2,1-aminomutase
VP0206		-1.7	Putative amidohydrolase
VP0207		-2.2	Putative oxidoreductase (Flagellin modification)
VP0214	*hldD*	-1.0	ADP-L-glycero-D-manno-heptose-6-epimerase
VP0222		-2.1	dTDP-glucose 4,6-dehydratase
VP0223		-2.5	Glucose-1-phosphate thymidylyltransferase

VP0224		-1.6	Putative dTDP-4-dehydrorhamnose reductase
VP0229		-3.0	dTDP-4-dehydrorhamnose 3,5-epimerase
VP0232		-1.5	Putative carbamoylphosphate synthase large subunit, short form
VP0233		-2.9	Uncharacterized protein
VP0234		-2.7	Pilin glycosylation protein
VP0236		-2.6	Nucleotide sugar dehydrogenase
VP0237		-2.0	UTP--glucose-1-phosphate uridylyltransferase
VP0239	*tpiA*	-2.0	Triosephosphate isomerase
VP0240		-5.0	Putative 5-carboxymethyl-2-hydroxymuconate delta isomerase
VP0243		-1.7	Uncharacterized protein
VP0244		-1.9	Fructose-1,6-bisphosphatase
VP0246	*zapB*	-1.6	Cell division protein ZapB
VP0247	*rraA*	-3.4	Regulator of ribonuclease activity A
VP0285		-1.8	Peptidyl-prolyl cis-trans isomerase
VP0286		-1.4	Uncharacterized protein
VP0290		-2.3	2',3'-cyclic-nucleotide 2'-phosphodiesterase
VP0293	*cysN*	-1.8	Sulfate adenylyltransferase subunit 1
VP0296	*cysC*	-1.7	Adenylyl-sulfate kinase
VP0297		-2.0	Uncharacterized protein
VP0311	*ppa*	-1.7	Inorganic pyrophosphatase
VP0313	*fbp*	-2.2	Fructose-1,6-bisphosphatase class 1
VP0314	*mpl*	-2.3	UDP-N-acetylmuramate--L-alanyl-gamma-D-glutamyl-meso-2,6-diaminoheptandioate ligase
VP0319		-1.3	Universal stress protein
VP0323		-3.9	Immunogenic protein
VP0325	*mdh*	-4.6	Malate dehydrogenase
VP0327		-1.4	Octaprenyl-diphosphate synthase
VP0333		-2.8	Dihydrofolate reductase
VP0335	*apaG*	-1.0	Protein ApaG
VP0337	*pdxA*	-2.4	4-hydroxythreonine-4-phosphate dehydrogenase
VP0338	*surA*	-1.5	Chaperone SurA
VP0343	*leuC*	-1.5	3-isopropylmalate dehydratase large subunit
VP0344	*leuB*	-3.0	3-isopropylmalate dehydrogenase
VP0346	*leuA*	-1.5	2-isopropylmalate synthase
VP0352		-1.6	Acetolactate synthase
VP0353		-1.2	Acetolactate synthase III, small subunit
VP0356		-1.4	Pyruvate kinase
VP0358		-2.4	Transcriptional regulator, DeoR family
VP0359	*glmS*	-1.6	Glutamine--fructose-6-phosphate aminotransferase [isomerizing]
VP0363		-2.1	Glycerol dehydrogenase GldH
VP0364		-2.9	Putative dihydroxyacetone kinase
VP0365		-1.9	Putative dihydroxyacetone kinase
VP0374		-2.1	Uncharacterized protein
VP0379		-2.8	Lipoprotein
VP0393		-2.1	Uncharacterized protein

VP0394		-2.2	Haemagglutinin associated protein
VP0395		-2.8	Type I restriction enzyme R protein
VP0405	*dnaG*	-1.6	DNA primase
VP0406		-1.6	Uncharacterized protein
VP0408	*tsaD*	-1.0	tRNA N6-adenosine threonylcarbamoyltransferase
VP0409		-2.6	Putative beta-ketoadipate enol-lactone hydrolase
VP0411		-1.4	7,8-dihydroneopterin aldolase
VP0423	*glnE*	-4.4	Glutamate-ammonia-ligase adenylyltransferase
VP0424	*hldE*	-1.9	Bifunctional protein HldE
VP0426		-1.9	MutT/nudix family protein
VP0428	*cpdA*	-3.6	3',5'-cyclic adenosine monophosphate phosphodiesterase CpdA
VP0429		-5.1	Uncharacterized protein
VP0433		-1.2	Protease DO
VP0434		-1.2	Uncharacterized protein
VP0436	*zapE*	-3.2	Cell division protein ZapE
VP0444		-2.5	Stringent starvation protein A
VP0445		-2.1	Stringent starvation protein B
VP0455	*murE*	-2.2	UDP-N-acetylmuramoyl-L-alanyl-D-glutamate--2,6-diaminopimelate ligase
VP0456	*murF*	-1.8	UDP-N-acetylmuramoyl-tripeptide--D-alanyl-D-alanine ligase
VP0458	*murD*	-3.3	UDP-N-acetylmuramoylalanine--D-glutamate ligase
VP0461	*murC*	-1.9	UDP-N-acetylmuramate--L-alanine ligase
VP0463	*ftsA*	-1.2	Cell division protein FtsA
VP0464	*ftsZ*	-1.4	Cell division protein FtsZ
VP0468		-1.8	Mutator MutT protein
VP0469	*dapB*	-3.1	4-hydroxy-tetrahydrodipicolinate reductase
VP0470	*carA*	-2.5	Carbamoyl-phosphate synthase small chain
VP0471	*carB*	-2.2	Carbamoyl-phosphate synthase large chain
VP0477	*btuF*	-2.2	Vitamin B12-binding protein
VP0479	*mtnN*	-2.8	5'-methylthioadenosine/S-adenosylhomocysteine nucleosidase
VP0482		-1.7	Glutamate synthase, large subunit
VP0487		-1.1	Sensor histidine kinase FexB
VP0494		-1.8	Aspartokinase I/homoserine dehydrogenase, threonine-sensitive
VP0495	*thrB*	-1.7	Homoserine kinase
VP0497	*grcA*	-1.5	Autonomous glycyl radical cofactor
VP0500	*ung*	-2.3	Uracil-DNA glycosylase
VP0504		-1.7	UPF0246 protein VP0504
VP0511		-2.6	Single-stranded-DNA-specific exonuclease RecJ
VP0513	*lysS*	-2.2	Lysine--tRNA ligase
VP0514		-1.2	Sigma-54 dependent transcriptional regulator
VP0516		-4.4	Oxidoreductase Tas, aldo/keto reductase family
VP0524	*thyA*	-3.6	Thymidylate synthase
VP0525		-2.4	Uncharacterized protein
VP0527		-1.6	Transcriptional activator protein NhaR

VP0534	ileS	-1.0	Isoleucine--tRNA ligase
VP0537	ispH	-1.7	4-hydroxy-3-methylbut-2-enyl diphosphate reductase
VP0539		-1.4	Uncharacterized protein
VP0540		-1.1	Putative carbon starvation protein A
VP0541		-1.1	Uncharacterized protein
VP0543	murQ1	-2.3	N-acetylmuramic acid 6-phosphate etherase 1
VP0544	anmK	-5.8	Anhydro-N-acetylmuramic acid kinase
VP0545	nagZ	-2.9	Beta-hexosaminidase
VP0546		-4.1	Phospho-2-dehydro-3-deoxyheptonate aldolase
VP0547		-2.7	T-protein
VP0551		-1.5	ABC transporter, ATP-binding protein
VP0552		-1.0	Soluble lytic murein transglycosylase
VP0555		-1.6	Chorismate mutase/prephenate dehydratase
VP0556		-1.8	Putative sigma-54 modulation protein
VP0561	clpB	-1.6	Chaperone protein ClpB
VP0569		-2.6	DNA-binding response regulator PhoB
VP0572		-1.6	Exopolyphosphatase
VP0573	ppk	-3.4	Polyphosphate kinase
VP0578		-1.5	Uncharacterized protein
VP0580		-3.9	Antioxidant, AhpC/Tsa family
VP0583		-3.4	Malate synthase
VP0585		-4.0	Putative acetoin utilization protein AcuB
VP0594	trmJ	-4.5	tRNA (cytidine/uridine-2'-O-)-methyltransferase TrmJ
VP0596	iscS	-1.0	Cysteine desulfurase IscS
VP0597		-2.0	Iron-sulfur cluster assembly scaffold protein IscU
VP0598		-3.9	Iron-binding protein IscA
VP0599	hscB	-2.2	Co-chaperone protein HscB homolog
VP0600	hscA	-1.9	Chaperone protein HscA homolog
VP0601		-2.5	Ferredoxin
VP0603	pepB	-1.7	Peptidase B
VP0604	ndk	-2.4	Nucleoside diphosphate kinase
VP0608	ispG	-1.8	4-hydroxy-3-methylbut-2-en-1-yl diphosphate synthase (flavodoxin)
VP0617	guaA	-1.6	GMP synthase [glutamine-hydrolyzing]
VP0622		-2.7	Sodium/alanine symporter
VP0625		-1.3	Uncharacterized protein
VP0626		-2.8	Uncharacterized protein
VP0628		-1.3	Uncharacterized protein
VP0629		-3.5	Homocysteine synthase
VP0634		-2.7	Uncharacterized protein
VP0637		-2.3	Uncharacterized protein
VP0650	nadK	-6.6	NAD kinase
VP0653	dnaK	-1.3	Chaperone protein DnaK
VP0666	purL	-3.0	Phosphoribosylformylglycinamidine synthase
VP0671		-2.9	Aminoacyl-histidine dipeptidase
VP0673	gpt	-2.5	Xanthine phosphoribosyltransferase
VP0674		-1.6	UPF0255 protein VP0674

VP0675	*crl*	-4.2	Sigma factor-binding protein Crl
VP0676	*proB*	-2.0	Glutamate 5-kinase
VP0677	*proA*	-2.0	Gamma-glutamyl phosphate reductase
VP0678	*nrdR*	-3.7	Transcriptional repressor NrdR
VP0681	*ribB*	-2.6	3,4-dihydroxy-2-butanone 4-phosphate synthase
VP0687		-1.2	Geranyltranstransferase
VP0698		-1.9	Uncharacterized protein
VP0700		-1.2	Uncharacterized protein
VP0703		-1.4	Uncharacterized protein
VP0704		-2.0	Lipoprotein
VP0705		-1.4	ABC transporter, permease protein
VP0706	*metN*	-1.7	Methionine import ATP-binding protein MetN
VP0708		-2.3	D,D-heptose 1,7-bisphosphate phosphatase
VP0709		-4.4	Trehalose operon repressor
VP0711		-1.2	Trehalose-6-phosphate hydrolase
VP0715	*glyA1*	-2.7	Serine hydroxymethyltransferase 1
VP0717	*lipB*	-2.2	Octanoyltransferase
VP0718		-2.0	UPF0250 protein VP0718
VP0727	*leuS*	-1.8	Leucine--tRNA ligase
VP0728		-1.6	Uncharacterized protein
VP0730		-1.5	Putative hemolysin
VP0735		-2.0	VisC-related protein
VP0737	*ychF*	-2.2	Ribosome-binding ATPase YchF
VP0739	*prs*	-1.0	Ribose-phosphate pyrophosphokinase
VP0747	*kdsA*	-1.3	2-dehydro-3-deoxyphosphooctonate aldolase
VP0749		-1.1	Cys-tRNA(Pro)/Cys-tRNA(Cys) deacylase
VP0753		-4.1	Uncharacterized protein
VP0758		-1.4	Cation transport ATPase, E1-E2 family
VP0762	*gltX*	-2.4	Glutamate--tRNA ligase
VP0768		-1.3	Uncharacterized protein
VP0773		-2.2	Chemotaxis CheV
VP0793		-2.9	PTS system, glucose-specific IIA component
VP0794		-1.2	Phosphoenolpyruvate-protein phosphotransferase
VP0795		-1.7	Phosphocarrier protein HPr
VP0797		-3.3	Cysteine synthase
VP0802		-2.3	Putative exported protein
VP0805		-2.1	Uncharacterized protein
VP0806		-2.2	Uncharacterized protein
VP0815		-2.1	Uncharacterized protein
VP0821	*htpG*	-1.0	Chaperone protein HtpG
VP0822	*adk*	-2.8	Adenylate kinase
VP0825	*rfaH*	-1.5	Transcription antitermination protein RfaH
VP0826		-2.4	Asparagine synthetase B, glutamine-hydrolyzing
VP0828		-1.6	N-acetylglucosamine repressor
VP0829		-1.6	N-acetylglucosamine-6-phosphate deacetylase
VP0832	*glnS*	-1.6	Glutamine--tRNA ligase

VP0833	*fur*	-1.6	Ferric uptake regulation protein
VP0835		-2.7	Flavodoxin
VP0837		-2.2	Putative esterase/lipase YbfF
VP0839		-2.5	Phosphoglucomutase
VP0842		-2.3	Citrate synthase
VP0849	*sucC*	-2.8	Succinyl-CoA ligase [ADP-forming] subunit beta
VP0850		-2.9	Succinyl-CoA ligase [ADP-forming] subunit alpha
VP0853		-1.8	Zinc ABC transporter, periplasmic zinc-binding protein
VP0860		-3.1	Histidine triad family protein
VP0861	*argS*	-1.8	Arginine--tRNA ligase
VP0864	*purU*	-3.4	Formyltetrahydrofolate deformylase
VP0872	*minE*	-2.6	Cell division topological specificity factor
VP0873		-2.0	Site-determining protein
VP0875		-1.5	YcgL domain-containing protein VP0875
VP0879	*folD*	-4.0	Bifunctional protein FolD
VP0883		-2.2	Putative beta-hydroxydecanoyl-ACP dehydrase
VP0900		-3.9	Putative oxidoreductase protein
VP0909		-3.8	UPF0061 protein VP0909
VP0910		-2.4	C4-dicarboxylate-binding periplasmic protein
VP0917	*clpP*	-1.1	ATP-dependent Clp protease proteolytic subunit
VP0918	*clpX*	-2.2	ATP-dependent Clp protease ATP-binding subunit ClpX
VP0920		-1.2	DNA-binding protein HU-beta
VP0925		-1.5	Deoxyguanosinetriphosphate triphosphohydrolase-like protein
VP0928		-2.5	Menaquinone-specific isochorismate synthase
VP0929	*menD*	-1.9	2-succinyl-5-enolpyruvyl-6-hydroxy-3-cyclohexene-1-carboxylate synthase
VP0931	*menB*	-2.3	1,4-dihydroxy-2-naphthoyl-CoA synthase
VP0932	*menC*	-1.5	o-succinylbenzoate synthase
VP0958		-5.4	Inosine monophosphate dehydrogenase-related protein
VP0959		-2.2	Cation transport ATPase, E1-E2 family
VP0960		-2.4	Uridine phosphorylase
VP0962		-1.2	Uncharacterized protein
VP0963		-1.0	Methyl-accepting chemotaxis protein
VP0964		-3.3	Hit family protein
VP0966		-1.0	Uncharacterized protein
VP0969		-3.2	UPF0227 protein VP0969
VP0975	*mfd*	-1.4	Transcription-repair-coupling factor
VP0984	*kdsB*	-1.6	3-deoxy-manno-octulosonate cytidylyltransferase
VP0990		-1.2	UPF0304 protein VP0990
VP0992		-1.4	Pyruvate formate-lyase-activating enzyme
VP0994		-2.7	Formate acetyltransferase
VP0998		-2.9	Amino acid ABC transporter, ATP-binding protein
VP0999		-2.4	Amino acid ABC transporter, periplasmic amino acid-binding protein
VP1000		-4.2	Amino acid ABC transporter, permease protein

VP1003		-1.2	Exodeoxyribonuclease III
VP1009		-2.2	UPF0319 protein VP1009
VP1011		-3.2	Isocitrate dehydrogenase
VP1014		-2.2	ATP-dependent Clp protease, ATP-binding subunit ClpA
VP1020	*aroA*	-3.6	3-phosphoshikimate 1-carboxyvinyltransferase
VP1023	*glgC1*	-2.6	Glucose-1-phosphate adenylyltransferase 1
VP1024	*glgA*	-2.6	Glycogen synthase
VP1047	*aspS*	-2.2	Aspartate--tRNA ligase
VP1060	*tolB*	-1.1	Protein TolB
VP1064		-1.2	Putative eukaryotic-type potassium channels
VP1072		-2.8	Putative helicase
VP1081		-2.5	Uncharacterized protein
VP1082		-2.8	Uncharacterized protein
VP1087		-6.7	Uncharacterized protein
VP1096		-6.8	Putative tryptophanyl-tRNA synthetase
VP1102		-5.3	Uncharacterized protein
VP1103		-2.6	Alanine dehydrogenase
VP1107		-1.1	Uncharacterized protein
VP1108	*serS*	-3.1	Serine--tRNA ligase
VP1116	*bioD*	-2.5	ATP-dependent dethiobiotin synthetase BioD
VP1118	*htpX*	-1.5	Protease HtpX
VP1128		-1.2	Adenylosuccinate lyase
VP1132		-1.7	Inosine-guanosine kinase
VP1133		-1.4	DNA-binding protein
VP1137	*hisG*	-2.0	ATP phosphoribosyltransferase
VP1138	*hisD*	-3.0	Histidinol dehydrogenase
VP1139	*hisC*	-1.4	Histidinol-phosphate aminotransferase
VP1140	*hisB*	-3.2	Histidine biosynthesis bifunctional protein HisB
VP1141	*hisH*	-3.5	Imidazole glycerol phosphate synthase subunit HisH
VP1142	*hisA*	-4.3	1-(5-phosphoribosyl)-5-[(5-phosphoribosylamino)methylideneamino] imidazole-4-carboxamide isomerase
VP1143	*hisF*	-3.1	Imidazole glycerol phosphate synthase subunit HisF
VP1144	*hisI*	-2.2	Histidine biosynthesis bifunctional protein HisIE
VP1149		-3.0	Peptidyl-prolyl cis-trans isomerase
VP1150	*cysS*	-2.0	Cysteine--tRNA ligase
VP1164		-2.4	Uncharacterized protein
VP1173		-2.2	Phage shock protein A
VP1182		-2.6	Cystathionine beta-lyase
VP1203		-1.9	Heat shock protein HslJ
VP1212		-1.4	DNA-binding response regulator
VP1217		-1.0	Uncharacterized protein
VP1230		-2.0	Oxidoreductase, acyl-CoA dehydrogenase family
VP1231	*fabV1*	-2.2	Enoyl-[acyl-carrier-protein] reductase [NADH] 1
VP1233		-1.9	Glutaredoxin 1
VP1247	*serC*	-3.1	Phosphoserine aminotransferase

VP1251		-3.5	Thioredoxin reductase
VP1252		-2.3	Uncharacterized protein
VP1253		-3.3	NifS-related protein
VP1263	*purC*	-1.3	Phosphoribosylaminoimidazole-succinocarboxamide synthase
VP1269		-2.0	Uncharacterized protein
VP1273	*hutH*	-2.4	Histidine ammonia-lyase
VP1274	*hutU*	-2.8	Urocanate hydratase
VP1276	*hutI*	-2.3	Imidazolonepropionase
VP1283		-2.4	UPF0145 protein VP1283
VP1294	*ihfA*	-1.0	Integration host factor subunit alpha
VP1297	*purT*	-2.2	Phosphoribosylglycinamide formyltransferase 2
VP1298	*cdd*	-1.1	Cytidine deaminase
VP1301		-2.5	Exodeoxyribonuclease I
VP1304	*cobT*	-4.1	Nicotinate-nucleotide--dimethylbenzimidazole phosphoribosyltransferase
VP1307		-2.4	Putative alpha-ribazole-5'-phosphate phosphatase CobC
VP1308		-2.8	Putative oligopeptidase
VP1310	*astE*	-1.7	Succinylglutamate desuccinylase
VP1313		-3.9	Uncharacterized protein
VP1325		-2.7	Uncharacterized protein
VP1326		-2.2	Uncharacterized protein
VP1328		-2.5	Putative transcription regulator
VP1329		-3.9	Fatty aldehyde dehydrogenase
VP1332		-5.7	Probable binding protein component of ABC transporter
VP1335		-3.0	Probable dihydrodipicolinate synthetase
VP1342		-2.9	Putative aminopeptidase
VP1343		-5.2	Oligopeptide ABC transporter, ATP-binding protein
VP1345		-5.2	Oligopeptide ABC transporter, permease protein
VP1347		-4.4	Oligopeptide ABC transporter, periplasmic oligopeptide-binding protein
VP1349		-4.0	4-hydroxyphenylpyruvate dioxygenase
VP1350		-4.8	Putative oxidoreductase
VP1351		-4.0	Uncharacterized protein
VP1376		-2.5	Putative chemotaxis protein CheY
VP1380		-3.5	Uncharacterized protein
VP1388		-1.4	Type VI secretion system 1 protein
VP1392		-1.0	Type VI secretion system 1 protein, Putative ClpA/B-type protease
VP1393		-1.1	Type VI secretion system 1, protein BfdA
VP1401		-2.0	Type VI secretion system 1 protein
VP1423		-3.1	Uncharacterized protein
VP1425		-4.5	Putative alcohol dehydrogenase
VP1431		-2.5	Putative ATP-binding component of a transport system
VP1443		-3.5	Uncharacterized protein
VP1455		-2.4	Uncharacterized protein
VP1480		-3.0	Riboflavin synthase, alpha chain

146

VP1481		-2.2	Uncharacterized protein VP1481
VP1494	*nagK*	-2.0	N-acetyl-D-glucosamine kinase
VP1495		-1.1	Uncharacterized protein
VP1517		-3.0	Putative Rhs-family protein
VP1518		-3.0	Uncharacterized protein
VP1524	*cobB*	-2.0	NAD-dependent protein deacylase
VP1525		-1.5	Putrescine-binding periplasmic protein
VP1526		-1.1	Putrescine-binding periplasmic protein
VP1532		-3.6	Uncharacterized protein
VP1533	*ttcA*	-1.1	tRNA 2-thiocytidine biosynthesis protein TtcA
VP1535		-2.2	Putative stress protein
VP1536		-1.1	Fumarate and nitrate reduction regulatory protein
VP1561		-2.9	Bacteriophage f237 ORF8
VP1564		-3.2	Uncharacterized protein
VP1588		-2.4	Uncharacterized protein
VP1591	*fabA*	-2.6	3-hydroxydecanoyl-[acyl-carrier-protein] dehydratase
VP1595		-1.1	ABC transporter, ATP-binding protein
VP1602		-1.3	Putative NAD-glutamate dehydrogenase
VP1604		-3.0	Aminopeptidase N
VP1606		-1.9	Tail-specific protease
VP1614		-1.2	Uncharacterized protein
VP1616		-1.5	Phospho-2-dehydro-3-deoxyheptonate aldolase
VP1617		-1.7	UPF0234 protein VP1617
VP1619		-1.7	Uroporphyrin-III C-methyltransferase
VP1626		-3.7	Sulfurtransferase
VP1633		-2.6	Putative RTX toxin
VP1635		-1.3	Putative outer membrane protein
VP1638	*queC*	-1.7	7-cyano-7-deazaguanine synthase
VP1640		-6.8	Uncharacterized protein
VP1644		-2.4	PrpE protein
VP1645		-2.0	Uncharacterized protein
VP1646		-3.0	Aconitate hydratase
VP1647		-3.0	Citrate synthase
VP1648	*prpB*	-3.8	2-methylisocitrate lyase
VP1649		-3.1	Transcriptional regulator, GntR family
VP1650		-4.3	Uncharacterized protein
VP1651		-3.3	Putative tricarboxylic transport TctC
VP1658		-2.1	Low calcium response locus protein H
VP1665		-1.6	Putative type III secretion protein
VP1703		-3.6	Aldehyde dehydrogenase
VP1708		-1.7	6-phosphogluconate dehydrogenase, decarboxylating
VP1709		-2.8	DevB protein
VP1712		-2.5	Putative sensor kinase CitA
VP1714		-3.1	Uncharacterized protein
VP1725		-2.1	Uncharacterized protein
VP1744		-3.8	Thermostable carboxypeptidase 1

VP1751	*metA*	-1.8	Homoserine O-succinyltransferase
VP1768		-4.1	Uncharacterized protein
VP1772		-1.4	Succinate-semialdehyde dehydrogenase
VP1774		-1.8	Putative carbon-nitrogen hydrolase
VP1779		-3.5	Putative glutamine amidotransferase
VP1789		-4.8	Uncharacterized protein
VP1802		-2.0	Uncharacterized protein
VP1839		-3.7	Uncharacterized protein
VP1845		-3.4	Uncharacterized protein
VP1853		-2.1	Uncharacterized protein
VP1866		-1.3	Uncharacterized protein
VP1870		-1.5	UPF0283 membrane protein VP1870
VP1871		-1.9	Uncharacterized protein
VP1883		-5.6	6-carboxy-5,6,7,8-tetrahydropterin synthase
VP1892		-3.2	Methyl-accepting chemotaxis protein
VP1893	*asnS*	-2.2	Asparagine--tRNA ligase
VP1900		-2.8	Aspartate aminotransferase
VP1920		-2.2	Putative iron-regulated protein A
VP1921	*ribA*	-4.2	GTP cyclohydrolase-2
VP1934		-1.6	Ribonucleoside-diphosphate reductase
VP1935		-1.8	Ribonucleoside-diphosphate reductase, beta subunit
VP1937		-7.4	CinA-like protein
VP1939		-1.8	Uncharacterized protein
VP1940		-2.3	Carboxynorspermidine/carboxyspermidine decarboxylase
VP1941		-2.5	Putative carboxynorspermidine dehydrogenase
VP1945		-1.7	Transcriptional regulator, LuxR family
VP1948		-2.3	Elongation factor P-like protein
VP1953		-1.8	Putative translation factor
VP1958	*trpD*	-4.3	Anthranilate phosphoribosyltransferase
VP1959	*trpC*	-2.4	Tryptophan biosynthesis protein TrpCF
VP1960	*trpB1*	-3.7	Tryptophan synthase beta chain 1
VP1961	*trpA*	-3.9	Tryptophan synthase alpha chain
VP1976		-9.0	Transcriptional activator MetR
VP1987		-1.5	Uncharacterized protein
VP1997		-1.3	Uncharacterized protein
VP2014		-1.6	Putative tetrathionate reductase, subunit A
VP2025		-3.3	Uncharacterized protein
VP2026	*pyrF*	-2.9	Orotidine 5'-phosphate decarboxylase
VP2027	*lapB*	-1.3	Lipopolysaccharide assembly protein B
VP2029	*ihfB*	-1.1	Integration host factor subunit beta
VP2031	*cmk*	-1.3	Cytidylate kinase
VP2033		-3.2	Oxidoreductase, short-chain dehydrogenase/reductase family
VP2037		-1.2	Chemotaxis protein CheV
VP2038		-2.0	Transcriptional regulator, ROK family
VP2039		-2.5	Pyruvate kinase

VP2048		-1.8	DNA polymerase III, delta prime subunit
VP2051		-1.6	4-amino-4-deoxychorismate lyase
VP2052		-1.9	3-oxoacyl-[acyl-carrier-protein] synthase 2
VP2053	*acpP*	-1.8	Acyl carrier protein
VP2054		-2.2	3-oxoacyl-(Acyl-carrier-protein) reductase
VP2055		-2.1	Malonyl CoA-acyl carrier protein transacylase
VP2064		-1.3	Phosphotyrosine protein phosphatase
VP2065		-2.3	Cob(I)alamin adenosyltransferase
VP2067	*udk*	-1.7	Uridine kinase
VP2068		-2.9	Iron-sulfur cluster carrier protein
VP2069	*metG*	-1.5	Methionine--tRNA ligase
VP2071	*fadR*	-1.1	Fatty acid metabolism regulator protein
VP2080		-3.5	ABC transporter substrate-binding protein
VP2082	*ackA1*	-1.9	Acetate kinase 1
VP2083		-1.3	Phosphate acetyltransferase
VP2091		-1.1	Oligopeptide ABC transporter, periplasmic oligopeptide-binding protein
VP2092		-2.3	Molybdenum cofactor biosynthesis protein E
VP2094	*moaC*	-2.3	Cyclic pyranopterin monophosphate synthase accessory protein
VP2099	*luxO*	-1.1	Regulatory protein LuxO
VP2100	*uvrB*	-1.9	UvrABC system protein B
VP2110		-2.4	Uncharacterized protein VP2110
VP2117		-3.0	Glutaredoxin
VP2118		-2.9	Superoxide dismutase
VP2121		-2.0	Aldehyde-alcohol dehydrogenase
VP2124	*asd*	-2.5	Aspartate-semialdehyde dehydrogenase
VP2126		-1.0	Uncharacterized protein
VP2127		-3.4	Uncharacterized protein
VP2134		-2.1	Uncharacterized protein
VP2135		-1.6	Putative phage-related protein
VP2145		-3.9	Histone deacetylase/AcuC/AphA family protein
VP2146		-4.3	Putative oxidoreductase protein
VP2150		-4.0	Putative nitroreductase
VP2153		-3.4	L-asparaginase I
VP2156	*msrB*	-2.6	Peptide methionine sulfoxide reductase MsrB
VP2157		-2.1	Glyceraldehyde-3-phosphate dehydrogenase
VP2158		-2.5	Uncharacterized protein
VP2172		-1.0	Uncharacterized protein
VP2177	*recR*	-1.3	Recombination protein RecR
VP2180	*apt*	-1.9	Adenine phosphoribosyltransferase
VP2185	*purF*	-1.8	Amidophosphoribosyltransferase
VP2193	*pdxB*	-3.0	Erythronate-4-phosphate dehydrogenase
VP2194		-1.7	3-oxoacyl-[acyl-carrier-protein] synthase I
VP2195	*mnmC*	-1.8	tRNA 5-methylaminomethyl-2-thiouridine biosynthesis bifunctional protein MnmC
VP2197		-3.0	Uncharacterized protein
VP2202	*aroC*	-1.8	Chorismate synthase

VP2205		-3.0	Phosphohistidine phosphatase
VP2206		-1.1	Peptidase, insulinase family
VP2225		-2.2	Chemotaxis protein CheW
VP2241		-1.0	Flagellar motor switch protein FliN
VP2242		-1.3	Flagellar motor switch protein FliM
VP2251		-1.6	FlaM
VP2262		-1.9	TyrA protein
VP2268		-3.6	Putative arsenate reductase
VP2269	*dapE*	-3.7	Succinyl-diaminopimelate desuccinylase
VP2273	*dapA*	-2.0	4-hydroxy-tetrahydrodipicolinate synthase
VP2274		-2.5	Putative glycine cleavage system transcriptional repressor
VP2278		-1.7	Putative beta-barrel assembly-enhancing protease
VP2279		-2.9	Arsenate reductase
VP2284	*upp*	-2.2	Uracil phosphoribosyltransferase
VP2285	*purM*	-2.5	Phosphoribosylformylglycinamidine cyclo-ligase
VP2286	*purN*	-5.8	Phosphoribosylglycinamide formyltransferase
VP2288	*gmhA*	-2.3	Phosphoheptose isomerase
VP2293	*rnhA*	-5.2	Ribonuclease HI
VP2295	*gloB*	-2.8	Hydroxyacylglutathione hydrolase
VP2299		-2.6	Nitrogen regulatory protein P-II
VP2312	*dxr*	-2.5	1-deoxy-D-xylulose 5-phosphate reductoisomerase
VP2315	*frr*	-1.2	Ribosome-recycling factor
VP2317	*tsf*	-2.2	Elongation factor Ts
VP2319	*map*	-1.6	Methionine aminopeptidase
VP2321		-1.5	UPF0325 protein VP2321
VP2324		-1.7	Uncharacterized protein
VP2333	*proS*	-2.1	Proline--tRNA ligase
VP2334		-1.8	Uncharacterized protein
VP2335		-5.6	UPF0253 protein VP2335
VP2340		-2.7	Putative ATP-dependent DNA helicase RecQ
VP2352		-2.9	Cell division protein BolA
VP2355		-2.4	Peptidyl-prolyl cis-trans isomerase
VP2368		-2.2	HesA/MoeB/ThiF family protein
VP2373	*recD*	-1.9	RecBCD enzyme subunit RecD
VP2374	*recB*	-2.5	RecBCD enzyme subunit RecB
VP2376		-2.3	Uncharacterized protein
VP2380	*dapD*	-2.5	2,3,4,5-tetrahydropyridine-2,6-dicarboxylate N-succinyltransferase
VP2381		-2.3	Glycerophosphoryl diester phosphodiesterase
VP2386	*glpK*	-2.9	Glycerol kinase
VP2389		-1.0	Putative membrane transport protein
VP2393		-1.3	Transcriptional regulator, LacI family
VP2425		-1.7	Putative long-chain-fatty-acid-CoA ligase
VP2428	*fusA2*	-2.2	Elongation factor G 2
VP2431		-1.9	Phosphoserine phosphatase
VP2433	*deoD1*	-2.3	Purine nucleoside phosphorylase DeoD-type 1

VP2434	*deoB*	-1.3	Phosphopentomutase
VP2435	*deoA*	-2.9	Thymidine phosphorylase
VP2436	*deoC*	-2.3	Deoxyribose-phosphate aldolase
VP2450		-1.9	Transcriptional regulator, MarR family
VP2461	*glmM*	-1.1	Phosphoglucosamine mutase
VP2462		-2.5	Dihydropteroate synthase
VP2466	*greA*	-2.5	Transcription elongation factor GreA
VP2468		-1.2	D-alanyl-D-alanine carboxypeptidase/D-alanyl-D-alanine-endopeptidase
VP2470	*tyrS2*	-1.7	Tyrosine--tRNA ligase 2
VP2473		-4.3	Uncharacterized protein
VP2475	*hemL*	-2.1	Glutamate-1-semialdehyde 2,1-aminomutase
VP2479		-3.7	Peptide ABC transporter, periplasmic peptide-binding protein
VP2488		-1.5	Putative phosphoglucomutase/phosphomannomutase
VP2491		-2.1	Iron(III) ABC transporter, periplasmic iron-compound-binding protein
VP2495		-1.9	Aconitate hydratase B
VP2500	*dksA*	-1.3	RNA polymerase-binding transcription factor DksA
VP2507	*panC*	-1.4	Pantothenate synthetase
VP2514		-2.1	Carbonic anhydrase
VP2515		-2.7	Hypoxanthine ribosyl transferase
VP2516		-1.3	OpaR
VP2521		-5.3	AmpD protein
VP2522		-2.5	NadC
VP2537	*luxS*	-2.9	S-ribosylhomocysteine lyase
VP2539	*gshA*	-1.8	Glutamate--cysteine ligase
VP2542		-4.6	Quinone oxidoreductase
VP2544		-1.2	Oxaloacetate decarboxylase, alpha subunit
VP2546	*csrA*	-1.3	Carbon storage regulator homolog
VP2548	*alaS*	-1.3	Alanine--tRNA ligase
VP2550	*recA*	-1.1	Protein RecA
VP2551		-3.9	CinA-related protein
VP2553	*rpoS*	-7.0	RNA polymerase sigma factor RpoS
VP2556	*surE*	-4.2	5'-nucleotidase SurE
VP2557	*truD*	-1.5	tRNA pseudouridine synthase D
VP2558	*ispF*	-8.6	2-C-methyl-D-erythritol 2,4-cyclodiphosphate synthase
VP2561	*eno*	-1.1	Enolase
VP2567		-1.1	Histidine kinase
VP2569	*pdxJ*	-2.1	Pyridoxine 5'-phosphate synthase
VP2580		-3.3	L-aspartate oxidase
VP2583		-1.1	tRNA-modifying protein YgfZ
VP2590		-1.7	Cell division protein ZapA
VP2592	*rpiA*	-2.0	Ribose-5-phosphate isomerase A
VP2593		-2.2	D-3-phosphoglycerate dehydrogenase
VP2599		-3.0	Fructose-bisphosphate aldolase, class II
VP2600	*pgk*	-2.7	Phosphoglycerate kinase

VP2601	*epd*	-2.4	D-erythrose-4-phosphate dehydrogenase
VP2605	*tkt1*	-2.2	Transketolase 1
VP2606	*metK*	-1.4	S-adenosylmethionine synthase
VP2611	*gshB*	-3.2	Glutathione synthetase
VP2613		-2.5	Putative pre-16S rRNA nuclease
VP2614		-1.5	Twitching motility protein PilT
VP2615		-2.2	Twitching motility protein PilT
VP2616		-2.1	FkuA
VP2617	*proC*	-1.2	Pyrroline-5-carboxylate reductase
VP2626		-1.8	A/G-specific adenine glycosylase
VP2627		-1.9	Probable Fe(2+)-trafficking protein
VP2630		-1.1	Aldehyde dehydrogenase
VP2632		-1.4	Transcriptional regulator, LacI family
VP2634		-4.2	6-phospho-beta-glucosidase
VP2639		-3.4	Putative short-chain dehydrogenase
VP2646	*valS*	-1.7	Valine--tRNA ligase
VP2648		-1.4	Putative acetyltransferase
VP2650	*rraB*	-2.6	Regulator of ribonuclease activity B
VP2652	*arcA*	-2.8	Arginine deiminase
VP2653	*argF*	-4.0	Ornithine carbamoyltransferase
VP2654	*pyrB*	-2.1	Aspartate carbamoyltransferase
VP2655	*pyrI*	-2.8	Aspartate carbamoyltransferase regulatory chain
VP2656		-3.0	Uncharacterized protein
VP2666		-2.2	Arabinose 5-phosphate isomerase
VP2670		-1.3	RNA polymerase sigma-54 factor
VP2671		-2.9	Putative sigma-54 modulation protein
VP2676		-3.9	PmbA protein
VP2678		-4.1	2-hydroxyacid dehydrogenase family protein
VP2683		-2.4	Uncharacterized protein
VP2684		-2.5	TldD protein
VP2691		-1.1	Rod shape-determining protein MreB
VP2692		-2.1	Uncharacterized protein
VP2698		-1.2	Putative V10 pilin
VP2701		-1.4	MSHA biogenesis protein MshE
VP2702		-3.4	MSHA biogenesis protein MshN
VP2704		-1.2	MSHA biogenesis protein MshL
VP2707		-1.2	MSHA biogenesis protein MshI
VP2711		-2.7	UTP--glucose-1-phosphate uridylyltransferase
VP2714		-3.1	Aminotransferase, class V
VP2715		-2.4	Aspartokinase
VP2717	*metH*	-2.1	Methionine synthase
VP2720	*cysH*	-3.3	Phosphoadenosine phosphosulfate reductase
VP2722	*cysJ*	-1.0	Sulfite reductase [NADPH] flavoprotein alpha-component
VP2727	*dusA*	-1.3	tRNA-dihydrouridine(20/20a) synthase
VP2729		-2.2	Putative zinc uptake regulation protein
VP2731	*pgi*	-2.3	Glucose-6-phosphate isomerase

VP2734	*alr1*	-2.5	Alanine racemase 1
VP2735		-1.9	Replicative DNA helicase
VP2741		-2.1	Ribulose-phosphate 3-epimerase
VP2743		-1.3	DamX-related protein
VP2744	*aroB*	-3.4	3-dehydroquinate synthase
VP2753		-1.5	Peroxiredoxin family protein/glutaredoxin
VP2761	*ppc*	-2.4	Phosphoenolpyruvate carboxylase
VP2763		-2.5	Methylenetetrahydrofolate reductase
VP2764		-3.4	Aspartokinase II/homoserine dehydrogenase, methionine-sensitive
VP2765		-2.0	Cystathionine gamma-synthase
VP2766	*metJ*	-3.9	Met repressor
VP2767		-2.5	Putative malate oxidoreductase
VP2770	*tufB*	-2.6	Elongation factor Tu
VP2771	*fusA1*	-2.0	Elongation factor G 1
VP2777		-1.7	Uncharacterized protein
VP2781		-3.8	Putative asparaginase
VP2783		-2.2	Peptidyl-prolyl cis-trans isomerase
VP2788		-1.8	ABC transporter, ATP-binding protein
VP2794		-5.1	Uncharacterized protein
VP2795	*astD*	-4.0	N-succinylglutamate 5-semialdehyde dehydrogenase
VP2796		-2.2	Arginine N-succinyltransferase
VP2797	*argD*	-3.0	Acetylornithine aminotransferase
VP2798		-1.8	Para-aminobenzoate synthase glutamine amidotransferase, component II
VP2804	*trpS*	-1.7	Tryptophan--tRNA ligase
VP2807	*rnr*	-1.2	Ribonuclease R
VP2812	*purA*	-2.7	Adenylosuccinate synthetase
VP2817	*hfq*	-1.0	RNA-binding protein Hfq
VP2818	*miaA*	-1.2	tRNA dimethylallyltransferase
VP2823	*orn*	-1.6	Oligoribonuclease
VP2829	*gpmI*	-1.9	2,3-bisphosphoglycerate-independent phosphoglycerate mutase
VP2831	*secB*	-1.9	Protein-export protein SecB
VP2833		-1.0	Serine acetyltransferase
VP2835		-2.8	Uncharacterized protein
VP2838	*epmA*	-1.7	Elongation factor P--(R)-beta-lysine ligase
VP2840		-1.0	Fumarate reductase flavoprotein subunit
VP2844		-1.7	Uncharacterized protein
VP2845	*efp*	-2.0	Elongation factor P
VP2852	*groS1*	-2.3	10 kDa chaperonin 1
VP2855	*pfkA*	-2.6	ATP-dependent 6-phosphofructokinase
VP2858		-2.7	Transcriptional regulator CpxR
VP2860		-4.4	Superoxide dismutase
VP2861	*trmL*	-1.3	tRNA (cytidine(34)-2'-O)-methyltransferase
VP2863		-2.4	Aspartate ammonia-lyase
VP2866		-10.6	Transcriptional regulator, LuxR family
VP2867	*nhaP2*	-1.1	K(+)/H(+) antiporter NhaP2

VP2869		-3.6	Sodium/solute symporter
VP2872		-5.4	Uncharacterized protein
VP2873	*fumC*	-3.5	Fumarate hydratase class II
VP2874		-1.9	Sensor histidine kinase
VP2876		-1.9	Uncharacterized protein
VP2877		-2.2	Putative DNA polymerase III, epsilon subunit
VP2878	*acsA*	-3.5	Acetyl-coenzyme A synthetase
VP2880		-1.3	Acetyl-CoA carboxylase, biotin carboxyl carrier protein
VP2881		-1.4	Acetyl-CoA carboxylase, biotin carboxylase
VP2896	*purH*	-1.8	Bifunctional purine biosynthesis protein PurH
VP2898	*purD*	-3.2	Phosphoribosylamine--glycine ligase
VP2899		-1.5	Uncharacterized protein
VP2900		-1.8	Uncharacterized protein
VP2903		-3.9	Putative phage protein
VP2905		-2.4	Uncharacterized protein
VP2916	*hemE*	-2.4	Uroporphyrinogen decarboxylase
VP2918		-2.5	Uncharacterized protein
VP2919	*nudC*	-2.4	NADH pyrophosphatase
VP2920		-3.8	Regulator of sigma D
VP2942	*sthA*	-2.6	Soluble pyridine nucleotide transhydrogenase
VP2944		-2.6	O-methyltransferase-related protein
VP2945	*lexA*	-1.6	LexA repressor
VP2952	*glpE*	-4.4	Thiosulfate sulfurtransferase GlpE
VP2953	*rpoH*	-1.3	RNA polymerase sigma factor RpoH
VP2956	*ftsY*	-2.2	Signal recognition particle receptor FtsY
VP2969		-1.3	Putative phosphatase
VP2970		-3.0	Glyceraldehyde-3-phosphate dehydrogenase
VP2974		-1.5	Lysophospholipase L2
VP2975		-3.4	Uncharacterized protein
VP2976		-2.6	Uncharacterized protein
VP2982		-5.4	Uncharacterized protein
VP2983	*dapF*	-1.2	Diaminopimelate epimerase
VP2984	*lysA*	-2.9	Diaminopimelate decarboxylase
VP2988	*hemC*	-3.7	Porphobilinogen deaminase
VP2989		-3.7	Uroporphyrinogen-III synthase
VP2990		-1.2	Putative uroporphyrin-III C-methyltransferase
VP2991		-1.4	HemY protein
VP2995		-4.1	NAD(P)H-flavin reductase
VP2997	*ubiD*	-1.4	3-octaprenyl-4-hydroxybenzoate carboxy-lyase
VP3001		-2.4	Thioredoxin
VP3003	*gppA*	-1.3	Guanosine-5'-triphosphate,3'-diphosphate pyrophosphatase
VP3013		-1.2	DNA helicase
VP3018		-1.4	Uncharacterized protein
VP3021		-2.4	Aminopeptidase P
VP3033	*aroE*	-6.8	Shikimate dehydrogenase (NADP(+))
VP3034	*hemF*	-3.9	Oxygen-dependent coproporphyrinogen-III oxidase

VP3036	*purE*	-2.2	N5-carboxyaminoimidazole ribonucleotide mutase
VP3037	*purK*	-7.1	N5-carboxyaminoimidazole ribonucleotide synthase
VP3042	*def1*	-1.4	Peptide deformylase 1
VP3043	*fmt*	-2.3	Methionyl-tRNA formyltransferase
VP3049		-4.5	SpoOM-related protein
VP3056		-2.1	Putative periplasmic protein
VP3058		-2.9	Acetolactate synthase
VP3059		-1.9	Acetolactate synthase II, small subunit
VP3060		-4.0	Branched-chain amino acid amiotransferase
VP3061	*ilvD*	-2.2	Dihydroxy-acid dehydratase
VP3062	*ilvA*	-2.4	L-threonine dehydratase
VP3065		-2.4	Putative cyclohexadienyl dehydratase signal peptide protein
VP3067	*glmU*	-1.4	Bifunctional protein GlmU
VPA0004		-4.5	Peptide ABC transporter, ATP-binding protein
VPA0011		-1.4	Probable transcriptional regulatory protein VPA0011
VPA0036		-1.7	Uncharacterized protein
VPA0038	*nagB*	-2.8	Glucosamine-6-phosphate deaminase
VPA0051		-1.8	NhaD
VPA0057		-5.0	UPF0345 protein VPA0057
VPA0071		-2.2	S-(hydroxymethyl)glutathione dehydrogenase
VPA0072		-5.1	Putative N-hydroxyarylamine O-acetyltransferase
VPA0075		-3.1	Uncharacterized protein
VPA0077		-2.8	2-deoxy-D-gluconate 3-dehydrogenase
VPA0089		-3.2	Putative siderophore utilization protein
VPA0099		-4.4	Uncharacterized protein
VPA0101		-3.3	Uncharacterized protein
VPA0102		-1.0	Putative isomerase
VPA0110		-1.0	Putative phosphatase
VPA0111		-1.9	Uncharacterized protein
VPA0112		-3.6	Putative peptidase
VPA0117		-4.4	Uncharacterized protein
VPA0127		-1.4	Cytochrome c-type protein YecK
VPA0131	*thiM*	-2.9	Hydroxyethylthiazole kinase
VPA0133		-3.1	Putative ABC transporter substrate-binding protein
VPA0138		-2.8	Putative TldD protein
VPA0139		-2.6	Putative PmbA-related protein
VPA0144		-2.5	D-lactate dehydrogenase
VPA0146		-1.8	Putative glycerophosphoryl diester phosphodiesterase
VPA0147		-3.0	Lactate dehydrogenase
VPA0166		-2.8	Putative outer membrane protein
VPA0167		-2.2	Putative protease
VPA0180		-2.4	Phospho-beta-glucosidase B
VPA0182		-5.2	Putative C4-dicarboxylate transport sensor protein
VPA0188		-8.9	Immunogenic protein
VPA0190		-2.6	Putative transcriptional regulator
VPA0192	*tnaA*	-4.2	Tryptophanase

VPA0196		-2.1	Uncharacterized protein
VPA0215		-5.7	Uncharacterized protein
VPA0228		-2.9	Uncharacterized protein
VPA0246		-1.3	Uncharacterized protein
VPA0248		-2.1	Putative outer membrane protein OmpA
VPA0257		-1.8	Hemolysin
VPA0296		-2.5	Putative oxidoreductase protein
VPA0298		-1.4	PTS system, fructose-specific IIA component
VPA0304		-4.1	Uncharacterized protein
VPA0305		-1.2	Catalase
VPA0307		-3.0	Putative pyrazinamidase/nicotinamidase
VPA0326		-8.0	Uncharacterized protein
VPA0337		-1.7	Uncharacterized protein
VPA0347		-1.8	Uncharacterized protein
VPA0348		-2.7	Uncharacterized protein
VPA0368	*tyrS1*	-5.4	Tyrosine--tRNA ligase 1
VPA0372		-1.1	Phosphoenolpyruvate synthase
VPA0373		-1.2	Putative phosphoenolpyruvate synthase regulatory protein
VPA0399		-3.6	Putative aminotransferase
VPA0402		-3.5	Uncharacterized protein
VPA0408	*pyrC*	-2.1	Dihydroorotase
VPA0411		-1.1	Uncharacterized protein
VPA0412	*nadE*	-3.8	NH(3)-dependent NAD(+) synthetase
VPA0423		-2.0	Hemin ABC transporter, periplasmic hemin-binding protein HutB
VPA0428		-1.0	Uncharacterized protein
VPA0429		-2.2	Uncharacterized protein
VPA0434		-2.9	Putative site-specific recombinase
VPA0436		-2.7	Putative resolvase
VPA0460		-5.1	PAS factor
VPA0464		-2.0	Putative TrkA family protein
VPA0466		-1.4	Universal stress protein
VPA0468		-2.7	Prolyl endopeptidase
VPA0475		-3.5	Uncharacterized protein
VPA0493		-4.0	Uncharacterized protein
VPA0535		-3.2	Putative phosphomannomutase
VPA0552		-1.8	Cold shock DNA-binding domain protein
VPA0562		-1.2	Putative chemotaxis transducer
VPA0563		-2.2	DPS family protein
VPA0566		-2.1	Alcohol dehydrogenase
VPA0567		-4.0	Sigma cross-reacting protein 27A
VPA0574		-2.4	Putative methyltransferase
VPA0575		-3.8	Acetyl-CoA synthase
VPA0576		-2.2	Phenylalanine-4-hydroxylase
VPA0577		-4.4	Putative pterin-4-alpha-carbinolamine dehydratase
VPA0585	*trpB2*	-1.2	Tryptophan synthase beta chain 2

VPA0589		-2.9	Putative cobalamin synthesis protein
VPA0595		-9.0	ATP-binding component of molybdate transport system
VPA0611	*ackA2*	-2.0	Acetate kinase 2
VPA0625		-4.6	3-hydroxyisobutyrate dehydrogenase
VPA0632		-8.1	Uncharacterized protein
VPA0641		-3.2	Putative transcriptional regulator, LysR family
VPA0657		-1.9	Iron(III) ABC transporter, periplasmic iron-compound-binding protein
VPA0662		-3.1	Transcriptional regulator, MerR family
VPA0663		-1.2	Putative transcriptional regulator, AraC/XylS family
VPA0664		-2.3	Putaive Fe-regulated protein B
VPA0673	*mgsA*	-3.8	Methylglyoxal synthase
VPA0704		-5.5	Uncharacterized protein
VPA0705		-1.3	Putative cytoplasmic membrane protein
VPA0708		-4.6	Putative acetyltransferase
VPA0709		-3.0	HAD superfamily hydrolase
VPA0710		-1.0	Sensor histidine kinase/response regulator LuxN
VPA0711		-2.4	Aminotransferase, class II
VPA0746		-2.2	Chemotaxis protein CheV
VPA0761		-2.2	Aldehyde dehydrogenase
VPA0768	*katG2*	-2.1	Catalase-peroxidase 2
VPA0776		-2.1	MazG-related protein
VPA0796		-5.3	Putative L-allo-threonine aldolase
VPA0797		-1.8	Uncharacterized protein
VPA0800		-3.3	Uncharacterized protein
VPA0801	*gcvP*	-2.2	Glycine dehydrogenase (decarboxylating)
VPA0802	*gcvH*	-3.3	Glycine cleavage system H protein
VPA0803	*glyA2*	-3.4	Serine hydroxymethyltransferase 2
VPA0804		-3.1	Transcriptional regulator, HTH_3 family
VPA0805		-2.8	Aminomethyltransferase
VPA0820		-4.6	Amino acid ABC transporter, periplasmic amino acid-binding protein
VPA0829		-2.1	Iron-containing alcohol dehydrogenase
VPA0834	*fhs*	-3.5	Formate--tetrahydrofolate ligase
VPA0841		-2.1	CbbY family protein
VPA0850		-3.6	UPF0312 protein VPA0850
VPA0854		-3.5	Uncharacterized protein
VPA0857		-1.9	Uncharacterized protein
VPA0861		-1.9	Uncharacterized protein
VPA0866		-3.8	Putative oxidoreductase iron/ascorbate family
VPA0884		-2.2	Putative acetyltransferase
VPA0886	*ddl*	-3.0	D-alanine--D-alanine ligase
VPA0918		-2.5	Uncharacterized protein
VPA0919		-2.7	Transcriptional regulator
VPA0928		-2.0	Uncharacterized protein
VPA0931		-1.8	Molybdenum ABC transporter, periplasmic molybdenum-binding protein

VPA0935		-1.3	Uncharacterized protein
VPA0936		-3.6	Amino acid biosynthesis aminotransferase
VPA0942		-4.0	Uncharacterized protein
VPA0949		-1.1	Putative NADH oxidase
VPA0961		-2.5	Putative transcriptional regulator
VPA0971	*fabH2*	-4.5	3-oxoacyl-[acyl-carrier-protein] synthase 3 protein 2
VPA0987		-3.2	Nitrite reductase (NAD(P)H), large subunit
VPA0988		-2.9	Regulator of nucleoside diphosphate kinase
VPA1005		-2.1	D-lactate dehydrogenase
VPA1009		-2.4	Uncharacterized protein
VPA1010		-3.2	MutT/nudix family protein
VPA1011		-3.5	L-allo-threonine aldolase
VPA1015		-1.6	Putative succinate dehydrogenase subunit Sdh
VPA1022	*sbcC*	-1.9	Putative exonuclease SbcC
VPA1026		-3.3	Type VI secretion system 2 protein
VPA1027		-5.5	Type VI secretion system 2 protein
VPA1028		-4.1	Putative ClpA/B-type chaperone, type VI secretion system 2 protein
VPA1030		-3.4	Type VI secretion system 2 protein
VPA1034		-2.4	Type VI secretion system 2 protein
VPA1035		-2.2	Type VI secretion system 2 protein
VPA1041		-2.4	Type VI secretion system 2 protein
VPA1042		-1.6	Type VI secretion system 2 protein
VPA1043		-3.8	Type VI secretion system 2 protein
VPA1044		-2.2	Type VI secretion system 2 protein
VPA1052		-3.7	Putative TetR-family
VPA1073		-8.5	Putative alkaline phosphatase
VPA1077		-2.3	Uncharacterized protein
VPA1082		-2.2	Ribose operon repressor
VPA1084		-2.2	Ribose ABC transporter, periplasmic D-ribose-binding protein
VPA1096		-4.4	Uncharacterized protein
VPA1117		-4.3	Putative short-chain dehydrogenase
VPA1118		-3.4	3-hydroxyisobutyrate dehydrogenase
VPA1120		-3.1	Putative enoyl-CoA hydratase/isomerase
VPA1121		-3.4	Putative acyl-CoA dehydrogenase
VPA1122		-4.2	Putative aldehyde dehydrogenase
VPA1123		-4.1	Putative acyl-CoA thiolase
VPA1125		-2.7	Putative acyl-CoA dehydrogenase
VPA1126		-3.5	Putative acyl-CoA carboxyltransferase beta chain
VPA1129		-2.4	Putative hydroxymethylglutaryl-CoA lyase
VPA1132		-2.5	Uncharacterized protein
VPA1147		-3.6	Putative phenylacetate-CoA ligase
VPA1148		-3.6	Putative high-affinity branched-chain amino acid transport ATP-binding protein
VPA1149		-4.6	Uncharacterized protein
VPA1150		-2.7	Putative high-affinity branched-chain amino acid transport permease protein

VPA1152		-3.2	Putative long-chain-fatty-acid-CoA ligase
VPA1153		-3.2	Putative high-affinity branched-chain amino acid transport ATP-binding protein
VPA1156		-4.1	Electron transfer flavoprotein, beta-subunit
VPA1157		-3.3	Electron transfer flavoprotein, alpha-subunit
VPA1158		-2.5	Acetyl-CoA synthase
VPA1159	*guaC*	-1.3	GMP reductase
VPA1162		-2.0	Response regulator
VPA1163		-4.2	Oxidoreductase, aldo/keto reductase 2 family
VPA1169	*folE*	-1.5	GTP cyclohydrolase 1
VPA1178		-1.4	Transcriptional regulator, SorC family
VPA1180	*tal*	-2.8	Transaldolase
VPA1181	*tkt2*	-1.7	Transketolase 2
VPA1185		-2.5	Phospho-2-dehydro-3-deoxyheptonate aldolase
VPA1186		-2.6	Outer membrane protein OmpA
VPA1191		-2.5	Putative multidrug efflux membrane fusion protein
VPA1195		-1.9	Nitrate/nitrite response regulator protein
VPA1202		-4.0	Polyhydroxyalkanoic acid synthase
VPA1203		-1.3	Uncharacterized protein
VPA1204		-3.4	Acetyl-CoA acetyltransferase
VPA1205		-3.1	Acetoacetyl-CoA reductase
VPA1211		-2.9	Uncharacterized protein
VPA1216		-3.0	Uncharacterized protein
VPA1230		-2.7	Glyceraldehyde-3-phosphate dehydrogenase
VPA1255		-1.2	Uncharacterized protein
VPA1256		-3.2	Uncharacterized protein
VPA1271		-1.4	Thiol:disulfide interchange protein
VPA1293		-2.1	Putative antioxidant
VPA1298		-3.9	Putative glutathione S-transferase
VPA1334		-2.9	Type III secretion system 2 protein
VPA1338		-1.6	Putative ATPase YscN, type III secretion system 2 protein
VPA1350		-3.7	Type III secretion system 2 protein
VPA1370		-3.7	Type III secretion system 2 protein
VPA1397		-3.2	Acyl-CoA thioester hydrolase-related protein
VPA1401		-2.3	Maltose ABC transporter, periplasmic maltose-binding protein
VPA1411		-4.6	Putative glycosyltransferase
VPA1416		-2.5	Putative oxidoreductase
VPA1418		-1.1	Catalase
VPA1419		-3.3	Putative 3-hydroxyisobutyrate dehydrogenase
VPA1428		-1.6	Azurin
VPA1445		-3.0	Putative secreted calcium-binding protein
VPA1448		-1.6	Uncharacterized protein
VPA1475	*deoD2*	-1.7	Purine nucleoside phosphorylase DeoD-type 2
VPA1480		-1.0	Uncharacterized protein
VPA1487		-3.2	Putative acetyltransferase
VPA1490		-3.3	Uncharacterized protein

VPA1493		-1.0	ATP-dependent protease LA-related protein
VPA1495		-1.8	ABC transporter, ATP-binding protein
VPA1496		-3.1	Prolyl endopeptidase
VPA1500		-3.1	Uncharacterized protein
VPA1502		-5.2	Carbonic anhydrase
VPA1509	*tdh*	-2.5	L-threonine 3-dehydrogenase
VPA1510	*kbl*	-3.2	2-amino-3-ketobutyrate coenzyme A ligase
VPA1511		-2.1	ScrC (Sensory box/GGDEF family protein) (Involved in swarmer cell regulation)
VPA1559		-3.2	Uncharacterized protein
VPA1567		-2.8	Putative pyruvate formate lyase
VPA1572		-3.1	Uncharacterized protein
VPA1584		-2.3	UPF0319 protein VPA1584
VPA1586		-3.5	Putative ferredoxin-NADP reductase
VPA1587		-2.5	Uncharacterized protein
VPA1589		-3.4	Transcriptional regulator, LysR family
VPA1591		-4.4	Oxygen-insensitive NAD(P)H nitroreductase
VPA1595		-1.3	Putative prolyl aminopeptidase
VPA1596		-4.7	Putative acetyltransferase
VPA1597		-1.2	UPF0176 protein VPA1597
VPA1599		-3.4	Uncharacterized protein
VPA1601		-2.6	NADPH-flavin oxidoreductase
VPA1602		-1.3	Capsular polysaccharide transport protein
VPA1616		-2.6	Alpha-amylase
VPA1618	*glgB*	-4.2	1,4-alpha-glucan branching enzyme GlgB
VPA1619		-2.6	4-alpha-glucanotransferase
VPA1620		-1.8	Alpha-1,4 glucan phosphorylase
VPA1626		-1.6	Sco1-related protein
VPA1632	*pdxY*	-3.2	Pyridoxal kinase PdxY
VPA1635		-2.1	Ornithine decarboxylase, inducible
VPA1642		-1.0	Putative CymC protein
VPA1644	*lamB*	-1.3	Maltoporin
VPA1645		-2.3	Glycogen operon protein GlgX homolog
VPA1648		-1.0	Uncharacterized protein
VPA1658		-2.3	Uncharacterized protein
VPA1659		-3.3	Uncharacterized protein
VPA1662		-3.9	Putative diaminopimelate decarboxylase protein
VPA1693		-1.6	Uncharacterized protein
VPA1714		-2.8	Uncharacterized protein
VPA1715		-1.5	ABC transporter, ATP-binding protein
VPA1717		-2.2	Transcriptional regulator, AsnC family
VPA1723		-2.8	Putative ribosomal protein N-acetyltransferase
VPA1725		-2.3	Uncharacterized protein
VPA1726		-2.3	Bifunctional protein PutA
VPA1730	*pdxH*	-2.2	Pyridoxine/pyridoxamine 5'-phosphate oxidase
VPA1739		-6.9	Oligopeptide ABC transporter, periplasmic oligopeptide-binding protein

VPA1740		-4.4	Uncharacterized protein
VPA1749		-1.8	Uncharacterized protein
VPA1750	*tmcA*	-1.6	tRNA(Met) cytidine acetyltransferase TmcA
VPA1752		-3.1	ParA family protein

Table 14. Proteins differentially expressed (log2 fold change (FC ≥1 or ≤-1) and statistically significant (FDR=0.01 S_0=0.2) between pairs of i) Center ii vs. Center i, ii) Center iii vs. Center i, iii) Center iv vs. Center i.

Protein number	Gene name	Cii vs. Ci (FC)	Ciii vs. Ci (FC)	Civ vs. Ci (FC)	Protein number
VP0163		4.32	2.25	2.40	Protein TonB
VP0168		1.79	1.98	2.23	Uncharacterized protein
VP0488		2.13	1.43	1.22	Putative DNA polymerase III, beta chain
VP0710		3.69	3.17	2.85	PTS system, trehalose-specific IIBC component
VP0755		4.75	1.58	1.52	N,N'-diacetylchitobiase
VP0845		1.47	2.07	1.96	Succinate dehydrogenase flavoprotein subunit
VP0846		1.31	1.51	1.40	Succinate dehydrogenase iron-sulfur subunit
VP0847		1.81	2.26	2.10	2-oxoglutarate dehydrogenase, E1 component
VP0848		1.77	2.33	2.19	Dihydrolipoyllysine-residue succinyltransferase component of 2-oxoglutarate dehydrogenase complex
VP0907		3.13	1.87	1.75	Uncharacterized protein
VP0920		1.73	2.48	2.39	DNA-binding protein HU-beta
VP0944		1.89	3.85	3.85	Putative outer membrane protein
VP1066		3.23	4.01	3.65	Uncharacterized protein
VP1088		1.71	2.46	2.36	Putative chemotaxis transducer
VP1117		4.52	7.61	7.81	Uncharacterized protein
VP1207		2.62	2.13	1.94	UDP-sugar hydrolase
VP1352		1.93	4.42	4.72	Putative glutathione S-transferase
VP1387		3.01	1.67	1.35	Type VI secretion system 1 protein
VP1389		2.26	3.00	2.82	Type VI secretion system 1 protein
VP1390		2.24	2.17	1.87	Type VI secretion system 1 protein
VP1391		3.20	2.20	1.79	Transcriptional regulator of type VI secretion system 1
VP1392		1.20	2.15	2.10	Type VI secretion system 1, Putative ClpA/B-type protease
VP1393		1.47	3.00	2.60	Type VI secretion system 1, protein BfdA
VP1394		2.31	3.88	3.67	Type VI secretion system 1, Putative VgrG protein

VP1396		4.55	3.70	3.29	Type VI secretion system 1 protein
VP1398		2.31	2.00	1.81	Type VI secretion system 1 protein
VP1400		1.95	1.28	1.04	Type VI secretion system 1 protein
VP1402		3.34	2.70	2.42	Type VI secretion system 1 protein
VP1403		3.12	2.35	1.98	Type VI secretion system 1 protein
VP1404		3.32	3.24	2.82	Type VI secretion system 1 protein
VP1405		2.89	3.58	3.34	Type VI secretion system 1 protein
VP1406		3.92	3.73	3.38	Type VI secretion system 1 protein
VP1409		1.80	1.30	1.00	Type VI secretion system 1 protein
VP1411		1.96	1.81	1.43	Type VI secretion system 1 protein
VP1412		1.93	1.51	1.48	Type VI secretion system 1 protein
VP1413		2.12	2.47	2.23	Type VI secretion system 1 protein
VP1415		2.13	2.18	2.03	Uncharacterized protein
VP1541		1.58	1.33	1.31	Cbb3-type cytochrome c oxidase subunit
VP1602		1.50	2.89	2.74	Putative NAD-glutamate dehydrogenase
VP1778		1.94	1.72	1.90	Putative transcriptional regulator
VP1805		3.24	5.64	5.45	Uncharacterized protein
VP1902		4.30	2.69	2.53	Uncharacterized protein
VP2010		4.27	2.60	2.06	Putative tetrathionate reductase complex: sensory transduction histidine kinase
VP2089		1.95	3.72	3.48	Oligopeptide ABC transporter, permease protein
VP2209	*fadI*	1.42	1.23	1.16	3-ketoacyl-CoA thiolase
VP2362	*ompK*	2.86	1.61	1.52	Outer membrane protein OmpK
VP2450		1.69	1.20	1.48	Transcriptional regulator, MarR family
VP2594		1.82	1.15	1.08	Uncharacterized protein
VP2750		2.52	1.95	1.54	Putative fimbrial assembly protein PilM
VP2799		2.86	1.67	1.58	Extracellular nuclease-related protein
VP2827		2.39	1.73	1.59	Methyl-accepting chemotaxis protein
VP2866		3.77	3.54	3.28	Transcriptional regulator, LuxR family
VP2938	*btuB*	1.30	1.15	1.02	Vitamin B12 transporter BtuB
VP2989		2.14	2.34	2.69	Uroporphyrinogen-III synthase
VPA0073		1.90	1.84	1.98	Putative transcriptional regulator
VPA0116		2.43	3.96	3.73	Permease
VPA0124		1.95	2.80	3.26	Putative acetyltransferase
VPA0166		1.21	5.36	5.32	Putative outer membrane protein
VPA0207		1.45	1.71	2.28	Peptide methionine sulfoxide reductase

VPA0242		7.88	5.33	4.99	Uncharacterized protein
VPA0341		8.12	11.27	10.81	Uncharacterized protein
VPA0466		1.23	2.13	2.49	Universal stress protein
VPA0595		1.49	1.43	1.42	ATP-binding component of molybdate transport system
VPA0621		2.59	1.95	1.66	Methylmalonate-semialdehyde dehydrogenase
VPA0754		3.41	1.54	1.13	Uncharacterized protein
VPA0842		1.29	1.52	1.38	Methyl-accepting chemotaxis protein
VPA0864		1.68	1.71	1.61	Putative ABC transporter periplasmic solute binding protein
VPA0979		1.48	1.19	1.03	Ferric aerobactin receptor
VPA1004		7.02	12.17	10.96	Putative transmembrane protein
VPA1087	rbsD	5.95	3.71	3.19	D-ribose pyranase
VPA1120		1.61	1.41	1.43	Putative enoyl-CoA hydratase/isomerase
VPA1176		2.14	1.59	1.25	Uncharacterized protein
VPA1182		2.63	1.23	1.02	Methyl-accepting chemotaxis protein
VPA1353		10.84	6.80	7.24	Putative outer membrane protein, type III secretion system 2 protein
VPA1424		6.06	3.94	4.04	PTS system, fructose-specific IIABC component
VPA1548	lafA	5.24	3.57	3.11	Lateral flagellin
VPA1556	lafT	5.15	3.44	2.99	Chemotaxis protein LafT
VPA1637		4.97	2.69	2.30	Uncharacterized protein
VPA1656		2.17	2.74	2.70	Ferric vibrioferrin receptor
VPA1657		1.65	2.11	2.10	Ferric siderophore receptor homolog
VPA1741		5.27	7.74	6.76	Uncharacterized protein
VP0130	hslO	-1.68	-2.00	-1.94	33 kDa chaperonin
VP0158		-1.42	-2.59	-2.67	tRNA methyltransferase
VP0197		-2.27	-1.87	-1.70	Putative capsular polysaccharide biosynthesis protein D
VP0408	tsaD	-2.08	-2.19	-2.29	tRNA N6-adenosine threonylcarbamoyltransferase
VP0461	murC	-2.64	-1.63	-1.36	UDP-N-acetylmuramate--L-alanine ligase

VP0465	lpxC	-2.74	-2.28	-2.13	UDP-3-O-acyl-N-acetylglucosamine deacetylase
VP0510		-1.56	-1.10	-1.13	Thiol:disulfide interchange protein DsbC
VP0513	lysS	-1.60	-1.30	-1.14	Lysine--tRNA ligase
VP0537	ispH	-2.40	-1.68	-1.65	4-hydroxy-3-methylbut-2-enyl diphosphate reductase
VP0551		-1.92	-1.58	-1.39	ABC transporter, ATP-binding protein

VP0608	*ispG*	-1.47	-1.22	-1.27	4-hydroxy-3-methylbut-2-en-1-yl diphosphate synthase (flavodoxin)
VP0617	*guaA*	-1.79	-1.61	-1.56	GMP synthase [glutamine-hydrolyzing]
VP0702	*syd*	-2.15	-2.04	-1.71	Protein Syd
VP0703		-1.78	-1.60	-1.23	Uncharacterized protein
VP0718		-1.29	-1.68	-1.87	UPF0250 protein VP0718
VP0730		-1.86	-1.10	-1.15	Putative hemolysin
VP0737	*ychF*	-2.26	-1.84	-1.68	Ribosome-binding ATPase YchF
VP0762	*gltX*	-1.63	-1.33	-1.19	Glutamate--tRNA ligase
VP0794		-1.81	-2.99	-2.98	Phosphoenolpyruvate-protein phosphotransferase
VP0832	*glnS*	-1.24	-1.16	-1.17	Glutamine--tRNA ligase
VP0837		-3.34	-1.89	-1.60	Putative esterase/lipase YbfF
VP0861	*argS*	-1.88	-1.76	-1.74	Arginine--tRNA ligase
VP0866	*tsaB*	-3.09	-2.40	-2.31	tRNA threonylcarbamoyladenosine biosynthesis protein TsaB
VP1045	*cmoA*	-4.16	-3.48	-3.23	tRNA (cmo5U34)-methyltransferase
VP1052	*ruvB*	-2.81	-2.32	-1.95	Holliday junction ATP-dependent DNA helicase RuvB
VP1130	*mnmA*	-1.82	-2.32	-2.21	tRNA-specific 2-thiouridylase MnmA
VP1132		-1.74	-2.72	-2.93	Inosine-guanosine kinase
VP1422		-3.81	-3.97	-3.96	SM-20-related protein
VP1439		-1.47	-2.27	-2.65	DnaK-related protein
VP1504		-3.74	-3.39	-3.55	ABC transporter, ATP-binding protein
VP1525		-2.57	-1.92	-1.60	Putrescine-binding periplasmic protein
VP1595		-1.84	-1.43	-1.36	ABC transporter, ATP-binding protein
VP1612	*rsmF*	-1.62	-3.08	-2.90	Ribosomal RNA small subunit methyltransferase F
VP1708		-1.67	-1.84	-1.85	6-phosphogluconate dehydrogenase, decarboxylating
VP1710	*zwf*	-2.05	-1.59	-1.50	Glucose-6-phosphate 1-dehydrogenase
VP1880		-2.13	-3.07	-3.14	L-serine dehydratase 1
VP1890	*rnr*	-2.07	-2.77	-2.90	Ribonuclease R
VP1940		-2.49	-2.18	-1.98	Carboxynorspermidine/carboxyspermidine decarboxylase
VP2049	*tmk*	-2.81	-2.20	-2.16	Thymidylate kinase
VP2052		-2.26	-1.82	-1.69	3-oxoacyl-[acyl-carrier-protein] synthase 2
VP2056	*fabH1*	-2.40	-2.10	-2.05	3-oxoacyl-[acyl-carrier-protein] synthase 3 protein 1
VP2075	*dusC*	-4.51	-8.25	-10.98	tRNA-dihydrouridine(16) synthase

VP2082	ackA1	-2.45	-2.63	-2.45	Acetate kinase 1
VP2118		-2.78	-1.80	-1.52	Superoxide dismutase
VP2167		-3.23	-4.35	-4.47	Uncharacterized protein
VP2177	recR	-5.27	-2.57	-2.34	Recombination protein RecR
VP2193	pdxB	-1.69	-1.42	-1.22	Erythronate-4-phosphate dehydrogenase
VP2284	upp	-1.59	-1.58	-1.38	Uracil phosphoribosyltransferase
VP2333	proS	-1.66	-2.18	-2.19	Proline--tRNA ligase
VP2428	fusA2	-2.43	-2.18	-2.05	Elongation factor G 2
VP2434	deoB	-2.11	-1.70	-1.67	Phosphopentomutase
VP2462		-3.43	-2.32	-1.90	Dihydropteroate synthase
VP2470	tyrS2	-1.45	-1.47	-1.42	Tyrosine--tRNA ligase 2
VP2547		-1.88	-4.66	-6.01	Aspartokinase
VP2606	metK	-1.56	-1.80	-1.55	S-adenosylmethionine synthase
VP2646	valS	-1.71	-1.72	-1.70	Valine--tRNA ligase
VP2727	dusA	-2.67	-3.19	-2.94	tRNA-dihydrouridine(20/20a) synthase
VP2771	fusA1	-2.49	-2.09	-1.97	Elongation factor G 1
VP2788		-1.25	-2.00	-1.93	ABC transporter, ATP-binding protein
VP2805	gph	-2.55	-2.44	-2.28	Phosphoglycolate phosphatase
VP2812	purA	-2.61	-1.72	-1.47	Adenylosuccinate synthetase
VP2818	miaA	-1.53	-1.98	-2.09	tRNA dimethylallyltransferase
VP2913		-4.12	-2.61	-2.04	Uncharacterized protein
VP2939	trmA	-2.38	-1.99	-1.99	tRNA/tmRNA (uracil-C(5))-methyltransferase
VP3079	rsmG	-2.66	-2.63	-2.33	Ribosomal RNA small subunit methyltransferase G
VPA0309	pncB	-6.55	-2.75	-3.51	Nicotinate phosphoribosyltransferase
VPA0461		-2.78	-1.95	-1.66	Alpha-amylase
VPA0773		-4.32	-3.74	-3.37	N-ethylmaleimide reductase
VPA0784	def2	-2.03	-2.40	-1.80	Peptide deformylase 2
VPA0829		-2.20	-3.14	-2.86	Iron-containing alcohol dehydrogenase
VPA0874		-5.59	-3.95	-3.23	Uncharacterized protein
VPA0943		-3.19	-2.53	-1.08	Putative AcrA/AcrE family protein
VPA1597		-1.78	-2.23	-2.40	UPF0176 protein VPA1597
VPA1681		-2.04	-4.20	-4.31	Putative organic hydroperoxide resistance protein

Table 15. Set of proteins specific to cells from swarm flares. Proteins differentially expressed (log2 fold change (FC ≥1 or ≤-1) and statistically significant (FDR=0.01 S_0=0.2) between pairs of i) Periphery vs. Center ii) Periphery vs. Solid, iii) Periphery vs. Liquid.

Protein number	Gene name	P vs. C (FC)	P vs. S (FC)	P vs. L (FC)	Description
NT01vpa1551		5.2	5.5	6.3	Cytoskeletal domain protein CcmA
VP0135		1.0	1.4	2.9	General secretion pathway protein F (Type IISS 1 protein)
VP0179	*lpxL*	1.3	1.4	1.2	Lipid A biosynthesis lauroyltransferase
VP0386		1.3	2.9	1.7	Putative inner membrane protein
VP0413	*uppP*	2.2	2.5	2.8	Undecaprenyl-diphosphatase
VP0903		1.1	2.9	1.4	Probable ATP-dependent RNA helicase RhlE
VP1386		1.2	3.7	5.5	Type VISS 1 protein
VP1387		1.4	3.7	5.0	Type VISS 1 protein
VP1390		1.1	3.6	3.7	Type VISS 1 protein
VP1407		1.9	3.0	2.8	Putative transcriptional regulator
VP1917		1.6	2.9	3.1	Uncharacterized protein
VP2159		2.1	2.5	2.0	Putative methyl-accepting chemotaxis transmembrane protein
VP2211		2.1	1.7	1.1	Uncharacterized protein
VP2224		2.0	1.5	4.4	Uncharacterized protein
VP2227		1.0	1.4	2.1	Soj-like protein
VP2228	*cheB*	1.2	1.4	2.1	Chemotaxis response regulator protein-glutamate methylesterase of group 1 operon
VP2243		2.5	2.4	1.7	Polar flagellar protein FliL
VP2497		2.2	4.1	2.8	Penicillin-binding protein 1B
VP2628		2.9	4.0	2.3	Membrane-bound lytic murein transglycosylase C
VP2629		1.8	1.7	3.1	Methyl-accepting chemotaxis protein
VP2664		1.3	1.3	2.8	ABC transporter, ATP-binding protein
VP2686		1.1	2.0	1.5	Uncharacterized protein
VP2739	*priB*	2.6	2.7	2.1	Primosomal replication protein N
VP2827		1.3	2.7	4.6	Methyl-accepting chemotaxis protein
VPA0262		1.0	3.5	3.0	LfgM
VPA0264		4.6	5.1	5.2	Flagellar basal body rod protein FlgB
VPA0267		3.6	5.7	5.9	Flagellar hook protein FlgE

VPA0268		5.1	4.6	5.6	Flagellar basal body protein
VPA0269		3.9	4.8	4.0	Flagellar basal-body rod protein FlgG
VPA0273	*flgK*	3.6	5.1	4.3	Flagellar hook-associated protein 1
VPA0274		3.7	5.7	6.0	Putative flagellar hook-associated protein
VPA0275		2.6	3.9	3.4	Putative flagellin
VPA0288		4.8	5.5	5.4	Uncharacterized protein
VPA0297		2.6	1.3	3.0	PTS system, fructose-specific IIBC component
VPA0390	*rhlE*	1.9	2.3	1.6	ATP-dependent RNA helicase RhlE
VPA0583		2.4	2.8	1.4	Putative ATP-dependent RNA helicase
VPA0754		2.3	3.1	3.9	Uncharacterized protein
VPA0917		1.7	1.9	3.2	Uncharacterized protein
VPA1000		2.8	2.9	1.7	Methyl-accepting chemotaxis protein
VPA1083		1.1	1.5	1.1	Ribokinase
VPA1086	*rbsA*	3.0	4.1	4.6	Ribose import ATP-binding protein RbsA
VPA1176		1.4	1.9	1.3	ci-d-GMP (EAL GGDEF) protein
VPA1182		1.1	2.5	3.7	Methyl-accepting chemotaxis protein
VPA1189		2.8	4.2	3.8	Methyl-accepting chemotaxis protein
VPA1294		3.1	7.0	6.8	Putative DamX-related protein
VPA1361		1.4	1.5	2.0	Type III SS protein
VPA1449		1.5	3.4	3.8	Methyl-accepting chemotaxis protein
VPA1492		2.5	4.1	3.0	Methyl-accepting chemotaxis protein
VPA1535		3.7	5.0	6.0	Putative flagellar motor switch protein
VPA1536		3.6	5.2	5.5	Flagellar M-ring protein
VPA1539		3.9	4.4	4.8	Putative sodium-type flagellar protein MotY
VPA1546		2.6	3.3	2.0	Flagellar biosynthesis protein
VPA1548	*lafA*	3.3	6.0	6.8	Lateral flagellin
VPA1550	*fliDL*	3.4	4.0	5.3	Lateral flagellar hook-associated protein 2
VPA1554	*lafL*	4.0	4.8	5.1	Flagellar protein LafL
VPA1556	*lafT*	3.7	6.4	7.1	Chemotaxis protein LafT
VPA1557	*lafU*	3.9	4.9	5.9	Chemotaxis protein LafU
VPA1639		4.4	7.8	6.7	Putative secreted ribonuclease
VPA1649		3.2	3.2	3.6	Putative TagE protein
VPA1651		1.6	2.2	3.1	Putative methyl-accepting chemotaxis protein
VPA1652		1.1	2.3	2.7	ATP-binding component of citrate-dependent iron
VPA1699		2.7	3.5	2.6	ATP-dependent RNA helicase, DEAD box family

VP0022	*glyQ*	-1.5	-2.1	-2.2	Glycine--tRNA ligase alpha subunit
VP0126	*dtd*	-1.7	-3.8	-2.8	D-aminoacyl-tRNA deacylase
VP0154		-2.8	-3.0	-1.6	Transcriptional regulator OmpR
VP0243		-1.7	-1.0	-1.5	DNA binding domain
VP0246	*zapB*	-1.6	-1.6	-2.6	Cell division protein ZapB
VP0504		-1.7	-1.6	-2.1	UPF0246 stress response to H2O2
VP0513	*lysS*	-2.2	-2.1	-2.0	Lysine--tRNA ligase
VP0514		-1.2	-1.6	-1.6	Sigma-54 dependent transcriptional regulator
VP0545	*nagZ*	-2.9	-2.6	-2.8	Beta-hexosaminidase
VP0552		-1.0	-1.9	-2.6	Soluble lytic murein transglycosylase
VP0561	*clpB*	-1.6	-2.7	-2.0	Chaperone protein ClpB
VP0569		-2.6	-2.2	-1.6	DNA-binding response regulator PhoB
VP0617	*guaA*	-1.6	-2.2	-1.4	GMP synthase [glutamine-hydrolyzing]
VP0653	*dnaK*	-1.3	-2.7	-1.6	Chaperone protein DnaK
VP0673	*gpt*	-2.5	-3.6	-2.3	Xanthine phosphoribosyltransferase
VP0676	*proB*	-2.0	-1.5	-1.6	Glutamate 5-kinase
VP0739	*prs*	-1.0	-1.7	-1.3	Ribose-phosphate pyrophosphokinase
VP0794		-1.2	-1.5	-1.9	Phosphoenolpyruvate-protein phosphotransferase
VP0832	*glnS*	-1.6	-1.2	-1.5	Glutamine--tRNA ligase
VP0833	*fur*	-1.6	-1.3	-1.4	Ferric uptake regulation protein
VP0975	*mfd*	-1.4	-1.5	-1.4	Transcription-repair-coupling factor
VP1102		-5.3	-5.6	-4.3	Uncharacterized protein
VP1118	*htpX*	-1.5	-2.7	-2.5	Protease HtpX
VP1128		-1.2	-1.7	-1.4	Adenylosuccinate lyase
VP1343		-5.2	-3.8	-5.0	Oligopeptide ABC transporter, ATP-binding protein
VP1425		-4.5	-4.2	-2.6	Putative alcohol dehydrogenase
VP1495		-1.1	-1.0	-2.0	Uncharacterized protein
VP1533	*ttcA*	-1.1	-1.9	-3.3	tRNA 2-thiocytidine biosynthesis protein TtcA
VP1591	*fabA*	-2.6	-2.0	-2.0	3-hydroxydecanoyl-[acyl-carrier-protein] dehydratase
VP1616		-1.5	-1.5	-1.0	Phospho-2-dehydro-3-deoxyheptonate aldolase
VP1617		-1.7	-2.3	-2.6	cyclic-di-GMP-binding
VP1633		-2.6	-3.6	-1.9	Putative RTX toxin
VP1779		-3.5	-8.6	-5.3	Putative glutamine amidotransferase
VP1845		-3.4	-4.1	-4.3	Uncharacterized protein
VP1866		-1.3	-1.7	-2.0	Uncharacterized protein
VP1921	*ribA*	-4.2	-5.4	-3.5	GTP cyclohydrolase-2
VP1934		-1.6	-1.9	-2.5	Ribonucleoside-diphosphate reductase

VP1935		-1.8	-2.0	-2.0	Ribonucleoside-diphosphate reductase, beta subunit
VP2048		-1.8	-1.5	-1.5	DNA polymerase III, delta prime subunit
VP2052		-1.9	-2.3	-2.5	3-oxoacyl-[acyl-carrier-protein] synthase 2
VP2054		-2.2	-2.2	-2.2	3-oxoacyl-
VP2083		-1.3	-1.3	-2.3	Phosphate acetyltransferase
VP2094	moaC	-2.3	-3.5	-2.5	Cyclic pyranopterin monophosphate synthase accessory protein
VP2268		-3.6	-3.6	-4.2	Putative arsenate reductase
VP2293	rnhA	-5.2	-3.8	-4.5	Ribonuclease HI
VP2319	map	-1.6	-1.5	-1.7	Methionine aminopeptidase
VP2333	proS	-2.1	-2.2	-2.2	Proline--tRNA ligase
VP2334		-1.8	-2.8	-1.8	Inner membrane protein
VP2376		-2.3	-2.1	-3.6	Uncharacterized protein
VP2470	tyrS2	-1.7	-2.5	-2.4	Tyrosine--tRNA ligase 2
VP2500	dksA	-1.3	-1.9	-1.4	RNA polymerase-binding transcription factor DksA
VP2521		-5.3	-5.0	-3.8	AmpD protein
VP2548	alaS	-1.3	-1.5	-1.8	Alanine--tRNA ligase
VP2556	surE	-4.2	-5.0	-3.2	5'-nucleotidase SurE
VP2557	truD	-1.5	-1.5	-1.2	tRNA pseudouridine synthase D
VP2646	valS	-1.7	-2.2	-2.0	Valine--tRNA ligase
VP2691		-1.1	-1.2	-1.0	Rod shape-determining protein MreB
VP2702		-3.4	-4.0	-3.6	MSHA biogenesis protein MshN
VP2704		-1.2	-1.4	-2.0	MSHA biogenesis protein MshL
VP2727	dusA	-1.3	-2.6	-2.7	tRNA-dihydrouridine
VP2735		-1.9	-2.1	-2.2	Replicative DNA helicase
VP2766	metJ	-3.9	-4.5	-5.5	Met repressor
VP2804	trpS	-1.7	-1.7	-1.6	Tryptophan--tRNA ligase
VP2845	efp	-2.0	-3.5	-1.8	Elongation factor P
VP2852	groS1	-2.3	-3.9	-2.3	10 kDa chaperonin 1
VP2858		-2.7	-2.9	-1.3	Transcriptional regulator CpxR
VP2863		-2.4	-2.5	-1.5	Aspartate ammonia-lyase
VP2880		-1.3	-1.4	-1.7	Acetyl-CoA carboxylase, biotin carboxyl carrier protein
VP2956	ftsY	-2.2	-2.8	-2.1	Signal recognition particle receptor FtsY
VP2976		-2.6	-1.7	-1.7	Uncharacterized protein
VP3049		-4.5	-4.6	-2.7	SpoOM-related protein
VPA0188		-8.9	-7.7	-3.3	Immunogenic protein
VPA0248		-2.1	-2.2	-2.9	Putative outer membrane protein OmpA
VPA0304		-4.1	-3.1	-2.2	Uncharacterized protein
VPA0399		-3.6	-4.1	-1.7	Putative aminotransferase
VPA0563		-2.2	-5.0	-6.1	DPS family protein
VPA0829		-2.1	-2.3	-2.6	Iron-containing alcohol dehydrogenase

VPA1052		-3.7	-3.5	-1.2	Putative TetR-family
VPA1096		-4.4	-3.8	-1.9	Uncharacterized protein
VPA1181	*tkt2*	-1.7	-2.0	-1.9	Transketolase 2
VPA1334		-2.9	-3.1	-2.3	Uncharacterized protein
VPA1475	*deoD2*	-1.7	-2.7	-3.4	Purine nucleoside phosphorylase DeoD-type 2
VPA1500		-3.1	-3.9	-2.4	DNA binding domain

Table 16. List of 15 genes selected for deletion based on proteomic analyses. Differences in fold change (FC) of protein LFQ intensities between pairs of i) Periphery vs. Center ii) Periphery vs. Solid, iii) Periphery vs. Liquid. SS –statistically significant protein in Students t-test with FDR=0.01 S_0=0.2.

Gene number	Description	P vs. C		P vs. S		P vs. L	
		SS	FC	SS	FC	SS	FC
vp0053	CinA Competence-damaged protein		0.8	+	1.7		2.3
vp1391	type VISS protein - transcriptional regulator		1.0	+	3.7	+	2.7
vp2240*	Polar flagella protein						
vp2972	Signal transduction c-di-GMP phosphodiesterase, EAL/HD-GYP		1.4	+	1.6		1.1
vpa0584*	DNA-binding protein VF530						
vpa0754	Endonuclease/Exonuclease/phosphatase family	+	2.3	+	3.1	+	3.9
vpa1176	EAL_domain (cyclic-di-GMP)	+	1.4	+	1.9	+	1.3
vpa1649	Metalloprotease, peptidase family M23	+	3.2	+	3.2	+	3.6
vp0649	Uncharacterized	+	2.5	+	2.6		2.4
vpa1083	Ribokinase	+	1.1	+	1.5	+	1.1
vp0764	Outer membrane protein OmpA		-0.8	+	-1.5	+	-4.1
vp0514	Sigma-54 dependent transcriptional regulator	+	-1.2	+	-1.6	+	-1.6
vp1945	Transcriptional regulator, LuxR family-two-component system, NarL family, invasion response regulator UvrY	+	-1.7	+	-2.3		-0.5
vpa0662	Transcriptional regulator, MerR family	+	-3.1	+	-1.2		-1.0
vp2178	Nucleoid-associated protein VP2178		-0.8	+	-1.8	+	-1.7

* These two genes were not detected in the final run of mass spectometry, therefore there are no LFQ values available. As they were detected in the first run of proteomics and were up-regulated in periphery versus center, solid and liquid, we decided to delete these two genes, as well.

Table 17. Set of proteins specific of cells from the center of a swarm colony. Proteins differentially expressed (log2 fold change (FC ≥1 or ≤-1) and statistically significant (FDR=0.01 S_0=0.2) between pairs of i) Center vs. Solid ii) Center vs. Periphery, iii) Center vs. Liquid.

Protein number	Gene name	C vs. S (FC)	C vs. P (FC)	C vs. L (FC)	Description
VP0028		1.07	2.82	2.15	Zinc-binding alcohol dehydrogenase
VP0066		2.37	2.94	1.97	Purine nucleoside phosphorylase
VP0080		2.45	4.67	4.16	Putative sigma-54 interacting response regulator transcription regulator protein
VP0124		1.80	1.42	3.24	Uncharacterized protein
VP0157	*recG*	1.29	1.75	1.32	ATP-dependent DNA helicase RecG
VP0297		1.49	2.04	3.59	Uncharacterized protein
VP0352		1.13	1.56	2.13	Acetolactate synthase
VP0353		1.19	1.15	2.78	Acetolactate synthase III, small subunit
VP0364		1.34	2.88	3.63	Putative dihydroxyacetone kinase
VP0393		1.43	2.10	7.27	Uncharacterized protein
VP0394		2.79	2.20	4.89	Haemagglutinin associated protein
VP0516		1.83	4.35	4.38	Oxidoreductase Tas, aldo/keto reductase family
VP0525		2.15	2.36	2.19	Uncharacterized protein
VP0539		2.79	1.36	3.06	Uncharacterized protein
VP0540		1.66	1.09	2.23	Putative carbon starvation protein A
VP0541		1.10	1.09	2.18	Uncharacterized protein
VP0573	*ppk*	1.33	3.41	3.81	Polyphosphate kinase
VP0598		1.51	3.90	3.55	Iron-binding protein IscA
VP0599	*hscB*	1.09	2.20	1.52	Co-chaperone protein HscB homolog
VP0650	*nadK*	2.09	6.62	5.38	NAD kinase
VP0704		1.72	1.98	2.45	Lipoprotein
VP0705		2.35	1.40	1.92	ABC transporter, permease protein
VP0706	*metN*	1.73	1.69	1.77	Methionine import ATP-binding protein MetN
VP0717	*lipB*	1.28	2.22	2.71	Octanoyltransferase
VP0758		2.55	1.37	2.86	Cation transport ATPase, E1-E2 family
VP0768		1.85	1.32	2.12	Uncharacterized protein

VP0805		1.43	2.07	3.64	Uncharacterized protein
VP0864	*purU*	1.73	3.35	3.58	Formyltetrahydrofolate deformylase
VP0909		5.58	3.84	5.14	UPF0061 protein VP0909
VP0920		1.33	1.16	2.87	DNA-binding protein HU-beta
VP0925		1.14	1.48	1.18	Deoxyguanosinetriphosphate triphosphohydrolase-like protein
VP0959		2.43	2.17	1.73	Cation transport ATPase, E1-E2 family
VP0962		1.67	1.17	1.16	Uncharacterized protein
VP1072		1.24	2.79	2.71	Putative helicase
VP1087		3.67	6.69	4.65	Uncharacterized protein
VP1144	*hisI*	1.44	2.18	3.01	Histidine biosynthesis bifunctional protein HisIE
VP1164		8.38	2.43	8.69	Uncharacterized protein
VP1203		1.58	1.86	2.04	Heat shock protein HslJ
VP1283		2.13	2.39	3.00	UPF0145 protein VP1283
VP1301		1.48	2.53	3.15	Exodeoxyribonuclease I
VP1304	*cobT*	1.62	4.09	3.69	Nicotinate-nucleotide--dimethylbenzimidazole phosphoribosyltransferase
VP1307		1.60	2.43	2.49	Putative alpha-ribazole-5'-phosphate phosphatase CobC
VP1308		1.29	2.79	4.53	Putative oligopeptidase
VP1325		1.30	2.70	3.59	Uncharacterized protein
VP1326		1.65	2.23	4.10	Uncharacterized protein
VP1329		2.64	3.92	5.46	Fatty aldehyde dehydrogenase
VP1332		3.89	5.68	4.05	Probable binding protein component of ABC transporter
VP1335		2.64	3.02	2.92	Probable dihydrodipicolinate synthetase
VP1342		3.37	2.85	3.36	Putative aminopeptidase
VP1345		4.00	5.17	4.38	Oligopeptide ABC transporter, permease protein
VP1347		4.80	4.38	4.34	Oligopeptide ABC transporter, periplasmic oligopeptide-binding protein
VP1380		3.13	3.49	3.74	Uncharacterized protein

VP1388		4.36	1.43	3.94	Uncharacterized protein
VP1392		3.64	1.02	3.91	Putative ClpA/B-type protease
VP1393		6.76	1.07	5.32	BfdA
VP1401		4.04	2.00	2.84	Uncharacterized protein
VP1431		2.95	2.54	3.26	Putative ATP-binding component of a transport system
VP1455		2.34	2.41	2.88	Uncharacterized protein
VP1517		1.53	2.99	3.54	Putative Rhs-family protein
VP1561		2.36	2.94	5.01	Bacteriophage f237 ORF8
VP1606		1.42	1.91	1.76	Tail-specific protease
VP1614		1.81	1.25	1.52	Uncharacterized protein
VP1703		2.09	3.56	3.60	Aldehyde dehydrogenase
VP1714		1.56	3.10	2.43	Uncharacterized protein
VP1768		2.03	4.14	3.44	Uncharacterized protein
VP1789		3.31	4.83	4.37	Uncharacterized protein
VP1839		1.74	3.73	2.87	Uncharacterized protein
VP1853		2.11	2.09	2.89	Uncharacterized protein
VP1883		2.54	5.65	3.42	6-carboxy-5,6,7,8-tetrahydropterin synthase
VP1920		3.08	2.16	3.44	Putative iron-regulated protein A
VP1960	*trpB1*	1.18	3.68	3.17	Tryptophan synthase beta chain 1
VP1976		4.40	8.96	8.51	Transcriptional activator MetR
VP2065		1.05	2.29	1.17	Cob(I)alamin adenosyltransferase
VP2110		3.55	2.44	2.91	Uncharacterized protein VP2110
VP2127		2.03	3.36	3.05	Uncharacterized protein
VP2135		1.01	1.62	2.97	Putative phage-related protein
VP2145		2.30	3.88	2.90	Histone deacetylase/AcuC/AphA family protein
VP2150		1.95	3.96	3.26	Putative nitroreductase
VP2158		1.74	2.55	2.61	Uncharacterized protein
VP2177	*recR*	1.19	1.34	1.40	Recombination protein RecR
VP2197		1.19	3.05	4.52	Uncharacterized protein

VP2340		3.63	2.72	2.67	Putative ATP-dependent DNA helicase RecQ
VP2381		1.46	2.31	2.50	Glycerophosphoryl diester phosphodiesterase
VP2386	*glpK*	1.63	2.88	3.32	Glycerol kinase
VP2389		2.48	1.02	2.26	Putative membrane transport protein
VP2431		1.85	1.94	3.82	Phosphoserine phosphatase
VP2473		4.98	4.27	7.12	Uncharacterized protein
VP2479		1.25	3.74	3.34	Peptide ABC transporter, periplasmic peptide-binding protein
VP2553	*rpoS*	2.77	6.95	5.01	RNA polymerase sigma factor RpoS
VP2580		1.05	3.33	2.98	L-aspartate oxidase
VP2630		1.94	1.11	2.71	Aldehyde dehydrogenase
VP2653	*argF*	2.77	4.00	2.82	Ornithine carbamoyltransferase
VP2654	*pyrB*	1.33	2.08	2.61	Aspartate carbamoyltransferase
VP2655	*pyrI*	1.36	2.85	2.67	Aspartate carbamoyltransferase regulatory chain
VP2678		1.48	4.10	2.53	2-hydroxyacid dehydrogenase family protein
VP2683		1.42	2.42	3.28	Uncharacterized protein
VP2698		2.60	1.17	1.44	Putative V10 pilin
VP2743		1.42	1.34	1.95	DamX-related protein
VP2744	*aroB*	1.61	3.36	3.11	3-dehydroquinate synthase
VP2761	*ppc*	1.73	2.36	2.75	Phosphoenolpyruvate carboxylase
VP2763		1.83	2.47	2.56	Methylenetetrahydrofolate reductase
VP2764		1.72	3.42	3.55	Aspartokinase II/homoserine dehydrogenase, methionine-sensitive
VP2765		1.17	2.01	3.00	Cystathionine gamma-synthase
VP2781		1.88	3.81	3.53	Putative asparaginase
VP2794		1.98	5.10	5.62	Uncharacterized protein
VP2807	*rnr*	1.55	1.25	1.80	Ribonuclease R
VP2817	*hfq*	2.20	1.01	1.78	RNA-binding protein Hfq
VP2844		3.51	1.68	2.81	Uncharacterized protein
VP2860		2.02	4.37	5.33	Superoxide dismutase

VP2872		4.47	5.45	2.69	Uncharacterized protein
VP2873	*fumC*	3.03	3.51	4.40	Fumarate hydratase class II
VP2899		1.43	1.55	1.55	Uncharacterized protein
VP2903		2.30	3.93	2.67	Putative phage protein
VP2905		2.29	2.36	2.28	Uncharacterized protein
VP2944		3.08	2.60	3.60	O-methyltransferase-related protein
VP2952	*glpE*	1.26	4.45	4.27	Thiosulfate sulfurtransferase GlpE
VP2953	*rpoH*	1.47	1.25	1.19	RNA polymerase sigma factor RpoH
VP3065		1.60	2.38	3.44	Putative cyclohexadienyl dehydratase signal peptide protein
VPA0004		3.16	4.50	2.55	Peptide ABC transporter, ATP-binding protein
VPA0036		1.57	1.70	1.82	Uncharacterized protein
VPA0038	*nagB*	1.36	2.83	2.08	Glucosamine-6-phosphate deaminase
VPA0072		1.86	5.08	5.35	Putative N-hydroxyarylamine O-acetyltransferase
VPA0089		1.72	3.19	3.44	Putative siderophore utilization protein
VPA0111		1.78	1.88	2.36	Uncharacterized protein
VPA0117		1.30	4.39	3.83	Uncharacterized protein
VPA0144		1.62	2.54	1.66	D-lactate dehydrogenase
VPA0147		2.27	2.95	3.01	Lactate dehydrogenase
VPA0190		1.40	2.60	3.70	Putative transcriptional regulator
VPA0215		6.21	5.75	8.22	Uncharacterized protein
VPA0246		1.01	1.35	1.39	Uncharacterized protein
VPA0296		1.35	2.55	2.44	Putative oxidoreductase protein
VPA0337		1.86	1.74	2.41	Uncharacterized protein
VPA0348		1.27	2.70	3.58	Uncharacterized protein
VPA0368	*tyrS1*	2.68	5.37	4.51	Tyrosine--tRNA ligase 1
VPA0423		2.44	1.95	3.08	Hemin ABC transporter, periplasmic hemin-binding protein HutB
VPA0429		1.66	2.25	3.81	Uncharacterized protein
VPA0436		1.26	2.67	1.40	Putative resolvase
VPA0460		1.73	5.06	5.84	PAS factor

VPA0464		2.70	1.99	3.18	Putative TrkA family protein
VPA0475		1.04	3.45	2.84	Uncharacterized protein
VPA0493		1.67	3.98	4.83	Uncharacterized protein
VPA0562		2.15	1.19	5.82	Putative chemotaxis transducer
VPA0575		2.28	3.80	3.29	Acetyl-CoA synthase
VPA0632		4.84	8.10	7.56	Uncharacterized protein
VPA0641		2.59	3.22	2.43	Putative transcriptional regulator, LysR family
VPA0657		2.31	1.91	2.27	Iron(III) ABC transporter, periplasmic iron-compound-binding protein
VPA0662		1.88	3.12	2.13	Transcriptional regulator, MerR family
VPA0664		3.38	2.28	3.76	Putaive Fe-regulated protein B
VPA0705		1.35	1.34	2.33	Putative cytoplasmic membrane protein
VPA0709		1.18	2.97	1.99	HAD superfamily hydrolase
VPA0761		2.01	2.22	3.26	Aldehyde dehydrogenase
VPA0796		4.19	5.29	5.99	Putative L-allo-threonine aldolase
VPA0797		2.39	1.82	2.62	Uncharacterized protein
VPA0820		1.30	4.62	4.91	Amino acid ABC transporter, periplasmic amino acid-binding protein
VPA0857		1.56	1.94	2.02	Uncharacterized protein
VPA0884		1.03	2.18	2.46	Putative acetyltransferase
VPA0935		1.16	1.31	1.42	Uncharacterized protein
VPA1005		1.05	2.14	4.67	D-lactate dehydrogenase
VPA1011		1.26	3.48	3.52	L-allo-threonine aldolase
VPA1022		1.05	1.90	1.06	Putative exonuclease SbcC
VPA1028		1.44	4.11	4.50	Putative ClpA/B-type chaperone
VPA1044		1.91	2.23	1.40	Uncharacterized protein
VPA1148		1.20	3.63	4.27	Putative high-affinity branched-chain amino acid transport ATP-binding protein
VPA1152		1.27	3.16	3.95	Putative long-chain-fatty-acid-CoA ligase
VPA1153		1.24	3.22	3.85	Putative high-affinity branched-chain amino acid transport ATP-binding protein

VPA1163		1.65	4.19	4.13	Oxidoreductase, aldo/keto reductase 2 family
VPA1202		2.80	4.00	4.93	Polyhydroxyalkanoic acid synthase
VPA1205		2.31	3.13	3.56	Acetoacetyl-CoA reductase
VPA1255		1.47	1.20	2.90	Uncharacterized protein
VPA1256		2.22	3.23	4.04	Uncharacterized protein
VPA1293		1.52	2.08	2.78	Putative antioxidant
VPA1298		1.08	3.87	3.28	Putative glutathione S-transferase
VPA1338		1.30	1.61	2.00	Putative ATPase YscN
VPA1397		1.39	3.15	3.54	Acyl-CoA thioester hydrolase-related protein
VPA1411		3.68	4.62	2.16	Putative glycosyltransferase
VPA1419		1.75	3.35	3.50	Putative 3-hydroxyisobutyrate dehydrogenase
VPA1445		2.13	2.97	3.55	Putative secreted calcium-binding protein
VPA1487		3.23	3.22	4.73	Putative acetyltransferase
VPA1495		2.34	1.78	3.66	ABC transporter, ATP-binding protein
VPA1511		1.74	2.09	2.15	ScrC (Sensory box/GGDEF family protein) (Involved in swarmer cell regulation)
VPA1567		1.02	2.85	4.34	Putative pyruvate formate lyase
VPA1586		2.70	3.52	3.09	Putative ferredoxin-NADP reductase
VPA1589		1.30	3.41	2.05	Transcriptional regulator, LysR family
VPA1595		1.67	1.32	1.30	Putative prolyl aminopeptidase
VPA1599		1.03	3.37	2.40	Uncharacterized protein
VPA1658		3.36	2.26	4.37	Uncharacterized protein
VPA1659		3.09	3.31	4.25	Uncharacterized protein
VPA1662		3.60	3.89	4.52	Putative diaminopimelate decarboxylase protein
VPA1715		1.05	1.53	3.12	ABC transporter, ATP-binding protein
VPA1739		1.96	6.85	5.49	Oligopeptide ABC transporter, periplasmic oligopeptide-binding protein
VP0350		-2.11	-1.30	-3.03	Transcriptional regulator, LysR family
VP0375		-2.88	-1.26	-1.23	Putative lipoprotein

VP0566		-4.42	-1.46	-3.18	Ferredoxin
VP0605	rlmN	-1.69	-2.52	-3.15	Dual-specificity RNA methyltransferase RlmN
VP0995		-2.98	-1.62	-2.23	Uncharacterized protein
VP1268		-2.16	-1.17	-2.92	Uncharacterized protein
VP1506	fdhD	-4.45	-2.97	-1.64	Formate dehydrogenase accessory protein
VP2329		-4.04	-3.08	-1.82	Efflux pump component MtrF
VP2349	nqrC	-1.08	-1.11	-1.29	Na(+)-translocating NADH-quinone reductase subunit C
VP2351	nqrA	-1.18	-1.18	-1.19	Na(+)-translocating NADH-quinone reductase subunit A
VP2504	pcnB	-1.03	-1.55	-1.34	Poly(A) polymerase I
VP2547		-2.70	-1.30	-2.02	Aspartokinase
VP2885	fis	-1.63	-3.18	-3.54	DNA-binding protein Fis
VP3007		-3.04	-4.21	-5.33	ATP-dependent DNA helicase RecQ
VPA0173	rimK	-1.07	-1.28	-2.11	Probable alpha-L-glutamate ligase
VPA0286	groS2	-2.12	-1.18	-1.60	10 kDa chaperonin 2
VPA0341		-1.47	-1.57	-1.65	Uncharacterized protein
VPA1452		-1.07	-1.60	-1.98	Uncharacterized protein

Table 18. Set of proteins specific to cells from liquid growth. Proteins differentially expressed (log2 fold change (FC ≥1 or ≤-1) and statistically significant (FDR=0.01 S_0=0.2) between pairs of i) Liquid vs. Center ii) Liquid vs. Periphery, iii) Liquid vs. Solid.

Protein number	Gene name	L vs. C (FC)	L vs. P (FC)	L vs. S (FC)	Description
VP0187		2.27	1.16	1.99	Putative Dca
VP0246	zapB	1.04	2.60	1.03	Cell division protein ZapB
VP0350		3.03	1.74	0.92	Transcriptional regulator, LysR family
VP0419		2.09	1.32	0.97	Uncharacterized protein
VP0498	nfo	3.66	4.18	3.22	Probable endonuclease 4
VP0567		2.27	2.38	1.35	Putative protease
VP0646		1.29	1.80	0.71	UPF0125 protein VP0646

VP0716	*lipA*	2.11	1.75	1.03	Lipoyl synthase
VP0764		3.26	4.08	2.58	Outer membrane protein OmpA
VP0766		3.58	3.74	3.08	Uncharacterized protein
VP0878		4.57	4.11	3.94	Nucleoside permease
VP0927		1.27	2.19	1.14	Putative aspartate aminotransferase
VP0950		2.28	2.90	1.60	Lipoprotein-related protein
VP1044	*cmoB*	3.09	2.74	1.56	tRNA U34 carboxymethyltransferase
VP1185		3.60	2.17	3.18	Putative chemotaxis transducer
VP1217		0.92	1.92	1.39	Uncharacterized protein
VP1254		2.87	1.98	1.33	Uncharacterized protein
VP1267		2.76	1.65	1.98	Putative lipoprotein
VP1268		2.92	1.75	0.76	Uncharacterized protein
VP1495		0.91	2.01	1.01	Uncharacterized protein
VP1533	*ttcA*	2.22	3.29	1.37	tRNA 2-thiocytidine biosynthesis protein TtcA
VP1934		0.82	2.47	0.54	Ribonucleoside-diphosphate reductase
VP1942		2.53	1.56	1.35	Diaminobutyrate-pyruvate transaminase & L-2,4-diaminobutyrate decarboxylase
VP2059		1.55	2.09	1.60	Uncharacterized protein
VP2083		1.00	2.29	1.03	Phosphate acetyltransferase
VP2126		0.85	1.82	0.96	Uncharacterized protein
VP2160		2.68	1.67	1.41	rRNA
VP2376		1.29	3.57	1.48	Uncharacterized protein
VP2467	*ompU*	2.10	1.22	1.67	Outer membrane protein U
VP2532	*rimM*	2.59	1.94	1.28	Ribosome maturation factor RimM
VP2766	*metJ*	1.56	5.49	1.04	Met repressor
VPA0172		1.73	1.81	0.88	Uncharacterized protein
VPA0232		1.68	1.73	1.94	Putative transcriptional regulator
VPA0312		4.79	3.60	2.84	Putative exported protein
VPA0392		2.55	3.37	4.42	Uncharacterized protein

VPA0394		4.30	1.94	3.48	Uncharacterized protein
VPA0607	*rnb*	0.78	1.53	1.20	Exoribonuclease 2
VPA0813		1.92	2.15	1.77	PTS system, fructose-specific IIA/FPR component
VPA0835		2.01	2.49	4.60	Inosine-guanosine kinase
VPA1476		1.34	1.39	0.89	Uncharacterized protein
VP0047		-2.08	-1.21	-2.29	Peptide ABC transporter, ATP-binding protein
VP0050		-2.57	-1.62	-2.57	Peptide ABC transporter, permease protein
VP0124		-3.24	-1.82	-1.44	Uncharacterized protein
VP0133		-0.97	-1.59	-0.65	General secretion pathway protein D
VP0134		-1.33	-1.53	-1.21	General secretion pathway protein E
VP0135		-1.89	-2.94	-1.51	General secretion pathway protein F
VP0353		-2.78	-1.62	-1.58	Acetolactate synthase III, small subunit
VP0393		-7.27	-5.17	-5.84	Uncharacterized protein
VP0394		-4.89	-2.69	-2.10	Haemagglutinin associated protein
VP0421		-2.66	-2.46	-2.16	Methyl-accepting chemotaxis protein
VP0488		-1.34	-1.64	-0.83	Putative DNA polymerase III, beta chain
VP0572		-2.68	-1.06	-1.97	Exopolyphosphatase
VP0625		-3.39	-2.08	-3.49	Uncharacterized protein
VP0790	*flaD*	-2.53	-2.01	-1.57	Polar flagellin B/D
VP0805		-3.64	-1.58	-2.21	Uncharacterized protein
VP0827		-1.77	-2.67	-1.23	Putative glutathione-regulated potassium-efflux system protein KefB
VP0847		-2.03	-1.60	-2.06	2-oxoglutarate dehydrogenase, E1 component
VP0848		-2.48	-1.70	-2.44	Dihydrolipoyllysine-residue succinyltransferase component of 2-oxoglutarate dehydrogenase complex

VP0870		-0.76	-1.08	-1.25	Long-chain-fatty-acid-CoA ligase
VP0898		-1.14	-1.53	-1.02	Hypothetical lipoprotein
VP0920		-2.87	-1.71	-1.55	DNA-binding protein HU-beta
VP0996		-1.74	-1.69	-1.08	Putative 54 kDa polar flagellar sheath protein A
VP1064		-3.76	-2.55	-3.14	Putative eukaryotic-type potassium channels
VP1088		-2.39	-2.60	-1.93	Putative chemotaxis transducer
VP1101		-1.72	-1.24	-0.85	Cys regulon transcriptional activator
VP1104		-1.45	-1.16	-1.10	Leucine-responsive regulatory protein
VP1163		-1.81	-2.09	-3.29	Putative alpha-1,6-galactosidase
VP1207		-1.63	-1.82	-2.28	UDP-sugar hydrolase
VP1245		-2.12	-2.12	-0.91	Response regulator
VP1270		-1.20	-2.56	-2.10	Uncharacterized protein
VP1271		-2.55	-1.79	-1.19	Uncharacterized protein
VP1278		-2.30	-1.98	-1.51	Putative SpoOM-related protein
VP1308		-4.53	-1.74	-3.23	Putative oligopeptidase
VP1326		-4.10	-1.87	-2.45	Uncharacterized protein
VP1386		-4.30	-5.48	-1.80	Uncharacterized protein
VP1387		-3.67	-5.02	-1.37	Uncharacterized protein
VP1391		-1.78	-2.73	1.01	Putative transcriptional regulator
VP1396		-3.29	-3.86	1.28	Uncharacterized protein
VP1398		-2.40	-3.06	1.35	Uncharacterized protein
VP1404		-7.63	-7.50	-1.35	Uncharacterized protein
VP1408		-3.39	-4.31	-1.79	Putative IcmF-related protein
VP1409		-7.21	-8.20	-2.94	Uncharacterized protein
VP1417		-2.75	-1.81	-0.84	Uncharacterized protein
VP1425		-1.99	2.56	-1.67	Putative alcohol dehydrogenase
VP1540		-1.04	-1.31	-1.36	Uncharacterized protein
VP1541		-1.30	-1.86	-2.35	Cbb3-type cytochrome c oxidase subunit

VP1543		-1.35	-1.76	-2.13	Cytochrome c oxidase, subunit CcoO
VP1561		-5.01	-2.07	-2.65	Bacteriophage f237 ORF8
VP1589	*matP*	-1.73	-1.28	-1.08	Macrodomain Ter protein
VP1590		-1.75	-2.02	-0.63	ATP-dependent protease LA-related protein
VP1602		-3.65	-2.33	-3.05	Putative NAD-glutamate dehydrogenase
VP1628		-1.88	-1.59	-1.34	Putative methyl-accepting chemotaxis protein
VP1723		-3.41	-2.88	-1.70	Transporter, BCCT family
VP1851		-1.58	-2.02	-2.21	Uncharacterized protein
VP1904		-1.10	-1.95	-0.68	Methyl-accepting chemotaxis protein
VP1918		-2.51	-2.47	-1.30	Uncharacterized protein
VP1991		-2.20	-1.75	-1.71	5-methyltetrahydropteroyltriglutamate-homocysteine methyltransferase
VP2072	*nhaB*	-2.14	-2.69	-2.03	Na(+)/H(+) antiporter NhaB
VP2076		-1.44	-2.29	-1.43	Putative GGDEF family protein
VP2077		-4.21	-3.24	-4.54	Putative maltodextrin glucosidase
VP2091		-2.82	-1.67	-3.02	Oligopeptide ABC transporter, periplasmic oligopeptide-binding protein
VP2135		-2.97	-1.35	-1.96	Putative phage-related protein
VP2142		-1.92	-1.44	-1.23	Uncharacterized protein
VP2155		-1.85	-2.39	-1.17	Uncharacterized protein
VP2174		-2.70	-2.96	-6.45	Putative regulatory protein
VP2191		-1.08	-1.65	-0.67	Uncharacterized protein
VP2208	*fadJ*	-1.51	-1.91	-1.74	3-hydroxyacyl-CoA dehydrogenase
VP2209	*fadI*	-1.19	-1.82	-1.69	3-ketoacyl-CoA thiolase
VP2224		-2.30	-4.35	-2.83	Uncharacterized protein
VP2227		-1.09	-2.12	-0.74	Soj-like protein
VP2248		-1.72	-2.53	-2.05	Flagellar motor switch protein FliG

VP2258	*flaA*	-2.68	-1.91	-1.43	Polar flagellin A
VP2385		-6.02	-4.91	-3.55	Glycerol uptake facilitator protein GlpF
VP2388		-2.47	-2.82	-1.39	Glycerol-3-phosphate dehydrogenase
VP2431		-3.82	-1.88	-1.97	Phosphoserine phosphatase
VP2516		-4.64	-3.30	-3.93	OpaR
VP2614		-3.28	-1.74	-2.68	Twitching motility protein PilT
VP2629		-1.36	-3.15	-1.45	Methyl-accepting chemotaxis protein
VP2660		-1.46	-2.13	-0.90	Putative anti-sigma B factor antagonist
VP2664		-1.53	-2.79	-1.47	ABC transporter, ATP-binding protein
VP2799		-2.33	-2.62	-1.75	Extracellular nuclease-related protein
VP2827		-3.40	-4.65	-1.98	Methyl-accepting chemotaxis protein
VP2900		-3.57	-1.80	-3.66	Uncharacterized protein
VPA0150		-3.70	-4.03	-0.94	Putative ferrichrome-iron receptor
VPA0163		-2.53	-3.88	2.37	Putative ATP-binding component of ABC transporter
VPA0166		-5.86	-3.09	-5.73	Putative outer membrane protein
VPA0188		-5.59	3.28	-4.45	Immunogenic protein
VPA0227		-4.07	-5.08	-1.36	Alkaline serine protease
VPA0399		-1.95	1.66	-2.46	Putative aminotransferase
VPA0490		-4.47	-5.96	-2.67	Putative membrane protein
VPA0516		-1.87	-1.59	-1.57	Uncharacterized protein
VPA0562		-5.82	-4.63	-3.67	Putative chemotaxis transducer
VPA0585	*trpB2*	-2.84	-1.62	-3.85	Tryptophan synthase beta chain 2
VPA0592		-2.48	-2.89	1.65	Uncharacterized protein
VPA0593		-1.13	-1.17	0.89	Putative transcriptional regulator
VPA0621		-6.91	-7.82	-2.79	Methylmalonate-semialdehyde dehydrogenase
VPA0754		-1.62	-3.94	-0.82	Uncharacterized protein

VPA0836		-2.49	-1.89	-1.06	CreA protein
VPA0859		-2.61	-2.34	-2.14	Putative lipase
VPA0860		-3.65	-3.00	-2.19	Long-chain fatty acid transport protein
VPA0917		-1.53	-3.19	-1.31	Uncharacterized protein
VPA0979		-2.83	-2.75	-0.62	Ferric aerobactin receptor
VPA1005		-4.67	-2.52	-3.62	D-lactate dehydrogenase
VPA1024		-2.42	-3.68	-1.43	Uncharacterized protein
VPA1096		-2.53	1.91	-1.86	Uncharacterized protein
VPA1128		-3.38	-3.46	-3.27	Putative acyl-CoA carboxylase alpha chain
VPA1135		-4.16	-4.33	-5.49	Putative acetyltransferase
VPA1155		-2.67	-2.46	-2.90	Electron transfer flavoprotein-ubiquinone oxidoreductase
VPA1182		-2.54	-3.66	-1.14	Methyl-accepting chemotaxis protein
VPA1186		-4.35	-1.75	-4.14	Outer membrane protein OmpA
VPA1255		-2.90	-1.70	-1.43	Uncharacterized protein
VPA1261		-2.58	-1.99	-1.74	Putative ATP-binding protein
VPA1478		-1.85	-1.72	-1.08	GGDEF family protein and
VPA1480		-2.86	-1.87	-1.23	Uncharacterized protein
VPA1495		-3.66	-1.88	-1.32	ABC transporter, ATP-binding protein
VPA1550	*fliDL*	-1.95	-5.31	-1.34	Lateral flagellar hook-associated protein 2
VPA1557	*lafU*	-1.94	-5.85	-0.95	Chemotaxis protein LafU
VPA1638		-3.04	-2.75	-3.95	Putative pullulanase
VPA1642		-3.03	-2.03	-2.94	Putative CymC protein
VPA1648		-2.22	-1.26	-2.11	Uncharacterized protein
VPA1655		-4.15	-4.88	-2.73	Putative FecB
VPA1656		-4.01	-3.38	-2.04	Ferric vibrioferrin receptor
VPA1657		-3.97	-3.05	-2.45	Ferric siderophore receptor homolog
VPA1658		-4.37	-2.11	-1.01	Uncharacterized protein

		-3.12	-1.59	-2.08	ABC transporter, ATP-binding protein
VPA1715		-3.12	-1.59	-2.08	ABC transporter, ATP-binding protein
VPA1735		-1.46	-0.75	-0.94	Uncharacterized protein
VPA1736		-2.20	-2.18	-2.01	Toxin secretion ATP-binding protein

Table 19. Set of housekeeping proteins. List of proteins non-differentially expressed (log2 fold change FC < 1 and > -1) between all combination pairs (P vs. C, P vs. S, P vs. L, C vs. S, C vs. L, L vs. S). Essential proteins and proteins containing essential domains are marked with green and orange colour respectively. Results regarding essential proteins and domains are published in (Hubbard *et al.*, 2016) and the terms „underrepresented", and „regional" are used in place of the standart classifications: "essential," and "domain-essential."

Protein number	Gene name	Description
VP0004	*rnpA*	Ribonuclease P protein component
VP0006		Amino acid ABC transporter, ATP-binding protein
VP0011	*dnaA*	Chromosomal replication initiator protein DnaA
VP0012		DNA polymerase III subunit beta
VP0014	*gyrB*	DNA gyrase subunit B
VP0033		Protoporphyrinogen oxidase
VP0034		Transcriptional activator IlvY
VP0041	*rep*	ATP-dependent DNA helicase Rep
VP0077		Ferritin
VP0079		Uncharacterized protein
VP0096		Uncharacterized protein
VP0097	*ubiB*	Probable protein kinase UbiB
VP0098	*tatA*	Sec-independent protein translocase protein TatA
VP0107		DNA polymerase I
VP0121		Glutamine synthetase
VP0143		General secretion pathway protein N
VP0150		Uncharacterized protein
VP0151		Uncharacterized protein
VP0159		Guanosine-3',5'-bis
VP0177	*rph*	Ribonuclease PH
VP0181	*coaBC*	Phosphopantothenate--cysteine ligase
VP0200		Putative N-acetylneuraminic acid synthetase
VP0211		KDO transferase
VP0212		ADP-heptose-LPS heptosyltransferase II
VP0219		Uncharacterized protein
VP0220		OtnA protein
VP0221		OtnB protein
VP0230		Putative glycosyltransferase
VP0235		Putative epimerase/dehydratase
VP0249	*hslU*	ATP-dependent protease ATPase subunit HslU
VP0275	*rpmD*	50S ribosomal protein L30

VP0282	*rpoA*	DNA-directed RNA polymerase subunit alpha
VP0307		Uncharacterized protein
VP0308		Uncharacterized protein
VP0315	*ubiX*	Flavin prenyltransferase UbiX
VP0324	*argR*	Arginine repressor
VP0339	*lptD*	LPS-assembly protein LptD
VP0387		Putative HsdS polypeptide, part of CfrA family
VP0404	*rpoD*	RNA polymerase sigma factor RpoD
VP0430	*parE*	DNA topoisomerase 4 subunit B
VP0431	*parC*	DNA topoisomerase 4 subunit A
VP0449	*lpoA*	Penicillin-binding protein activator LpoA
VP0450	*rsmI*	Ribosomal RNA small subunit methyltransferase I
VP0452	*rsmH*	Ribosomal RNA small subunit methyltransferase H
VP0460	*murG*	UDP-N-acetylglucosamine--N-acetylmuramyl-
VP0467	*secA*	Protein translocase subunit SecA
VP0558	*bamD*	Outer membrane protein assembly factor BamD
VP0559	*rluD*	Ribosomal large subunit pseudouridine synthase D
VP0568	*rdgC*	Recombination-associated protein RdgC
VP0588	*tgt*	Queuine tRNA-ribosyltransferase
VP0589		Uncharacterized protein
VP0590	*secD*	Protein translocase subunit SecD
VP0591	*secF*	Protein-export membrane protein SecF
VP0607		Uncharacterized protein
VP0610		Uncharacterized protein
VP0611	*bamB*	Outer membrane protein assembly factor BamB
VP0612	*der*	GTPase Der
VP0644	*smpB*	SsrA-binding protein
VP0648		DNA repair protein RecN
VP0680		Riboflavin synthase, alpha subunit
VP0682	*ribH*	6,7-dimethyl-8-ribityllumazine synthase
VP0686	*dxs*	1-deoxy-D-xylulose-5-phosphate synthase
VP0692		Transcriptional regulator, LysR family
VP0693		Uncharacterized protein
VP0702	*syd*	Protein Syd
VP0720		Putative rare lipoprotein A
VP0722		Penicillin-binding protein 2
VP0726	*lptE*	LPS-assembly lipoprotein LptE
VP0748	*nutA*	5'-nucleotidase
VP0799		Cell division protein ZipA
VP0800	*ligA*	DNA ligase
VP0820	*toxR*	Cholera toxin homolog transcriptional activator
VP0831		PTS system, N-acetylglucosamine-specific IIABC component
VP0838	*seqA*	Negative modulator of initiation of replication
VP0841		GTP cyclohydrolase 1 type 2 homolog
VP0866	*tsaB*	tRNA threonylcarbamoyladenosine biosynthesis protein TsaB

VP0868		Putative outer membrane lipoprotein Slp
VP0882		Putative beta-ketoacyl-ACP reductase
VP0916	*tig*	Trigger factor
VP0919	*lon*	Lon protease
VP0939		Uncharacterized protein
VP0967		Uncharacterized protein
VP0977		Uncharacterized protein
VP1005		Primosomal replication protein N
VP1022	*topA*	DNA topoisomerase 1
VP1030	*purR*	HTH-type transcriptional repressor PurR
VP1033		Uncharacterized protein
VP1040		Uncharacterized protein
VP1041		Gonadoliberin III-related protein
VP1043		Uncharacterized protein
VP1051	*ruvA*	Holliday junction ATP-dependent DNA helicase RuvA
VP1057		TolQ protein
VP1059		TolA protein
VP1062		Uncharacterized protein
VP1083		DNA helicase
VP1106	*lolA*	Outer-membrane lipoprotein carrier protein
VP1123		Cyclopropane-fatty-acyl-phospholipid synthase
VP1129	*hflD*	High frequency lysogenization protein HflD homolog
VP1161		Cytochrome c-type protein TorC
VP1171		Peptide ABC transporter, periplasmic peptide-binding protein
VP1237		Putative glutamate decarboxylase
VP1250		Transport ATP-binding protein CydD
VP1258	*maeA*	NAD-dependent malic enzyme
VP1266		Uncharacterized protein
VP1280	*thrS*	Threonine--tRNA ligase
VP1285		Putative transcriptional regulator
VP1290	*pheS*	Phenylalanine--tRNA ligase alpha subunit
VP1291	*pheT*	Phenylalanine--tRNA ligase beta subunit
VP1436		Uncharacterized protein
VP1438		DnaK-related protein
VP1439		DnaK-related protein
VP1440		Uncharacterized protein
VP1453		ATP-dependent helicase HrpA
VP1496		Molybdopterin biosynthesis MoeA protein
VP1545		Uncharacterized protein
VP1601	*pyrD*	Dihydroorotate dehydrogenase
VP1739		Uncharacterized protein
VP1869		Transcriptional regulator TyrR
VP1932	*gyrA*	DNA gyrase subunit A
VP1933	*ubiG*	Ubiquinone biosynthesis O-methyltransferase
VP1944	*uvrC*	UvrABC system protein C

VP2018		Paraquat-inducible protein B
VP2019		Uncharacterized protein
VP2056	*fabH1*	3-oxoacyl-[acyl-carrier-protein] synthase 3 protein 1
VP2062	*rne*	Ribonuclease E
VP2066		AsmA protein
VP2130		Uncharacterized protein
VP2189	*accD1*	Acetyl-coenzyme A carboxylase carboxyl transferase subunit beta 1
VP2192	*asd*	Aspartate-semialdehyde dehydrogenase
VP2203	*prmB*	50S ribosomal protein L3 glutamine methyltransferase
VP2215		Putative cytochrome c-type biogenesis protein
VP2217		Thiol:disulfide interchange protein DsbE
VP2218		Cytochrome c-type biogenesis protein CcmF
VP2219	*ccmE*	Cytochrome c-type biogenesis protein CcmE
VP2234		Flagellar biosynthesis protein FlhF
VP2253		Polar flagellar protein FlaK
VP2304	*rnhB*	Ribonuclease HII
VP2305	*lpxB*	Lipid-A-disaccharide synthase
VP2308	*lpxD*	UDP-3-O-acylglucosamine N-acyltransferase
VP2309		Chaperone protein skp
VP2310	*bamA*	Outer membrane protein assembly factor BamA
VP2347	*nqrE*	Na
VP2353	*rlmG*	Ribosomal RNA large subunit methyltransferase G
VP2354		Putative lipoprotein
VP2369		Membrane-bound lytic murein transglycosylase A
VP2429	*radA*	DNA repair protein RadA
VP2437		Nucleoside permease
VP2446		C-di-GMP phosphodiesterase A-related protein
VP2452	*pnp*	Polyribonucleotide nucleotidyltransferase
VP2454	*truB*	tRNA pseudouridine synthase B
VP2456	*infB*	Translation initiation factor IF-2
VP2460		Preprotein translocase, SecG subunit
VP2474	*erpA*	Iron-sulfur cluster insertion protein ErpA
VP2477	*rsmC*	Ribosomal RNA small subunit methyltransferase C
VP2478		Histidine kinase
VP2498		ATP-dependent helicase HrpB
VP2511		ABC transporter, ATP-binding protein
VP2517	*lpd*	Dihydrolipoyl dehydrogenase
VP2528		Cell division protein ZapD
VP2534	*ffh*	Signal recognition particle protein
VP2552	*mutS*	DNA mismatch repair protein MutS
VP2562	*pyrG*	CTP synthase
VP2564		GTP pyrophosphokinase
VP2571	*era*	GTPase Era
VP2574	*lepA*	Elongation factor 4

VP2587		UbiH protein
VP2598		Uncharacterized protein
VP2610		Ribosomal RNA small subunit methyltransferase E
VP2618		FkuB
VP2657		1-acyl-sn-glycerol-3-phosphate acyltransferase
VP2661		Uncharacterized protein
VP2668	*lptA*	Lipopolysaccharide export system protein LptA
VP2673		Nucleotide-binding protein *VP*2673
VP2682	*rapA*	RNA polymerase-associated protein RapA
VP2690		Cell shape-determining protein MreC
VP2706		MSHA biogenesis protein MshJ
VP2724		Uncharacterized protein
VP2751		Penicillin-binding protein 1A
VP2773	*rpsL*	30S ribosomal protein S12
VP2792		Phosphoribulokinase
VP2806	*rlmB*	23S rRNA
VP2814	*hflC*	Protein HflC
VP2815	*hflK*	Protein HflK
VP2816	*hflX*	GTPase HflX
VP2819	*mutL*	DNA mismatch repair protein MutL
VP2820		N-acetylmuramoyl-L-alanine amidase
VP2830		Uncharacterized protein
VP2850		Uncharacterized protein
VP2911		DNA-binding protein HU-2
VP2921	*rpoC*	DNA-directed RNA polymerase subunit beta'
VP2922	*rpoB*	DNA-directed RNA polymerase subunit beta
VP2927	*nusG*	Transcription termination/antitermination protein NusG
VP2934		CDP-diacylglycerol--serine O-phosphatidyltransferase
VP2938	*btuB*	Vitamin B12 transporter BtuB
VP2947	*plsB*	Glycerol-3-phosphate acyltransferase
VP3000	*rho*	Transcription termination factor Rho
VP3044	*rsmB*	Ribosomal RNA small subunit methyltransferase B
VP3045		Potassium uptake protein TrkA
VP3072	*atpH*	ATP synthase subunit delta
VP3073	*atpF*	ATP synthase subunit b
VP3077		ParB family protein
VPA0041		Transcriptional regulator, LysR family
VPA0076		Putative regulator
VPA0140		Putative pseudouridine methyltransferase
VPA0149		Putative two-component system sensor kinase
VPA0202		GGDEF family protein
VPA0224	*macB*	Macrolide export ATP-binding/permease protein MacB
VPA0240		Putative repressor protein PhnR
VPA0279		Uncharacterized protein
VPA0303		Putative regulatory protein

VPA0379		Putative nucleoprotein/polynucleotide-associated enzyme
VPA0517		Uncharacterized protein
VPA0545		Peptidyl-prolyl cis-trans isomerase
VPA0546		Putative disulfide oxidoreductase
VPA0550		Uncharacterized protein
VPA0672		DNA helicase
VPA0712		Ribosome biogenesis GTPase A
VPA0806		Transcriptional regulator, TetR family
VPA0852		Transcriptional regulator, LysR family
VPA0920		Sensor histidine kinase
VPA0921		NAD
VPA1018		Lipoprotein Blc
VPA1170		Molybdopterin biosynthesis MoeA protein
VPA1223		UPF0502 protein VPA1223
VPA1456		Uncharacterized protein
VPA1477		Uncharacterized protein
VPA1501		Putative membrane protein
VPA1512		ScrB
VPA1733		Secretion protein, HlyD family
VPA1751		ParB family protein

7.2 Supplementary figures
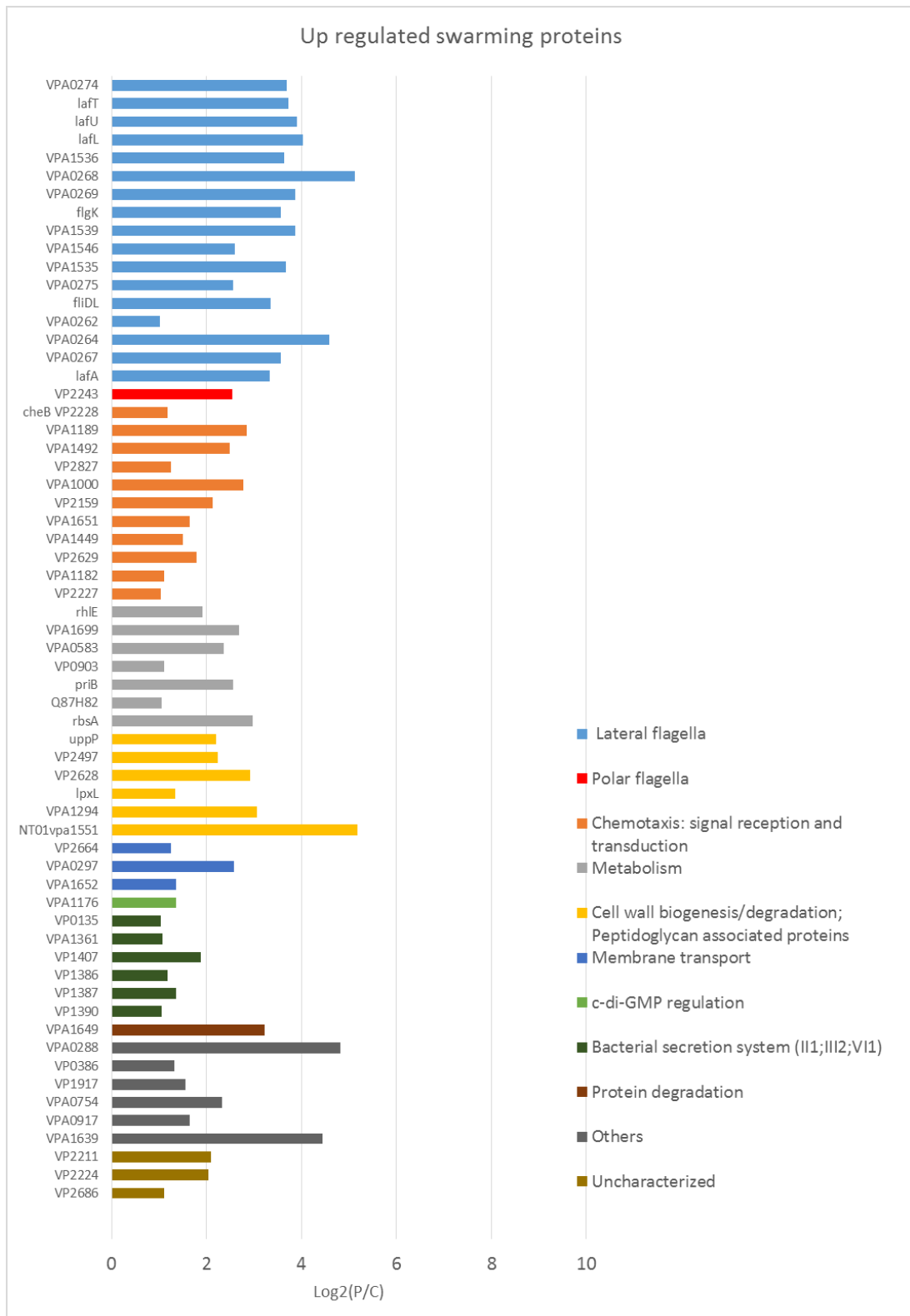
Figure 30. Up-regulated swarming specific proteins. Plot using log2 of the intensities ratio of cell from the periphery versus cell from the center of a swarm colony (P vs. C). These are proteins that are significantly up- regulated in all three comparison sets : P vs.C, P vs.S and P vs.L
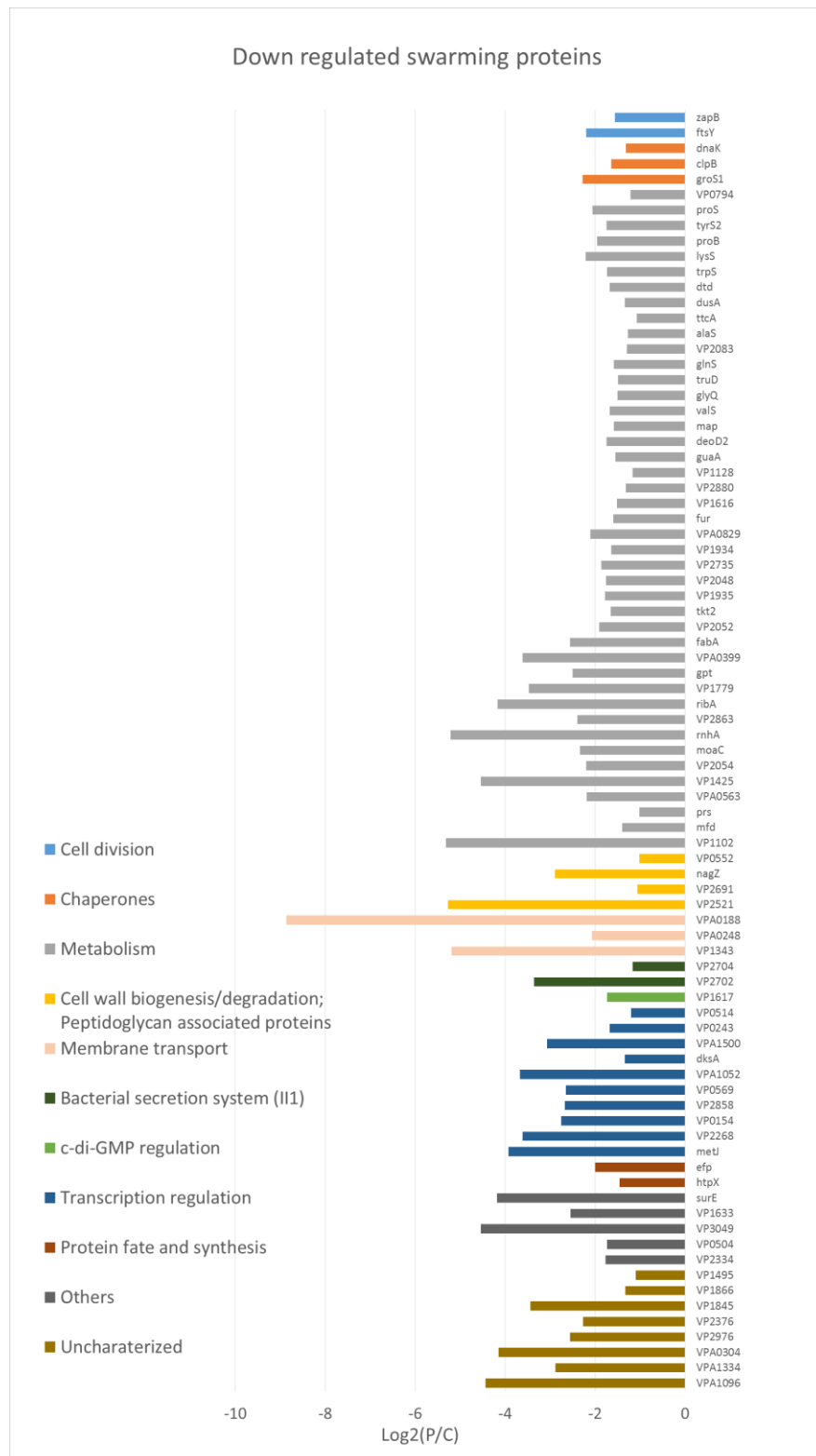
Figure 31. Down-regulated swarming specific proteins. Plot using log2 of the intensities ratio of cell from the periphery versus cell from the center of a swarm colony (P vs. C). These are proteins that are significantly up- regulated in all three comparison sets : P vs.C, P vs.S and P vs.L

Chapter VIII - References

References

Aagesen, A.M., Phuvasate, S., Su, Y.C., and Häse, C.C. (2013) Persistence of *Vibrio parahaemolyticus* in the pacific oyster, crassostrea gigas, is a multifactorial process involving pili and flagella but not type III secretion systems or phase variation. *Appl Environ Microbiol* **79**: 3303–3305.

Ait-Ouazzou, A., Mañas, P., Condón, S., Pagán, R., and García-Gonzalo, D. (2012) Role of general stress-response alternative sigma factors σ S (RpoS) and σ B (SigB) in bacterial heat resistance as a function of treatment medium pH. *Int J Food Microbiol* **153**: 358–364.

Al-Bassam, M.M., Haist, J., Neumann, S.A., Lindenberg, S., and Tschowri, N. (2018) Expression patterns, genomic conservation and input into developmental regulation of the GGDEF/EAL/HD-GYP domain proteins in Streptomyces. *Front Microbiol* **9**.

Alberti, L., and Harshey, R.M. (1990) Differentiation of *Serratia marcescens* 274 into swimmer and swarmer cells. *J Bacteriol* **172**: 4322–4328.

Allison, C., Emody, L., Coleman, N., and Hughes, C. (1994) The role of swarm cell differentiation and multicellular migration in the uropathogenicity of *Proteus mirabilis*. *J Infect Dis* **169**: 1155–1158.

Allison, D.G., Ruiz, B., Sanjose, C., Jaspe, A., and Gilbert, P. (1998) Extracellular products as mediators of the formation and detachment of *Pseudomonas fluorescens* biofilms. *FEMS Microbiol Lett* **167**: 179–184.

Altuvia, S., Almiron, M., Huisman, G., Kolter, R., and Storz, G. (1994) The dps promoter is activated by OxyR during growth and by IHF and σs in stationary phase. *Mol Microbiol* **13**: 265–272.

Alvarado, A., Kjær, A., Yang, W., Mann, P., Briegel, A., Waldor, M.K., and Ringgaard, S. (2017) Coupling chemosensory array formation and localization. *Elife* **6**: e31058.

An, S., Wu, J., and Zhang, L.H. (2010) Modulation of *Pseudomonas aeruginosa* biofilm dispersal by a cyclic-di-gmp phosphodiesterase with a putative hypoxia-sensing domain. *Appl Environ Microbiol* **76**: 8160–8173.

Ariel, G., Be'Er, A., and Reynolds, A. (2017) Chaotic Model for Lévy Walks in Swarming Bacteria. *Phys Rev Lett* **118**.

Ariel, G., Rabani, A., Benisty, S., Partridge, J.D., Harshey, R.M., and Be'Er, A. (2015) Swarming bacteria migrate by Lévy Walk. *Nat Commun* **6**: 8396.

Atkinson, S., Chang, C.Y., Sockett, R.E., Cámara, M., and Williams, P. (2006) Quorum sensing in *Yersinia enterocolitica* controls swimming and swarming motility. *J Bacteriol* **188**: 1451–1461.

Atkinson, S., and Williams, P. (2009) Quorum sensing and social networking in the microbial world. *J R Soc Interface* **6**: 959–978.

Baker-Austin, C., Stockley, L., Rangdale, R., and Martinez-Urtaza, J. (2010) Environmental occurrence and clinical impact of *Vibrio vulnificus* and *Vibrio parahaemolyticus*: A European perspective. *Environ Microbiol Rep* **2**: 7–18.

Barraud, N., Hassett, D.J., Hwang, S.H., Rice, S.A., Kjelleberg, S., and Webb, J.S. (2006) Involvement of nitric oxide in biofilm dispersal of *Pseudomonas aeruginosa*. *J Bacteriol* **188**: 7344–7353.

Barraud, N., Schleheck, D., Klebensberger, J., Webb, J.S., Hassett, D.J., Rice, S.A., and Kjelleberg, S. (2009a) Nitric oxide signaling in *Pseudomonas aeruginosa* biofilms mediates phosphodiesterase activity, decreased cyclic di-GMP levels, and enhanced dispersal. *J Bacteriol* **191**: 7333–7342.

Barraud, N., Storey, M. V., Moore, Z.P., Webb, J.S., Rice, S.A., and Kjelleberg, S. (2009b) Nitric oxide-mediated dispersal in single- and multi-species biofilms of clinically and industrially relevant microorganisms. *Microb Biotechnol* **2**: 370–378.

Baty, A.M., Eastburn, C.C., Techkarnjanaruk, S., Goodman, A.E., and Geesey, G.G. (2000) Spatial and temporal variations in chitinolytic gene expression and bacterial biomass production during chitin degradation. *Appl Environ Microbiol* **66**: 3574–3585.

Be'er, A., Smith, R.S., Zhang, H.P., Florin, E.L., Payne, S.M., and Swinney, H.L. (2009a) *Paenibacillus dendritiformis* bacterial colony growth depends on surfactant but not on bacterial motion. *J Bacteriol* **191**: 5758–5764.

Be'er, A., Strain, S.K., Hernández, R.A., Ben-Jacob, E., and Florin, E.L. (2013) Periodic reversals in *Paenibacillus dendritiformis* swarming. *J Bacteriol* **195**: 2709–2717.

Be'er, A., Zhang, H.P., Florin, E.-L., Payne, S.M., Ben-Jacob, E., and Swinney, H.L. (2009b) Deadly competition between sibling bacterial colonies. *Proc Natl Acad Sci* **106**: 428–433.

Belas, R., Erskine, D., and Flaherty, D. (1991) *Proteus mirabilis* mutants defective in swarmer cell differentiation and multicellular behavior. .

Belas, R., Goldman, M., and Ashliman, K. (1995) Genetic analysis of *Proteus mirabilis* mutants defective in swarmer cell elongation. *J Bacteriol* **177**: 823–828.

Ben-Jacob, E., Cohen, I., Czirók, A., Vicsek, T., and Gutnick, D.L. (1997) Chemomodulation of cellular movement, collective formation of vortices by swarming bacteria, and colonial development. *Phys A Stat Mech its Appl* **238**: 181–197.

Ben-Jacob, E., Cohen, I., and Gutnick, D.L. (2002) Cooperative organization of bacterial colonies: From Genotype to Morphotype. .

Ben-Jacob, E., Schochet, O., Tenenbaum, A., Cohen, I., Czirók, A., and Vicsek, T. (1994) Generic modelling of cooperative growth patterns in bacterial colonies. *Nature* **368**: 46–49.

Benisty, S., Ben-Jacob, E., Ariel, G., and Be'er, A. (2015) Antibiotic-induced anomalous statistics of collective bacterial swarming. *Phys Rev Lett* **114**.

Boehme, D.E., Vincent, K., and Brown, O.R. (1976) Oxygen and toxicity inhibition of amino acid biosynthesis. *Nature* **262**: 418–420.

Böer, S.I., Heinemeyer, E.A., Luden, K., Erler, R., Gerdts, G., Janssen, F., and Brennholt, N. (2013) Temporal and Spatial Distribution Patterns of Potentially Pathogenic *Vibrio* spp. at Recreational Beaches of the German North Sea. *Microb Ecol* **65**: 1052–1067.

Boles, B.R., and Horswill, A.R. (2008) Agr-mediated dispersal of *Staphylococcus aureus* biofilms. *PLoS Pathog* **4**: e1000052.

Boles, B.R., and McCarter, L.L. (2002) *Vibrio parahaemolyticus scrABC*, a novel operon affecting swarming and capsular polysaccharide regulation. *J Bacteriol* **184**: 5946–5954.

Böttcher, T., and Clardy, J. (2014) A Chimeric Siderophore Halts Swarming *Vibrio*. *Angew Chemie Int Ed* **53**: 3510–3513.

Böttcher, T., Elliott, H.L., and Clardy, J. (2016) Dynamics of snake-like swarming behavior of *Vibrio alginolyticus*. *Biophys J* **110**: 981–992.

Boylan, J.A., Lawrence, K.A., Downey, J.S., and Gherardini, F.C. (2008) *Borrelia burgdorferi* membranes are the primary targets of reactive oxygen species. *Mol Microbiol* **68**: 786–799.

Brennan, C. (2013) Chemoattraction of *Vibrio fischeri* to serine, nucleosides,. *Appl …* **69**: 7527–7530.

Cárcamo-Oyarce, G., Lumjiaktase, P., Kümmerli, R., and Eberl, L. (2015) Quorum sensing triggers the stochastic escape of individual cells from *Pseudomonas putida* biofilms. *Nat Commun* **6**.

Chan, C., Paul, R., Samoray, D., Amiot, N., Giese, B., Jenal, U., and Schirmer, T. (2005) Structural basis for the activity and allosteric control of diguanylate cyclase. *Acta Crystallogr Sect A Found Crystallogr* **61**: c235–c235.

References

Cho, C., Chande, A., Gakhar, L., Bakaletz, L.O., Jurcisek, J.A., Ketterer, M., *et al.* (2015) Role of the Nuclease of *Nontypeable Haemophilus influenzae* in dispersal of organisms from biofilms. *Infect Immun* **83**: 950–957.

Christen, M., Christen, B., Folcher, M., Schauerte, A., and Jenal, U. (2005) Identification and characterization of a cyclic di-GMP-specific phosphodiesterase and its allosteric control by GTP. *J Biol Chem* **280**: 30829–30837.

Chua, S.L., Liu, Y., Yam, J.K.H., Chen, Y., Vejborg, R.M., Tan, B.G.C., *et al.* (2014) Dispersed cells represent a distinct stage in the transition from bacterial biofilm to planktonic lifestyles. *Nat Commun* **5**: 4462.

Chung, C.T., Niemela, S.L., and Miller, R.H. (1989) One-step preparation of competent *Escherichia coli*: transformation and storage of bacterial cells in the same solution. *Proc Natl Acad Sci U S A* .

Cochran, W.L., Suh, S.J., McFeters, G.A., and Stewart, P.S. (2000) Role of RpoS and AlgT in *Pseudomonas aeruginosa* biofilm resistance to hydrogen peroxide and monochloramine. *J Appl Microbiol* **88**: 546–553.

Cohen, I., Ron, I.G., and Ben-Jacob, E. (2000) From branching to nebula patterning during colonial development of the *Paenibacillus alvei* bacteria. .

Copeland, M.F., and Weibel, D.B. (2009) Bacterial Swarming: A Model System for Studying Dynamic Self-assembly. *Soft Matter* **5**: 1174–1187.

Cox, J., and Mann, M. (2008) MaxQuant enables high peptide identification rates, individualized p.p.b.-range mass accuracies and proteome-wide protein quantification. *Nat Biotechnol* **26**: 1367–1372.

Cusick, K., Lee, Y.-Y., Youchak, B., and Belas, R. (2012) Perturbation of FliL interferes with *Proteus mirabilis* swarmer cell gene expression and differentiation. *J Bacteriol* **194**: 437–447.

Dean, S.N., Chung, M.-C., and Hoek, M.L. van (2015) *Burkholderia* diffusible signal factor signals to *Francisella novicida* to disperse biofilm and increase siderophore production. *Appl Environ Microbiol* **81**: 7057–7066.

Deepanjali, A., Kumar, H.S., Karunasagar, I., and Karunasagar, I. (2005) Seasonal variation in abundance of total and pathogenic *Vibrio parahaemolyticus* bacteria in oysters along the southwest coast of India. *Appl Environ Microbiol* **71**: 3575–80.

Dengler, V., Foulston, L., DeFrancesco, A.S., and Losick, R. (2015) An electrostatic net model for the role of extracellular DNA in biofilm formation by *Staphylococcus aureus* . *J Bacteriol* **197**: 3779–3787.

Deriu, E., Liu, J.Z., Pezeshki, M., Edwards, R.A., Ochoa, R.J., Contreras, H., *et al.* (2013) Probiotic bacteria reduce *Salmonella typhimurium* intestinal colonization by competing for iron. *Cell Host Microbe* **14**: 26–37.

Deutscher, J., Francke, C., and Postma, P.W. (2006) How Phosphotransferase System-Related Protein phosphorylation regulates carbohydrate metabolism in bacteria. *Microbiol Mol Biol Rev* **70**: 939–1031.

Di, D.Y.W., Lee, A., Jang, J., Han, D., and Hur, H.G. (2017) Season-specific occurrence of potentially pathogenic *Vibrio* spp. on the southern coast of South Korea. *Appl Environ Microbiol* **83**.

Donnenberg, M.S., and Kaper, J.B. (1991) Construction of an *eae* deletion mutant of enteropathogenic *Escherichia coli* by using a positive-selection suicide vector. *Infect Immun* **59**: 4310–7.

Dow, J.M., Crossman, L., Findlay, K., He, Y.-Q., Feng, J.-X., and Tang, J.-L. (2003) Biofilm dispersal in *Xanthomonas campestri*s is controlled by cell-cell signaling and is required for full virulence to plants. *Proc Natl Acad Sci* **100**: 10995–11000.

Eberl, L., Christlansen, G., Molin, S., and Givskov, M. (1996) Differentiation of *Serratia liquefaciens* into swarm cells is controlled by the expression of the *flhD* master operon. *J Bacteriol* **178**: 554–559.

Fernandez, N.L., Srivastava, D., Ngouajio, A.L., and Waters, C.M. (2018) Cyclic di-GMP positively regulates DNA repair in *Vibrio cholerae*. *J Bacteriol* **200**.

Fiebig, A., Varesio, L.M., Alejandro Navarreto, X., and Crosson, S. (2019) Regulation of the *Erythrobacter litoralis* DSM 8509 general stress response by visible light. *Mol Microbiol* **0**: mmi.14310.

Fields, A. (2014) Genome sequence of *Vibrio parahaemolyticus*: a pathogenic mechanism distinct from that of *Vibrio cholerae*. **6736**: 2–3.

Finkelshtein, A., Roth, D., Jacob, E. Ben, and Ingham, C.J. (2015) Bacterial swarms recruit cargo bacteria to pave the way in toxic environments. *MBio* **6**: 1–10.

Foulston, L., Elsholz, A.K.W., DeFrancesco, A.S., and Losick, R. (2014) The extracellular matrix of *Staphylococcus aureus* biofilms comprises cytoplasmic proteins that associate with the cell surface in response to decreasing pH. *MBio* **5**.

Fraser, G.M., and Hughes, C. (1999) Swarming motility. *Curr Opin Microbiol* **2**: 630–635.

Furness, R.B., Fraser, G.M., Hay, N.A., and Hughes, C. (1997) Negative feedback from a *Proteus* class II flagellum export defect to the *flhDC* master operon controlling cell division and flagellum assembly. *J Bacteriol* **179**: 5585–5588.

Gamble, M.D., and Lovell, C.R. (2011) Infaunal burrows are enrichment zones for *Vibrio parahaemolyticus* †. *Appl Environ Microbiol* **77**: 3703–3714.

Gao, X., Mukherjee, S., Matthews, P.M., Hammad, L.A., Kearns, D.B., Dann, C.E., and III (2013) Functional characterization of core components of the *Bacillus subtilis* cyclic-di-GMP signaling pathway. *J Bacteriol* **195**: 4782–4792.

Gavín, R., Rabaan, A.A., Merino, S., Tomás, J.M., Gryllos, I., and Shaw, J.G. (2002) Lateral flagella of *Aeromonas* species are essential for epithelial cell adherence and biofilm formation. *Mol Microbiol* **43**: 383–397.

Gjermansen, M., Ragas, P., Sternberg, C., Molin, S., and Tolker-Nielsen, T. (2005) Characterization of starvation-induced dispersion in *Pseudomonas putida* biofilms. *Environ Microbiol* **7**: 894–904.

Gjermansen, M., Ragas, P., and Tolker-Nielsen, T. (2006) Proteins with GGDEF and EAL domains regulate *Pseudomonas putida* biofilm formation and dispersal. *FEMS Microbiol Lett* **265**: 215–224.

Glick, R., Gilmour, C., Tremblay, J., Satanower, S., Avidan, O., Déziel, E., *et al.* (2010) Increase in rhamnolipid synthesis under iron-limiting conditions influences surface motility and biofilm formation in *Pseudomonas aeruginosa*. *J Bacteriol* **192**: 2973–2980.

Gode-Potratz, C.J., Chodur, D.M., and McCarter, L.L. (2010) Calcium and iron regulate swarming and type III secretion in *Vibrio parahaemolyticus*. *J Bacteriol* **192**: 6025–6038.

Gode-Potratz, C.J., Kustusch, R.J., Breheny, P.J., Weiss, D.S., and McCarter, L.L. (2011) Surface sensing in *Vibrio parahaemolyticus* triggers a programme of gene expression that promotes colonization and virulence. *Mol Microbiol* **79**: 240–63.

Gode-Potratz, C.J., and McCarter, L.L. (2011) Quorum sensing and silencing in *Vibrio parahaemolyticus*. *J Bacteriol* **193**: 4224–4237.

Greco, R.S., Prinz, F.B., and Lane Smith, R. (2004) Nanoscale technology in biological systems. *Nanoscale Technol Biol Syst* **49**: 1–485.

Guilhen, C., Charbonnel, N., Parisot, N., Gueguen, N., Iltis, A., Forestier, C., and Balestrino, D. (2016) Transcriptional profiling of *Klebsiella pneumoniae* defines signatures for planktonic, sessile and biofilm-dispersed cells. *BMC Genomics* **17**: 237.

References

Guilhen, C., Forestier, C., and Balestrino, D. (2017) Biofilm dispersal: multiple elaborate strategies for dissemination of bacteria with unique properties. *Mol Microbiol* **105**: 188–210.

Guttenplan, S.B., Shaw, S., and Kearns, D.B. (2013) The cell biology of peritrichous flagella in *Bacillus subtilis*. *Mol Microbiol* **87**: 211–229.

Gygi, D., Rahman, M.M., Lai, H. -C, Carlson, R., Guard-Petter, J., and Hughes, C. (1995) A cell-surface polysaccharide that facilitates rapid population migration by differentiated swarm cells of *Proteus mirabilis*. *Mol Microbiol* **17**: 1167–1175.

Hall, A.N., Subramanian, S., Oshiro, R.T., Canzoneri, A.K., and Kearns, D.B. (2018) SwrD (YlzI) promotes swarming in *Bacillus subtilis* by increasing power to flagellar motors. *J Bacteriol* **200**.

Hall, P.G., and Krieg, N.R. (2010) Swarming of *Azospirillum brasilense* on solid media . *Can J Microbiol* **29**: 1592–1594.

Harshey, R.M. (1994) Bees aren't the only ones: swarming in Gram-negative bacteria. *Mol Microbiol* **13**: 389–394.

Harshey, R.M. (2003) Bacterial Motility on a Surface: Many Ways to a Common Goal. *Annu Rev Microbiol* **57**: 249–273.

Harshey, R.M., and Matsuyama, T. (2006) Dimorphic transition in *Escherichia coli* and Salmonella typhimurium: surface-induced differentiation into hyperflagellate swarmer cells. *Proc Natl Acad Sci* **91**: 8631–8635.

Harshey, R.M., and Partridge, J.D. (2015) Shelter in a Swarm. *J Mol Biol* **427**: 3683–3694.

Hart, B.R., and Blumenthal, R.M. (2011) Unexpected coregulator range for the global regulator Lrp of *Escherichia coli* and *Proteus mirabilis*. *J Bacteriol* **193**: 1054–1064.

Hay, N.A., Tipper, D.J., Gygi, D., and Hughes, C. (1997) A nonswarming mutant of *Proteus mirabilis* lacks the Lrp global transcriptional regulator. *J Bacteriol* **179**: 4741–4746.

Heering, J., Alvarado, A., and Ringgaard, S. (2017b) Induction of cellular differentiation and single cell imaging of *Vibrio parahaemolyticus* swimmer and swarmer cells. *J Vis Exp* **e55842**.

Heering, J., and Ringgaard, S. (2016) Differential localization of chemotactic signaling arrays during the lifecycle of *Vibrio parahaemolyticus*. *Front Microbiol* **7**: 1767.

Henke, J.M., and Bassler, B.L. (2004) Bacterial social engagements. *Trends Cell Biol* **14**: 648–656.

Herrera, C.M., Hankins, J. V., and Trent, M.S. (2010) Activation of PmrA inhibits LpxT-dependent phosphorylation of lipid A promoting resistance to antimicrobial peptides. *Mol Microbiol* **76**: 1444–1460.

Hirano, T., Aoki, M., Kadokura, K., Kumaki, Y., Hakamata, W., Oku, T., and Nishio, T. (2011) Heterodisaccharide 4-O-(N-acetyl-β-d-glucosaminyl)-d-glucosamine is an effective chemotactic attractant for *Vibrio* bacteria that produce chitin oligosaccharide deacetylase. *Lett Appl Microbiol* **53**: 161–166.

Hood, R.D., Singh, P., Hsu, F.S., Güvener, T., Carl, M.A., Trinidad, R.R.S., *et al.* (2010) A Type VI secretion system of *Pseudomonas aeruginosa* targets a toxin to bacteria. *Cell Host Microbe* **7**: 25–37.

Hornstrup, M.K., and Gahrn-Hansen, B. (1993) Extraintestinal infections caused by *Vibrio parahæmolyticus* and *Vibrio alginolyticus* in a danish county, 1987-1992. *Scand J Infect Dis* **25**: 735–740.

Huang, C., Xu, K.D., Mcfeters, G.A., Stewart, S., and Feters, G.A.M.C. (1998) Weapons of a pathogen : Proteases and their role in virulence of *Pseudomonas aeruginosa* hosphate Starvation Spatial Patterns of Alkaline Phosphatase Expression within Bacterial Colonies and Biofilms in Response to Phosphate Starvation. *Appl Environ Microbiol* **64**: 1526–1531.

Hubbard, T.P., Chao, M.C., Abel, S., Blondel, C.J., Abel zur Wiesch, P., Zhou, X., *et al.* (2016)

Genetic analysis of *Vibrio parahaemolyticus* intestinal colonization . *Proc Natl Acad Sci* **113**: 6283–6288.

Humphries, N.E., and Sims, D.W. (2014) Optimal foraging strategies: Lévy walks balance searching and patch exploitation under a very broad range of conditions. *J Theor Biol* **358**: 179–193.

Ilari, A., Ceci, P., Ferrari, D., Rossi, G.L., and Chiancone, E. (2002) Iron incorporation into *Escherichia coli* Dps gives rise to a ferritin-like microcrystalline core. *J Biol Chem* **277**: 37619–37623.

Ilkanaiv, B., Kearns, D.B., Ariel, G., and Beer, A. (2017) Effect of Cell Aspect Ratio on Swarming Bacteria. *Phys Rev Lett* **118**: 158002.

Ingham, C.J., and Jacob, E. Ben (2008) Swarming and complex pattern formation in *Paenibacillus vortex* studied by imaging and tracking cells. *BMC Microbiol* **8**: 36.

Jaques, S., and McCarter, L.L. (2006) Three new regulators of swarming in *Vibrio parahaemolyticus*. *J Bacteriol* **188**: 2625–2635.

Jeckel, H., Jelli, E., Hartmann, R., Singh, P.K., Mok, R., Totz, J.F., *et al.* (2019) Learning the space-time phase diagram of bacterial swarm expansion. *Proc Natl Acad Sci* **116**: 1489–1494.

Jensen, L.J., Kuhn, M., Stark, M., Chaffron, S., Creevey, C., Muller, J., *et al.* (2009) STRING 8-- a global view on proteins and their functional interactions in 630 organisms. *Nucleic Acids Res* **37**: D412-6.

Ji, G., Beavis, R.C., and Novick, R.P. (2006) Cell density control of staphylococcal virulence mediated by an octapeptide pheromone. *Proc Natl Acad Sci* **92**: 12055–12059.

Jiang, Z.Y., Gest, H., and Bauer, C.E. (1997) Chemosensory and photosensory perception in purple photosynthetic bacteria utilize common signal transduction components. *J Bacteriol* **179**: 5720–5727.

Jiang, Z.Y., Rushing, B.G., Bai, Y., Gest, H., and Bauer, C.E. (1998) Isolation of *Rhodospirillum centenum* mutants defective in phototactic colony motility by transposon mutagenesis. *J Bacteriol* **180**: 1248–1255.

Jones, B. V., Young, R., Mahenthiralingam, E., and Stickler, D.J. (2004) Ultrastructure of *Proteus mirabilis* swarmer cell rafts and role of swarming in catheter-associated urinary tract infection. *Infect Immun* **72**: 3941–3950.

Jones, J.L., Kinsey, T.P., Johnson, L.W., Porso, R., Friedman, B., Curtis, M., *et al.* (2016) Effects of Intertidal Harvest Practices on Levels of *Vibrio parahaemolyticus* and *Vibrio vulnificus* Bacteria in Oysters. *Appl Environ Microbiol* **82**: 4517–4522.

Kamatkar, N.G., and Shrout, J.D. (2011) Surface hardness impairment of quorum sensing and swarming for *Pseudomonas aeruginosa*. *PLoS One* **6**.

Kaneko, T., and Colwell, R.R. (1973) Ecology of *Vibrio parahaemolyticus* in Chesapeake Bay. *J Bacteriol* **113**: 24–32.

Kaneko, T., and Colwell, R.R. (1974) Distribution of *Vibrio parahaemolyticus* and related organisms in the Atlantic Ocean off South Carolina and Georgia. *Appl Microbiol* **28**: 1009–17.

Kaneko, T., and Colwell, R.R. (1975) Adsorption of *Vibrio parahaemolyticus* onto Chitin and Copepods. *Appl Envir Microbiol* **29**: 269–274.

Kaneko, T., and Colwell, R.R. (1977) The annual cycle of *Vibrio parahaemolyticus* in chesapeake bay. *Microb Ecol* **4**: 135–155.

Kaplan, J.B., Velliyagounder, K., Ragunath, C., Rohde, H., Mack, D., K-M Knobloch, J., and Ramasubbu, N. (2004) Genes Involved in the Synthesis and Degradation of Matrix Polysaccharide in *Actinobacillus actinomycetemcomitans* and *Actinobacillus pleuropneumoniae* Biofilms. *J Bacteriol* **186**: 8213–8220.

References

Karatan, E., and Watnick, P. (2009) Signals, regulatory networks, and materials that build and break bacterial biofilms. *Microbiol Mol Biol Rev* **73**: 310–47.

Kawagishi, I., Imagawa, M., Imae, Y., McCarter, L., and Homma, M. (1996) The sodium-driven polar flagellar motor of marine *Vibrio* as the mechanosensor that regulates lateral flagellar expression. *Mol Microbiol* **20**: 693–699.

Kearns, D.B. (2010) A field guide to bacterial swarming motility. *Nat Rev Microbiol* **8**: 634–44.

Kearns, D.B., Chu, F., Rudner, R., and Losick, R. (2004) Genes governing swarming in *Bacillus subtilis* and evidence for a phase variation mechanism controlling surface motility. *Mol Microbiol* **52**: 357–369.

Kearns, D.B., and Losick, R. (2003) Swarming motility in undomesticated *Bacillus subtilis*. *Mol Microbiol* **49**: 581–90.

Kearns, D.B., and Losick, R. (2005) Cell population heterogeneity during growth of *Bacillus subtilis*. *Genes Dev* **19**: 3083–3094.

Kelley, L.A., and Sternberg, M.J.E. (2009) Protein structure prediction on the web: A case study using the phyre server. *Nat Protoc* **4**: 363–373.

Kibbe, W.A. (2007) OligoCalc: An online oligonucleotide properties calculator. *Nucleic Acids Res* **35**.

Kim, W., and Surette, M.G. (2004) Metabolic differentiation in actively swarming *Salmonella*. *Mol Microbiol* **54**: 702–714.

Kim, W., and Surette, M.G. (2005) Prevalence of surface swarming behavior in *Salmonella*. *J Bacteriol* **187**: 6580–6583.

Kim, Y.K., and McCarter, L.L. (2000) Analysis of the polar flagellar gene system of *Vibrio parahaemolyticus*. *J Bacteriol* **182**: 3693–3704.

Kim, Y.K., and McCarter, L.L. (2004) Cross-regulation in *Vibrio parahaemolyticus*: Compensatory activation of polar flagellar genes by the lateral flagellar regulator LafK. *J Bacteriol* **186**: 4014–4018.

Kim, Y.K., and McCarter, L.L. (2007) ScrG, a GGDEF-EAL protein, participates in regulating swarming and sticking in *Vibrio parahaemolyticus*. *J Bacteriol* **189**: 4094–4107.

Kirov, S.M., Tassell, B.C., Semmler, A.B.T., O'Donovan, L.A., Rabaan, A.A., and Shaw, J.G. (2002) Lateral flagella and swarming motility in *Aeromonas* species. *J Bacteriol* **184**: 547–555.

Lai, H.C., Gygi, D., Fraser, G.M., and Hughes, C. (1998) A swarming-defective mutant of *Proteus mirabilis* lacking a putative cation-transporting membrane P-type ATPase. .

Lamb, E., Trimble, M.J., and McCarter, L.L. (2019) Cell-cell communication, chemotaxis and recruitment in *Vibrio parahaemolyticus*. *Mol Microbiol* mmi.14256.

Lee, K.J., Kim, J.A., Hwang, W., Park, S.J., and Lee, K.H. (2013) Role of capsular polysaccharide (CPS) in biofilm formation and regulation of CPS production by quorum-sensing in *Vibrio vulnificus*. *Mol Microbiol* **90**: 841–857.

Letchumanan, V., Chan, K.G., and Lee, L.H. (2014) *Vibrio parahaemolyticus*: A review on the pathogenesis, prevalence, and advance molecular identification techniques. *Front Microbiol* **5**.

Li, W., Hu, L., Xie, Z., Xu, H., Li, M., Cui, T., and He, Z.G. (2018) Cyclic di-GMP integrates functionally divergent transcription factors into a regulation pathway for antioxidant defense. *Nucleic Acids Res* **46**: 7270–7283.

Little, K., Austerman, J., Zheng, J., and Gibbs, K.A. (2019) Cell Shape and Population Migration Are Distinct Steps of *Proteus mirabilis* Swarming That Are Decoupled on High-Percentage Agar . *J Bacteriol* **201**: 1–15.

Liu, Y., Bauer, S.C., and Imlay, J.A. (2011) The YaaA protein of the *Escherichia coli* OxyR regulon

_____

lessens hydrogen peroxide toxicity by diminishing the amount of intracellular unincorporated iron. *J Bacteriol* **193**: 2186–2196.

Liu, Z., Stirling, F.R., and Zhu, J. (2007) Temporal quorum-sensing induction regulates *Vibrio cholerae* biofilm architecture. *Infect Immun* **75**: 122–126.

Livny, J., Zhou, X., Mandlik, A., Hubbard, T., Davis, B.M., and Waldor, M.K. (2014) Comparative RNA-Seq based dissection of the regulatory networks and environmental stimuli underlying *Vibrio parahaemolyticus* gene expression during infection. *Nucleic Acids Res* **42**: 12212–12223.

López-Hernández, K.M., Pardío-Sedas, V.T., Lizárraga-Partida, L., Williams, J. de J., Martínez-Herrera, D., Flores-Primo, A., *et al.* (2015) Environmental parameters influence on the dynamics of total and pathogenic *Vibrio parahaemolyticus* densities in Crassostrea virginica harvested from Mexico's Gulf coast. *Mar Pollut Bull* **91**: 317–329.

Ma, C., Deng, X., Ke, C., He, D., Liang, Z., Li, W., *et al.* (2013) Epidemiology and etiology characteristics of foodborne outbreaks caused by *Vibrio parahaemolyticus* During 2008–2010 in Guangdong Province, China . *Foodborne Pathog Dis* **11**: 21–29.

MacIntyre, D.L., Miyata, S.T., Kitaoka, M., and Pukatzki, S. (2010) The *Vibrio cholerae* type VI secretion system displays antimicrobial properties. *Proc Natl Acad Sci* **107**: 19520–19524.

Macnab, R.M. (1999) The bacterial flagellum: Reversible rotary propellor and type III export apparatus. *J Bacteriol* **181**: 7149–7153.

Macnab, R.M., and Minamino, T. (1999) Components of the *Salmonella* Flagellar Export Apparatus and Classification of Export Substrates. *J Bacteriol* **181**: 1388–1394.

Magariyama, Y., Sugiyama, S., Muramoto, K., Kawagishi, I., Imae, Y., and Kudo, S. (1995) Simultaneous measurement of bacterial flagellar rotation rate and swimming speed. *Biophys J* **69**: 2154–2162.

Maira-Litrán, T., Allison, D.G., and Gilbert, P. (2000) Expression of the multiple antibiotic resistance operon (mar) during growth of *Escherichia coli* as a biofilm. *J Appl Microbiol* **88**: 243–247.

Makino, K., Oshima, K., Kurokawa, K., Yokoyama, K., Uda, T., Tagomori, K., *et al.* (2003) Genome sequence of *Vibrio parahaemolyticus*: A pathogenic mechanism distinct from that of V cholerae. *Lancet* **361**: 743–749.

Mandel, M.J., and Silhavy, T.J. (2005) Starvation for different nutrients in *Escherichia coli* results in differential modulation of RpoS levels and stability. *J Bacteriol* **187**: 434–442.

Mariconda, S., Wang, Q., and Harshey, R.M. (2006) A mechanical role for the chemotaxis system in swarming motility. *Mol Microbiol* **60**: 1590–1602.

Marks, L.R., Davidson, B.A., Knight, P.R., and Hakansson, A.P. (2013) Interkingdom signaling induces *Streptococcus pneumoniae* biofilm dispersion and transition from asymptomatic colonization to disease. *MBio* **4**.

Martinez-Urtaza, J., Blanco-Abad, V., Rodriguez-Castro, A., Ansede-Bermejo, J., Miranda, A., and Rodriguez-Alvarez, M.X. (2012) Ecological determinants of the occurrence and dynamics of *Vibrio parahaemolyticus* in offshore areas. *ISME J* **6**: 994–1006.

Martinez-Urtaza, J., Huapaya, B., Gavilan, R.G., Blanco-Abad, V., Ansede-Bermejo, J., Cadarso-Suarez, C., *et al.* (2008) Emergence of asiatic *vibrio* diseases in south america in phase with El Niño. *Epidemiology* **19**: 829–837.

Mauriello, E.M.F., Mignot, T., Yang, Z., and Zusman, D.R. (2010) Gliding Motility Revisited: How Do the *Myxobacteria* Move without Flagella? *Microbiol Mol Biol Rev* **74**: 229–249.

McCarter, L. (1999) The multiple identities of *Vibrio parahaemolyticus*. *J Mol Microbiol Biotechnol* **1**: 51–57.

McCarter, L., Hilmen, M., and Silverman, M. (1988) Flagellar dynamometer controls swarmer cell differentiation of *V. parahaemolyticus*. *Cell* **54**: 345–351.

References

McCarter, L., and Silverman, M. (1989) Iron regulation of swarmer cell differentiation of *Vibrio parahaemolyticus*. *J Bacteriol* **171**: 731–737.

McCarter, L., and Silverman, M. (1990) Surface-induced swarmer cell differentiation of *Vibrio parahaemolyticus*. *Mol Microbiol* **4**: 1057–1062.

McCarter, L.L. (2003) Polar Flagellar Motility of the Vibrionaceae. *Microbiol Mol Biol Rev* **65**: 445–462.

McCarter, L.L. (2004) Dual flagellar systems enable motility under different circumstances. *J Mol Microbiol Biotechnol* **7**: 18–29.

McCarter, L.L. (2006) Regulation of flagella. *Curr Opin Microbiol* **9**: 180–186.

McClain, J., Rollo, D.R., Rushing, B.G., and Bauer, C.E. (2002) *Rhodospirillum centenum* utilizes separate motor and switch components to control lateral and polar flagellum rotation. *J Bacteriol* **184**: 2429–2438.

McKee, R.W., Harvest, C.K., and Tamayo, R. (2018) Cyclic diguanylate regulates virulence factor genes via multiple riboswitches in *Clostridium difficile* . *mSphere* **3**.

Merino, S., Shaw, J.G., and Tomás, J.M. (2006) Bacterial lateral flagella: An inducible flagella system. *FEMS Microbiol Lett* **263**: 127–135.

Miller, V.L., and Mekalanos, J.J. (1988) A novel suicide vector and its use in construction of insertion mutations: osmoregulation of outer membrane proteins and virulence determinants in *Vibrio cholerae* requires *toxR*. *J Bacteriol* **170**: 2575–2583.

Miramontes, O., Boyer, D., and Bartumeus, F. (2012) The effects of spatially heterogeneous prey distributions on detection patterns in foraging seabirds. *PLoS One* **7**.

Miyata, S.T., Kitaoka, M., Brooks, T.M., McAuley, S.B., and Pukatzki, S. (2011) *Vibrio cholerae* requires the type VI secretion system virulence factor vasx to kill dictyostelium discoideum. *Infect Immun* **79**: 2941–2949.

Mobley, H.L.T., and Belas, R. (1995) Swarming and pathogenicity of *Proteus mirabilis* in the urinary tract. *Trends Microbiol* **3**: 280–284.

Morgan, R., Kohn, S., Hwang, S.H., Hassett, D.J., and Sauer, K. (2006) BdlA, a chemotaxis regulator essential for biofilm dispersion in *Pseudomonas aeruginosa*. *J Bacteriol* **188**: 7335–7343.

Murakami, H., Niizato, T., Tomaru, T., Nishiyama, Y., and Gunji, Y.P. (2015) Inherent noise appears as a Lévy walk in fish schools. *Sci Rep* **5**.

Muraleedharan, S., Freitas, C., Mann, P., Glatter, T., and Ringgaard, S. (2018) A cell length-dependent transition in MinD-dynamics promotes a switch in division-site placement and preservation of proliferating elongated *Vibrio parahaemolyticus* swarmer cells. *Mol Microbiol* **109**: 365–384.

Mustapha, S., Mustapha, E.M., and Nozha, C. (2013) *Vibrio alginolyticus* : An Emerging Pathogen of Foodborne Diseases. *Int J Sci Technol* **2**: 302–309.

Newton, A., Kendall, M., Vugia, D.J., Henao, O.L., and Mahon, B.E. (2012) Increasing rates of vibriosis in the United States, 1996-2010: Review of surveillance data from 2 systems. *Clin Infect Dis* **54**.

Nordstrom, J.L., Kaysner, C.A., Blackstone, G.M., Vickery, M.C.L., Bowers, J.C., And Depaola, A. (2016) Effect of Intertidal Exposure on *Vibrio parahaemolyticus* Levels in Pacific Northwest Oysters. .

O'Rear, J., Alberti, L., and Harshey, R.M. (1992) Mutations that impair swarming motility in *Serratia marcescens* 274 include but are not limited to those affecting chemotaxis or flagellar function. *J Bacteriol* **174**: 6125–6137.

Ohnishi, K., Fan, F., Schoenhals, G.J., Kihara, M., and Macnab, R.M. (1997) The fliO, fliP, fliQ,

and fliR proteins of *Salmonella typhimurium:* Putative components for flagellar assembly. *J Bacteriol* **179**: 6092–6099.

Ono, T., Park, K.S., Ueta, M., Iida, T., and Honda, T. (2006) Identification of proteins secreted via *Vibrio parahaemolyticus* type III secretion system 1. *Infect Immun* **74**: 1032–1042.

Overhage, J., Bains, M., Brazas, M.D., and Hancock, R.E.W. (2008) Swarming of *Pseudomonas aeruginosa* is a complex adaptation leading to increased production of virulence factors and antibiotic resistance. *J Bacteriol* **190**: 2671–2679.

Paranjpye, R., Hamel, O.S., Stojanovski, A., and Liermann, M. (2012) Genetic Diversity of Clinical and Environmental *Vibrio parahaemolyticus* Strains from the Pacific Northwest. *Appl Environ Microbiol* **78**: 8631–8638.

Park, K.-S., Arita, M., Iida, T., and Honda, T. (2005a) *vpaH*, a Gene Encoding a Novel Histone-Like Nucleoid Structure-Like Protein That Was Possibly Horizontally Acquired, Regulates the Biogenesis of Lateral Flagella in trh-Positive *Vibrio parahaemolyticus* TH3996. *Infect Immun* **73**: 5754–5761.

Park, S., You, X., and Imlay, J.A. (2005b) Substantial DNA damage from submicromolar intracellular hydrogen peroxide detected in Hpx- mutants of *Escherichia coli*. *Proc Natl Acad Sci* **102**: 9317–9322.

Patrick, J.E., and Kearns, D.B. (2008) MinJ (YvjD) is a topological determinant of cell division in *Bacillus subtilis*. *Mol Microbiol* **70**: 1166–1179.

Patrick, J.E., and Kearns, D.B. (2009) Laboratory strains of *Bacillus subtilis* do not exhibit swarming motility. *J Bacteriol* **191**: 7129–7133.

Pearson, M.M., Rasko, D.A., Smith, S.N., and Mobley, H.L.T. (2010) Transcriptome of swarming *Proteus mirabilis*. *Infect Immun* **78**: 2834–2845.

Petrova, O.E., and Sauer, K. (2016) Escaping the biofilm in more than one way: Desorption, detachment or dispersion. *Curr Opin Microbiol* **30**: 67–78.

Pettigrew, M.M., Marks, L.R., Kong, Y., Gent, J.F., Roche-Hakansson, H., and Hakansson, A.P. (2014) Dynamic Changes in the *Streptococcus pneumoniae* Transcriptome during Transition from Biofilm Formation to Invasive Disease upon Influenza A Virus Infection. *Infect Immun* **82**: 4607–4619.

Rashid, M.H., and Kornberg, A. (2000) Inorganic polyphosphate is needed for swimming, swarming, and twitching motilities of *Pseudomonas aeruginosa*. *Proc Natl Acad Sci* **97**: 4885–4890.

Rather, P.N. (2005) Swarmer cell differentiation in *Proteus mirabilis*. *Environ Microbiol* **7**: 1065–1073.

Rauprich, O., Matsushita, M., Weijer, C.J., Siegert, † Florian, Esipov, S.E., and Shapiro, J.A. (1996) Periodic Phenomena in *Proteus mirabilis* Swarm Colony Development. .

Ringgaard, S., Zepeda-Rivera, M., Wu, X., Schirner, K., Davis, B.M., and Waldor, M.K. (2014) ParP prevents dissociation of CheA from chemotactic signaling arrays and tethers them to a polar anchor. *Proc Natl Acad Sci* **111**: E255–E264.

Ross, P., Weinhouse, H., Aloni, Y., Michaeli, D., Weinberger-Ohana, P., Mayer, R., *et al.* (1987) Regulation of cellulose synthesis in *Acetobacter xylinum* by cyclic diguanylic acid. *Nature* **325**: 279–281.

Roy, V., Adams, B.L., and Bentley, W.E. (2011) Developing next generation antimicrobials by intercepting AI-2 mediated quorum sensing. *Enzyme Microb Technol* **49**: 113–123.

Rutherford, S.T., Kessel, J.C. Van, Shao, Y., and Bassler, B.L. (2011) AphA and LuxR/HapR reciprocally control quorum sensing in *vibrios*. *Genes Dev* **25**: 397–408.

Ryjenkov, D.A., Tarutina, M., Moskvin, O. V., and Gomelsky, M. (2005) Cyclic diguanylate is a ubiquitous signaling molecule in bacteria: Insights into biochemistry of the GGDEF protein

domain. *J Bacteriol* **187**: 1792–1798.

Saak, C.C., and Gibbs, K.A. (2016) The Self-Identity Protein IdsD Is Communicated between Cells in Swarming *Proteus mirabilis* Colonies. *J Bacteriol* **198**: 3278–3286.

Salomon, D., Gonzalez, H., Updegraff, B.L., and Orth, K. (2013) *Vibrio parahaemolyticus* Type VI Secretion System 1 is activated in marine conditions to target bacteria, and is differentially regulated from system 2. *PLoS One* **8**.

Sar, N., McCarter, L., Simon, M., and Silverman, M. (1990) Chemotactic control of the two flagellar systems of *Vibrio parahaemolyticus*. *J Bacteriol* **172**: 334–341.

Sauer, K., and Camper, A.K. (2001) Characterization of Phenotypic Changes in *Pseudomonas putida* in Response to Surface-Associated Growth. *J Bacteriol* **183**: 6579–6589.

Sauer, K., Camper, A.K., Ehrlich, G.D., Costerton, J.W., and Davies, D.G. (2002) *Pseudomonas aeruginosa* displays multiple phenotypes during development as a biofilm. *J Bacteriol* **184**: 1140–1154.

Sauer, K., Cullen, M.C., Rickard, A.H., Zeef, L.A.H., Davies, D.G., and Gilbert, P. (2004) Characterization of Nutrient-Induced Dispersion in *Pseudomonas aeruginosa* PAO1 Biofilm. *J Bacteriol* **186**: 7312–7326.

Schindelin, J., Arganda-Carreras, I., Frise, E., Kaynig, V., Longair, M., Pietzsch, T., *et al.* (2012) Fiji: An open-source platform for biological-image analysis. *Nat Methods* **9**: 676–682.

Schreiber, F., Beutler, M., Enning, D., Lamprecht-Grandio, M., Zafra, O., González-Pastor, J., and Beer, D. De (2011) The role of nitric-oxide-synthase-derived nitric oxide in multicellular traits of *Bacillus subtilis* 3610: Biofilm formation, swarming, and dispersal. *BMC Microbiol* **11**: 111.

Schwarz, S., West, T.E., Boyer, F., Chiang, W.C., Carl, M.A., Hood, R.D., *et al.* (2010) *Burkholderia* type vi secretion systems have distinct roles in eukaryotic and bacterial cell interactions. *PLoS Pathog* **6**: 77–78.

Senesi, S., Celandroni, F., Salvetti, S., Beecher, D.J., Wong, A.C.L., and Ghelardi, E. (2002) Swarming motility in *Bacillus cereus* and characterization of a fliY mutant impaired in swarm cell differentiation. *Microbiology* **148**: 1785–1794.

Simm, R., Morr, M., Kader, A., Nimtz, M., and Römling, U. (2004) GGDEF and EAL domains inversely regulate cyclic di-GMP levels and transition from sessibility to motility. *Mol Microbiol* **53**: 1123–1134.

Singh, P.K., Bartalomej, S., Hartmann, R., Jeckel, H., Vidakovic, L., Nadell, C.D., and Drescher, K. (2017) *Vibrio cholerae* combines individual and collective sensing to trigger biofilm dispersal. *Curr Biol* **27**: 3359-3366.e7.

Sokolov, A., and Aranson, I.S. (2012) Physical properties of collective motion in suspensions of bacteria. *Phys Rev Lett* **109**.

Srivastava, D., and Waters, C.M. (2012) A tangled web: Regulatory connections between quorum sensing and cyclic Di-GMP. *J Bacteriol* **194**: 4485–4493.

Stacy, A., Everett, J., Jorth, P., Trivedi, U., Rumbaugh, K.P., and Whiteley, M. (2014) Bacterial fight-and-flight responses enhance virulence in a polymicrobial infection. *Proc Natl Acad Sci* **111**: 7819–7824.

Stahl, S.J., Stewart, K.R., and Williams, F.D. (1983) Extracellular slime associated with *Proteus mirabilis* during swarming. *J Bacteriol* **154**: 930–937.

Steichen, C.T., Cho, C., Shao, J.Q., and Apicella, M.A. (2011) The *Neisseria gonorrhoeae* biofilm matrix contains DNA, and an endogenous nuclease controls its incorporation . *Infect Immun* **79**: 1504–1511.

Stephens, C.M., and Shapiro, L. (1993) An unusual promoter controls cell-cycle regulation and dependence on DNA replication of the *Caulobacter* fliLM early flagellar operon. *Mol Microbiol* **9**: 1169–1179.

Stewart, B.J., and McCarter, L.L. (2003) Lateral flagellar gene system of *Vibrio parahaemolyticus*. *J Bacteriol* **185**: 4508–4518.

Stoodley, P., Wilson, S., Hall-Stoodley, L., Boyle, J.D., Lappin-Scott, H.M., and Costerton, J.W. (2001) Growth and Detachment of Cell Clusters from Mature Mixed-Species Biofilms. *Appl Environ Microbiol* **67**: 5608–5613.

Sturgill, G., and Rather, P.N. (2004) Evidence that putrescine acts as an extracellular signal required for swarming in *Proteus mirabilis*. *Mol Microbiol* **51**: 437–446.

Tambalo, D.D., Yost, C.K., and Hynes, M.F. (2010) Characterization of swarming motility in Rhizobium leguminosarum bv. viciae. *FEMS Microbiol Lett* **307**: 165–174.

Thiel, V., Kunze, B., Verma, P., Wagner-Döbler, I., and Schulz, S. (2009) New structural variants of homoserine lactones in bacteria. *ChemBioChem* **10**: 1861–1868.

Thompson, C.C., Vicente, A.C.P., Souza, R.C., Vasconcelos, A.T.R., Vesth, T., Alves, N., *et al.* (2009) Genomic taxonomy of *vibrios*. *BMC Evol Biol* **9**.

Thormann, K.M., Duttler, S., Saville, R.M., Hyodo, M., Shukla, S., Hayakawa, Y., and Spormann, A.M. (2006) Control of formation and cellular detachment from *Shewanella oneidensis* MR-1 biofilms by cyclic di-GMP. *J Bacteriol* **188**: 2681–2691.

Thormann, K.M., Saville, R.M., Shukla, S., and Spormann, A.M. (2005) Induction of rapid detachment in *Shewanella oneidensis* MR-1 biofilms. *J Bacteriol* **187**: 1014–1021.

Toguchi, A., Siano, M., Burkart, M., and Harshey, R.M. (2000) Genetics of swarming motility in *Salmonella enterica serovar Typhimurium*: Critical role for lipopolysaccharide. *J Bacteriol* **182**: 6308–6321.

Touati, D., Jacques, M., Tardat, B., Bouchard, L., and Despied, S. (1995) Lethal oxidative damage and mutagenesis are generated by iron in Δfur mutants of *Escherichia coli*: Protective role of superoxide dismutase. *J Bacteriol* **177**: 2305–2314.

Tremblay, J., and Déziel, E. (2010) Gene expression in *Pseudomonas aeruginosa* swarming motility. *BMC Genomics* **11**: 587.

Trimble, M.J., and McCarter, L.L. (2011) Bis-(3'-5')-cyclic dimeric GMP-linked quorum sensing controls swarming in *Vibrio parahaemolyticus*. *Proc Natl Acad Sci* **108**: 18079–18084.

Tuson, H.H., Copeland, M.F., Carey, S., Sacotte, R., and Weibel, D.B. (2013) Flagellum Density Regulates *Proteus mirabilis* Swarmer Cell Motility in Viscous Environments. *J Bacteriol* **195**: 368–377.

Tyanova, S., Temu, T., Sinitcyn, P., Carlson, A., Hein, M.Y., Geiger, T., *et al.* (2016) The Perseus computational platform for comprehensive analysis of (prote)omics data. *Nat Methods* **13**: 731–740.

Ueda, A., and Wood, T.K. (2009) Connecting quorum sensing, c-di-GMP, pel polysaccharide, and biofilm formation in *Pseudomonas aeruginosa* through tyrosine phosphatase TpbA (PA3885). *PLoS Pathog* **5**.

Ulitzer, S. (1975) The mechanism of swarming of *Vibrio alginolyticus*. *Arch Microbiol* **104**: 67–71.

Ulitzur, S. (1974) Induction of swarming in *Vibrio parahaemolyticus*. *Arch Microbiol* **101**: 357–363.

Ulitzur, S. (1975) Effect of temperature, salts, pH and other factors on the development of peritrichous flagella in *Vibrio alginolyticus*. *Arch Microbiol* **104**: 285–288.

Uppuluri, P., Acosta Zaldívar, M., Anderson, M.Z., Dunn, M.J., Berman, J., Lopez Ribot, J.L., and Köhler, J.R. (2018) *Candida albicans* dispersed cells are developmentally distinct from biofilm and planktonic cells. *MBio* **9**.

Utada, A.S., Bennett, R.R., Fong, J.C.N., Gibiansky, M.L., Yildiz, F.H., Golestanian, R., and Wong, G.C.L. (2014) *Vibrio cholerae* use pili and flagella synergistically to effect motility switching and conditional surface attachment. *Nat Commun* **5**: 1–8.

Velazquez-Roman, J., León-Sicairos, N., Flores-Villaseñor, H., Villafaña-Rauda, S., and Canizalez-Roman, A. (2012) Association of Pandemic *Vibrio parahaemolyticus* O3:K6 Present in the Coastal Environment of Northwest Mexico with Cases of Recurrent Diarrhea between 2004 and 2010. *Appl Environ Microbiol* **78**: 1794–1803.

Venturi, V., Bertani, I., Kerényi, Á., Netotea, S., and Pongor, S. (2010) Co-swarming and local collapse: Quorum sensing conveys resilience to bacterial communities by localizing cheater mutants in *Pseudomonas aeruginosa*. *PLoS One* **5**.

Verstraeten, N., Braeken, K., Debkumari, B., Fauvart, M., Fransaer, J., Vermant, J., and Michiels, J. (2008) Living on a surface: swarming and biofilm formation. *Trends Microbiol* **16**: 496–506.

Wallace, M.A., Liou, L.-L., Martins, J., Clement, M.H.S., Bailey, S., Longo, V.D., *et al.* (2004) Superoxide Inhibits 4Fe-4S Cluster Enzymes Involved in Amino Acid Biosynthesis. *J Biol Chem* **279**: 32055–32062.

Walters, M.C., Roe, F., Bugnicourt, A., Franklin, M.J., and Stewart, P.S. (2003) Contributions of antibiotic penetration, oxygen limitation, and low metabolic activity to tolerance of *Pseudomonas aeruginosa* biofilms to ciprofloxacin and tobramycin. *Antimicrob Agents Chemother* **47**: 317–323.

Wang, Q., Frye, J.G., McClelland, M., and Harshey, R.M. (2004) Gene expression patterns during swarming in *Salmonella typhimurium*: Genes specific to surface growth and putative new motility and pathogenicity genes. *Mol Microbiol* **52**: 169–187.

Wang, R., Zhong, Y., Gu, X., Yuan, J., Saeed, A.F., and Wang, S. (2015) The pathogenesis, detection, and prevention of *Vibrio parahaemolyticus*. *Front Microbiol* **6**.

Wang, T., Cai, Z., Shao, X., Zhang, W., Xie, Y., Zhang, Y., *et al.* (2019) Pleiotropic effects of c-di-GMP content in *Pseudomonas syringae*. *Appl Environ Microbiol* **85**.

Waters, C.M., Rowe-Magnus, D.A., Fernandez, N., Pu, M., Coulter, P., Isaacs, J., and Chodur, D.M. (2018) Environmental Calcium Initiates a Feed-Forward Signaling Circuit That Regulates Biofilm Formation and Rugosity in *Vibrio vulnificus* . *MBio* **9**: 1–14.

Watts, R.E., Totsika, M., Challinor, V.L., Mabbett, A.N., Ulett, G.C., Voss, J.J.D., and Schembri, M.A. (2012) Contribution of siderophore systems to growth and urinary tract colonization of asymptomatic bacteriuria *Escherichia coli*. *Infect Immun* **80**: 333–344.

Webb, J.S., Thompson, L.S., James, S., Charlton, T., Tolker-Nielsen, T., Koch, B., *et al.* (2003) Cell death in *Pseudomonas aeruginosa* biofilm development. *J Bacteriol* **185**: 4585–4592.

Wenren, L.M., Sullivan, N.L., Cardarelli, L., Septer, A.N., and Gibbs, K.A. (2013) Two independent pathways for self-recognition in *Proteus mirabilis* are linked by type VI-dependent export. *MBio* **4**.

Xue, D., Tian, F., Yang, F., Chen, H., Yuan, X., Yang, C.H., *et al.* (2018) Phosphodiesterase EdpX1 promotes *Xanthomonas oryzae pv. oryzae* virulence, exopolysaccharide production, and biofilm formation. *Appl Environ Microbiol* **84**.

Yang, F., Qian, S., Tian, F., Chen, H., Hutchins, W., Yang, C.H., and He, C. (2016) The GGDEF-domain protein GdpX1 attenuates motility, exopolysaccharide production and virulence in *Xanthomonas oryzae pv. oryzae*. *J Appl Microbiol* **120**: 1646–1657.

Yao, Y., Sturdevant, D.E., and Otto, M. (2004) Genomewide Analysis of Gene Expression in *Staphylococcus epidermidis* Biofilms: Insights into the Pathophysiology of *S. epidermidis* Biofilms and the Role of Phenol-Soluble Modulins in Formation of Biofilms . .

Yu, Y., Yan, F., He, Y., Qin, Y., Chen, Y., Chai, Y., and Guo, J.H. (2018) The ClpY-ClpQ protease regulates multicellular development in *Bacillus subtilis*. *Microbiol (United Kingdom)* **164**: 848–862.

Zhang, J.J., Chen, T., Yang, Y., Du, J., Li, H., Troxell, B., *et al.* (2018) Positive and negative regulation of glycerol utilization by the c-di-GMP binding protein plza in borrelia burgdorferi. *J Bacteriol* **200**.

Zhou, J., Ma, Q., Yi, H., Wang, L., Song, H., and Yuan, Y.J. (2011) Metabolome profiling reveals metabolic cooperation between *Bacillus megaterium* and *Ketogulonicigenium vulgare* during

_____

induced swarm motility. *Appl Environ Microbiol* **77**: 7023–7030.

Acknowlegments

First of all, I would like to sincerely thank my supervisor, Dr. Simon Ringgaard. Thank you for giving me the opportunity to work in your lab and for giving me all the wise and enthusiatic input throughout the time I worked under your oversight during my PhD studies. I also would like to thank the members of my Thesis Advisory Committee, Prof. Dr. Lotte Søgaard-Andersen and Prof. Dr. Martin Thanbichler for giving me helpful feedback along the project progress. I also thank our collaborator Timo for guiding me through the proteomics procedure and analyses. Also, a special thanks goes to Shankar Iyer for the proofreading of this thesis, and to Dr. Kathrin Schirner for the translation of the abstract.

Likewise, I want to thank all the present and former members of Ringgard´s lab:
My dear Shankar, we both moved suddendly and together from our previous lab, and it has been a great experience to take all the important steps of our PhD side by side. Thanks for making my days a time full of jokes, puns and updates on the lastest political news, pop musics and new netflix shows. Also, I want to thank you again for reading and commenting my thesis. Petra, you are an amazing professional and an amazing person. Thanks for having always helped me whenever I asked anything. Jan, thanks for our nice coffee breaks and for making the coolest logos for our epic Viking Chess´ teams. Erick, it has been a pleasure meeting you this last year (I will probably request your skills in Tarot again soon). Our WUP Ale, thank you not only for throwing pillows at me, but specially for all the funny moments you provided us with your jokes and stories. Sam, thank you for our conversations always followed by your wise pieces of advice. To former members that left the lab longer ago: Stephan, who stayed close by in the lab next door, our baby quinoa Barbara, our kickers´master Marco and our activist Karo. It was a pleasure sharing the lab with you with such a nice atmosphere. Thank you Karo for always bringing to our lab your big smile, positive energy and desire to learn. It was a pleasure supervising you during your bachelor studies.

Thanks to everyone from A2 floor and also people from A1 floor, including our dear honorary lab member Dorota: you all provided a joyfull athmosphere in our coffee corner where we gathered many times. Particular thanks to Stephan and Bailey. It was a pleasure to share our duties as PhD representatives as well as so many nice moments outside the lab.

I also want to thank all the amazing people, which I didn´t mention yet, and with whom I spent great times in this lovely city of Marburg: Hanna, Stefano, Joana, Luís, Nicole, Mariana, Manuel, Francisco, Govind, Bartoz, Sofia, Dobro and more. I also would like to thank my dear neighbour Susanne, for our tandem meetings and relaxing celebrations of our work progress and for all the care and sympathy she has showed me as a neighbour from the moment I came to live nextdoor. I equally want to thank all the friends I made in Dusseldorf. Thank you, Abhi - the best guide in India someone could wish for - Manu, Bidesh, Sven and all the members of the core group for the nice times we spent together.

All my friends from Portugal deserve a BIG Thanks. Even though separated by 2000 km I could always count on them. It was great to see you everytime I had the opportunity to go back home. I miss you.

I want to thank my dear family for all the support. The fact that they are always there for me makes all my dreams seem possible. You give me encouragement and strength. I also want to thank my grandparents for being an amazing and inspiring example of sucessful and humble people, which I will always try to follow.

A special thanks goes to Tiago. Thank you for always supporting me, not only before but also during my PhD, for being there for the good and for the not so good moments. It has been great going with you in our nice trips together. These years have been amazing.

Thank you all for everything.

Curriculum Vitae

Carolina Duarte de Freitas

Date of Birth: 06.04.1991

Nationality: Portuguese

EDUCATION

2015-present **MPI for Terrestrial Microbiology**   **Marburg, Germany**

Ph.D (Dr.rer.nat)

Thesis title: Characterization of swarm-colony development reveals the release of a distinct cell type facilitating dissemination of *Vibrio parahaemolyticus*

2012-2014 **NOVA University**   **Lisboa, Portugal**

Masters degree in Molecular Genetics and Biomedicine. Faculty of Sciences and Technoloy.

Final average: 18 (out of 20).

Thesis title: Polyphosphorylation of a structural component of *Bacillus subtilis* spore

2009-2012 **Universidade de Lisboa (University of Lisbon)**   **Lisboa, Portugal**

Bachelors degree in Molecular Biology and Genetics. Faculty of Sciences of *Universidade de Lisboa*.

PUBLICATIONS

Freitas, C., Glatter, T. and Ringgaard, S. The release of a distinct cell type from swarm colonies facilitates dissemination of *Vibrio parahaemolyticus* in the environment. *Under review,* The ISME Journal

Fernandes, CG., Martins, D., Hernandez, G., Sousa, AL., Freitas C., et al. (2019) Temporal and spatial regulation of protein cross-linking by the pre-assembled substrates of a *Bacillus subtilis* spore coat transglutaminase. PLOS Genetics 15(4): e1007912. https://doi.org/10.1371/journal.pgen.1007912

Carolina Freitas, Jarnaja Plannic, Rachele Isticato, Assunta Pelosi, Rita Zilhao, Monica Serrano, Loredana Baccigalupi, Ezio Ricca, Alexander KW Elsholz, Richard Losick, Adriano O Henriques. (2018) A protein phosphorylation module patterns the *Bacillus subtilis* spore outer coat. bioRxiv. 469122; doi: https://doi.org/10.1101/469122

Muraleedharan, S., Freitas, C., Mann, P., Glatter, T., & Ringgaard, S. (2018). A cell length-dependent transition in MinD-dynamics promotes a switch in division-site placement and preservation of proliferating elongated *Vibrio parahaemolyticus* swarmer cells. Molecular Microbiology, 109(3), 365–384. https://doi.org/10.1111/mmi.13996

Nunes, F., Fernandes, C., Freitas, C., et al. (2018) SpoVID functions as a non-competitive hub that connects the modules for assembly of the inner and outer spore coat layers in *Bacillus subtilis*. Molecular Microbiology, 110(4):576-595 https://doi.org/10.1111/mmi.14116

Erklärung

Hermit versichere ich, dass ich die vorliegende Dissertation mit dem Titel **„Characterization of swarm-colony development reveals the release of a distinct cell type facilitating dissemination of *Vibrio parahaemolyticus*"** selbstständing verfasst, keine anderen als die Text angegebenen Hilfsmittel verwendet und sämttliche Stellen, die im Wortlaut oder dem Sinn nach anderen Werken entnommen sind, mit Quellenangaben kenntlich gemacth habe.

Die Dissertation wurde in der jetzigen oder einer ähnlichen From noch bei keoner anderen Hochschule eingereicht und hat noch keinen sonstigen Prüfungswecjen gedient.

_____   _____

Ort, Datum   Carolina Duarte de Freitas

Einverständniserklärung

Ich erkläre mich dam einverstanden, dass die vorliegende Dissertation

„Characterization of swarm-colony development reveals the release of a distinct cell type facilitating dissemination of *Vibrio parahaemolyticus*"

in Bibliotheken allgemein zugänglich gemacht wird. Dazu gehört, dass sie

- von der Bibliothek der Einrichtung, in der ich meine Arbeit anfertig habe, zur Benutzung in ihren Räumen bereitgehalten wird;

- in konventionellen und maschinenlesbaren Katalogen, Verzeichnissen und Datenbanken verzeichnet wird;

- im Rahmen der urheberrechtichen Bestimmungen für Kopierzwecke genutzt werden kann.

Marburg, den __.__.2019

_____

Carolina Duarte de Freitas

_____

Dr. Simon Ringgaard